



Philip Williams & Associates, Ltd.
Consultants in Hydrology

Pier 35, The Embarcadero
San Francisco, CA 94133
Phone: (415) 981-8363
Fax: (415) 981-5021

**CITY OF STOCKTON
WATER QUALITY MODEL
VOLUME I: MODEL DEVELOPMENT
AND CALIBRATION**

prepared for

The City of Stockton

prepared by

Robert Schanz, M.S., P.E.
Philip Williams & Associates, Ltd.

and

Carl Chen, Ph.D., P.E.
Systech Engineering

August, 1993

#824

25\824\stock.doc\08-06-93

Environmental Hydrology Engineering Hydraulics Sediment Hydraulics Water Resources

D - 0 4 1 2 5 4

D-041254

TABLE OF CONTENTS

	<u>Page No.</u>
I. INTRODUCTION	1
II. ENVIRONMENTAL SETTING AND BACKGROUND	3
A. Operation of the Stockton Municipal Wastewater Treatment Plant	3
B. Hydrology of the San Joaquin River/Delta System	3
C. Major Dischargers and Pollutant Sources	5
D. Previous Studies and Modeling Efforts	6
III. SUMMARY OF EXISTING WATER QUALITY DATA	8
A. Introduction	8
B. Effluent Characteristics	8
C. Receiving Water Monitoring	9
IV. DYE MIXING STUDY	11
A. Introduction	11
B. Field Study	11
C. Results	14
V. NEAR-FIELD MODEL CALIBRATION	16
A. Introduction	16
B. Existing Models	16
C. Data and Results	17

	<u>Page No.</u>
D. Summary and Conclusions	21
VI. FAR-FIELD MODEL	22
A. Introduction	22
B. Model Grid System	22
C. Model Input and Output	22
D. Hydrodynamic Calibration	25
E. Transport and Dispersion of Dye	26
F. Water Quality Calibration	26
G. Verification	32
H. Response to Plant Shutdown	33
I. Status of the Model	34
J. Summary and Conclusions	34
VII. CONCLUSIONS	36

REFERENCES

LIST OF FIGURES

- Figure II-1. Location of the Stockton Outfall and Study Area
- Figure II-2. Monthly Average Flows in the San Joaquin River at Vernalis
- Figure II-3. Changes in San Joaquin River Flow with Distance Downstream

- Figure II-4. DWR Relationship Defining the San Joaquin - Old River Flow Split
- Figure II-5. River and Effluent Flow Rate from 7/90 to 12/91
- Figure II-6. Typical Cross-section of the Stockton Shipping Channel
- Figure II-7. Typical Cross-section of the San Joaquin River near the Stockton Outfall
- Figure IV-1. Location of Temporary Tide Gages
- Figure IV-2. Side View of Stockton Outfall
- Figure IV-3. Water Level During Near Field Sampling Periods
- Figure IV-4a-b. Near Field Sampling Locations
- Figure IV-5. Far Field Sampling Locations for Dye Study
- Figure IV-6. Fluorometer Calibrations for Rhodamine WT
- Figure IV-7. Stage Measurements at Paradise Point
- Figure IV-8. Stage Measurements at Light 16 in Deep Water Channel
- Figure IV-9. Stage Measurements at Turner Cut (Tiki Lagoon)
- Figure IV-10. Near Field Dye Distribution along Transect 177 Downstream of Outfall During Ebb Tide
- Figure IV-11. Plan View of Dye Distribution in River for Three Near Field Periods
- Figure IV-12. Far Field Dye Concentration Near Outfall
- Figure V-1a-b. Measured and Simulated Centerline Dilutions in Near Field
- Figure V-2. Effects of River Current on UDKHDEN Model Prediction of Minimum Dilution
- Figure V-3. Effects of Density Difference on UDKHDEN Model Prediction of Minimum Dilution
- Figure VI-1. Sampling Stations Along San Joaquin River near Stockton
- Figure VI-2. Link-Node Network of San Joaquin River near Stockton

- Figure VI-4a-b. Stockton Effluent Water Quality from 7/90 to 12/91
- Figure VI-5. Effect of Algae Concentration on Total BOD Measurement at Station R0A (7/90 to 7/91)
- Figure VI-6. Comparison of Observed and Simulated Tidal Depths near Station R5
- Figure VI-7. Comparison of Observed and Simulated Tidal Depths at Santa Fe Railroad
- Figure VI-8. Simulated Currents in the San Joaquin River
- Figure VI-9. Comparison of Observed and Simulated Dye Concentration Profiles in the Far Field
- Figure VI-10. Comparison of Observed and Simulated Far Field Dye Concentrations at Stations 3 and 8
- Figure VI-11. Measured Chlorophyll-a and Light Penetration at Stations R2 and R4 from 7/90 to 7/91
- Figure VI-12a-b. Comparison of Observed and Simulated Dissolved Oxygen Profiles from 7/90 to 7/91
- Figure VI-13a-c. Comparison of Observed and Simulated Dissolved Oxygen Concentration at Station R0A to R8 from 7/90 to 7/91
- Figure VI-14. Comparison of Observed and Simulated Cumulative Frequency of Dissolved Oxygen for Station R1 to R6 from 7/90 to 7/91
- Figure VI-15. Oxygen Budget at Stations R1 to R4 for Calibration Period (7/90 to 7/91)
- Figure VI-16. Effluent and River conditions During Verification Period (7/91 to 12/91)
- Figure VI-17a-b. Comparison of Observed and Simulated Dissolved Oxygen concentration at Stations R0A to R8 During Verification Period (7/91 to 12/91)
- Figure VI-18. Comparison of Observed and Simulated Dissolved Oxygen Profiles During Verification Period (7/91 to 12/91)
- Figure VI-19. Response of River Dissolved Oxygen to a Plant Shutdown During Winter Condition with Positive River Flow.
- Figure VI-20. Response of River Dissolved Oxygen to a Plant Shutdown During Summer Condition with Positive River Flow.

Figure VI-21. Response of River Dissolved Oxygen to a Plant Shutdown During Winter Condition with Reverse River Flow.

Figure VI-22. Response of River Dissolved Oxygen to a Plant Shutdown During Summer Condition with Reverse River Flow.

LIST OF TABLES

Table II-1. Summary of Corps of Engineers Data on San Joaquin River Tributaries.

Table II-2. Summary of Peak Flood Discharges in the San Joaquin River at Burns Cutoff.

Table II-3. Summary of 100-Year Peak Discharges in San Joaquin River Tributaries.

Table II-4. NPDES-Permitted Industrial discharges in the Stockton Area.

Table IV-1. Near Field Study Dosing Conditions, July 20, 1992.

Table IV-2. Time Lags of Tides at the Downstream boundaries from the DWR Gage Station at Venice Island.

Table V-1. Survey of Plume Models.

Table V-2. TDS, Temperature, and Density of Effluent and River Water in 1991.

Table V-3. Length Scales During the Tracer Study.

Table V-4. Modeled Centerline Dilutions from the Stockton Outfall.

Table V-6. Initial Dilutions of the Stockton Outfall Under Different Discharge Rates*

Table VI-1. Ammonia Nitrogen at Vernalis.

Table VI-2. River Flow Rates During Dye Study.

Table VI-3. Rate Coefficients.

Table VI-4. Temperature Coefficient Used in the Model.

Table VI-5. Estimated Productivity Rates of Algae in the San Joaquin River Near Stockton.

Table VI-6. Conditions During Winter and Summer Scenarios.

LIST OF APPENDICES

- Appendix A: Dye Concentration Profiles Across River Transects in the Near Field
- Appendix B: Observed and Simulated Time Concentrations of Dye at the Far Field Stations
- Appendix C: Observed and Simulated Dye Concentration Profiles in the Far Field
- Appendix D: Method for Estimating San Joaquin River Flows at Stockton for Times with No Rock Barriers at Old River
- Appendix E: Simulated and Observed Concentration Profiles and Time Concentrations of Total Dissolved solid From July 1990 to July 1991
- Appendix F: Simulated and Observed concentration Profiles and Time Concentrations of Carbonaceous BOD From July 1990 to July 1991
- Appendix G: Simulated and Observed Concentration Profiles and Time Concentrations of Ammonia Nitrogen From July 1990 to July 1991
- Appendix H: Simulated and Observed concentration Profiles and Time Concentrations of Nitrate Nitrogen From July 1990 to July 1991
- Appendix I: Simulated and Observed Concentration Profiles and Time Concentrations of Dissolved Oxygen From July 1990 to July 1991

I. INTRODUCTION

The City of Stockton, which discharges about 40 million gallons per day (MGD) of tertiary-treated municipal wastewater to the San Joaquin River, is required under the Clean Water Act to obtain an National Pollutant Discharge Elimination System (NPDES) permit from the Regional Water Quality Control Board. This permit specifies discharge limits for various pollutants, and mandates that the City monitor water quality of the effluent and receiving water.

(22 on average)
(misread Table V-6)

The purpose of NPDES discharge limits is to protect the water quality of the receiving water. The limits are derived to protect identified beneficial uses of the river; including recreation, water supply, fisheries, and wildlife. Important factors that determine discharge limits are the mixing characteristics of the receiving water, the chemical and biological reactions that transform pollutants as they are transported in the river, and the requirements/sensitivity of the aquatic ecosystem.

Water quality in the San Joaquin River system is determined by a complex set of interacting factors, including Delta water withdrawals, tidal influences, upstream inflows, urban runoff, as well as municipal, agricultural, and industrial discharges. Because of the complexity of the system, it is important that discharge limits be derived as scientifically as possible. They should account for the interaction between river flow and water quality, under a variety of seasonal and water withdrawal scenarios. The limits should also reflect the contributions of all the various pollutant sources, and the transport mechanisms within the receiving water. The best method for achieving an understanding of such a complex system is through a coordinated modeling and data collection effort. The model provides a theoretical framework for projecting water quality under a variety of conditions. The field data collection program provides data for model development and calibration.

This report describes the development and calibration of a computerized water quality model of the lower San Joaquin River system. This model simulates the transport of pollutants from the Stockton wastewater treatment outfall; based on upstream inflows, Delta water withdrawals, tides, and pollutant loading rates. The model includes a near-field component that simulates mixing and dilution in the immediate vicinity of the outfall, and a far-field component that simulates mass transport of pollutants through the river and Stockton shipping channel. The model has been calibrated against dye mixing data collected as part of this study, and water quality data collected by the City of Stockton for their discharge permit. This initial phase of the model focuses on critical water quality conditions during the dry season; later phases will also include a stormwater pollutant loading component.

Section II of the report describes the environmental setting, including operation of the treatment plant, hydrology of the river system, and pollutant sources. Section III focuses on the existing water quality data for the system, and Section IV details the results of the field dye-mixing study. Near- and far-field model calibration are described in Sections V and VI. Section VII provides

our conclusions on the key water quality issues, based on the results of selected model simulations. A user's manual for the model is provided in a separate report.

II. ENVIRONMENTAL SETTING AND BACKGROUND

A. OPERATION OF THE STOCKTON WASTEWATER TREATMENT PLANT

The City of Stockton treats its municipal wastewater at a treatment plant located adjacent to the San Joaquin River upstream of the Stockton Deep Water Channel. Figure II-1 is a location map of the treatment plant and San Joaquin River system. The plant provides tertiary treatment of wastewater through a series of flotation tanks, re-aeration facilities, and dual-media filters before being chlorinated and discharged to the San Joaquin River. The plant includes a large algae pond which serves as a tertiary polishing pond, and provides storage during weekends and other off-line periods. The facility has a capacity of 86 MGD, and typically operates at about 40 MGD. *average 15-20 MGD*

Treated effluent is discharged through one of two 4-foot outfall pipes on the west bank of the San Joaquin River. The outfall extends about 50 feet offshore at high tide, and discharges perpendicular to the San Joaquin River flow at a depth of 5 to 10 feet. The plume from the outfall is slightly buoyant, and travels in the downriver direction during winter and ebb tide periods. During summer flow reversals and flood tides, the plume is carried upriver. *15'*

(frequently negatively buoyant although sometimes positive)

B. HYDROLOGY OF THE SAN JOAQUIN RIVER/DELTA SYSTEM

1. Upstream Inflows

The San Joaquin River originates in the southern Sierra Mountains, and drains a total area of 14,685 square miles at Stockton. Major tributaries include the Merced, Tuolumne, Stanislaus, and Mokelumne rivers. Sources of water include snowmelt, stormwater runoff, irrigation drainage, and wastewater discharges. The river eventually enters the Central Valley Delta and San Francisco Bay through the Stockton Deep Water Channel, a shipping channel maintained by the U.S. Army Corps of Engineers.

Flow in the river is monitored by the U.S. Geological Survey (USGS) at five locations upstream of the study reach, with the nearest gage at Vernalis (representing a drainage area of 13,536 square miles). The mean annual flow at Vernalis is 4,540 cubic feet per second (cfs). The annual hydrograph for the river at Vernalis is typical of snowmelt-dominated systems, with the highest monthly flows in the spring (Figure II-2). Mean monthly flows range from 1,321 cfs in August to 7,759 cfs in May. Figure II-3 shows the effects of agricultural withdrawals on flows at different locations along the River. During the winter when withdrawals are minimal, flows increase with distance downstream. In the summer, flows decrease by about 400 cfs between Friant and Newman.

Major tributaries flowing into the San Joaquin River near Stockton include French Camp Slough, Duck Creek, Littlejohn Creek, Walker Slough, Mormon Slough, the Calaveras River, 14-mile

Slough, and Mosher Slough. As summarized in Table II-1, there is limited flow data on these tributaries, with the exception of data collected on selected streams by the U.S. Army Corps of Engineers. Tributaries are tidally-influenced near the mouth, and observed daily average flows range from 8,500 cfs during storms to 0.0 cfs during dry periods. Littlejohn Creek, Bear Creek, and the Calaveras River are regulated upstream by reservoirs, and have extensive agricultural diversions downstream of the reservoirs. All of these streams have been channelized and altered for flood control and drainage purposes.

2. Effects of Delta Water Operations

Flow in the San Joaquin River is strongly influenced by the pumped export of water at two locations in the Delta. The Clifton Court Forebay facility, located northwest of Tracy, pumps an average of 3,400 cfs of Delta water into the California Aqueduct, and is operated by the State of California. The Tracy pumping station is operated by the U.S. Bureau of Reclamation and exports about 4,600 cfs of water to the South via the Delta Mendota Canal. Total exports from these two sources can be greater than 10,000 cfs.

The net effect of these exports is to draw water from the San Joaquin River into the Old River. These withdrawals frequently cause flow reversals in which all of the San Joaquin River water is drawn southward into the Old River. To minimize the effects of these withdrawals on water quality and fish, the California Department of Water Resources (DWR) has periodically installed flow barriers in various Delta channels. These barriers are constructed of loose rock and are fitted with 48 inch gated culverts and a weir overflow spillway. During the study period, rock barriers were installed in the Old River at its confluence with the San Joaquin River, and in the Middle River at the Victoria Canal confluence. With barriers in place, 30 percent or more of the San Joaquin River water flows past the Old River confluence (Harte et al., 1986).

The primary reach of concern in this study is the San Joaquin River extending from Brandt's Bridge through the Stockton Deep Water Channel to Venice Island in the Delta. While there is no flow gage in this portion of the river, DWR has developed empirical relationships that calculate flow past the Stockton wastewater treatment plant based on the flow at Vernalis, estimated channel depletions, and withdrawals at Tracy and Clifton Court. Most of these are based on the relationship shown in Figure II-4 from DWR Bulletin No. 76 (1962). This graph was developed from flow data obtained during tidal cycle measurements in the southern Delta, and relates the river flow at Brandt's Bridge to the ratio of exports to the river flow at Mossdale. These flow relationships are highly empirical, are based on data that are over 30 years old, and rely heavily on reported export and diversion rates. Thus, the estimated flow in the study reach of the river is highly uncertain. To improve the accuracy of flow estimates, the City of Stockton is currently constructing a flow gage in the river near the wastewater treatment plant outfall.

Figure II-5 shows flows past the Stockton outfall for July 1990 through December 1991, based on the DWR relationships. Rock barriers were in place from mid-September through late November of each year. Without barriers, net upstream flows occur frequently. Consistent

downstream flows occur only during the spring snowmelt period and when rock barriers are in place. Figure II-5 also shows that during flow reversal periods the Stockton wastewater discharge is the largest contributor of freshwater to the lower San Joaquin River.

3. Tides and Bathymetry

This reach of the river is also subject to tidal influence. At the tide gage at Rough and Ready Island, the mean diurnal tidal cycle ranges from a mean lower low water (MLLW) of -0.15 feet NGVD to a mean higher high water (MHHW) of +3.35 feet NGVD (H.T. Harvey and Associates, 1991).

Bathymetric data for the area are available from a variety of sources. The Army Corps of Engineers recently surveyed the entire length of the Stockton ship channel (1988), and has previously performed soundings of the river between Vernalis and Stockton for the local FEMA flood insurance studies. This reach of the river was also surveyed for the Weston Ranch flood study (Gill and Pulver Engineers, Inc., 1987). To supplement the available data, PWA and Kjeldsen-Sinnock and Associates, Inc. surveyed over 20 cross-sections near the treatment plant and in various delta sloughs and tributaries.

Typical river cross-sections in the shipping channel and in the river near the treatment plant are shown in Figures II-6 and II-7. The deep water channel is dredged for ship traffic, and has a wide regular cross-section. The remainder of the river in the study area has also been channelized, and is flanked by steep levees armored with rip-rap. Because of the steep banks and poor soil conditions, riparian vegetation occurs only in backwater bends and remnant floodplain areas in front of the levees.

4. Flood Discharges

The San Joaquin River is leveed on both sides throughout the study reach. Nonetheless, flooding occurs in locations where there is inadequate levee freeboard and structural instability. Table II-2 summarizes the 10-, 50-, 100-, and 500-year discharges used in the San Joaquin County flood insurance study (Federal Emergency Management Agency, 1989). Table II-3 summarizes estimated 100-year discharges in the major tributaries to the study reach.

C. MAJOR DISCHARGERS AND POLLUTANT SOURCES

Municipal dischargers include the Cities of Stockton, Modesto, Turlock, and Newman. The Stockton and Modesto wastewater treatment plants are by far the largest point dischargers to the River, with mean daily flow rates of about 40 and 23 MGD, respectively. All of these plants discharge tertiary-treated wastewater. These types of discharges contribute nitrates, ammonia, phosphates, and biochemical oxygen demand (BOD) loads to the river system, resulting in

increased oxygen demand. Municipal wastewater may also contain trace amounts of metals and toxic organics.

Table II-4 summarizes the NPDES-permitted industrial facilities that discharge directly into the San Joaquin River system in the Stockton area. As of 1987, there were no industrial dischargers upstream of Vernalis (State Water Resources Control Board, 1987). The primary constituents of concern from these facilities include Chemical Oxygen Demand (COD), various metals, temperature, and chlorine residual. The flow rates from these permitted facilities are fairly low in comparison to other sources, and probably do not cause large-scale water quality problems. However, they may result in localized degradation of water quality.

Nonpoint source discharges to the River include agricultural drainage and urban runoff. Agricultural input to the system occurs primarily upstream of Vernalis, and may derive from both subsurface tile drainage and surface drainage (irrigation return water and spills). Agricultural drainage contributes nutrient, sediment, and pesticide loadings, and are generally thought to be the major sources of selenium in the river. In their mass balance model of the upper river, the State Water Resources Control Board (1987) estimates an average annual input of 7,806 acre-ft per year from subsurface drainage, and about 230,000 to 290,000 acre-ft per year from surface drainage.

Urban runoff is generated primarily during storm events, when pollutants are washed off of impervious surfaces into the storm drainage system. Urban runoff may contain metals, oil and grease, sediment, nutrients, and trace amounts of various toxic organics. These discharges occur primarily in the winter, when freshwater flows in the river are high. The City of Stockton currently discharges its stormwater through over 60 pump-station outfalls.

- ✓ Dredging activities in the ship channel and river have also been identified as a source of water quality problems. In the short term, dredging resuspends solids and pollutants into the water column. In the long term, channel deepening decreases dissolved oxygen by reducing velocities and re-aeration of the water column, and increasing oxygen uptake by phytoplankton (Resource Management Associates, 1985). The U.S. Army Corps of Engineers has performed a number of studies of the impacts of ship channel dredging on dissolved oxygen in the river system.)

D. PREVIOUS STUDIES AND MODELING EFFORTS

A number of other modeling studies have been conducted in the area to evaluate water quantity and quality. To simulate the impacts of water withdrawals on the Delta, DWR and other investigators have applied the link-node model developed by Fischer. The domain of this model generally extends upstream to Vernalis, and covers most of the Sacramento-San Joaquin Delta. The model uses monthly average flow data, and has been applied to simulate salinity intrusion and water circulation through the system. The Contra Costa Water District maintains a version of the model to evaluate the potential for salinity intrusion into the Delta near their water supply intakes (Contra Costa Water District, 1991).

Harte et al. (1986) developed the Delta Net-Flow Accounting Model (DNFAM) to assess water quality in the delta. This model simulates the transport of conservative substances on a monthly time step, and is based on a simplified water balance approach. Because the model uses monthly average DWR DAYFLOW data to simulate flows, it is not capable of simulating the effects of daily flow variations or tides.

The State Water Resources Control Board has developed a mass-balance water quantity and water quality model of the San Joaquin River upstream of Vernalis (State Water Resources Control Board, 1987). This model, referred to as the San Joaquin River Input-Output Model (SJRIO), focuses on the impacts of agricultural drainages on salinity, selenium, and boron loadings to the river. The Environmental Defense Fund is currently applying and refining this model in their efforts to further characterize the selenium problem.

Hydroscience (1976) assessed the impacts of pollutant loads from municipal and agricultural sources on the San Joaquin River. A preliminary model was used to assess the projected loadings of chlorophyll, Nitrates, Phosphates, biological oxygen demand, and dissolved oxygen to the river. Resources Management Associates (1985) applied the link-node model to evaluate the impacts of deepening the Stockton Ship Channel on dissolved oxygen.

A number of hydraulic models have been developed to assess flooding in the river. The Corps of Engineers has developed a HEC-2 backwater model of the San Joaquin River from the ship channel to Vernalis for the local FEMA flood insurance studies. This model was later refined and applied to evaluate the Weston Ranch development (Gill and Pulver Engineers, 1987).

III. WATER QUALITY DATA

A. INTRODUCTION

This chapter describes the historic water quality data that have been compiled and used to support the modeling study. Actual analyses of the data will be made in conjunction with the modeling sections of this report.

B. EFFLUENT CHARACTERISTICS

The laboratory of the Stockton Wastewater Control Facility measured and recorded the effluent characteristics as a part of their discharge permit issued by the State Regional Water Quality Control Board. The parameters include:

- Flow
- 5-day BOD
- Total Suspended Solids (TSS)
- Settleable Solids
- Total Solids
- Total Dissolved Solids (TDS)
- Specific Conductivity
- pH
- Bioassay, % survival
- Total Coliform
- Fecal Coliform
- Chlorine Residual
- Oil and Grease
- Temperature
- Total Organic Carbon
- Total Phosphorus
- Orthophosphate
- Nitrogen Series (NH₃, Kjeldahl, NO₃, NO₂, and Total)
- Chemical Oxygen Demand
- Turbidity
- Volatile Suspended Solids
- Chlorophyll-a
- Alkalinity
- Dissolved Oxygen

The majority of these parameters are measured daily. The bioassay and oil and grease measurements are performed on an infrequent basis.

The City has furnished a diskette that contains the effluent data from 1988 to 1991. The data were used to prepare the input for the model calibrations and verifications. The data were also used in the statistical characterization of effluent discharge for the sensitivity analysis with the model.

C. RECEIVING WATER MONITORING

As a part of the NPDES, the City also performs daily monitoring of the receiving water quality. The parameters include:

- Dissolved Oxygen
- Temperature
- pH
- Turbidity
- TDS
- Specific Conductivity
- NH3-N
- NO3-N
- NO2-N
- Kjeldahl Nitrogen
- Total Nitrogen
- Light Penetration

The monitoring program takes samples from 8 stations in the river extending from Bowman Road (referred to as R1) , upstream of the outfall, to Light 18 (referred to as R8) in the Stockton Ship Channel.

A special field program was carried out from July 1990 to July 1991. During this period, two stations were added further upstream of Bowman Road. One was at the confluence of San Joaquin River and Old River. This station was referred to as R0A. The other station was R0B, situated between stations R0A and R1. During this period, the following water quality parameters were added:

- Total Soluble Inorganic Nitrogen
- Dissolved Ortho-Phosphate
- 5-day BOD
- Total Suspended Solids
- Chlorophyll-a
- Screening Bioassay

The data for the special field program were more complete, and were used to calibrate the far field model in this study.

In addition to the City's monitoring program, the US Geological Survey (USGS) maintains a station in the San Joaquin River at Vernalis. This station is used by DWR to monitor the water quality of the San Joaquin River before entering the delta system. Some 52 water quality parameters including 20 trace metals were monitored on a bi-monthly basis. The California Department of Water Resources (DWR) has measured dissolved oxygen in Stockton Ship Channel extensively as a part of the Interagency Ecological Monitoring Program of the Delta.

IV. DYE MIXING STUDY

A. INTRODUCTION

An intensive field program was carried out between July 18 and August 1, 1992 to collect data for model calibration. The plan was to obtain a data set for which the boundary conditions and waste discharge were known and well defined. A tracer was introduced through the outfall. The distribution of the tracer in the receiving water was measured in the near-field and far-field for each tide over a one week period.

B. FIELD STUDY

The field study was conducted in two phases: near field and far field. The near field study characterized the initial dilution of the plume in the region near the outfall where discharge momentum and buoyancy are important. The focus of the far field study was on the large scale transport and dispersion of pollutants by oscillating river currents. Throughout the field study, we also measured tides, velocities, and river bathymetry to characterize the physical geometry of the receiving water system.

1. Tidal Measurements

The downstream end of the San Joaquin River meets the Sacramento River before entering Suisun Bay and San Francisco Bay. The San Joaquin River near Stockton is subject to tidal influence from tides propagated from Golden Gate through Suisun Bay.

To quantify the tidal boundary conditions at the downstream end of the model domain, three temporary gages were installed at (1) Paradise Point at Turner Cut, (2) Light 16 in the Deep Water Channel, and (3) Tiki Lagoon at Bishop Cut and Disappointment Slough. To obtain data for comparison against model results, a fourth gage was installed at the Santa Fe Railroad Bridge which is just upstream of the outfall. In addition, stage measurements at the confluence of the Calaveras River and the Deep Water Channel were available from the Corps of Engineers.

Figure IV-1 shows the locations of temporary tidal gages. These gages were deployed from July 18 to August 1, 1992. They recorded tidal heights continuously at 6 minute intervals.

2. Stockton Outfall

The Water Pollution Control Plant of Stockton has a large algae pond which serves as a tertiary polishing unit. The pond also serves as a storage facility that can hold water over weekends or other extended periods. The treated waste water travels along a chlorine contact canal, over a

weir crest, into a siphon box under highly turbulent conditions, and is then siphoned over a levee to the San Joaquin River.

The outfall comprises two parallel pipes 4 feet in diameter. The pipes extend about 14 feet from the shoreline (at MLLW) of the west bank. There is no diffuser at the end of the pipes. The treated waste water is simply discharged perpendicular to the river flow. Only one outfall is used at a time. The centerline of the pipe is about 7 feet below mean lower low water. The average river depth from 0 NGVD is 11 feet and has a maximum depth of 18 feet towards the east side of the river. Figure IV-2 shows a cross-section of the outfall.

The treatment plant discharge rate was maintained at about 34 MGD during the field study. The outlet velocity was 4 ft/sec. Because of the relatively shallow discharge, the jet was observed to surface about 20 to 40 feet away from the outfall when the water surface was below mean tide level. Turbulent boils in a circular area about 6 feet in diameter was visible at the surfacing point.

3. Near Field Study

Dilution measurements for the near-field study were conducted for three tidal conditions: (1) ebb tide, (2) low tide, and (3) flood tide. Each period lasted about an hour.

The plan was to release the tracer at the ebb tide first. The dye would be carried downstream with the current by the time of low tide. This would prevent the released tracer during the ebb tide from interfering with the study for low tide. Several hours after the low tide, the study for flood tide would begin. By this time, the dye released during the ebb tide would still be downstream of the outfall while the dye released during low tide would be upstream.

The dye, Rhodamine WT, was injected at the weir crest. It was observed to mix rapidly in the siphon box before being siphoned to the river.

A peristaltic pump was used to pump the tracer solution at a steady rate of about 35 ml/min. The dosing continued for one hour for each tidal condition. The dosing stopped for approximately two hours between tides. The dosing concentration was increased progressively from one tidal condition to the next. This was done to minimize possible interference of dye introduced earlier. Background samples were taken before each period to detect any carry over of dye from previous injections.

Figure IV-3 shows the dosing periods with respect to the tide and Table IV-1 presents the dosing conditions for the near-field study.

To measure tracer concentrations in the receiving water, samples were taken by a boat. A 10-foot weighted cable was suspended from the side of the boat. Three submersible pumps were

attached to the cable at 2-, 7-, and 10-foot depths. The water was pumped up to the surface via plastic tubings. Twelve-ounce bottles were used to collect water samples on board.

The procedure of sampling was as follows. The boat traveled along a predetermined transect. Every minute and half, the boat stopped for sampling. The plastic tubings were flushed for 10 to 15 seconds before collecting samples. Bottles for three depths were filled quickly in 10 to 15 seconds. Once a set of samples was collected at a location, a surveyor determined the position of the boat using a range finder.

River currents caused the boat to drift off station while sampling. Over the course of collecting one set of samples, the boat might have drifted as much as 20 feet. The drift also made it difficult to accurately measure the current velocities with a current meter mounted on the boat. As a result, we relied on drogues to measure the flow velocity.

Two drogues, one suspended at 3 feet and the other at 6 feet, were used to measure the current velocity. The current velocity was 0.4 feet per second at low-slack-water. At ebb tide, the current speed was 0.7 feet per second. For flood tide, the current speed was 0.8 feet per second.

Figure IV-4 shows the sampling locations for the near-field study. The boat traced over four to six river transects for each study period. Sample points do not fall exactly on each transect because of boat drift.

All told, samples were collected at about 35 locations in each study period. Approximately 105 samples were collected per period.

4. Far Field Study

In the far field study, a slug of tracer, 5.49 kilograms of Rhodamine WT was released into the effluent at 21:00 on July 20, 1992. Water samples were collected at 12 monitoring stations along the San Joaquin River (see Figure IV-5). Samples were taken for each low and high tide of the next four days.

At each station, samples were taken at three locations across the river: center, left, and right. Two boats were deployed in order to collect the samples over a short time span (typically about 40 minutes). The samples were stored in 12 ounce plastic bottles and promptly delivered to the laboratory for analysis.

5. Laboratory Procedures

A field laboratory was set up at the chemical laboratory of Stockton Water Pollution Control Plant. The laboratory provided a bench for our Turner Fluorometer, working space, and bottle

washer. The laboratory was opened for our use around the clock which permitted us to perform a very large number of measurements during the field study.

Dye concentration is determined by calibrating the instrument to standards. The standards were prepared using river water in order to eliminate any background effects. The calibration curves for the four instrument scales (30X, 10X, 3X, and 1X) and the regression equations are shown in Figure IV-6. At the most sensitive scale (30X), the instrument can accurately detect concentrations as low as 0.1 ug/L.

Before using the calibration curves, all fluorescence readings are corrected to the same temperature by the equation

$$F_o = F \exp(n(T-T_o))$$

where F is the fluorescence reading at sample temperature T in degrees Celsius, F_o is the fluorescence at a standard temperature T_o, and n is a constant equal to 0.027 (Smart, 1979).

The instrument was zeroed with distilled water each time the scale was changed to prevent instrument drifting. Duplicate readings were made for approximately 25 percent of the samples. In order to prevent any bias, the sample bottles were randomly shuffled before analyzing.

C. RESULTS

1. Tides at the Boundaries

The purposes of the tidal measurements were to provide 1) the downstream boundary conditions for the period of dye studies; 2) the tidal data at the railroad bridge for checking against the model results; and 3) time lag and elevation adjustment factors for the boundary tides. The time lag and elevation adjustment factors can then be used to derive the boundary tides for other periods based on tides at the Venice Island gaging station maintained by California Department of Water Resources.

Figures IV-7, 8, and 9 show the measured tides at Paradise Point, Light 16, and Tiki Lagoon for July 18 through August 4, 1992. Comparing these data to concurrent data from Venice Island show similar tidal patterns and tidal ranges (2.5 to 4 feet). There are also time lags of 1.43 to 19.31 minutes from the tides measured at Venice Island. This is reasonable because the waters at those stations are interconnected by channels.

However, the absolute tidal elevations measured from National Geodetic Vertical Datum (NGVD) exhibit unreasonable differences. After researching this problem, we concluded that the benchmarks used to survey in the temporary tide gages have shifted and are no longer accurate.

Because all of the gages had similar tidal ranges, we assumed that the observed height differences were due primarily to errors of the survey benchmarks. Therefore, no height adjustment factors are required to calculate the boundary tides from the tides at Venice Island. However, there are time lags for high and low tides as shown in Table IV-2. These assumed tidal corrections resulted in reasonable circulation and tidal height predictions from the link-node hydrodynamic model.

2. Near Field Dispersion

Figure IV-10 shows an example of the concentration profile on an average transect during ebb tide. The concentration distribution across the river follows a bell-shaped gaussian curve.

The complete set of similar plots can be found in Appendix A. Background samples were taken before each study period. They all had zero dye concentration indicating that the dye introduced in the earlier periods did not interfere with those introduced in the latter periods.

No clear pattern could be detected in the vertical concentration. It appears the plume was vertically well-mixed for the most part. Some of the vertical deviations may be attributed to the drifting of the boat.

Figure IV-11 shows the top view of the plume-jet. The maximum concentration is located at the center of the plume. As expected, the maximum concentration decreases and the plume-jet broadens with increasing distance downstream of the outfall.

3. Far Field Dispersion

Figure IV-12 shows the dye concentration measured at station 5 near the outfall. The figure compares the measurements made on the left bank, the middle of the river, and the right bank. The first measurement was taken during a low tide, 8 hours after the slug was released. At this time, concentrations varied across the river, suggesting that the dye was not completely mixed across the river. After 16 hours, the dye appeared to be well mixed across the river. Based on these observations, it was concluded that the procedure of taking samples from three points (left, middle, and right) in a river cross-section was adequate to characterize the far field dispersion of the tracer.

The changes in concentration with time at the various sampling locations are given in Appendix B. The concentration distribution throughout the river for each sampling trip are provided in Appendix C. The results will be discussed in further detail in conjunction with the modeling efforts.

V. NEAR FIELD MODELING

A. INTRODUCTION

When the wastewater is discharged from the outfall, dilution and mixing are induced by the momentum and buoyancy of the jet. The initial jet rises and spreads radially until it reaches surface and bottom boundaries and loses momentum. The region where this occurs, described as the "near field", defines the initial dilution of the discharge. Beyond the near field, the jet continues to spread laterally across the channel. Eventually, the waste discharge becomes well-mixed with the river flow

To characterize near field dilution, we applied several standard EPA plume models. These models were calibrated against the data collected in the near field dye study discussed in Chapter IV of this report.

B. EXISTING MODELS

Most of the existing outfall models were originally designed for deep ocean discharges. In these models, it is assumed that the receiving water has an infinite depth and width relative to the outfall dimension. The plume jet can expand indefinitely until it loses all its momentum and/or its density reaches neutral buoyancy with respect to the ambient water. Often, this terminal point of neutral buoyancy is below the water surface. The water available for dilution is therefore infinite. All entrained waters are "uncontaminated" under the assumption of uni-directional flow in the ambient.

For Stockton discharge, the outfall diameter (4 feet) is on the same order of magnitude as the river depth (12 feet). The plume-jet probably touches both the water surface and the river bottom during the first stage of jet mixing. After that, additional dilution is not acquired from the rising or sinking plume. Rather, it is attained from lateral mixing across the river from the west bank to the east bank. The flow is bi-directional, meaning the ambient water may recirculate the waste water of previous discharges.

From a strictly theoretical standpoint, none of the existing plume models would be applicable. A number of models and analytical equations were reviewed to determine their strengths, weakness, and potential applicability to the Stockton discharge. Results are summarized in Table V-1.

The anticipated overprediction of dilution was based on the knowledge that the plume model would continue to assume increasing dilution before the centerline reached the surface. For the Stockton outfall, the additional dilution was curtailed when the edges of the plume became bounded by the surface and the bottom of the river. The dilution predicted by the plume model

included entrainment across all sides of the plume and was larger than that from mixing laterally across the river.

Based on the review and testing of all models, it appears that UDKHDEN is the most suitable for the application. UDKHDEN is a fully three-dimensional model based on the developments of Hirst, Davis, and Kannberg (EPA 1985). It is one of the six plume models available from EPA. The model considers the development of the plume through the zone of flow establishment. The model outputs such parameters as plume trajectory, travel time, plume width, average dilution, and minimum dilution. It provides intermediate results instead of providing answers only for the terminal point, as most other EPA plume models do. We need all those intermediate results to make a judgement on when and where the assumptions of the model are still valid.

UDKHDEN, like other plume models, can only handle steady-state conditions, in which the effluent and receiving water are maintained constant. In the Stockton case, the currents change dynamically with the tide. We therefore applied the model for multiple segments of the time. We assumed that the discharge and receiving water conditions were approximately constant over the short intervals. This is a good assumption, because the plume jet reaches its equilibrium point very quickly. When the calculations are provided for a sufficient number of time segments, the results can be reconstructed to provide a dynamic picture of the real situation.

C. DATA AND RESULTS

1. Current Velocity

In the summer, the ambient current velocity in the receiving water near the Stockton outfall is tidally driven. During the dye study, currents fluctuated between +1 to -1 foot per second, based on the hydrodynamic simulation of San Joaquin River using the far-field link-node model. These results were confirmed in part by the drogue measurement carried out during the tracer study. The drogue measurements, which were not performed during the peak velocity, gave velocities of 0.7 to 0.8 foot per second.

2. Density of Plume

To determine if the Stockton outfall issued a rising or sinking plume, we calculated the density of effluent and river water. During the dye study, the effluent was heavier than the river water by about 0.08 kg/m³. The discharge would therefore not rise buoyantly, and mixing would be momentum-dominated.

Table V-2 presents the TDS and temperature of effluent and river water for 1991. The density differences are also presented in the table and show that the effluent is usually heavier than the river water.

3. Discharge Rates

In 1991, the discharge rates had the following statistics:

Average flow:	42.2 MGD
Standard deviation:	11.7 MGD
Minimum:	9.9 MGD
Maximum:	74.0 MGD

4. Length Scale Analysis

Wright (1977) compared the length scales of jet and length scale of plume to determine the relative importance of momentum and density difference. He used the following terms:

- Q = discharge rate, (L³/T)
- V = jet velocity, (L/T)
- M = momentum flux = VQ, (L⁴/T²)
- B = buoyancy flux = G(Δρ/ρ) Q, (L⁴/T³)
- U_a = ambient current, (L/T)

and

- L_m = length scale of jet in a crossflow = M^{0.5}/U_a
- L_b = length scale of plume in a crossflow = B/U_a³

The calculated length scales L_m and L_b for the study period are shown in Table V-3.

The L_m to L_b ratios are much greater than one. This means that buoyancy effects on mixing are relatively unimportant. The momentum mixing is much more important in the near field.

According to Wright (1977), the momentum dominated near field will occur at a trajectory distance less than the scale length of L_m. In this zone, the dilution is not influenced significantly by the ambient current. At a trajectory distance larger than the length scale of L_m, the intermediate mixing zone will develop. In this zone, the dilution will be influenced by the residual momentum and the ambient current.

5. Definition of Initial Dilution

The initial dilution is defined as the "dilution achieved in a plume due to the combined effects of momentum and buoyancy of the fluid discharged from an orifice." (EPA 1985). For ocean discharges, the plume has two sections in the zone of initial dilution. The first section is where momentum mixing dominates. The second section is where the buoyancy jet of rising (or sinking) plume dominates. The important point is that the initial dilution, according to the definition, includes both the entrainment mixings of initial momentum and subsequent buoyancy.

For the Stockton case, the density of the treated water is very close to that of the San Joaquin river water. As shown in Table V-2, the plume was sinking more often than rising. During the dye study, the plume was sinking. The boils that we saw near the outfall pipe were caused by the momentum of the jet, rather than the rising plume.

After the initial mixing of momentum jet, the plume is confined by both the water surface and the river bottom. However, the plume can continue to expand laterally across the river for additional dilution. The initial dilution for the Stockton outfall should be defined at the point beyond where the major momentum of the jet gets dissipated. Where that point is can be determined semi-empirically. It requires model calculations in comparison to the data from the tracer study.

6. Model vs Tracer Data

We used the UDKHDEN model to track the first few minutes of the momentum jet. Figure V-1 shows the comparison between the model calculations and the measured dilutions for ebb, low, and flood tides.

The circles are the measured centerline dilutions. They are plotted as a function of distance downstream from the outfall. The solid lines are the model results for the centerline dilution for 120 seconds after the discharge. The simulated lines and measured dilutions are not strictly comparable, because the flow of the San Joaquin River changes speed and direction with tides continuously. The model simulation on the other hand assumes for a constant velocity for the simulated period. However, the error introduced by this simplified assumption is believed to be small.

For the condition of flood tide, the model appears to underpredict the measured dilution. This can result from the experimental error in which lesser amount of tracer was actually introduced due to the disengagement of dosing tube. However, as indicated in the last chapter, the field program appeared to have recovered majority of the presumed dose of tracer. With these conflicting indirect evidences and the direct evidence of seeing the disruption of dosing tube, we believe that the simulated dilution of 10 is more correct than the observed dilution of 13.

The current changes speed and direction with tide continuously as does the shape of the plume. Thus, it is more convenient to define the point of initial dilution by the time of mixing after the discharge, rather than using distance from outfall as the yardstick of mixing.

Table V-4 presents the centerline dilutions calculated for 60 and 120 seconds after the discharge. Table V-5 presents the measured centerline dilutions. From the comparison of the data presented in Tables V-4 and V-5 and the observation of quick boil near the outfall pipe, we estimate that the initial momentum mixing at the Stockton outfall occurs in 60 seconds after discharge. At that point, the dilution was approximately 7. The jet at that point still contains considerable energy. It spends another 60 seconds mixing laterally across the river to acquire another 3 units of dilution. The dilution at the end of 120 seconds after discharge is approximately 10. After that, the additional lateral mixing becomes dominated by the ambient current.

The approximate location where the initial dilution occurs depends on tidal conditions. Based on calculations shown in Table V-4, it occurs within approximately 1100 feet of the outfall.

7. Sensitivity Analyses

The initial dilutions are a function of discharge rates as shown in Table V-6. In this table, the average discharge is the average of 1991 flows during the times of discharge (i.e. the zero discharges on the weekends are not included). The low and high flows are the flows at one standard deviation from the average.

The results indicate that the initial dilution is higher for higher discharge rate. Higher discharge rates produce higher momentum which causes more mixing with the river water. This is not to say that higher discharge will result in better water quality, since this will also increase mass loadings of pollutants to the river system.

Figure V-2 presents the sensitivity of centerline dilution with respect to the current speed of the receiving water. The important conclusion to draw is that the centerline dilution does not significantly change for large differences in current speed. It is more sensitive to discharge rates. In the other words, the major driving force for the initial dilution is the jet momentum rather than the current velocity.

Figure V-3 compares the centerline dilutions calculated for two density differences between the waste effluent and the river water. The ambient current velocity used in this analysis was 0.9 feet per second. The small differences in the calculated initial dilution confirm the conclusion that buoyancy induced mixing is not important for the Stockton outfall.

8. Maximum Dilution

Based on the field data and the modeling results, it is clear that the Stockton outfall only disperses its effluent to the western half of the San Joaquin river. What is the maximum dilution when the effluent is mixed completely with the water passing by the outfall? By using the maximum current velocity of 1 foot per second and a cross-sectional area of 3,000 square feet, the maximum dilution is approximately 56.

However, there is a real question if the water quality will improve by having a better initial mixing. Because the tide moves the water back and forth, the dilution water cannot be all fresh. Much of the discharged water will be recirculated back and forth several times. Unless the waste effluent is very toxic which requires a large dilution to lower its concentration to a safe level, there is no advantage to a higher initial dilution than what it has now.

D. SUMMARY AND CONCLUSION

Analyses were made with the data observed in the tracer study and the model simulations based on the EPA three-dimensional UDKHDEN plume model. Based on the analyses presented, it is concluded:

1. The Stockton outfall provides a strong momentum jet which causes a rapid mixing. The momentum mixing causes the plume to touch the water surface and the river bottom in 60 seconds after the discharge. However, the momentum jet does not cause the lateral mixing across the river from the west bank of the discharge to the east bank. The jet spends another 60 seconds entraining water laterally across the river section.
2. The majority of EPA plume models were designed for deep ocean discharges of infinite depth and width under a stratified environment. They are suitable for calculating dilution acquired through momentum mixing and rising plume. They cannot handle the situation in Stockton outfall where the plume is confined by the water surface and the river bottom and where the dilution is acquired through momentum mixing and lateral mixing across the river.
3. The EPA 3-D UDKHDEN plume model can be used to track the momentum jet for the first few minutes after the discharge. The ability to provide intermediate results for every few seconds allows us to make an empirical judgement as to when the model becomes no longer applicable due to the confinements at the water surface and the river bottom.
4. The initial dilution of the Stockton outfall occurs at the end of 120 seconds after discharge. At that point, the dilution is approximately 10.
5. The initial dilution of 10 is applicable to all tides as simulated by the model and observed by the tracer study.
6. The current near the Stockton outfall is tidally influenced. The velocity fluctuated between +1 to -1 feet per second. This velocity fluctuation will cause a recirculation of discharge water which cannot be accounted for by the near field model, but is accounted for in the far field model.

On the average, the total soluble nitrogen concentration is about 1.5 mg/L and the dissolved orthophosphate is about 0.5 mg/L. These concentrations are well excess of the nutrient requirements for green algae. The algae growth rate is not limited by nutrient concentrations, and is mainly controlled by temperature and sunlight.

An attempt was made to simulate algae in the model. The observed algal density was slightly higher from November 1990 to April 1991 than in the summer. This is counter to the model predictions which predicted higher algae in the summer than in the winter. The only explanation is that the turbidity of the water was higher in the summer than in the winter. This might have been true according to the light penetration data shown in Figure VI-11. It is not known why the turbidity is lower in the winter than in the summer.

Instead of turning on the portion of the model which simulates the algal-nutrient dynamics, the model was modified to accept algal productivity data. The productivity is defined as the difference between the growth and respiration rate in a column of water. The units are in milligrams of dry weight algae per day per feet squared. For every gram of algae which grows, about 1.6 grams of oxygen are produced and 0.07 grams of nitrogen are consumed (EPA Rates Manual 1985). The monthly estimate of productivity are shown in Table VI-5. The estimate was based in part on earlier model calculations and in part on the observed data which showed high algal density in the winter.

The effects of algae on DO were small and made up less than 2 percent of the total oxygen resources. Because the nutrient concentrations are very large, the effect of algae on nitrogen was also very small compared to the nitrification rate.

7. Dissolved Oxygen

Figure VI-12 presents the comparison for the simulated and observed concentration profiles of DO. Figure VI-13 presents the comparison of the simulated and observed concentrations of DO over time.

The time variations of DO indicate that low DO (4 to 6 mg/L) occurred in July and August. During this period the rive

VI. FAR FIELD MODELING

A. INTRODUCTION

Calibration of the far field model can be divided into three parts: (1) hydrodynamics, (2) transport and dispersion, and (3) water quality. The tidal measurements taken in the two-week field study are used to calibrate the hydrodynamics. The far field dye measurements are used to calibrate the transport and dispersion of a conservative substance. After the transport is correctly simulated, the next step is to calibrate other water quality parameters such as BOD, DO, and ammonia. This entails determining the rate constants for various water quality processes in order for the model to match one-year's water quality data monitored in the San Joaquin River.

The far field model tracks the transport, dispersion, and decay of pollutants in the river. As such, it accounts for the cumulative effects of continuous discharge including the recirculation caused by the back and forth movement of water by tides.

B. MODEL GRID SYSTEM

Figure VI-1 shows the water quality monitoring stations of the San Joaquin River. The river section of interest extends from station R0A at the Old River intersection in the south to station R8 between Rindge Tract and McDonald Tract in the Stockton Shipping Channel. The Stockton outfall is in the middle as marked in the figure. Although the actual flow direction in the river changes depending on pumping, for discussion, the term "downstream" refers to the Delta end of the system.

In the link-node model, the water body is segmented into a series of nodes which are connected by links. Figure VI-2 presents the grid system adapted to the San Joaquin River system near Stockton. As shown, the grid system covers a much larger waterway than the San Joaquin River alone. It includes the 14 Miles Slough, the Calaveras River, the Mormon Slough, the Stockton Diverting Canal and the French Camp Slough.

C. MODEL INPUT AND OUTPUT

1. Input Requirements

The model requires the following input data:

- Downstream boundary conditions (tides, water quality)
- Upstream boundary conditions (flow, water quality)
- Stockton effluent (flow, water quality)

- Storm water (hourly flow, water quality)
- Model coefficients.

Water quality refers to the concentrations of dissolved oxygen (DO), ammonia, biochemical oxygen demand (BOD), nitrate, total dissolved solid (TDS), and coliform. The model tracks BOD as carbonaceous BOD (CBOD). The model also tracks ammonia as a water quality parameter that exerts an oxygen demand separately. For the Stockton effluent, the concentration of BOD should be the first stage 5-day BOD, which does not include the oxygen demand from nitrification.

2. Tidal Data

The tide data for the gaging station at Venice Island includes time and elevation of high and low tides for each day of the year. The data was obtained from the California Department of Water Resources (DWR). The data was translated to the tides for the 3 downstream boundary nodes by the use of a time lag factor measured during the tracer study.

3. Stream Flow Data

The river flow for the upstream node was calculated from an equation developed by DWR, based on the 1962 data collected by US Bureau of Reclamation (USBR). A description of the methodology was provided by DWR and included in Appendix D.

Since 1988, DWR has placed a rock barrier at the head of the Old River typically from September to November. This barrier impedes flow from the San Joaquin River to the Old River and then to the state and federal pumps at the Clifton Court Forebay. The barrier had a significant impact on the river flow.

When we used the original 1962 DWR equation, we were unable to accurately simulate water quality when the barriers were in place. After discussing this problem with DWR staff, we obtained a new equation that accounts for the effects of the barriers. The equation is:

$$Q_s = 0.5 (Q_v - 50) - 50$$

where Q_s is the river flow at Stockton outfall and Q_v is the stream flow at Vernalis. Both flows are in cfs.

Although the use of the new equation has improved the simulation, there is still a large uncertainty in the magnitude of the calculated flows since the equation has never been verified with actual field measurements. It is suspected the flow equation may still underestimate the magnitude of the river flow.

Figure VI-3 shows the river flow data from July 1990 to December 1991 as calculated from the DWR equations. As shown, the stream flows were often negative, indicating that the net flows went upstream (reverse flow). Only during the spring melt period and when the rock barrier was up between September and November, did the river flow towards the Stockton Ship Channel.

4. Effluent Data

The measured daily effluent flows were used as the model input. The data is plotted as a dotted line in Figure VI-3. As shown, the flows had a weekly cycle. The City of Stockton did not discharge their effluent to the San Joaquin River typically on the weekends.

Figure VI-4 shows the effluent water quality data which includes ammonia, nitrogen, 5-day BOD, total suspended solids (TSS), chlorophyll-a, nitrate, and TDS. The daily effluent water quality data were used as the model input. Also shown is the river temperature to compare with effluent trends. The effluent dissolved oxygen, not shown here, was based on measurements made at the siphon station.

The 5-day BOD is a total BOD measurement, meaning it includes demands from both ammonia and CBOD. However, since CBOD is typically exerted before nitrogenous biochemical oxygen demand, it was assumed the 5-day measurements include effects mainly from CBOD. This assumption appears reasonable in light of the patterns of effluent ammonia and BOD. Ammonia was low in the summer and high in the winter, a pattern not followed by 5-day BOD. The effluent ammonia might not have contributed to effluent 5-day BOD.

Algae further complicates the interpretation of BOD data. It may artificially increase the BOD by consuming oxygen from the laboratory bottle through respiration. This is most obvious in the measurements taken at the head of the Old River, where the chlorophyll-a can be very high (Figure IV-5). 100 ug/L of chlorophyll-a artificially increases the BOD by about 4.6 g/L. The effluent BOD was reduced by the chlorophyll-a factor for use in the model input. The largest effects are in November to December 1990 and March to April 1991 when chlorophyll-a was 50 to 150 ug/L.

5. Boundary Water Quality

The water quality of the upstream boundary condition at the head of the Old River was defined by data collected at the upstream sampling system (R0A). DO, TDS, and nitrate are based on biweekly measurements. The CBOD was set to zero because as mentioned previously the BOD measurements are questionable because of the effects of algae.

The ammonia measured at the upstream boundary can also be quite high during reverse flow conditions. Under this condition, the major source of the ammonia is from the plant and not from upstream. Because it is quite possible that the calculation of flow direction can be wrong

(as will be discussed later), using the measured ammonia concentrations to fix the upstream boundary condition can lead to an erroneously high waste load attributed to the upstream. The average of the measured values cannot be used to set the boundary condition for the normal flow. To correct this problem, we chose to use the measurements taken by DWR about 15 miles upstream at Vernalis. The values are summarized in Table VI-1.

The downstream boundary conditions are defined at Turner Cut, Light 18, and Disappointment Slough at Bishop Cut. These nodes are defined as exchange nodes. Over a tidal cycle, the water ebbing out of the node is allowed to mix with the background water before flooding back into the node. The background water quality is based on daily or weekly measurements taken at stations R7 and R8.

6. Output Data

The link-node model has two modules: hydrodynamic and water quality. The hydrodynamic module generates the output data of tidal elevations for each node and flows for each link. These data are produced for each time step (40 seconds) and are integrated to hourly values which are saved in the hydrodynamics file.

The water quality module takes flow data from the hydrodynamics file and performs mass balance calculations for pollutants by accounting for advection, diffusion, sink and source associated with chemical and biological reactions. The output is the concentrations of various water quality parameters for each node and each hourly time step.

D. HYDRODYNAMIC CALIBRATION

The hydrodynamic model is calibrated by comparing the simulated and measured tidal depths. If the depths are correctly simulated then the currents must also be correct since the currents supply the tidal prism. The Mannings roughness coefficients of the links in the model are adjusted until there is an adequate match in tidal depths.

The stage measurements taken at the downstream during the dye study were used to fix the tidal conditions. The effluent flow was maintained at about 52 cfs (34 MGD). The river flow determined by the flow equation are given in Table VI-2. During this time period, the Old River Barrier was down and the pump exports had a considerable influence on the river. The flow was less than the effluent and moving in the reverse (negative) direction at times.

Figure VI-6 shows the simulated and measured tidal depths at the location where Calaveras River intersects the Deep Water Channel. Figure VI-7 shows tidal depths at the Santa Fe Railroad Bridge near the outfall. The matches are quite good throughout the period. A discrepancy occurs at the Santa Fe Railroad on hour 192. The erratic measurements indicate the gage data was probably incorrect.

The currents at the two locations are shown in Figure VI-8. The peak current speed in the upstream section of the river at the Santa Fe Railroad is about 1.0 feet/sec whereas the peak speed in the Deep Water Channel location is only about 0.5 feet/sec.

E. TRANSPORT AND DISPERSION OF DYE

The model dispersion is calibrated by adjusting a dispersion coefficient until the model can correctly simulate the longitudinal dispersion of the slug of dye released in the field study. The dye is treated as conservative and no reactions are assumed to take place. (Over long time periods, Rhodamine WT can photochemically decay. However, no significant decay could occur here since the light penetration is less than 2 feet.)

Based on calibration, the model dispersion coefficient was set to 400 ft²/sec. The actual physical dispersion in the river may be different because of numerical dispersion inherent in the model.

Figure VI-9 shows the concentration profiles along the river for the morning of each day. The concentration profiles describe the spatial distribution of water quality at a given time. They are represented by the model which captures a snap shot of the profile. However, the observed data were not collected simultaneously at all stations. This may lead to slight discrepancies.

The profiles have the characteristic bell-shaped curve. The model correctly simulated the sharp curve on day one and the gradual flattening of the curve as time progressed due to dispersion. Overall, the model predictions are very close to the observed.

The model underpredicted the maximum concentration on the first day (7/21/92 5:30). As discussed in the field results section, the dye may not have completely mixed across the river width at this time. The model assumes that the nodes are completely mixed from the west bank to the east bank of the river. This may have led to prediction of lower concentration.

Figure VI-10 shows the time-concentration of water quality at French Camp Slough in the upstream section and at Smith Canal in the Deep Water Channel. The match between the simulated and the measured are close. In the beginning, the dye was appearing and disappearing as it passed back and forth with the tide. As time progressed, the dye began to spread along the river. The tidal variation of water quality became less evident.

The complete set of profile and time series plots of concentration are provided in Appendix B and C.

F. WATER QUALITY CALIBRATION

The model has been shown to correctly simulate the transport and dispersion of a conservative substance. The next step is to determine rate constants necessary for model predictions to match

observed water quality data. Sources of calibration errors include (1) uncertainty in model input data, (2) errors in the model formulation, and (3) uncertainty in the observed water quality data.

To determine how well the simulated matches the observed, there are a large number of plots generated in this section. To prevent interruptions of the text, majority of the plots are placed in appendices and are referred to by the text.

Two types of plots were made to compare the simulated and the observed data. The first type is the profile of concentrations at nodes along the river at a given time. The second type is the time variation of concentration at a given station.

Both types of plots for a water quality parameter are placed in the same appendix. The appendix E is for TDS, F for carbonaceous BOD, G for ammonia nitrogen, H for nitrate nitrogen, and I for dissolved oxygen.

1. Rate Constants

The rate coefficients include re-aeration rate, sediment oxygen demand rate, nitrification rate, and CBOD decay rate. Each rate constant is influenced by temperature.

The O'Conner and Dobbins equation (1958) was used without adjustment to calculate the re-aeration coefficient. Because the tidal velocities in the upstream reach of the San Joaquin River are about twice as high as in the Deep Water Channel and the depths are much less, the calculated re-aeration coefficients for the upstream reach are more than twice that in the Deep Water Channel.

Sediment oxygen demand (SOD) has a large influence on the DO of the whole system. The SOD rate was adjusted to match the overall background dissolved oxygen levels (DO of river with no load from plant). We believe that SOD represents all background BOD from diffused sources of organic matters including those in the sediment.

The impact of the plant effluent on the river DO is through ammonia and CBOD loading. The nitrification rate was adjusted to simulate the ammonia and nitrate levels measured in the river.

Rate coefficients were adjusted to help match the observed with the simulated results. The strategy of calibration is to adjust the coefficients within the range of literature values. Table VI-3 shows the values we used were well within the ranges reported in the literature.

The rates are adjusted to the temperature according to:

$$k = k_{20}\theta(T-20)$$

where k is the rate constant at temperature T , k_{20} is the rate constant at 20 degrees Celsius, and θ is the temperature coefficient. The temperature coefficients used are given in Table IV-4.

2. Total Dissolved Solid

The first part of Appendix E presents the comparison of observed and simulated TDS profiles for each month of the simulation. From this comparison, it is clear that the model simulated the observed spatial gradient of TDS in the San Joaquin River. In August, the river flow was negative. The low salinity water from the Sacramento River was found to be pushed upstream to the location of Stockton outfall. In November when the river flow was high due to the rock barrier, the high salinity water of the San Joaquin River was found to push all the way downstream to R6.

The second part of Appendix E presents the comparison of simulated and observed time concentration of TDS for stations R0A to R8. The model simulated the time changes of TDS from July of 1990 to July of 1991 reasonably well. The discrepancies were traced to the uncertainty in the river flow data and also TDS data at R0A which was monitored only bi-weekly.

3. Carbonaceous BOD

The first part of Appendix F presents the comparison of simulated and observed BOD profiles. The second part presents the comparison of BOD concentrations over time. The model predicted a lower CBOD than the observed data.

There are many explanations for the discrepancy. First, the simulated BOD is for the BOD derived from the plant effluent. The measured BOD includes algal respiration, among other. The effect of algae on measured BOD is most obvious from the BOD profile of June 20, 1991. The measured BOD was highest at the head of the Old River (station R0A), decreasing gradually downstream toward the Stockton outfall. This was caused by the high algal (chlorophyll) concentration, not the high BOD derived from the plant effluent. The distribution of plant effluent BOD should follow the profile predicted by the model. Second, the detection limit of BOD is 2 mg/l. This limit is often above the BOD concentration which would result from dilution of the effluent by the river alone. For this reason, the measurements cannot track the actual effluent BOD for many times of the year.

4. Ammonia

The first part of Appendix G presents the comparison of simulated and observed ammonia profiles. The second part compares the observed and simulated time concentrations of ammonia concentration over time.

The model has accurately simulated the observed seasonal variation of ammonia, i.e. high concentrations in the winter and low concentrations in the summer. For the winter months when the ammonia concentrations are high, the model has accurately simulated the spatial distribution of ammonia. This has three important implications: 1) ammonia in this river reach can be accounted for by the ammonia from the plant effluent; 2) ammonia in the plant effluent is higher in the winter due to a lower algal uptake in the polishing ponds; 3) the high ammonia concentrations in the winter may not have as much effect on DO due to a lower water temperature.

One notable discrepancy in the time concentration is during January to February 1991. The ammonia concentration is underestimated at the Deep Water Channel Stations (R3-R6) and overestimated at the upstream stations (R1 and R2). During this period the DWR flow equation estimated a small negative (upstream) flow rate (Figure 3). In reality the flow rate was probably positive causing the ammonia load to move downstream instead of upstream.

Review of the TDS time series data (Appendix E) at stations R3 to R5 also show that the model predicted lower levels of TDS than observed during this period. Apparently, the model was drawing fresher water from the downstream section of the Deep Water Channel and moving it upstream, when in reality the higher salinity water from upstream was moving downstream.

It is clear that the flow data has to be accurate in order for the model to be accurate. Uncertainties in the flow data can lead to errors in the model output.

5. Nitrate

The first part of Appendix H presents the comparison for the simulated and observed concentration profiles of nitrate nitrogen. The second part compares the observed and simulated concentrations of nitrate over time.

Overall, the model has simulated the nitrate concentrations in time and space well. Because nitrate was uniformly high throughout the river reach, it means that nitrate is derived from both the plant and river water from the upstream. We also noted that the model overpredicted nitrate for stations R1 and R2 from January to February of 1991. This was probably caused by the error in the river flow data observed in the ammonia calibration.

6. Algae

Algae in the San Joaquin River was quite high throughout the year. Figure VI-11 shows chlorophyll-a measured at stations R2 and R4 during the calibration period. The concentration is typically 10 to 20 ug/L but may be as high as 100 ug/L in the upstream reach of the river.

On the average, the total soluble nitrogen concentration is about 1.5 mg/L and the dissolved orthophosphate is about 0.5 mg/L. These concentrations are well excess of the nutrient requirements for green algae. The algae growth rate is not limited by nutrient concentrations, and is mainly controlled by temperature and sunlight.

An attempt was made to simulate algae in the model. The observed algal density was slightly higher from November 1990 to April 1991 than in the summer. This is counter to the model predictions which predicted higher algae in the summer than in the winter. The only explanation is that the turbidity of the water was higher in the summer than in the winter. This might have been true according to the light penetration data shown in Figure VI-11. It is not known why the turbidity is lower in the winter than in the summer.

✓ Instead of turning on the portion of the model which simulates the algal-nutrient dynamics, the model was modified to accept algal productivity data. The productivity is defined as the difference between the growth and respiration rate in a column of water. The units are in milligrams of dry weight algae per day per feet squared. For every gram of algae which grows, about 1.6 grams of oxygen are produced and 0.07 grams of nitrogen are consumed (EPA Rates Manual 1985). The monthly estimate of productivity are shown in Table VI-5. The estimate was based in part on earlier model calculations and in part on the observed data which showed high algal density in the winter.

The effects of algae on DO were small and made up less than 2 percent of the total oxygen resources. Because the nutrient concentrations are very large, the effect of algae on nitrogen was also very small compared to the nitrification rate.

7. Dissolved Oxygen

Figure VI-12 presents the comparison for the simulated and observed concentration profiles of DO. Figure VI-13 presents the comparison of the simulated and observed concentrations of DO over time.

The time variations of DO indicate that low DO (4 to 6 mg/L) occurred in July and August. During this period the river temperature was high at 23 degrees Celsius which resulted in a lower saturated DO (8.6 mg/L) and higher SOD rate. The river flow rate was about -150 cfs during this period. Ammonia and BOD were not particularly high.

September 1990 is an interesting period because this is the time the rock barrier at the Head of Old River was built. The rock barrier was constructed on September 10 and removed on November 27, 1990. Without the barrier on September 4 (Figure 15), the DO effect of the Stockton effluent was toward the upstream (R1 and R2). With the barrier on September 18, the DO sag curve was toward the downstream (R3, R4, R5, and R6). The model was able to simulate the observed phenomenon.

At the end of September, the observed and simulated DO time concentration in the Deep Water Channel (R3-R8) began to diverge. The observed DO increased rapidly at this time whereas the simulated DO stayed constant at about 5 mg/L until the middle of October when it rapidly increased. Examination of the effluent data shows that the ammonia and BOD steadily increased from the time the barrier was in place until the middle of October. The river temperature only decreased 3 degrees Celsius (21 to 18 degrees). Since the load was moving downstream, it is difficult to explain why the observed DO at the Deep Water Channel stations increased over this time period.

One explanation is that the DWR flow equation with the rock barrier grossly underestimates the flow rate. The profiles on October 17 and November 13 in Figure VI-12 show that the DO sag curve is very broad and located far downstream. The DO at stations R7 and R8 are actually depressed at these times. It is possible that the flow rate was much higher than the 300 to 500 cfs predicted by the equation.

The simulated DO began to recover in the middle of October when the plant was shut down from October 22 to November 1. The river temperature also rapidly decreased during this period. After November 27 when the barrier was removed, the simulated DO was high (9 to 10 mg/L) and the match was better.

From December to March, the river water temperature was low but climbing. During that period, both BOD and ammonia were high. These combined factors caused DO to have a decreasing trend with time.

The model appears to have accurately simulated all these interacting processes. It has predicted the observed time concentrations of DO in the San Joaquin River near Stockton.

Another way to evaluate the model is to compare frequency distributions of simulated and observed data. Figure VI-14 are the comparisons for stations R1 to R6. The comparisons are close, with a less than 0.5 mg/L difference in the low-DO region. The model underpredicts the DO in the high-DO region possibly because of the suspected error in the rock barrier flow equation.

8. Oxygen Budget

The model allows an accounting of various process that control DO in the river. The results for station R1 to R4 are shown in Figure VI-15. Re-aeration is the dominant source of DO (about 40 percent) whereas SOD is the dominant sink (also about 40 percent).

The model uses a CBOD decay rate of 0.15 per day and a nitrification rate of 0.09 per day at 20 degree Celsius. For that reason, the importance of CBOD on the oxygen resources becomes more important near the outfall. Away from the outfall, CBOD would have already been expended. Therefore, the effect of nitrification on the oxygen resources becomes more important. This

phenomena can be demonstrated by comparing the oxygen budget for R2 (closest to the outfall), R3, and R4 (furthest from the outfall). The percentage of the oxygen consumption is 11% for nitrification and 8.8% for BOD at the near station (R2). The percentage changes to 15.7% for nitrification and 7.5% for BOD at the far station (R4).

G. VERIFICATION

The model was extended to simulate the water quality from July 1991 to November 1991. In this simulation, the calibrated model coefficients were not altered. This allows us to evaluate how accurately the model can simulate conditions not encountered in the calibration period.

Figure VI-16 shows effluent and river conditions during the period. The river flow rate was about -100 cfs until the rock barrier was installed on September 13. After the installation, the flow direction changed and the rate increased to 300 cfs in September and October, and increased further to 500 cfs in November. The flow decreased to about 100 cfs after the barrier was removed on November 27.

The river temperature was high (20-23 degrees Celsius) until the middle of October when it sharply decreased to about 10 degrees Celsius by December. While the temperature was high, the effluent ammonia steadily increased from less than 1 mg/L in July to about 20 mg/L at the middle of October. As will be seen, this led to a very low DO in the river. The 5-day BOD was fairly constant at about 6 mg/L until the middle of November when it sharply increased to about 20 mg/L. Unfortunately, no effluent chlorophyll-a measurements were made during the verification period so it is not certain whether the sudden increase in 5-day BOD was due to algae.

Figure VI-17 presents the comparison of the time variation of DO and Figure VI-18 presents the DO profiles. The DO predictions were good for the summer conditions in July and August when the river barrier was not yet installed. As the river temperature and effluent ammonia increased in September, and the river began to flow downstream, the observed and simulated DO decreased downstream of the outfall (R3-R8).

At the latter half of September the simulated DO stopped decreasing to about 3.5 mg/L because the effluent was cut on September 21-22 and on September 26-31. However, the observed DO at the downstream stations continued to descend for some reason even though the temperature was constant. Then in October, the observed DO dipped to very low values (less than 1 mg/L at station R5) on two different occasions. These two occurrences could not be related to any sudden changes in the input conditions to the model.

In the past, dredging activity in this region of the Deep Water Channel has caused the DO to drop below 2 mg/L. However, the Corps of Engineers informed us that no dredging occurred in 1991. For now, we can only speculate that the large depression in DO was caused by some source not taken into account by the model.

At the beginning of November, the temperature dropped suddenly from 20 to 13 degrees Celsius. This caused the observed and simulated DO to rapidly increase. At the latter half of November, the simulated DO stopped increasing because the temperature was relatively constant and the effluent BOD increased from about 5 mg/L to about 20 mg/L over a short time period.

Overall, the calibrated model was successfully extended to the verification period. It was able to accurately predict the decrease in DO to 3.5 mg/L. This was caused by high river temperature and the large increase in ammonia which was not encountered in the calibration period. The further drastic decrease in DO is attributed to an unknown source. This should serve as a warning that the input conditions must be accurately defined for the model to completely track the behavior of the river.

H. RESPONSE TO PLANT SHUTDOWN

The model was applied to see how the model simulates the response of the river to the stoppage of plant effluent. This evaluation was made for summer and winter conditions.

The winter scenario was based on the river and effluent conditions during February 1991 and the summer scenario was based on August 1990 conditions. These conditions are summarized in Table VI-6.

The simulations lasted 60 days. From day 1 to day 19 the effluent flow rate was set to 35 cfs (22.6 MGD) which is the average flow rate in 1990 and 1991, including the days of discharge and days of no discharge. On day 20 the effluent was cut for the next 40 days. There were two river flow conditions +200 cfs and -200 cfs.

Figure VI-19 shows the DO for the winter condition with a positive river flow rate. The top figure indicates that the minimum DO near station R4 is about 6.5 mg/L with plant operation and about 9 mg/L without. It took almost 30 days for the DO at station R4 to reach a steady-state value after the effluent was cut.

Figure VI-20 shows the DO for the summer condition with a positive river flow rate. The DO near station R4 is about 4.5 mg/L with and 5.5 mg/L without plant operation. Because the effluent ammonia and CBOD was less in the summer, the DO was only depressed by 1.0 mg/L compared to 2.5 mg/L in the winter. However, because the ambient DO is much lower in the summer, it did not take much to depress the DO below 5 mg/L.

Figures VI-21 and VI-22 show the DO for the summer and winter conditions during reverse flow. In the winter, the DO increased from 7.5 mg/L to 9.5 mg/L in the upstream region. In the summer, the DO increased from 5.0 mg/L to 6.0 mg/L. Thus, with a reverse flow during the summer condition, the DO did not drop to 4.0 mg/L as occurred with a positive flow rate. However, the DO was depressed over a much longer stretch of the river during reverse flow than during positive flow conditions.

The DO recovered more quickly (about 10 days) with the reverse flow. This is in part because the upstream stretch is more shallow and narrow than the Deep Water Channel enabling it to be flushed more quickly.

I. STATUS OF THE MODEL

Accuracy of the model depends on the accuracy of data. Even if the model is all theoretically correct, the model results cannot match the observed data perfectly.

Based on the results presented in this report, it appears that the model has been calibrated to simulate the important features of the hydrodynamic and water quality processes in the San Joaquin River near Stockton. Most of the significant discrepancies can be attributed to errors in the input data. The model can now be used to perform waste load allocation and other water quality analyses to support the application of the waste discharge permit.

An user friendly graphic interface has been developed for the model. This will allow users to run the model using menus. The results can be viewed graphically on the computer screen.

J. SUMMARY AND CONCLUSIONS

Based on the analyses performed, it is concluded:

1. The link-node model has successfully been calibrated to simulate the tidal movement of the water and the transport and dispersion of tracer with data collected during the dye study.
2. The link-node model has been calibrated to simulate the hydrodynamics and water quality of the San Joaquin River with monitoring data collected from July 1990 to July 1991. The water quality parameters considered include TDS, BOD, ammonia, nitrate, and DO.
3. The link-node model has been verified with data from July 1991 to November, 1991.
4. The far field model is ready to perform waste load allocation and other water quality analyses needed for the application of City's waste discharge permit.
5. Critical water quality conditions occur in the seasonal transitional periods of fall and spring. In the fall when the river temperature does not decrease as fast as expected, a high dose of BOD and ammonia can cause a sharp

decrease of DO in the river. In the spring, a similar situation can also occur when the river temperature rises too fast.

VII. CONCLUSIONS

The model described in this report has been successfully calibrated against field data, and will provide an accurate tool for analyzing the impacts of the Stockton wastewater discharge on the San Joaquin River. The model includes a near-field component that simulates mixing in the initial mixing zone, and a far-field component that tracks transport of pollutants through the lower San Joaquin River system. The model simulates the transport and fate of conservative substances, TDS, BOD, Ammonia, Nitrate, and Dissolved Oxygen.

The near-field model was calibrated against dye mixing data collected during ebb, slack, and flood tides in August of 1992. A variety of EPA initial dilution models were tested, and the model UDKHDEN was found to best simulate the observed discharge jet. Both the data and the model predicted initial dilutions on the order of 10.

The far-field model was calibrated in three phases. First, the hydrodynamic portion of the model was calibrated against observed water surface elevations measured at various locations along the River. After minor adjustment of hydraulic roughness coefficients, the model was able to accurately predict the observed water surface elevations. In the second phase, the transport component of the model was calibrated against dye mixing data collected in the field, to ensure that the model was correctly simulating the dispersion of the wastewater plume in the far-field. Finally, the model was calibrated and verified against observed water quality data collected by the City of Stockton in 1990 and 1991. Model predictions for TDS, BOD, Ammonia, Nitrate, Algae, and Dissolved Oxygen were compared to field data, and chemical rate coefficients were adjusted to produce the optimal fit between model results and field data.

The calibrated model, when used in conjunction with field data, will provide a useful tool for analyzing the impacts of various wastewater discharge scenarios. Based on our model runs to date, the following conclusions can be made about the behavior of the discharge:

1. The wastewater discharge is neutrally-buoyant, and mixing is dominated by momentum effects. The initial dilution of the discharge is about 10 under most conditions.
2. When the dominant flow direction is downriver, the DO sag due to the Stockton effluent is located downstream of the outfall in the Deep Water Channel. During flow reversals, the sag point may shift upstream as far as station R2.
3. Water quality limited conditions occur in the summer (May to October) when the river temperature is high. High water temperatures lead to lower saturated DO, and higher SOD rates, nitrification, and BOD decay. A

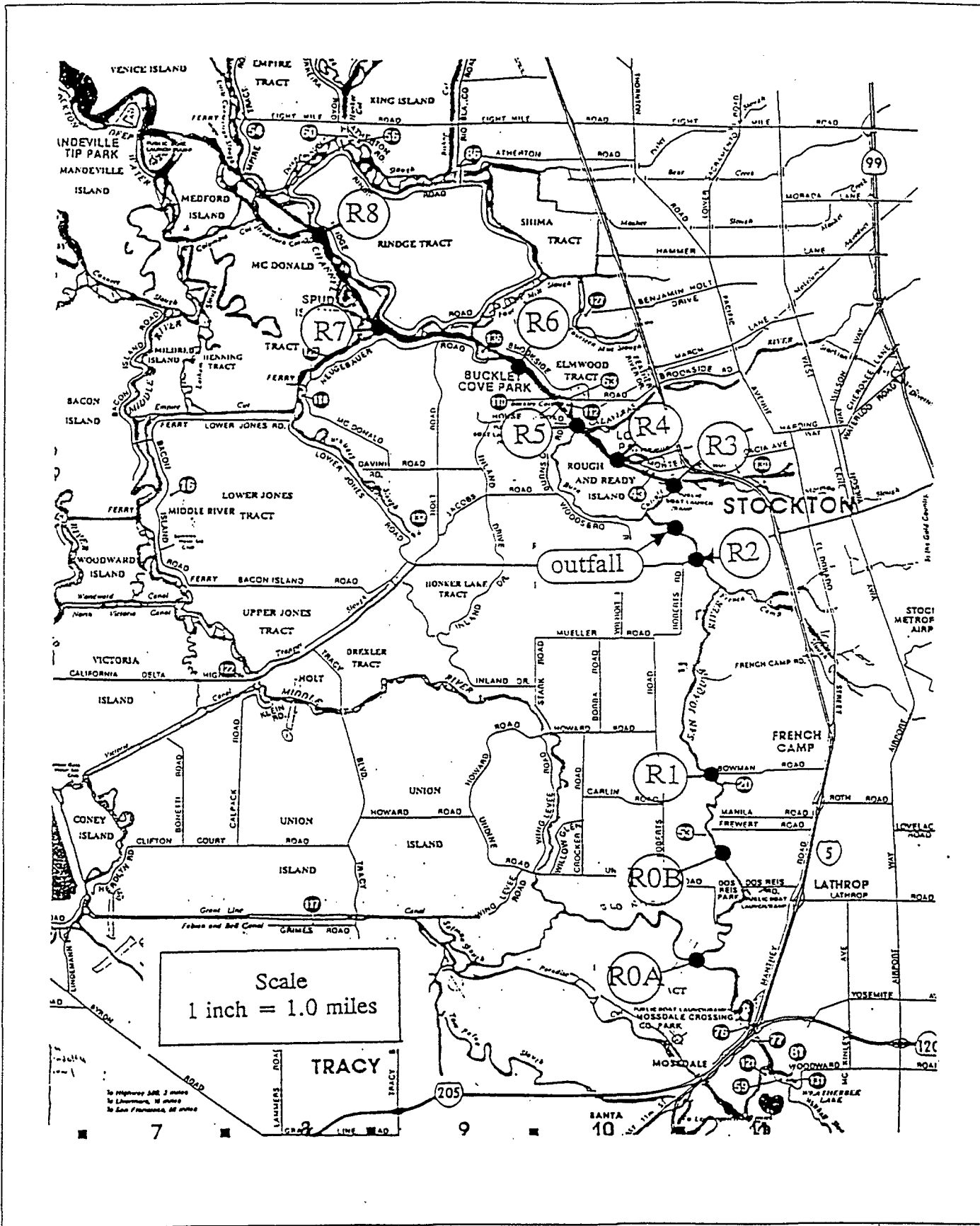
critical condition occurs in the transition fall and spring periods, when lower temperatures in the treatment plant algae pond result in higher ammonia and BOD loads to the river.

4. Water quality in the river is strongly related to river flow conditions. As a result, the accuracy of the upstream flow rate estimates is of critical importance. The installation of a flow gage at the outfall will greatly improve the model predictions.
5. Delta water management has a strong influence on river flows and water quality. Of particular importance are the Clifton Court and Tracy pumping facilities, and the rock barrier installations at the Old River confluence.

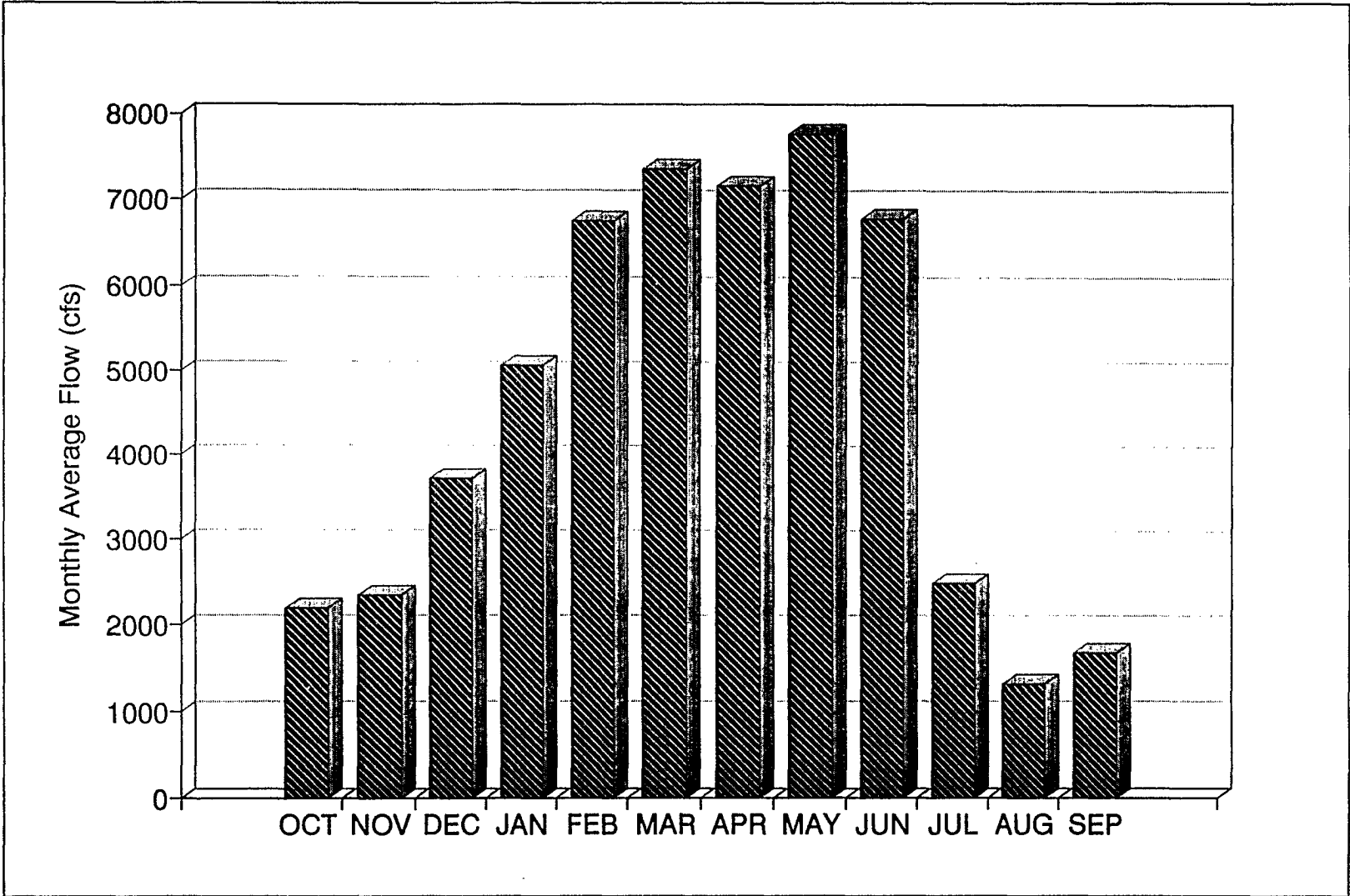
REFERENCES

- Contra Costa Water District. 1991. Assumptions Used in the Fischer Delta Model. Water Resources Department. Concord, CA.
- Division of Water Resources. 1962. Salinity Incursion and Water Resources, Delta Water Resources. Bulletin No. 76, April.
- Federal Emergency Management Agency. 1989. Flood Insurance Study, San Joaquin County, California. December.
- Gill and Pulver Engineers, Inc. 1987. Weston Ranch Hydraulic Study. Sacramento.
- Harte, J., K.G. Harrison, M. Turner, and D. Yargas. 1986. Preliminary Investigation of San Joaquin River Water Quality and Its Implications for Drinking Water Exports to Southern California. Prepared for the California Senate Office of Research. University of California Energy Resources Group, Berkeley, CA.
- H.T. Harvey and Associates. 1991. Weston Ranch Marina, Draft Supplemental EIR, Hydrology and Water Quality. Prepared for Valley Planning Consultants, Inc. Merced, CA.
- Hydroscience, Inc. 1976. Preliminary Evaluation of Observed Water Quality in San Joaquin River. Prepared for the Department of Water Resources, Sacramento, CA.
- Resources Management Associates. 1985. Effects of the Stockton Ship Channel Deepening on the Hydraulics and Water Quality Near the Port of Stockton, California. Lafayette, CA.
- Schaaf and Wheeler. 1992. Proposed 100-year Flow Rates for San Joaquin County and City of Stockton Flood Insurance Study. Letter to Stockton City Engineer, February 24.
- State Water Resources Control Board. 1987. Regulation of Agricultural Drainage to the San Joaquin River. Appendix C - An Input-Output Model of the San Joaquin River from the Lander Ave. Bridge to the Airport Way Bridge. August.
- U.S. Army Corps of Engineers. 1988. Condition Soundings in the Stockton Ship Channel. Geotechnical Division, Sacramento, CA.

FIGURES



 <p>Philip Williams & Associates, Ltd. Consultants in Hydrology</p>	<p>Location of the Stockton Outfall and Study Area</p>	<p>Figure II-1</p>
--	---	-------------------------------



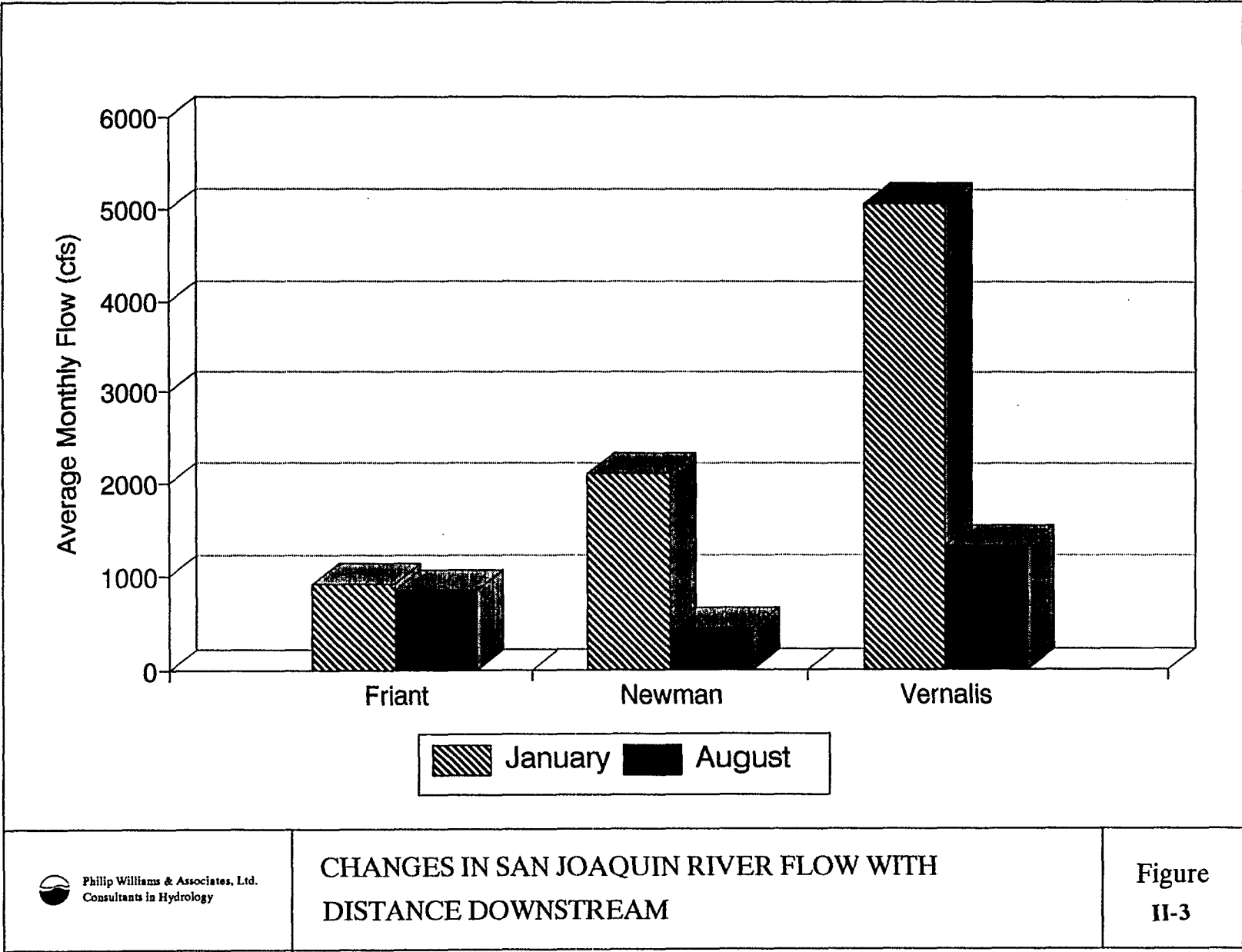
Philip Williams & Associates, Ltd.
 Consultants in Hydrology

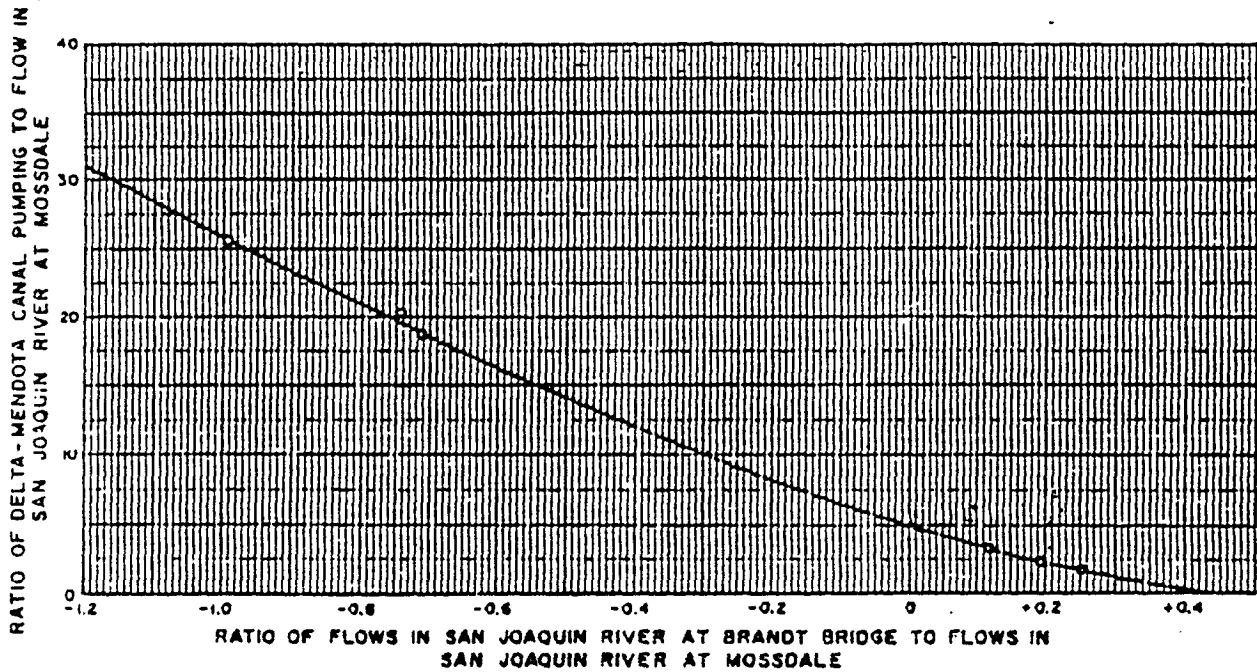
MONTHLY AVERAGE FLOWS IN THE SAN JOAQUIN
 RIVER AT VERNALIS

Figure
 II-2

D-041302

D-041302





NOTE: Flows in northwesterly direction in San Joaquin River at Brant Bridge positive and in opposite direction negative.

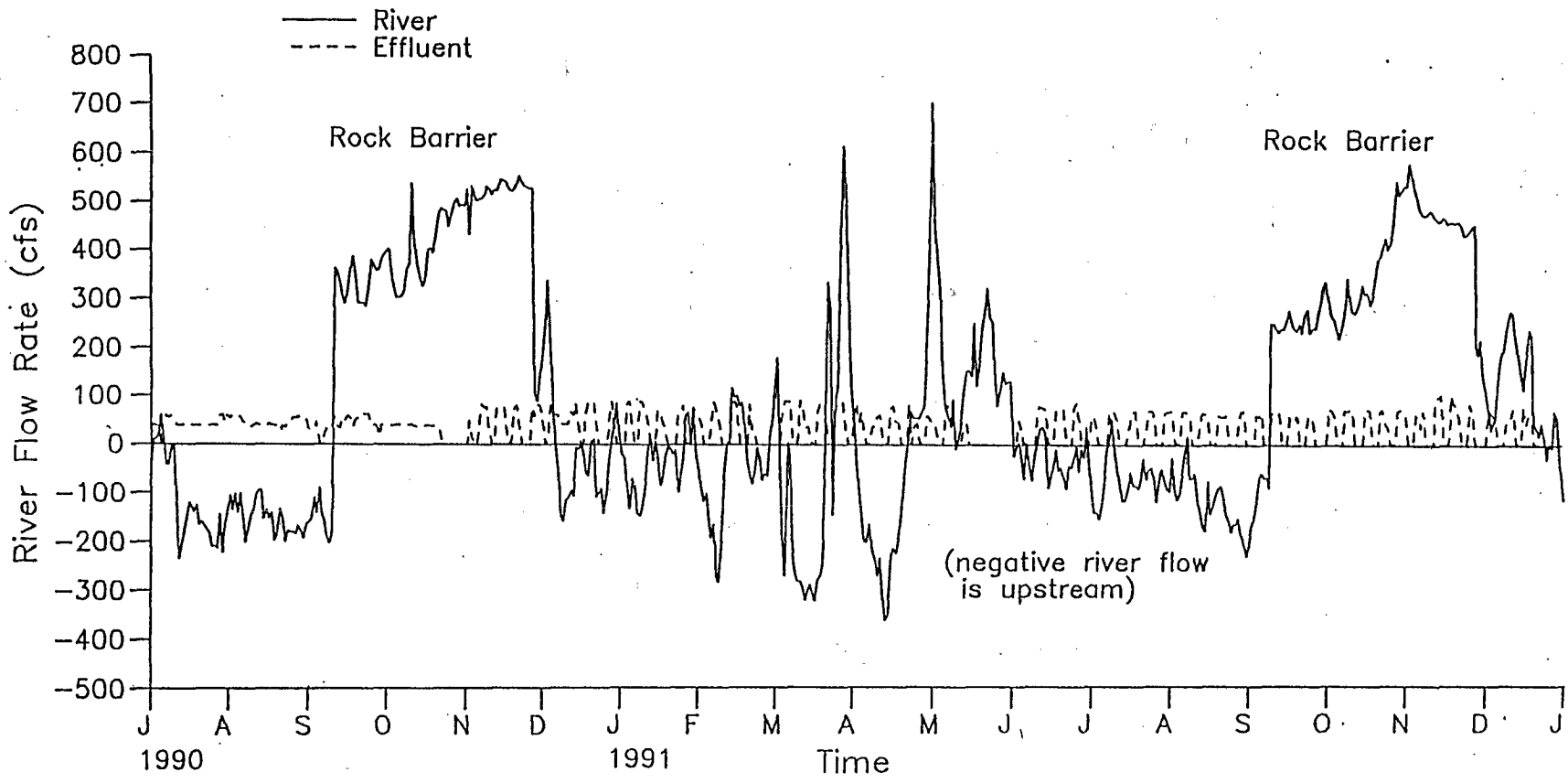
STATE OF CALIFORNIA
 THE RESOURCES AGENCY OF CALIFORNIA
 DEPARTMENT OF WATER RESOURCES
 DELTA BRANCH
 DELTA WATER FACILITIES
 RATIO OF FLOW AT TWO LOCATIONS
 ON SAN JOAQUIN RIVER AS INFLUENCED
 BY DELTA-MENDOTA CANAL PUMPING
 APRIL 1962



Philip Williams & Associates, Ltd.
 Consultants in Hydrology

DWR Relationship Defining the
 San Joaquin - Old River Flow Split

Figure
 II-4



D-041305



Philip Williams & Associates, Ltd.
Consultants in Hydrology

River and Effluent Flow Rate
from 7/90 to 12/91

Figure
II-5

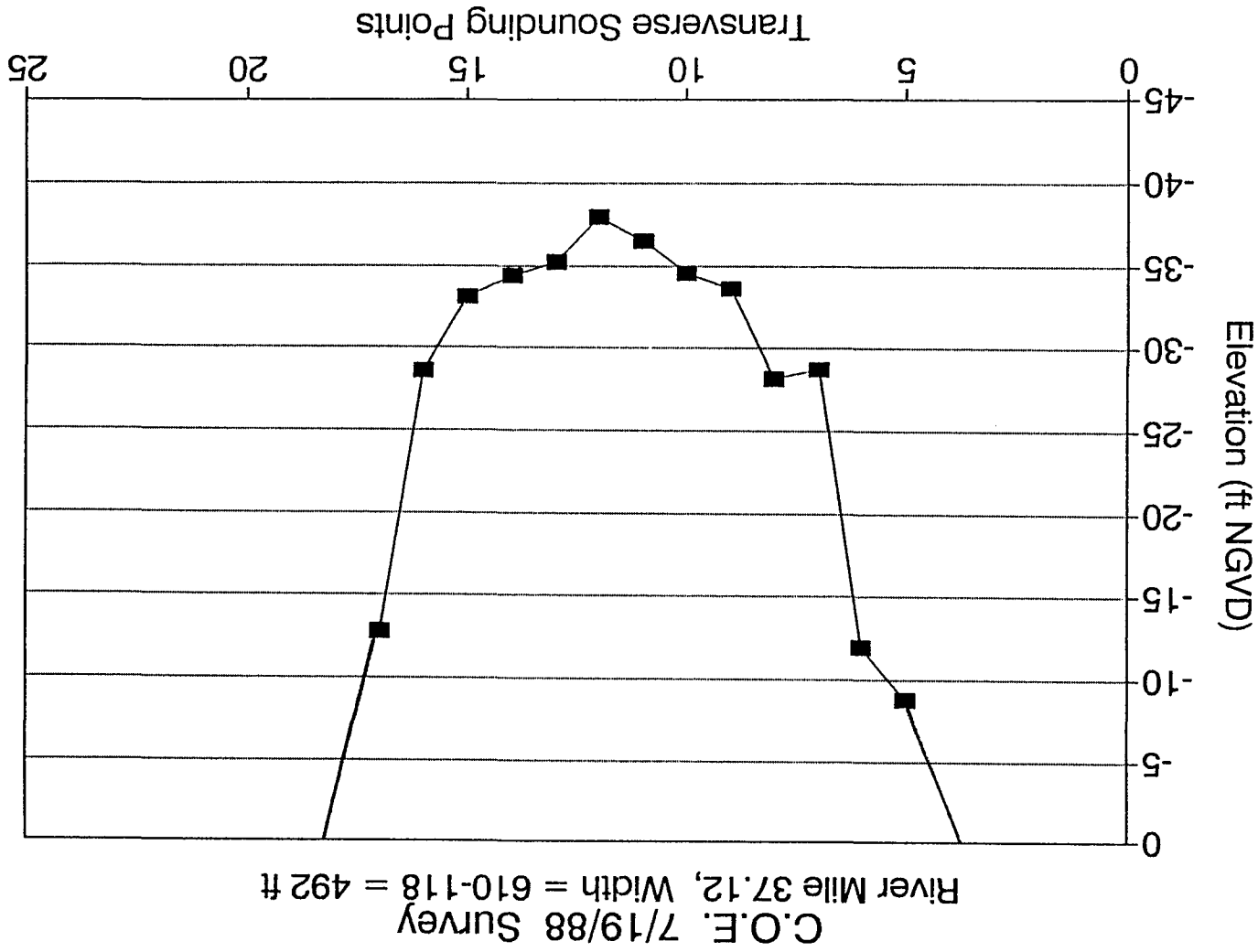


Philip Williams & Associates, Ltd.
Consultants in Hydrology

Typical Cross-Section of the Stockton Shipping Channel

SOURCE: *System Engineers*

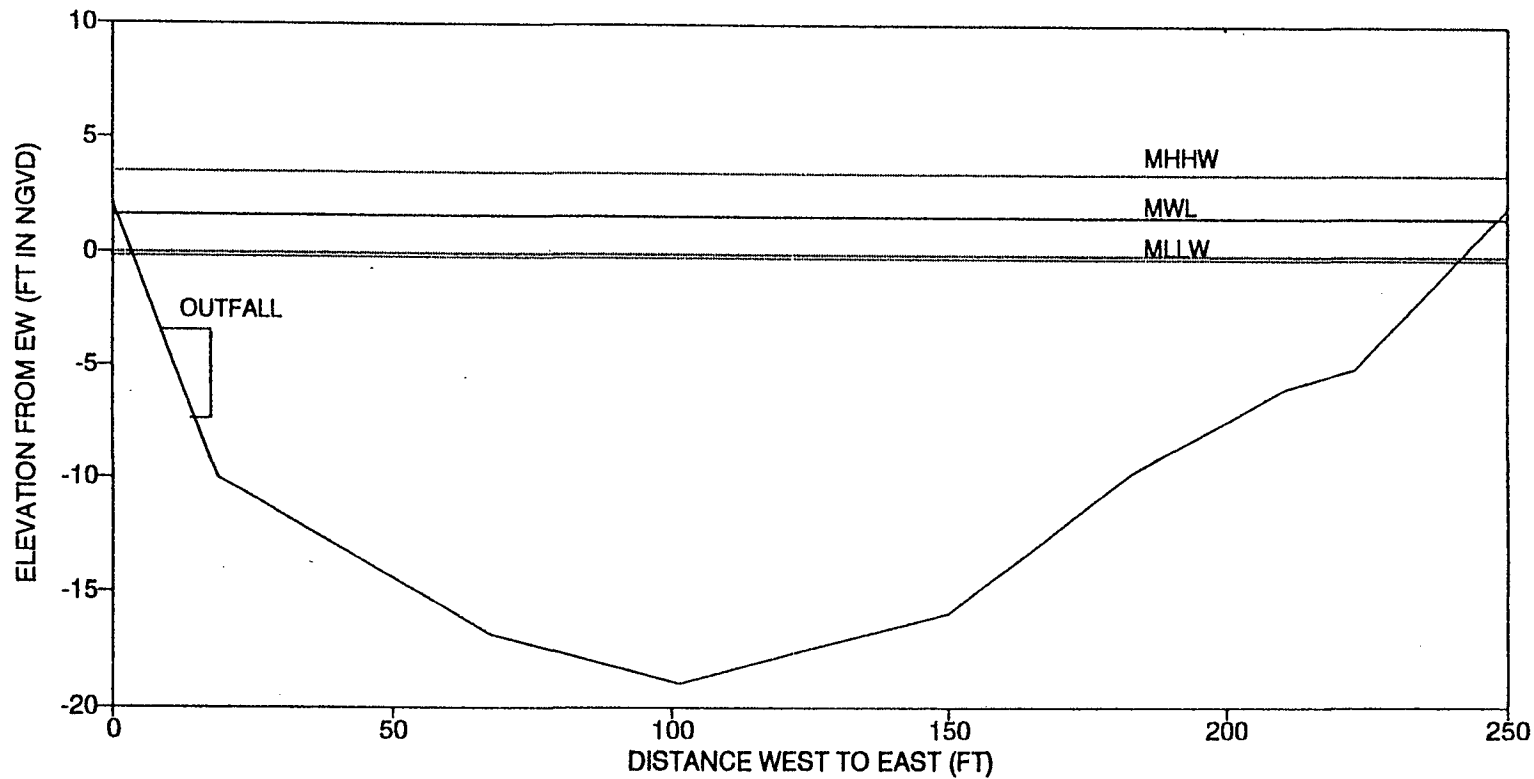
Figure II-6



D-041306

D-041306

SAN JOAQUIN RIVER
CROSS-SECTION: 100 FT U/S OF OUTFALL



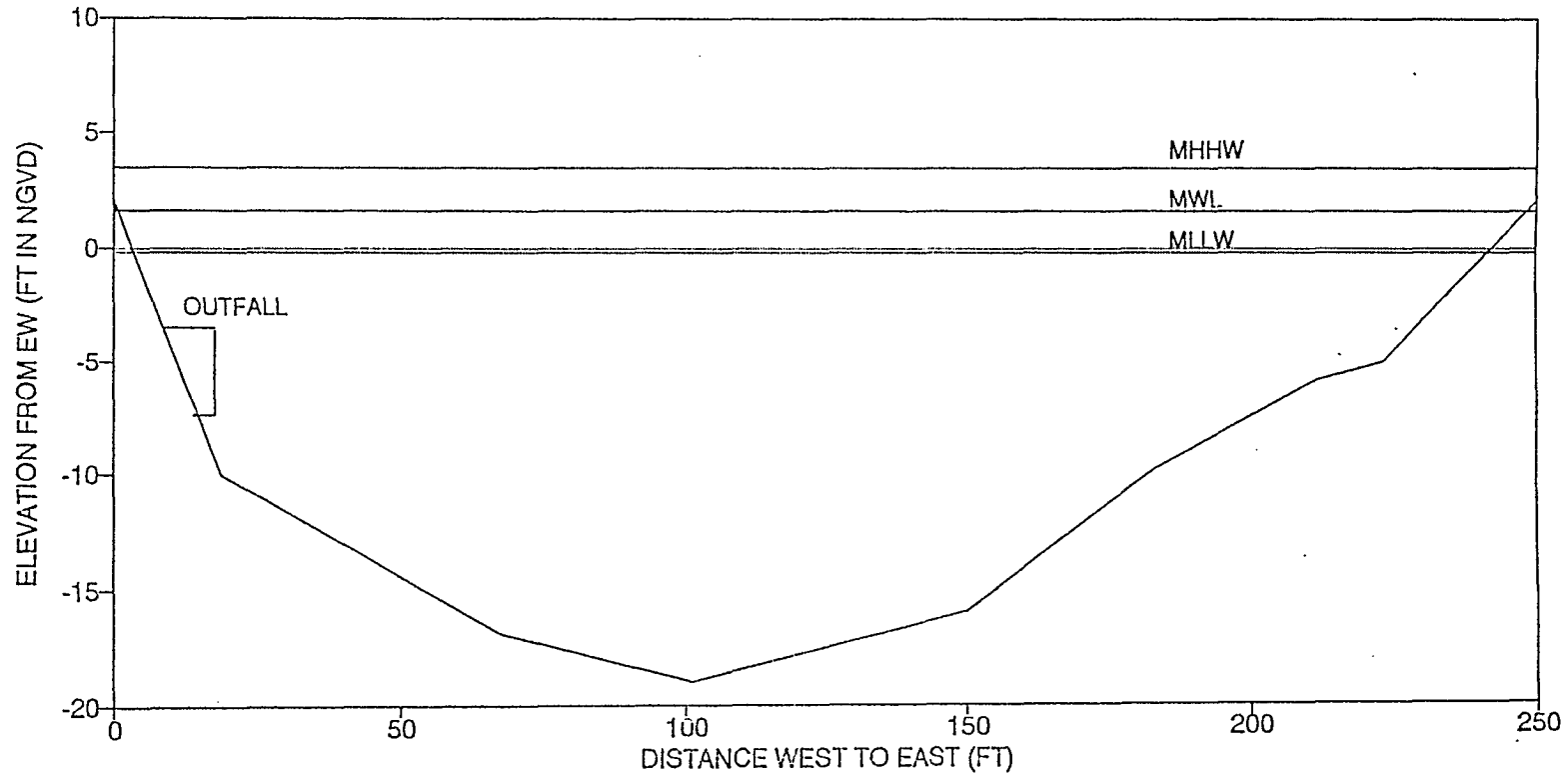
Philip Williams & Associates, Ltd.
Consultants in Hydrology

Typical Cross-Section of the San Joaquin River near the Stockton Outfall

SOURCE: Systech Engineers

Figure
II-7

SAN JOAQUIN RIVER
CROSS-SECTION: 100 FT U/S OF OUTFALL



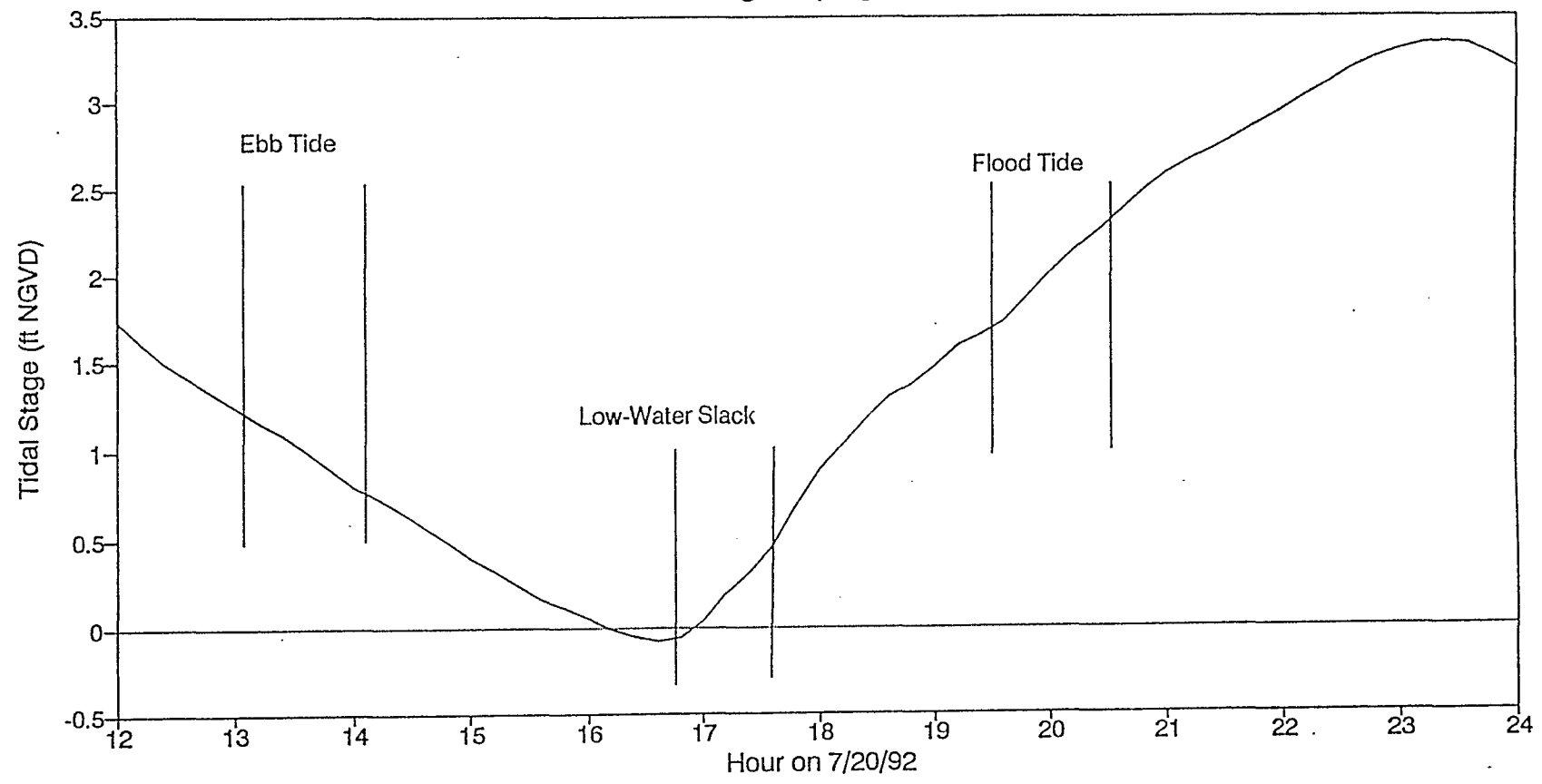
Philip Williams & Associates, Ltd.
Consultants in Hydrology

Side View of Stockton Outfall

SOURCE: Systech Engineers

Figure
IV-2

Tide During Sampling Periods

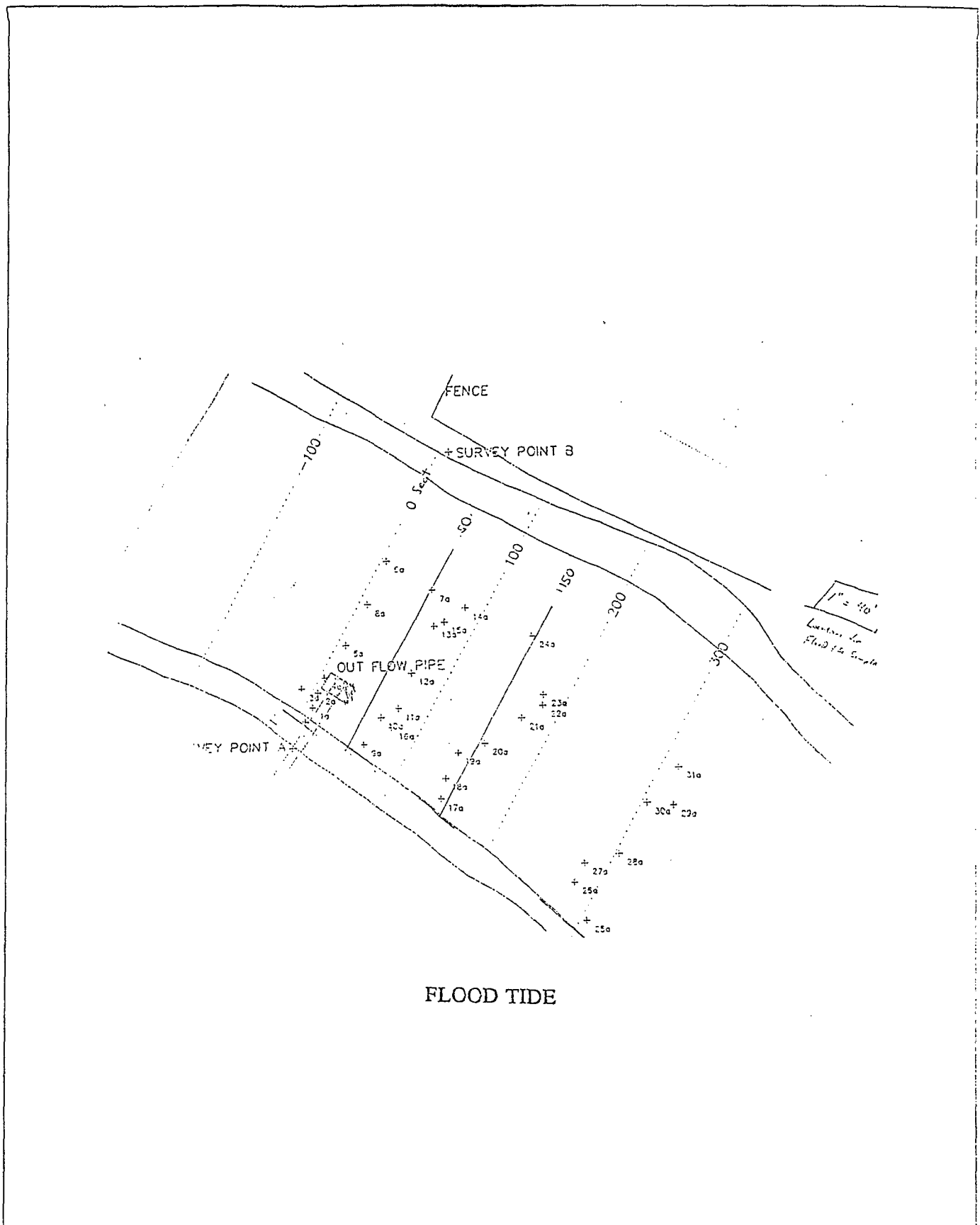


Philip Williams & Associates, Ltd.
Consultants in Hydrology

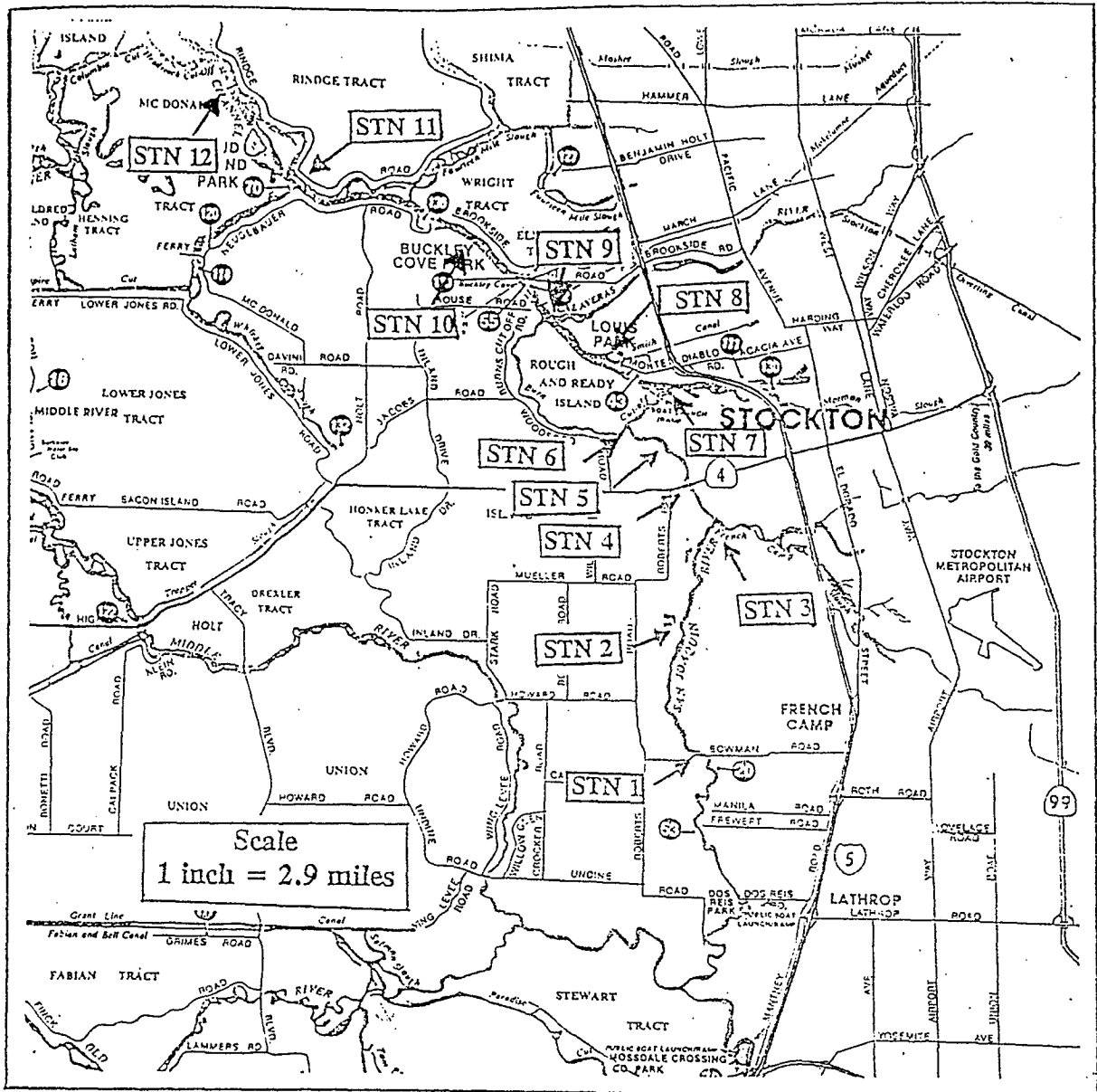
Water Level During Near Field Sampling Periods

SOURCE: Systech Engineers

Figure
IV-3



 <p>Philip Williams & Associates, Ltd. Consultants in Hydrology</p>	<p>Near Field Sampling Locations (continued)</p> <p><i>SOURCE: Systech Engineers</i></p>	<p>Figure IV-4b</p>
--	---	-------------------------



Location of Sampling Stations

- | | |
|---|---------------------------------------|
| 1. Bowman Road | 7. Burns Cutoff at Deep Water Channel |
| 2. Old Smoke Stack | 8. Smith Canal |
| 3. French Camp Slough | 9. Calaveras River |
| 4. Highway 4 | 10. Light 36 |
| 5. Outfall (SF Railroad bridge) | 11. Turner Cut |
| 6. Burns Cutoff (0.7 miles downstream of outfall) | 12. Light 18 |



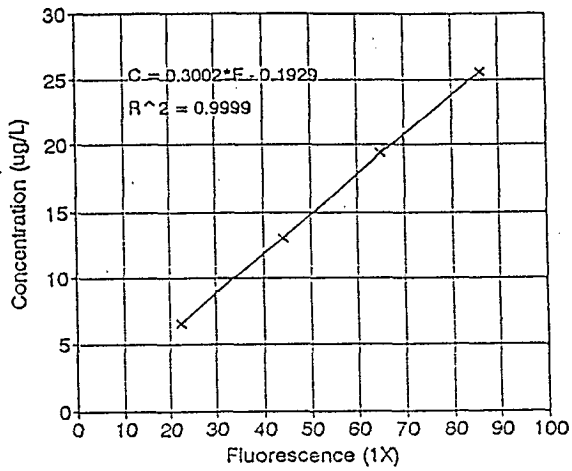
Philip Williams & Associates, Ltd.
Consultants in Hydrology

Far Field Sampling Stations for Dye Study

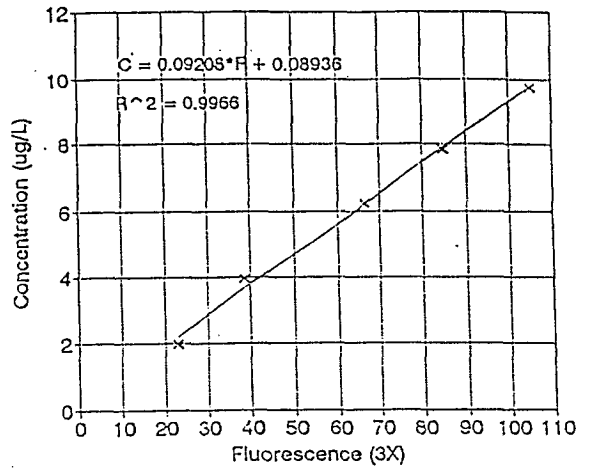
SOURCE: Systech Engineers

Figure
IV-5

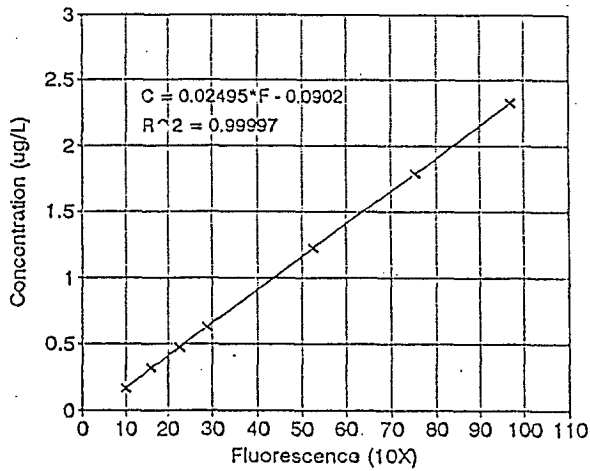
1X Fluorometer Calibration
(Temperature = 20 C)



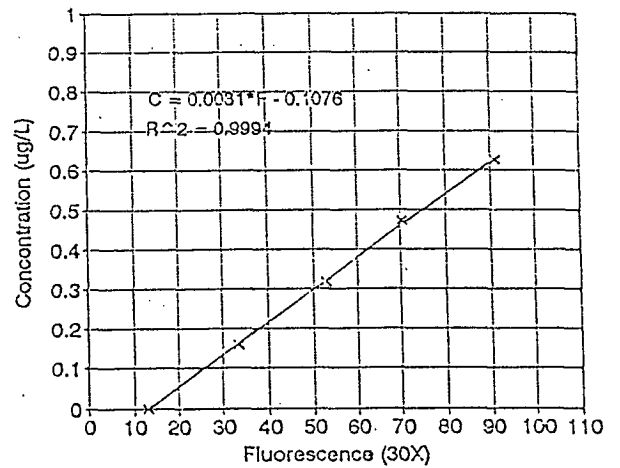
3X Fluorometer Calibration
(Temperature = 20 C)



10X Fluorometer Calibration
(Temperature = 20 C)



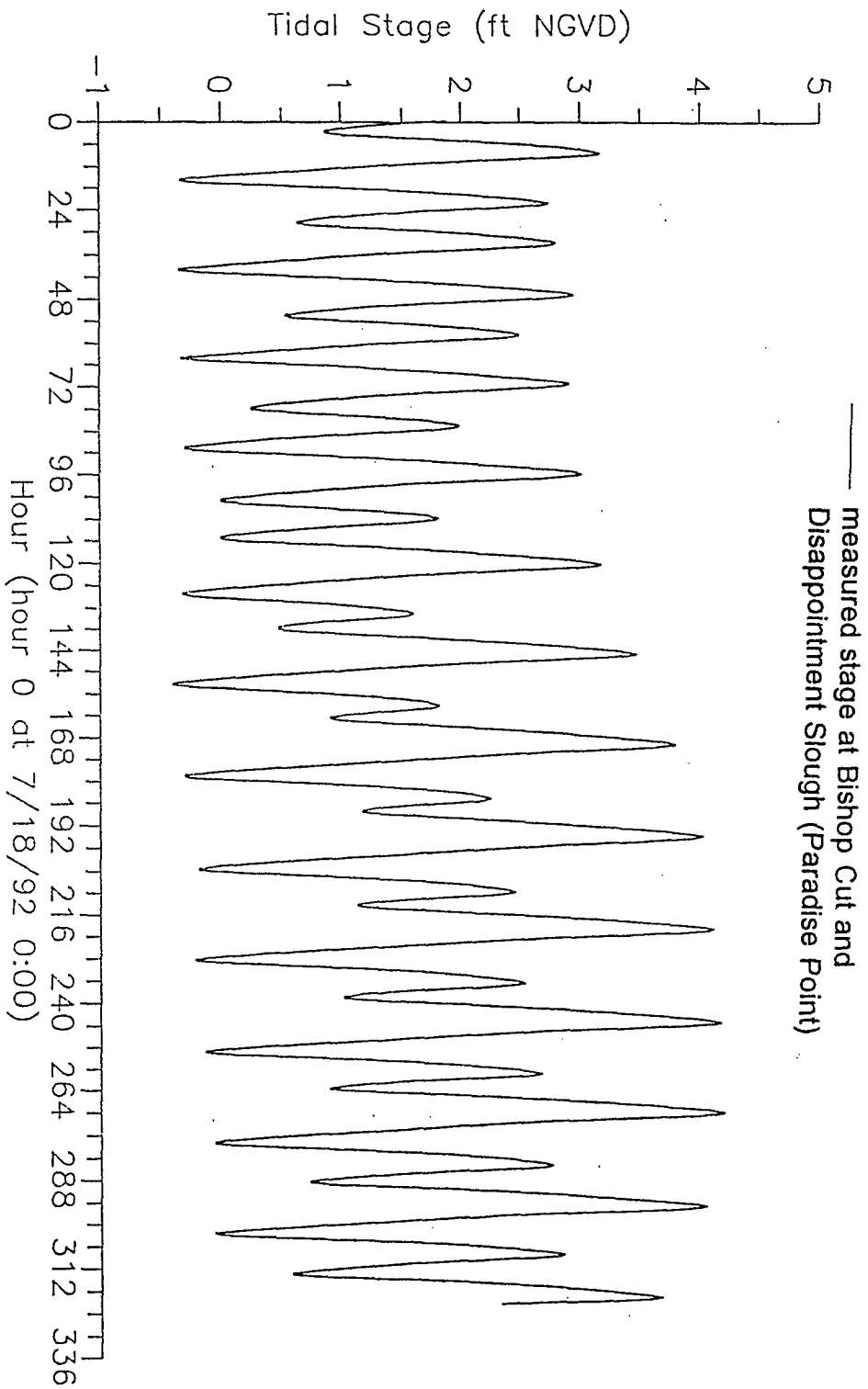
30X Fluorometer Calibration
(Temperature = 20 C)



Philip Williams & Associates, Ltd.
Consultants in Hydrology

Fluorometer Calibrations for Rhodamine WT
SOURCE: Systech Engineers

Figure
IV-6



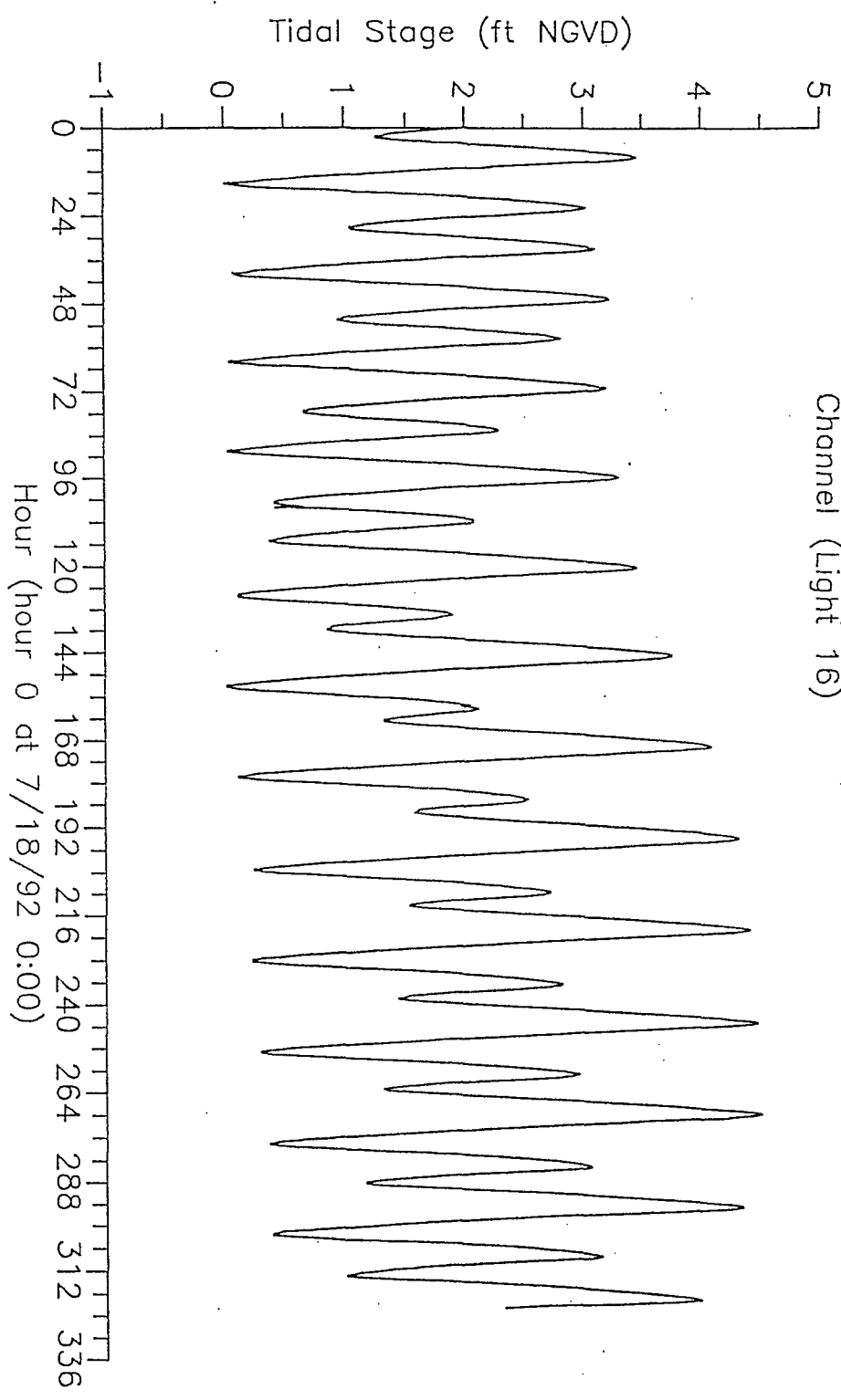
Philip Williams & Associates, Ltd.
Consultants in Hydrology

Stage Measurements at Paradise Point (7/18-7/31/92)

SOURCE: Systech Engineers

Figure
IV-7

— measured stage at Deep Water Channel (Light 16)

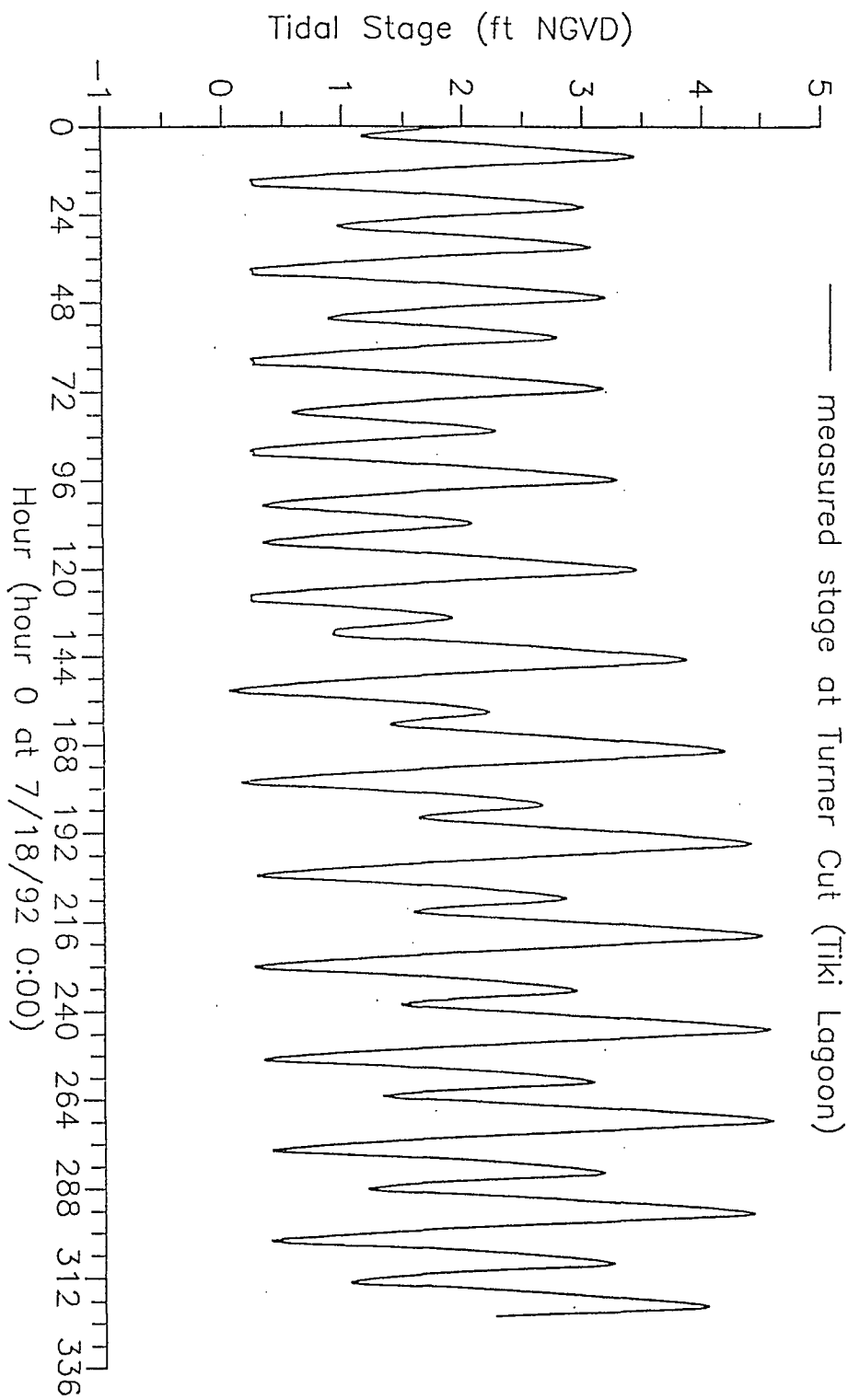


Philip Williams & Associates, Ltd.
Consultants in Hydrology

Stage Measurements at Light 16 in Deep Water Channel (7/18-7/31/92)

SOURCE: Systech Engineers

Figure
IV-8

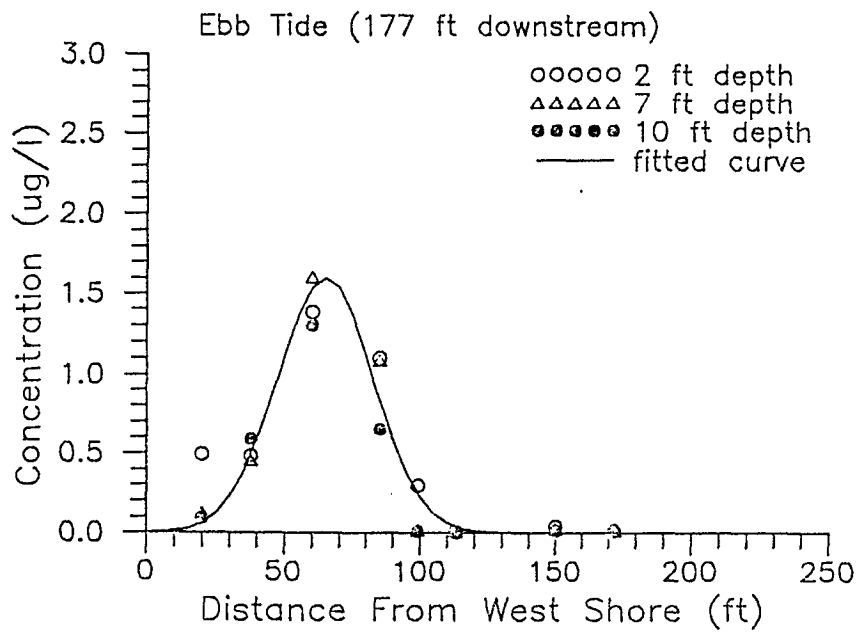


Philip Williams & Associates, Ltd.
Consultants in Hydrology

Stage Measurements at Turner Cut (Tiki Lagoon) (7/18-7/31/92)

SOURCE: Systech Engineers

Figure
IV-9

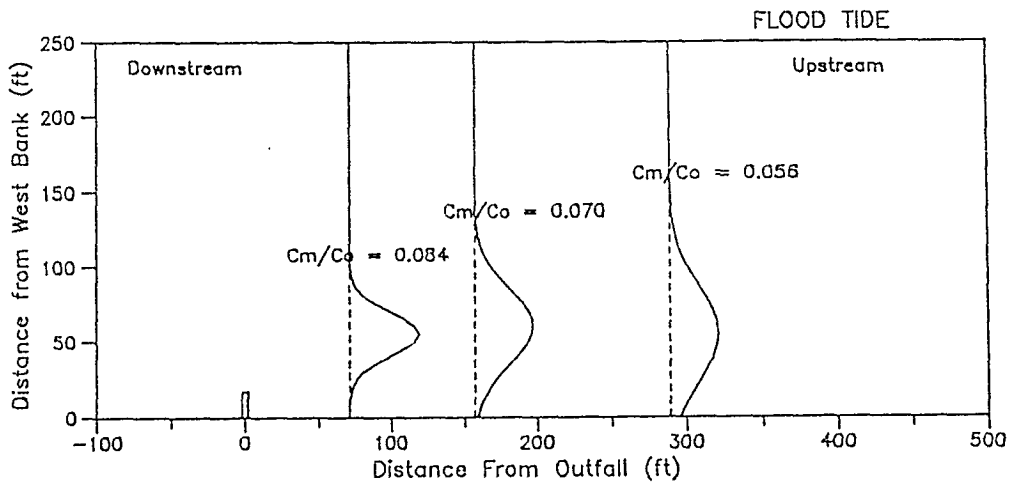
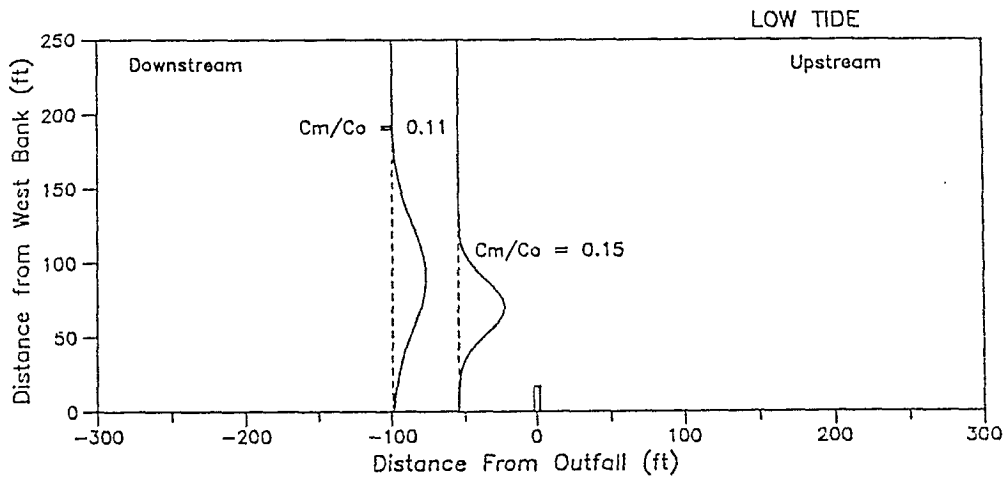
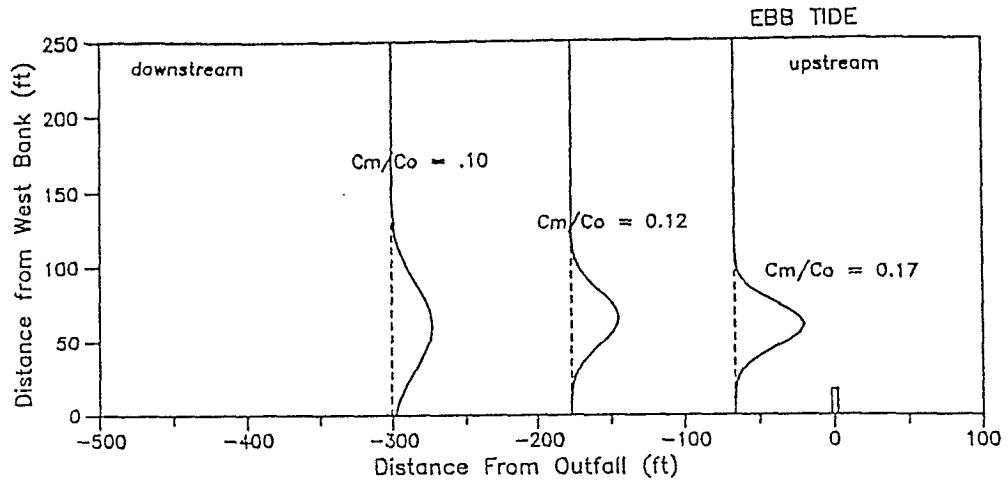


Philip Williams & Associates, Ltd.
 Consultants in Hydrology

**Near Field Dye Distribution along Transect
 177 feet Downstream of Outfall During Ebb
 Tide**

SOURCE: Systech Engineers

Figure
 IV-10

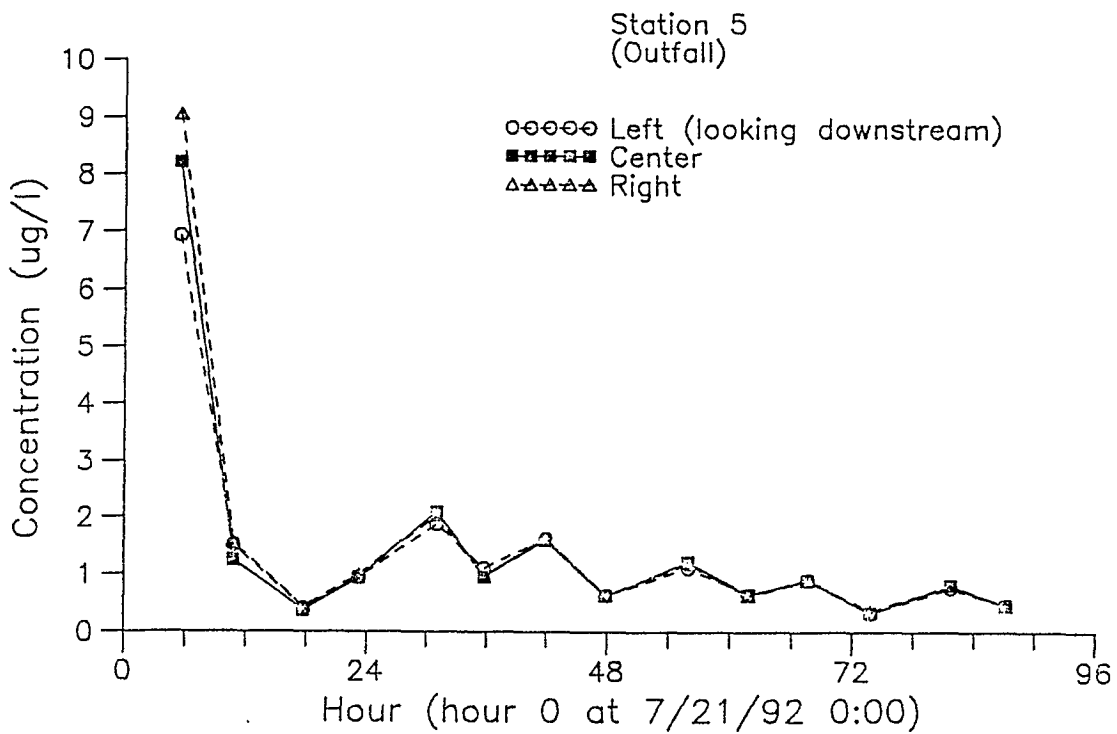


Philip Williams & Associates, Ltd.
Consultants in Hydrology

**Plan View of Dye Distribution in River for 3
Near Field Periods**

SOURCE: Systech Engineers

Figure
IV-11

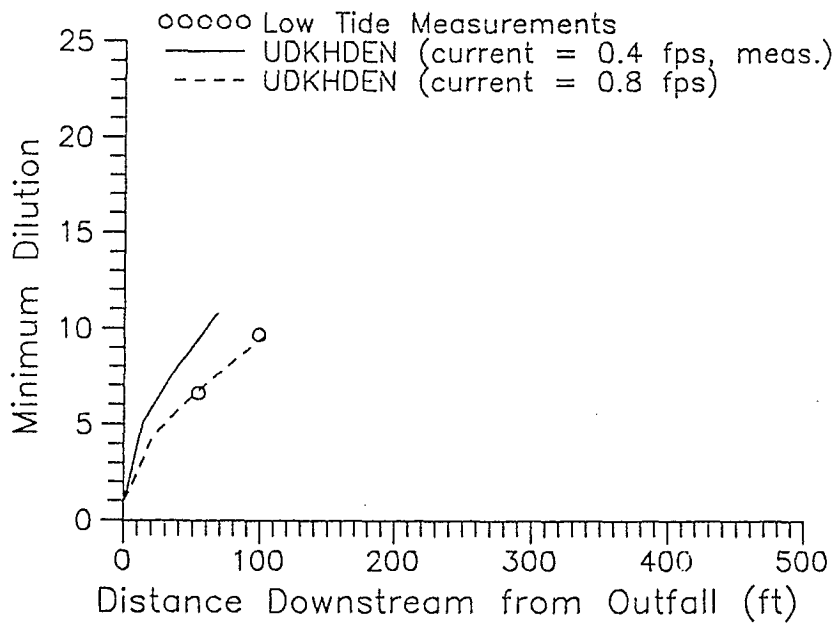
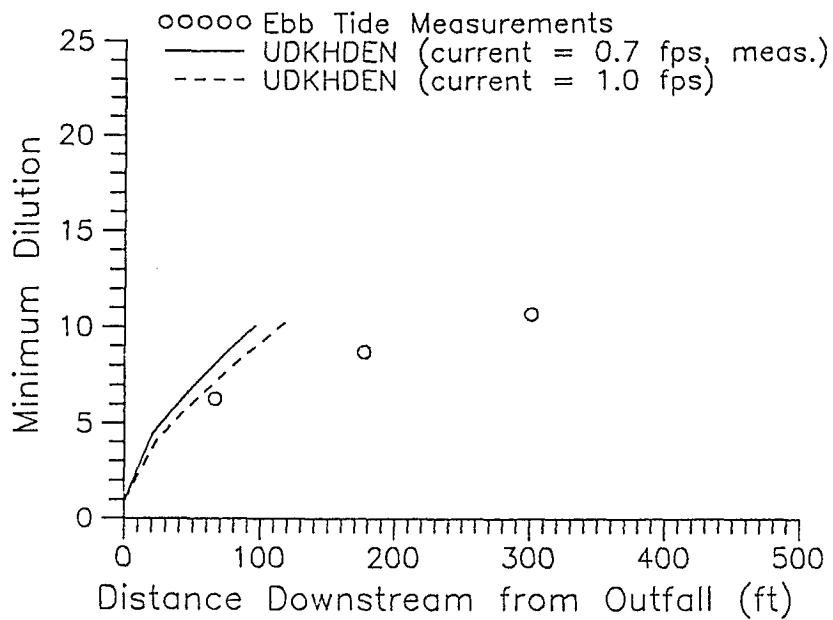


Philip Williams & Associates, Ltd.
 Consultants in Hydrology

Far Field Dye Concentration near Outfall
 (7/21-7/24/92)

SOURCE: Systech Engineers

Figure
 IV-12

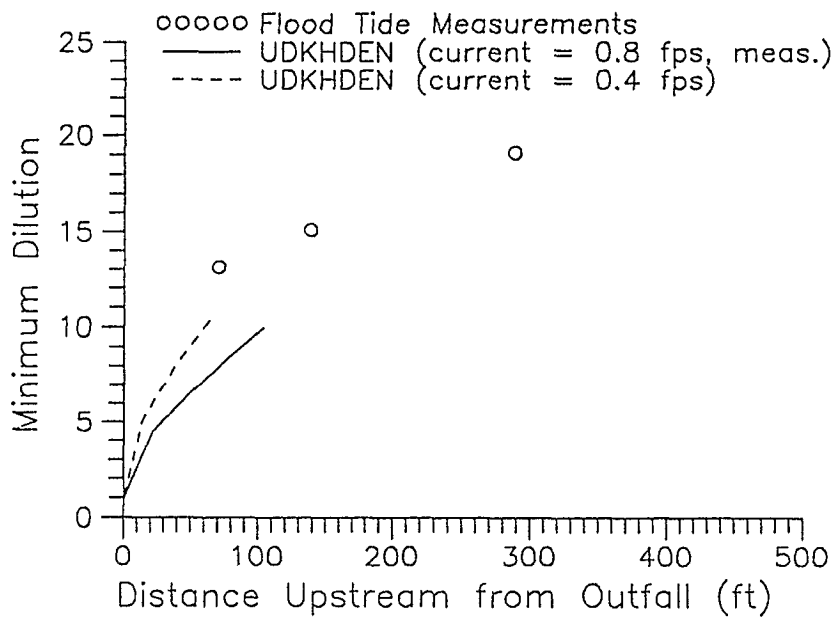


Philip Williams & Associates, Ltd.
Consultants in Hydrology

**Measured and Simulated Centerline Dilutions
in Near Field** (simulation stopped 120 seconds
after discharge)

SOURCE: Systech Engineers

Figure
V-1a

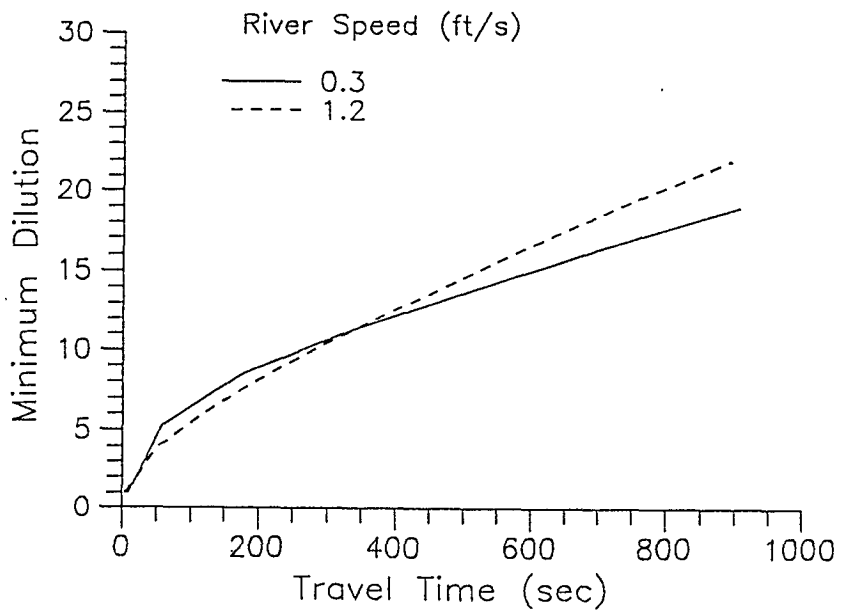


Philip Williams & Associates, Ltd.
Consultants in Hydrology

**Measured and Simulated Centerline Dilutions
in Near Field** (simulation stopped 120 seconds
after discharge)

SOURCE: Systech Engineers

Figure
V-1b

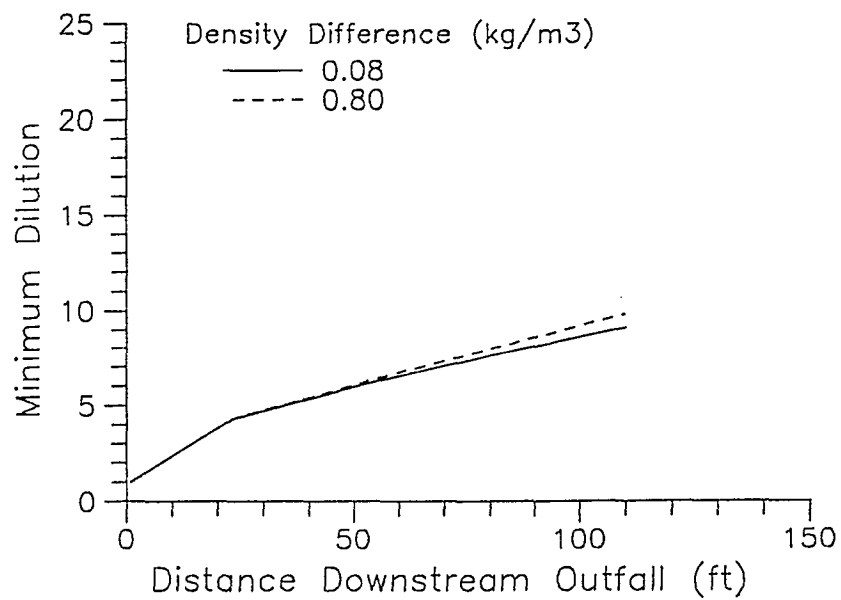


Philip Williams & Associates, Ltd.
 Consultants in Hydrology

**Effects of River Current on UDKHDEN
 Model Prediction of Minimum Dilution**

SOURCE: Systech Engineers

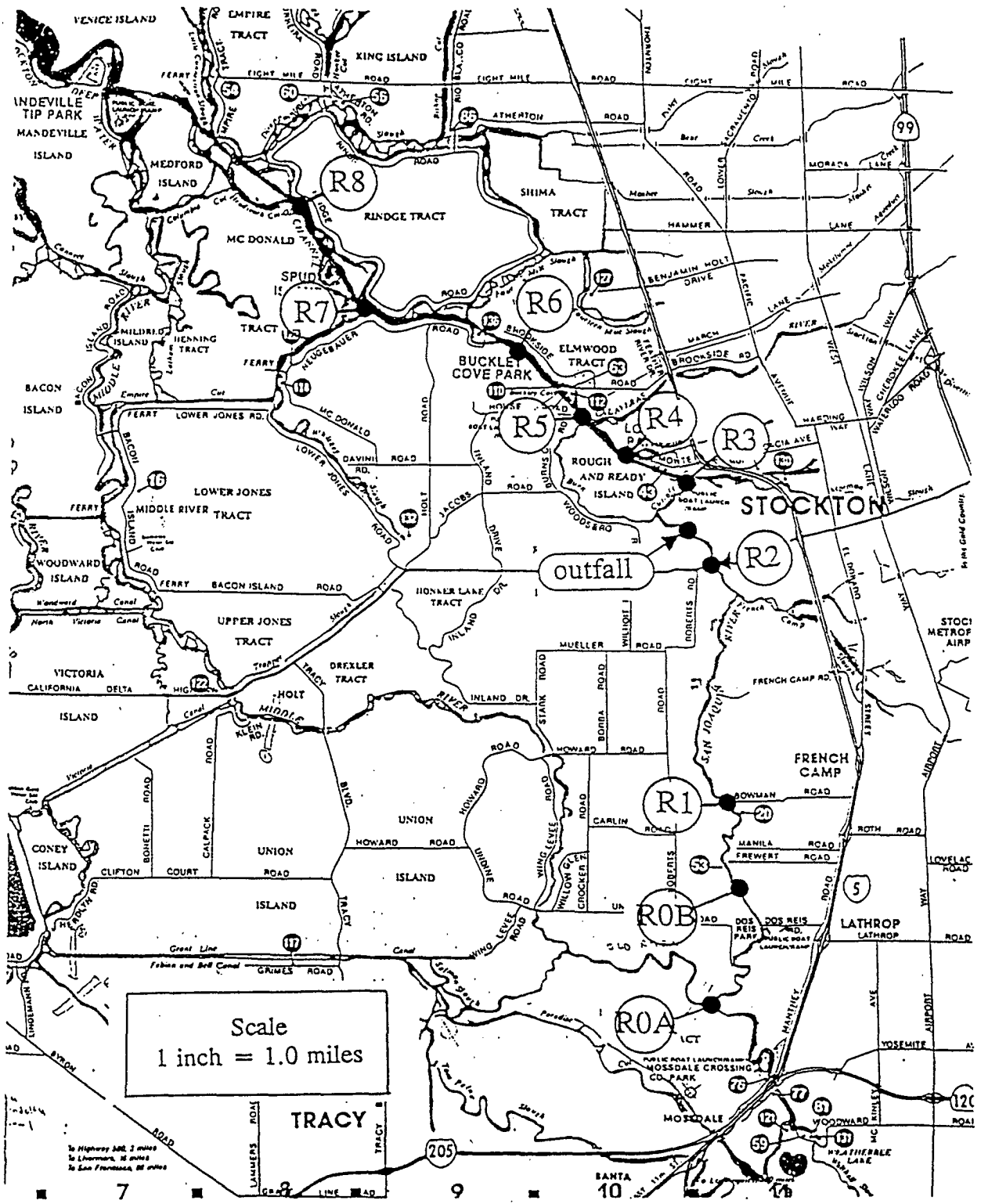
Figure
V-2



Philip Williams & Associates, Ltd.
Consultants in Hydrology

**Effects of Density Difference on UDKHDEN
Model Prediction of Minimum Dilution (river
current = 0.9 fps)**
SOURCE: Systech Engineers

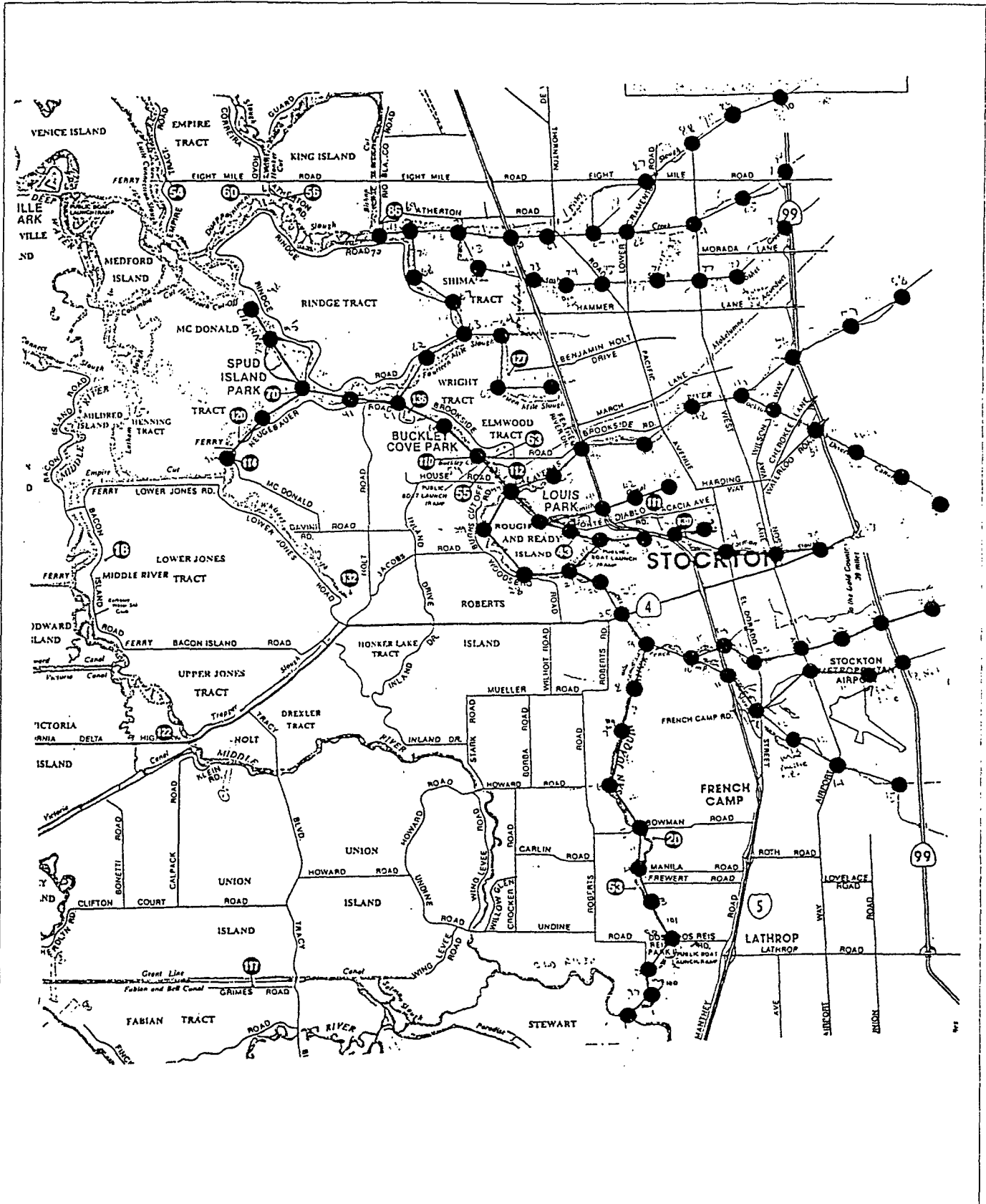
Figure
V-3



Philip Williams & Associates, Ltd.
 Consultants in Hydrology

Sampling Stations along San
 Joaquin River near Stockton

Figure
 VI-1

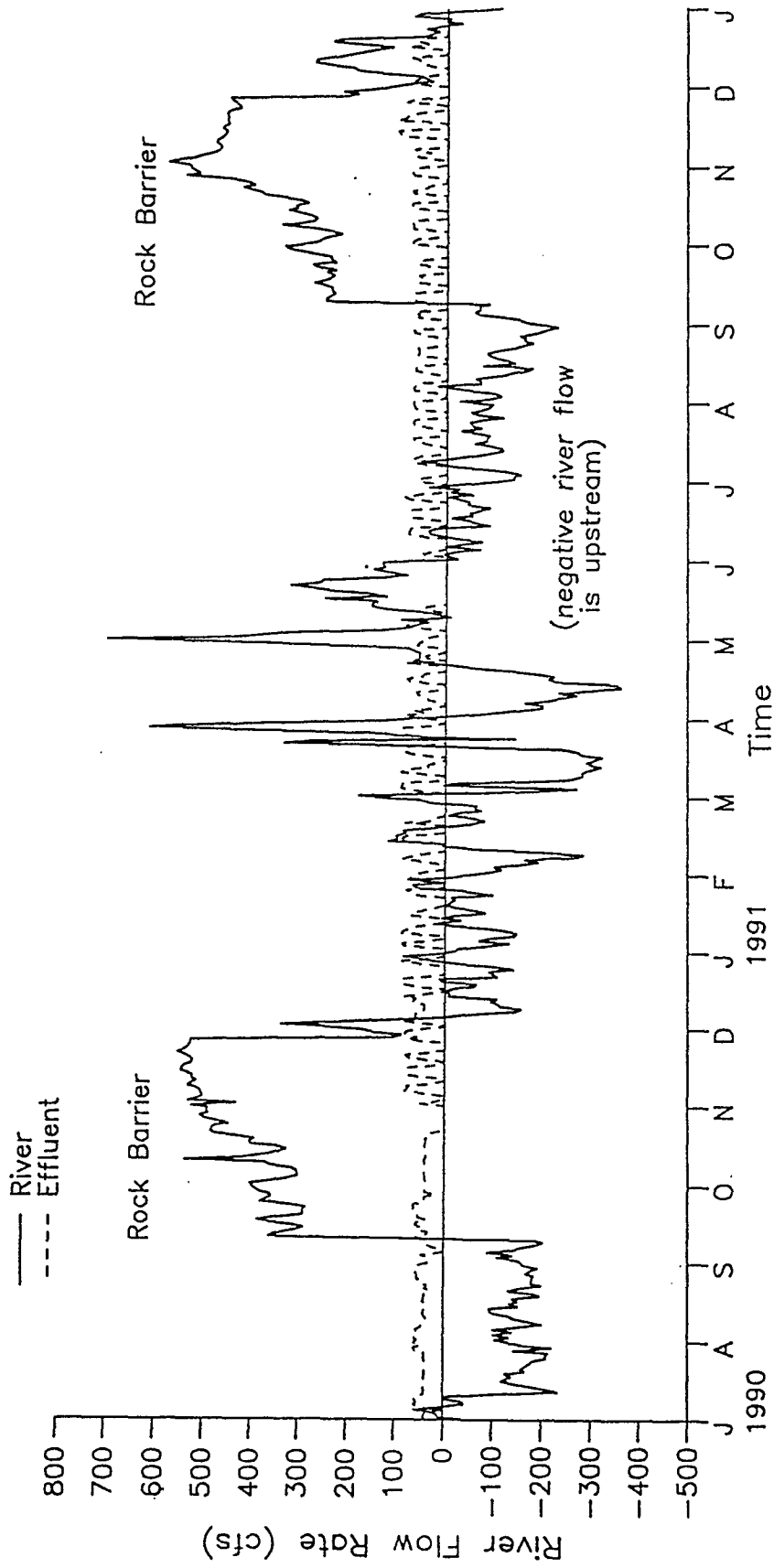


SOURCE: Systech Engineers


 Philip Williams & Associates, Ltd.
 Consultants in Hydrology

Link-Node Network of San
 Joaquin River near Stockton

Figure
 VI-2

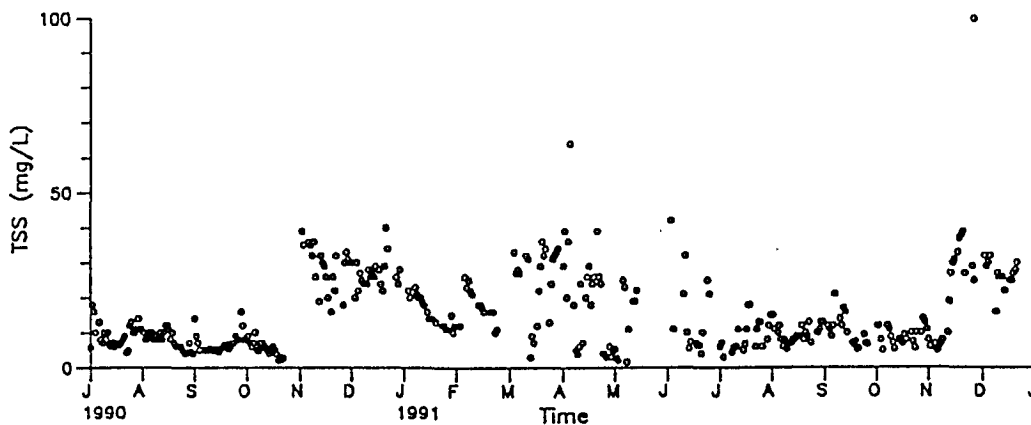
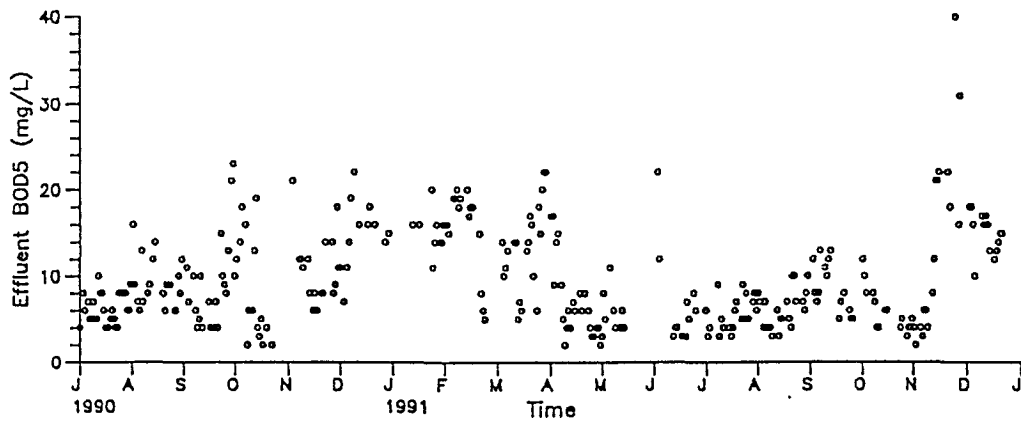
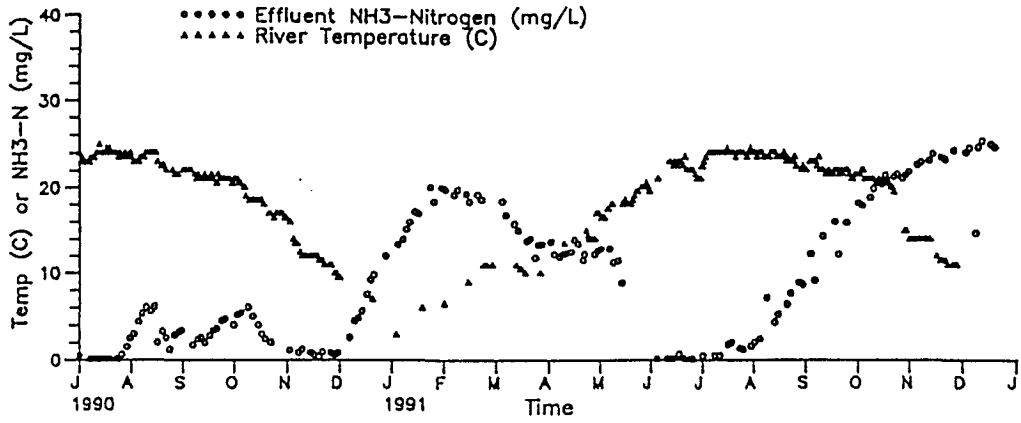


SOURCE: Systech Engineers

Philip Williams & Associates, Ltd.
 Consultants in Hydrology

River and Effluent Flow Rate from 7/90 to 12/91

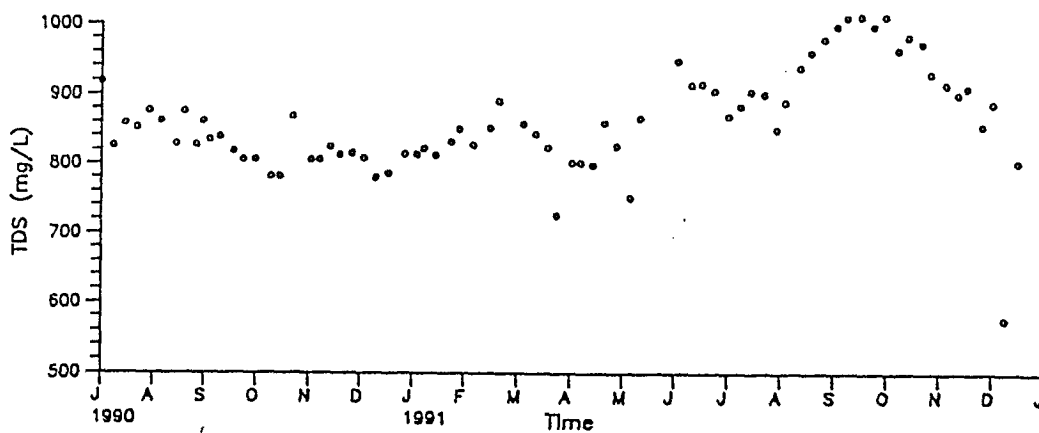
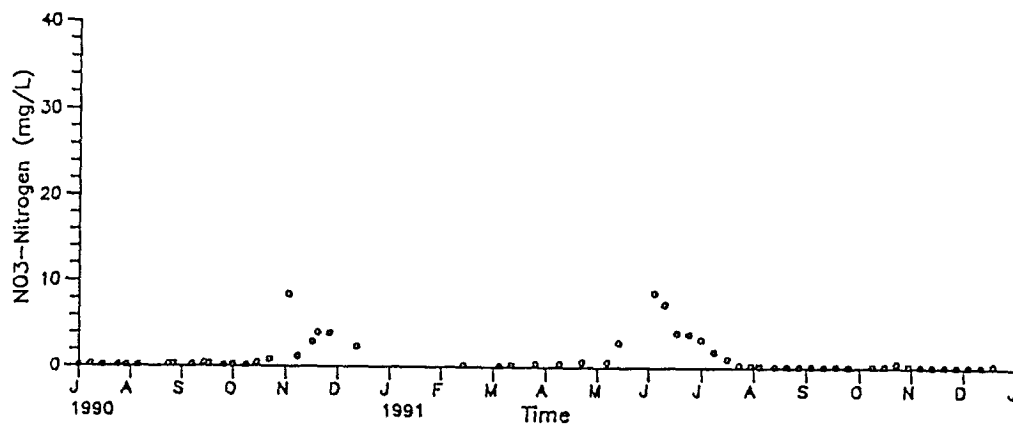
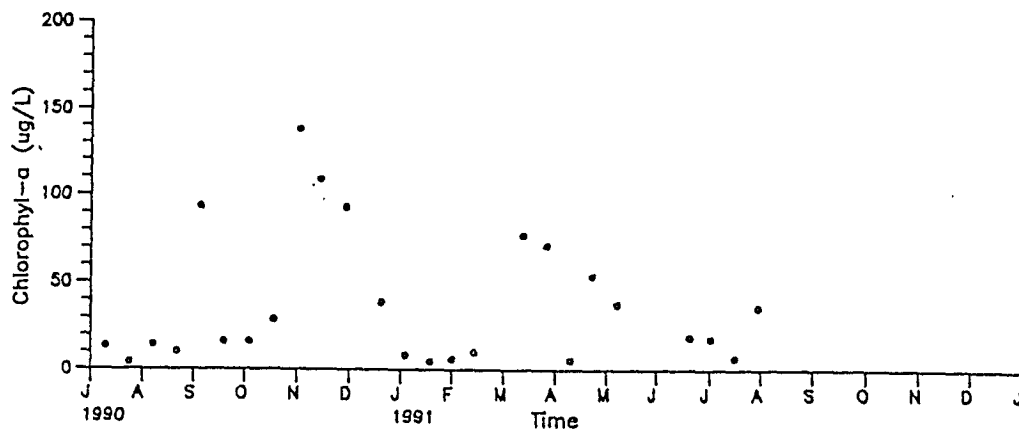
Figure VI-3



Philip Williams & Associates, Ltd.
Consultants in Hydrology

Stockton Effluent Water Quality
from 7/90 to 12/91

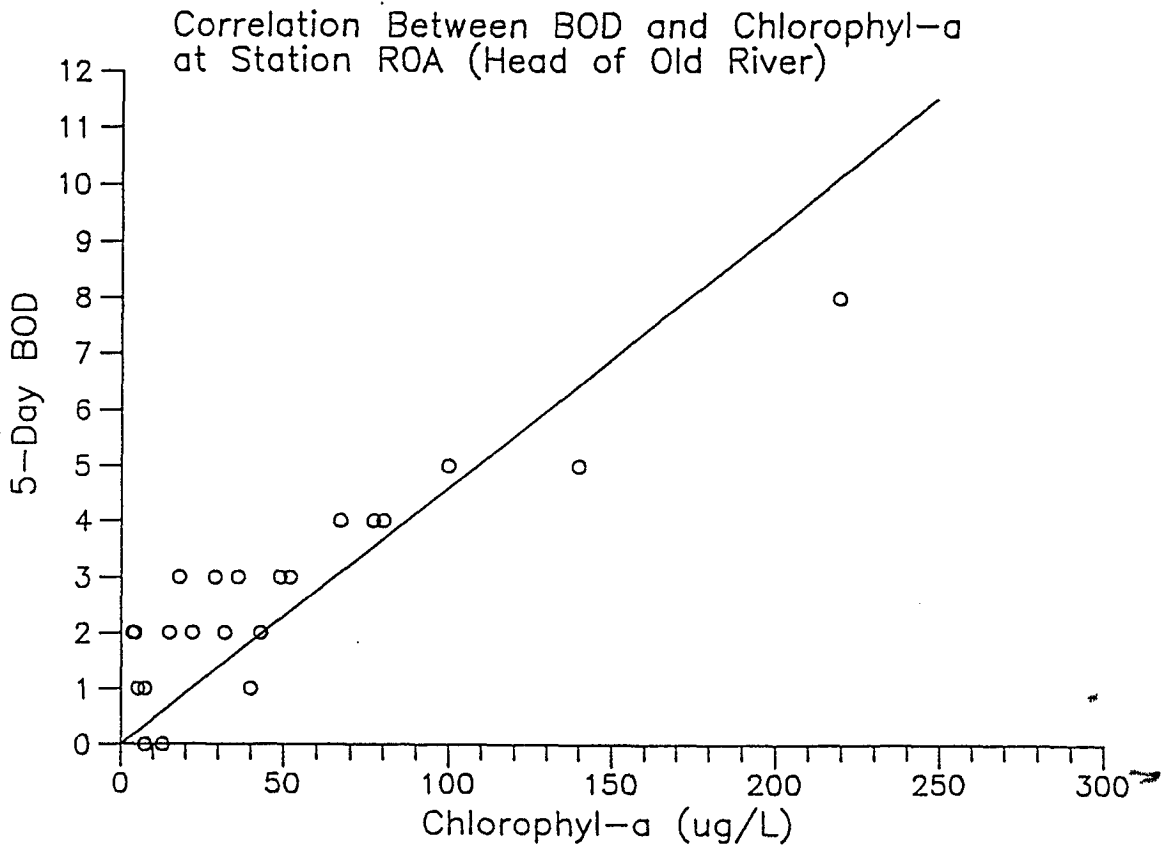
Figure
VI-4a



Philip Williams & Associates, Ltd.
Consultants in Hydrology

Stockton Effluent Water Quality
from 7/90 to 12/91

Figure
VI-4b



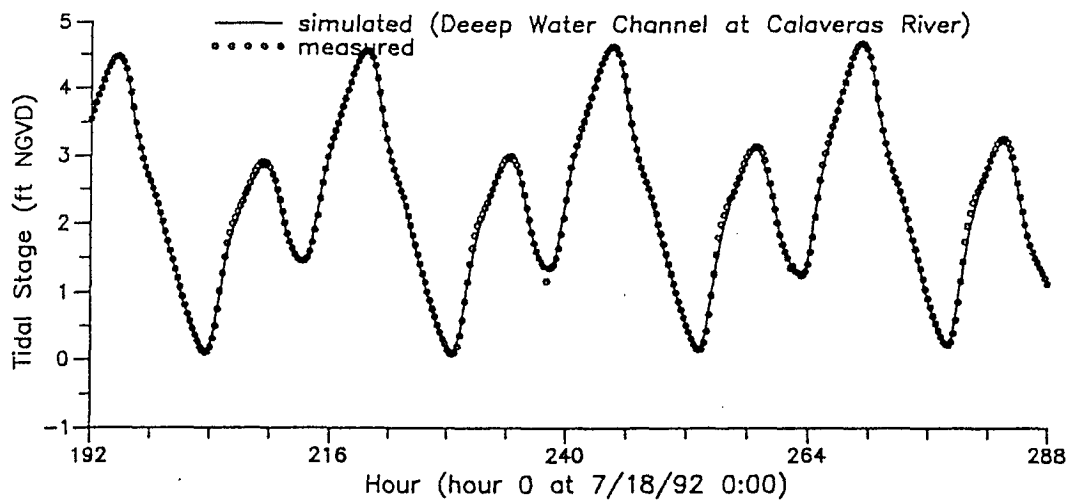
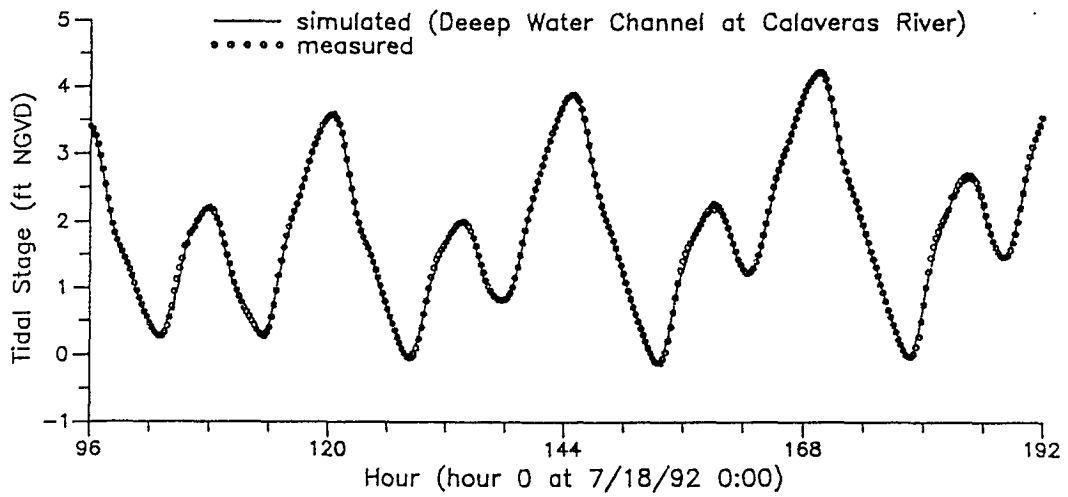
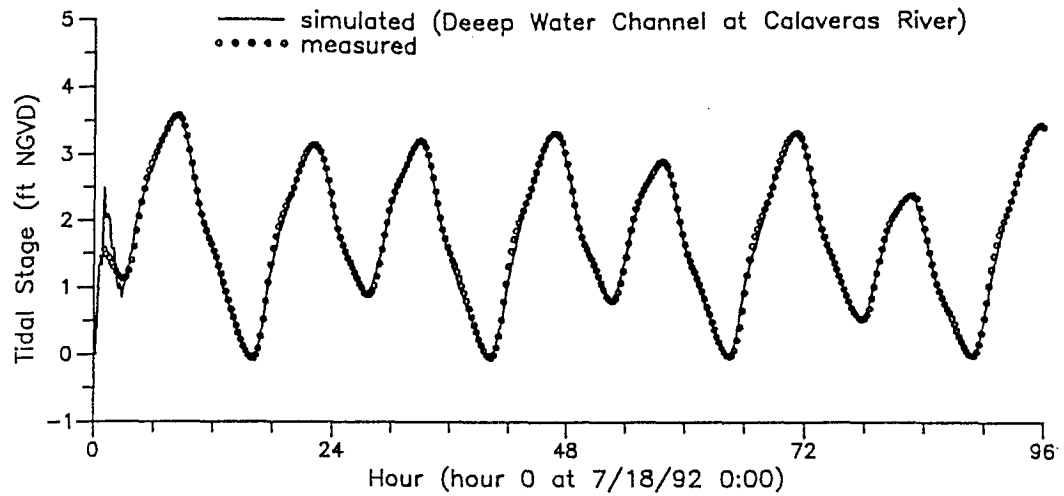
SOURCE: Systech Engineers



Philip Williams & Associates, Ltd.
Consultants in Hydrology

Effect of Algae Concentration on Total
BOD Measurement at Station ROA
(7/90 to 7/91)

Figure
VI-5

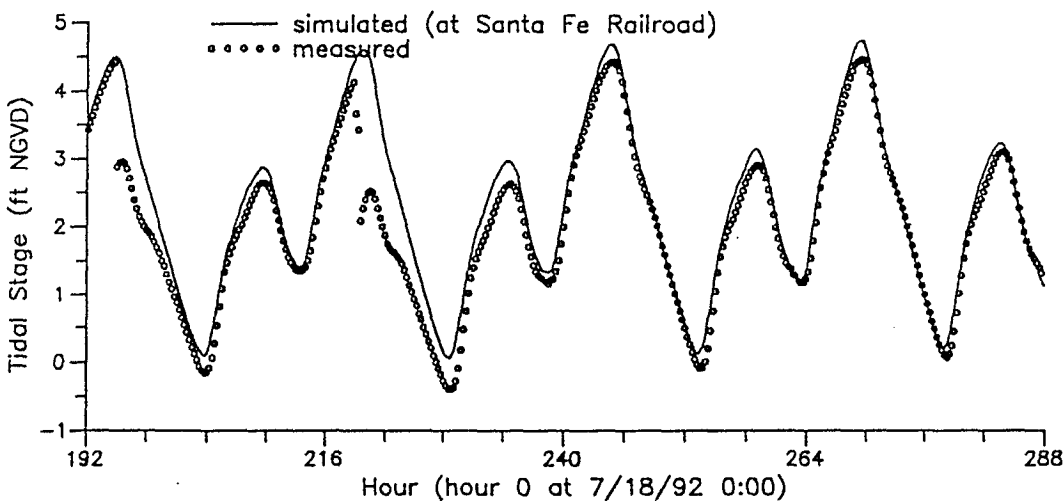
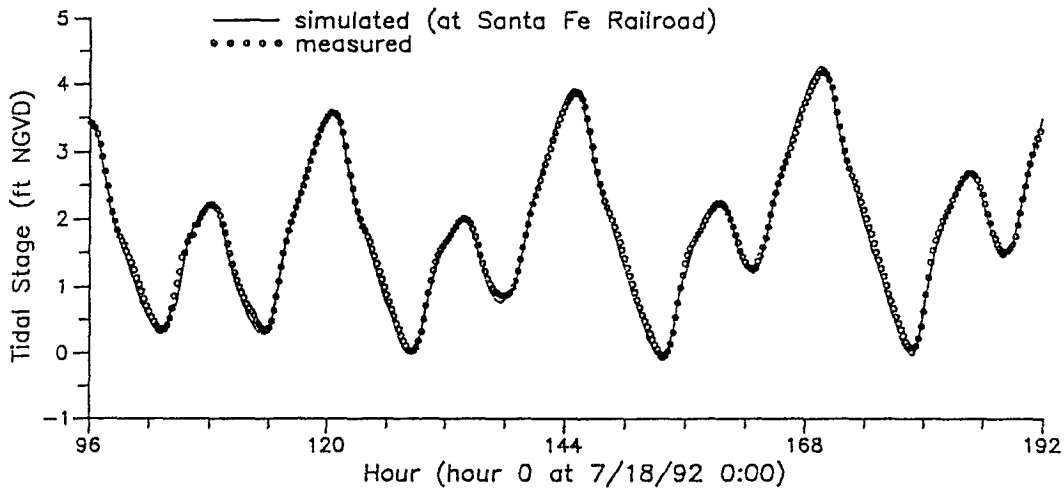
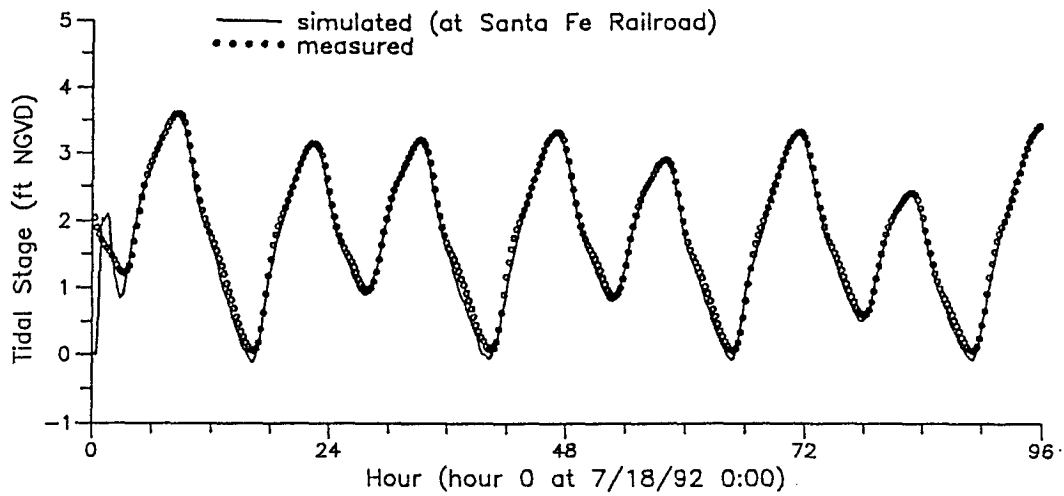


Philip Williams & Associates, Ltd.
Consultants in Hydrology

**Comparison of Observed and Simulated Tidal
Depths near Station R5 (7/18 - 7/29/92)**

SOURCE: Systech Engineers

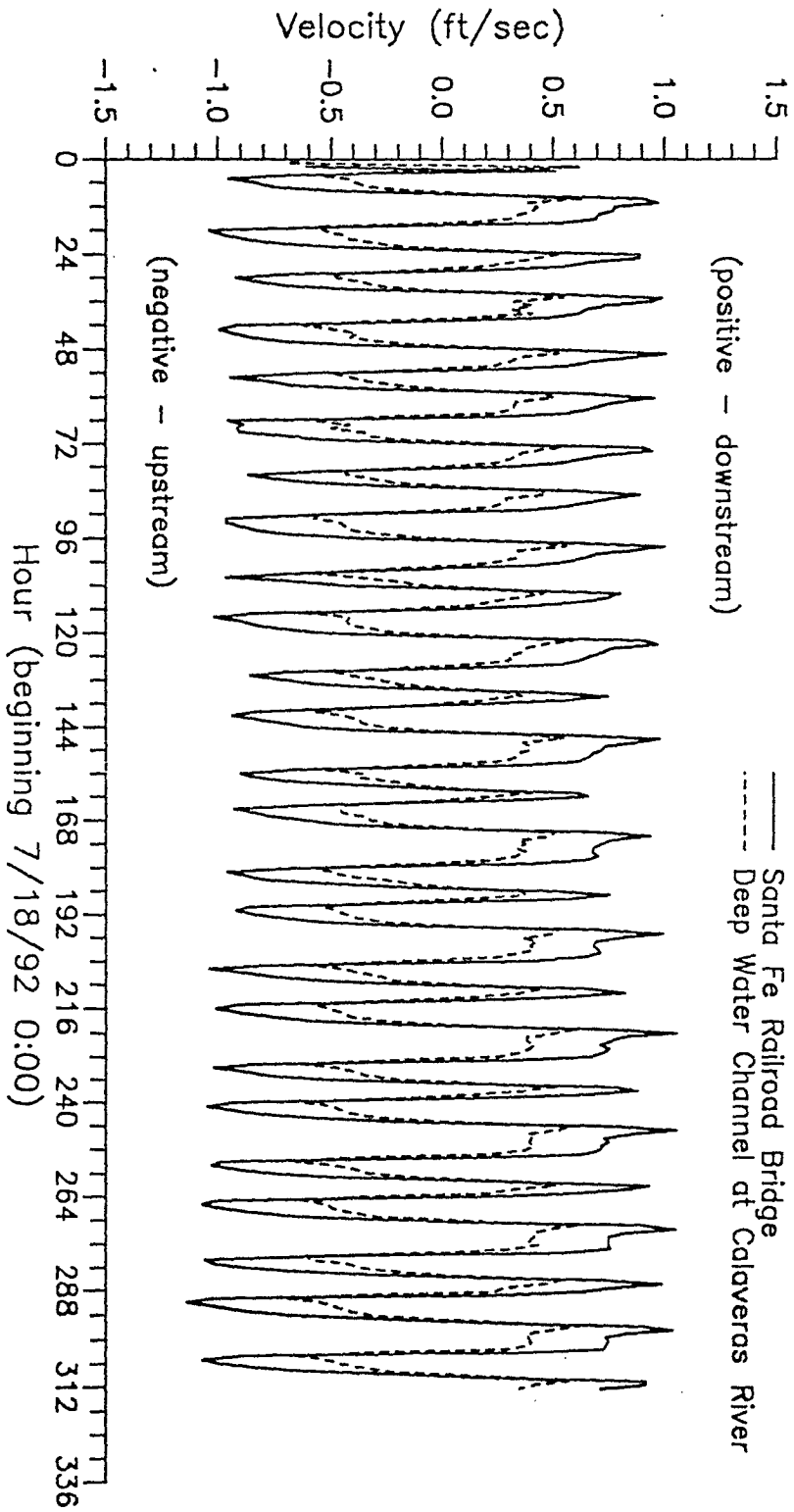
**Figure
VI-6**



Philip Williams & Associates, Ltd.
Consultants in Hydrology

**Comparison of Observed and Simulated Tidal
Depths at Santa Fe Railroad**
(7/18-7/24/92)
SOURCE: Systech Engineers

Figure
VI-7

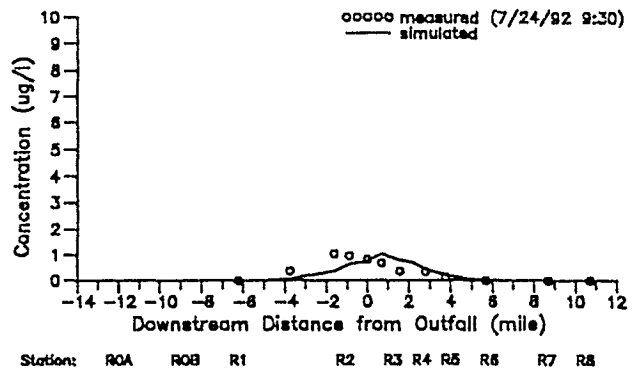
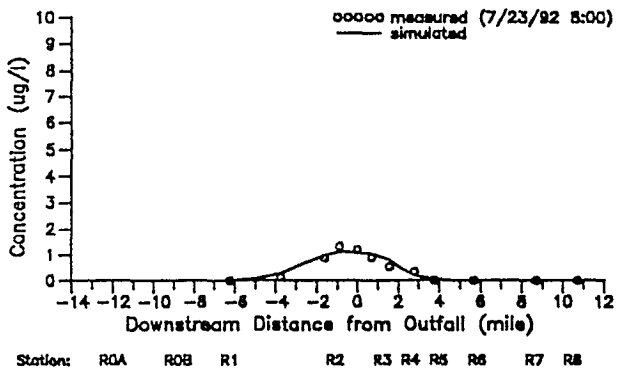
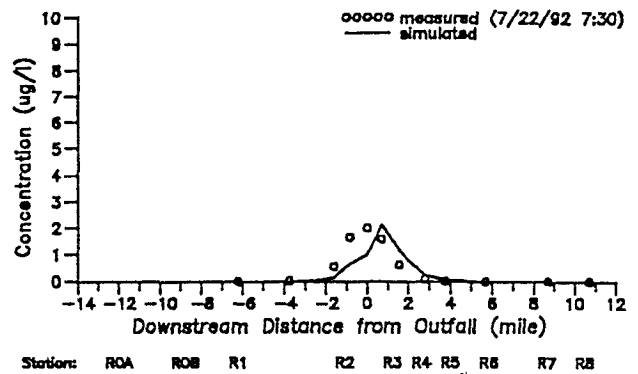
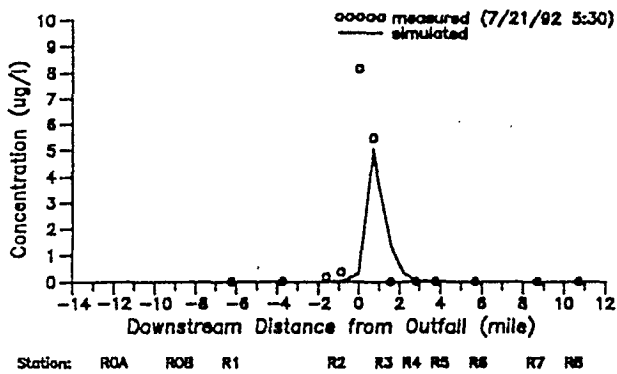


Philip Williams & Associates, Ltd.
Consultants in Hydrology

Simulated Currents in San Joaquin River (7/18-7/29/92)

SOURCE: Systech Engineers

Figure
VI-8

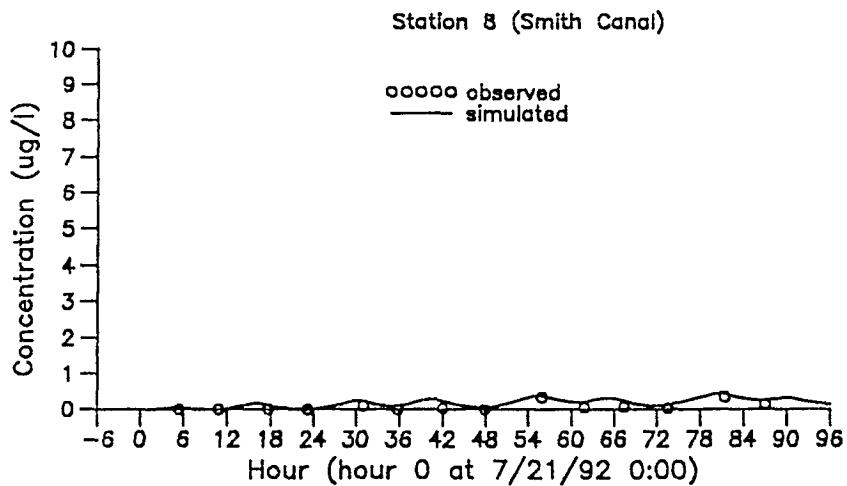
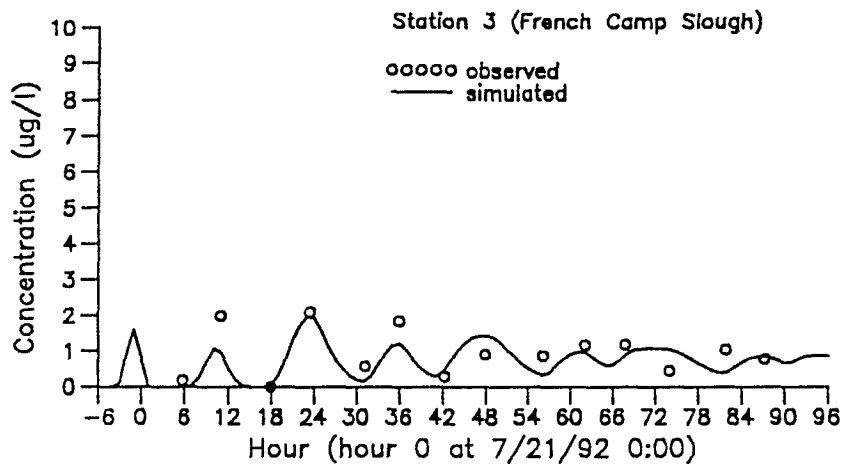


Philip Williams & Associates, Ltd.
 Consultants in Hydrology

**Comparison of Observed and Simulated Dye
 Concentration Profiles in the Far Field**

SOURCE: Systech Engineers

Figure
 VI-9

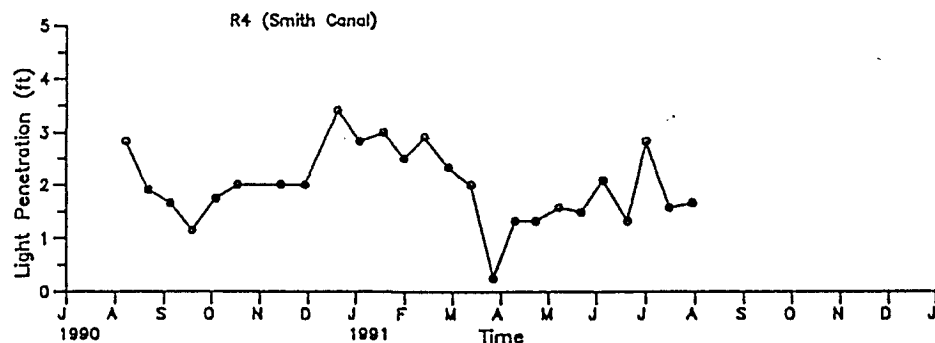
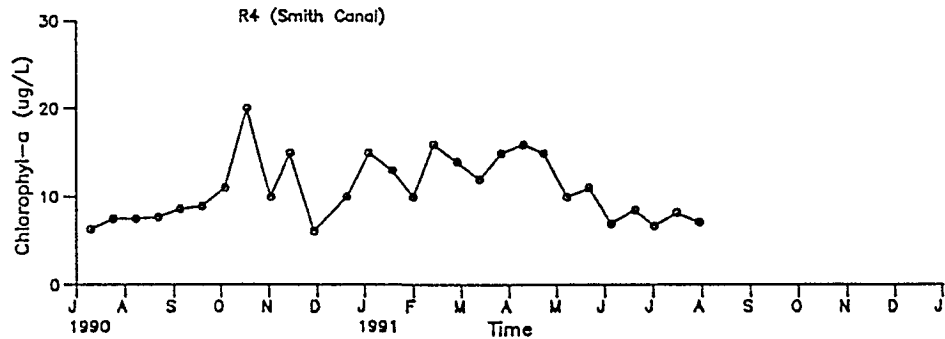
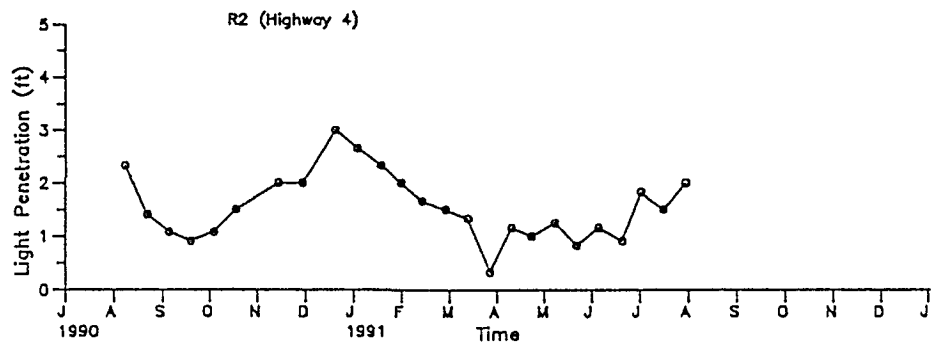
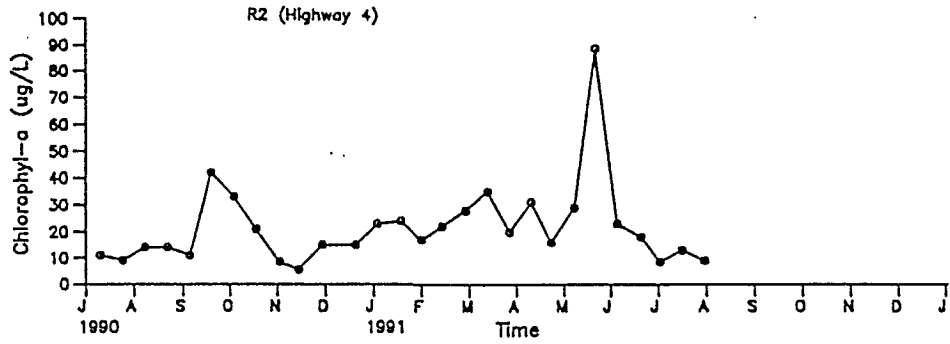


Philip Williams & Associates, Ltd.
Consultants in Hydrology

Comparison of Observed and Simulated Far
Field Dye Concentrations at Stations 3 and 8

SOURCE: Systech Engineers

Figure
VI-10



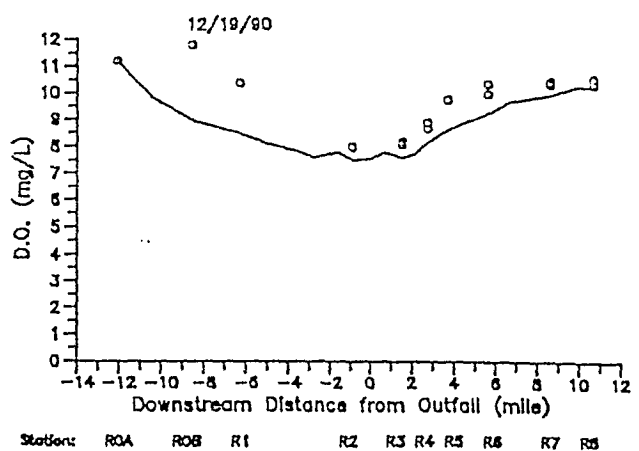
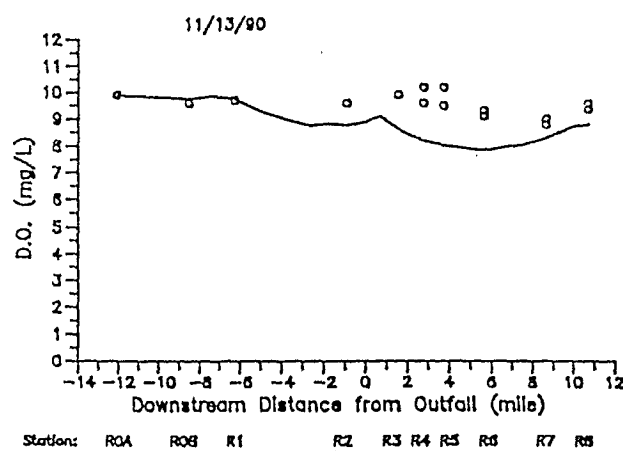
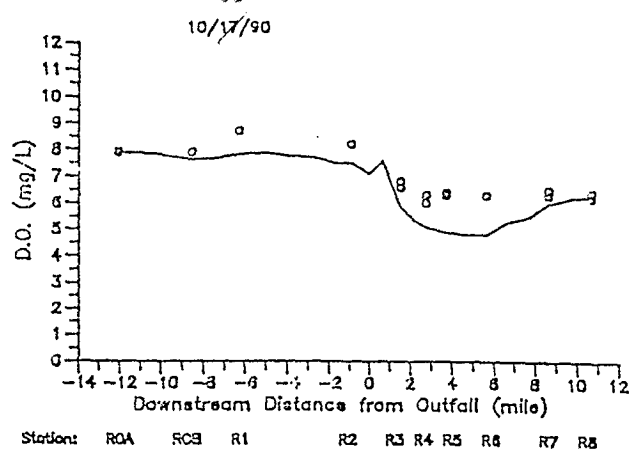
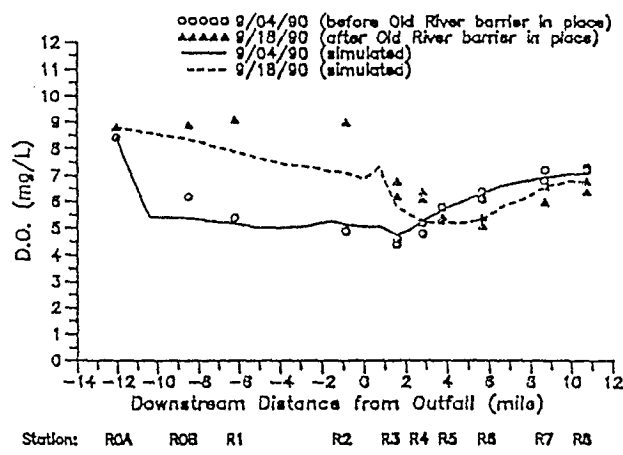
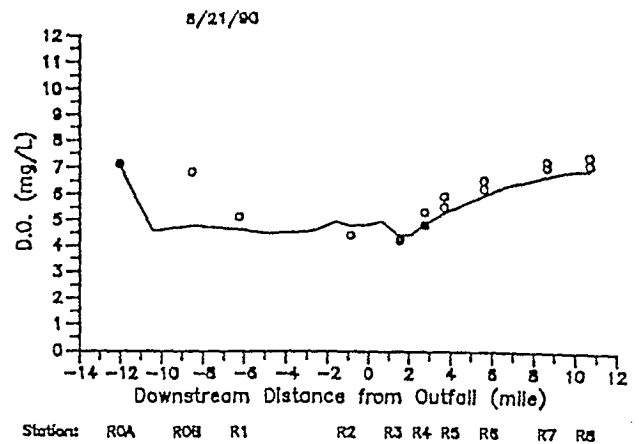
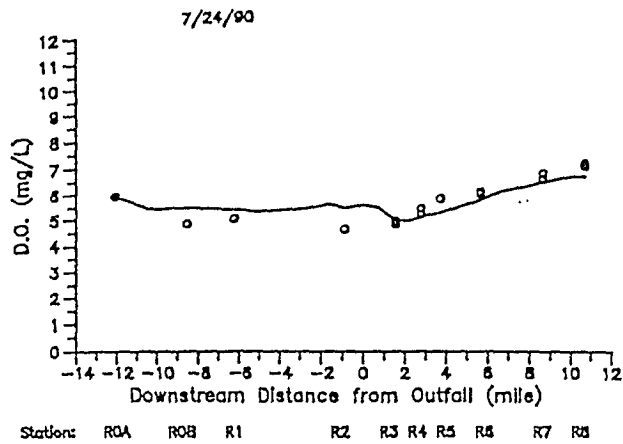
SOURCE: Systech Engineers



Philip Williams & Associates, Ltd.
Consultants in Hydrology

Measured Chlorophyll-a and Light Penetration
at Stations R2 and R4 from 7/90 to 7/91

Figure
VI-11



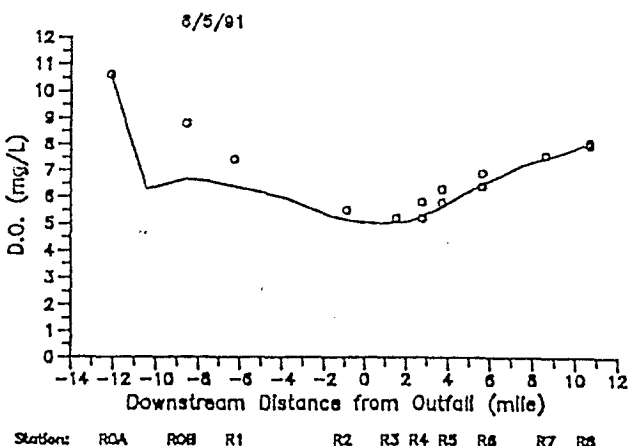
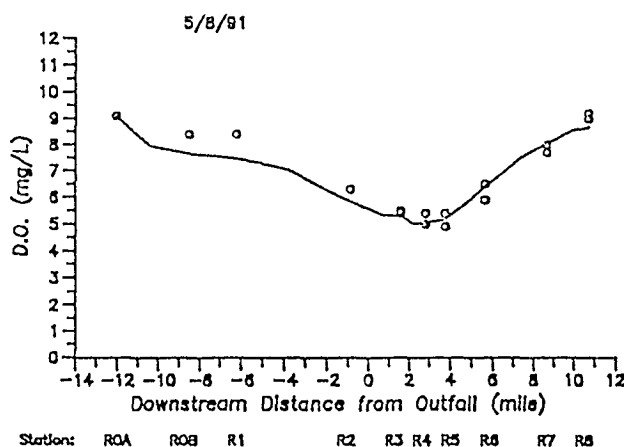
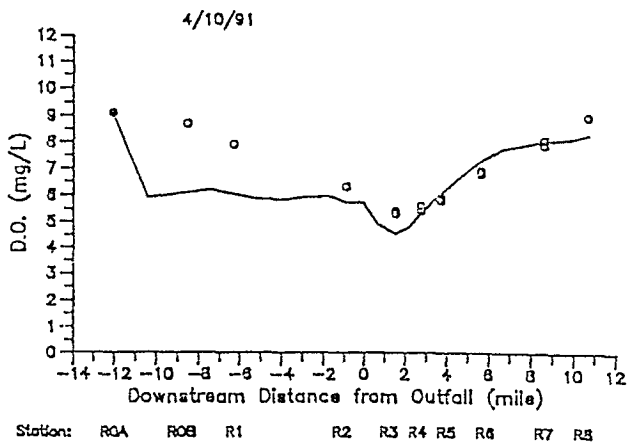
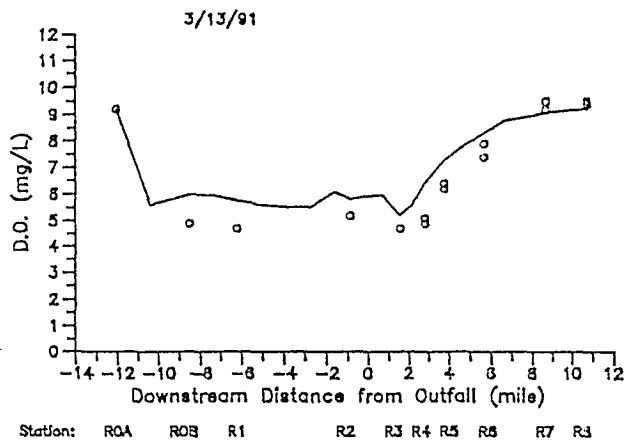
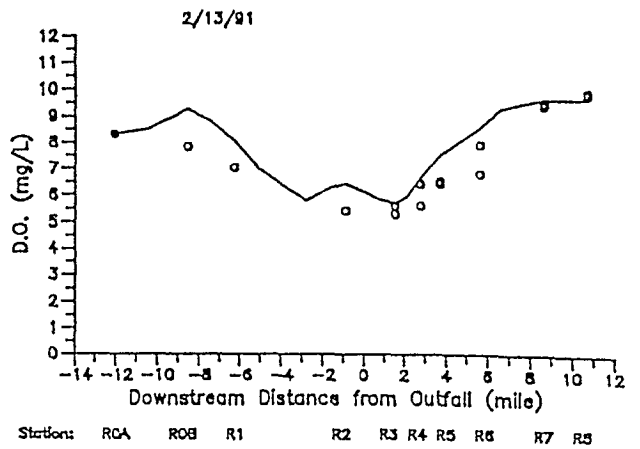
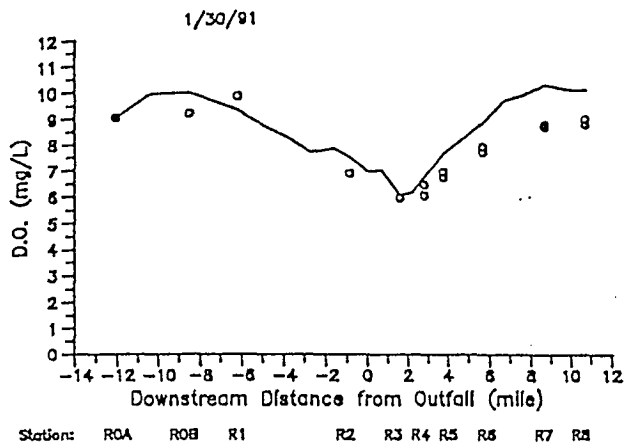
SOURCE: Systech Engineers



Philip Williams & Associates, Ltd.
Consultants in Hydrology

Comparison of Observed and Simulated
Dissolved Oxygen Profiles from 7/90 to 7/91

Figure
VI-12a



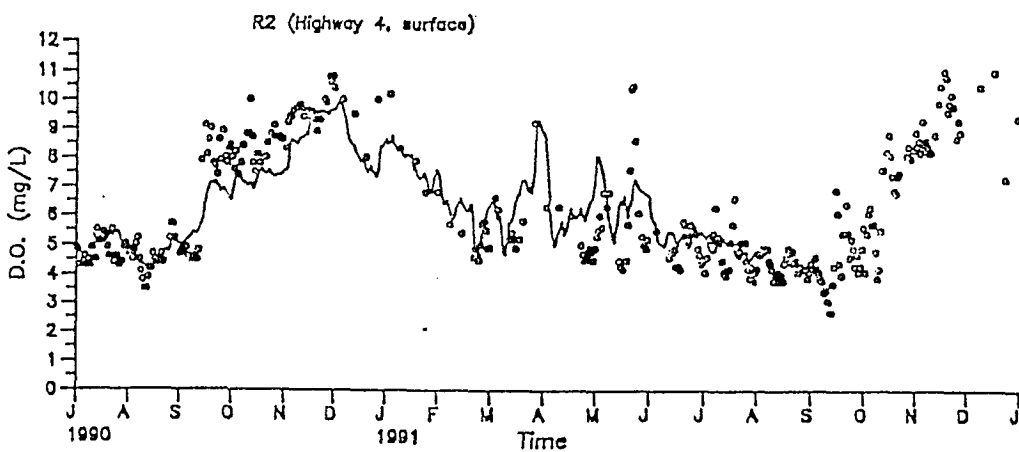
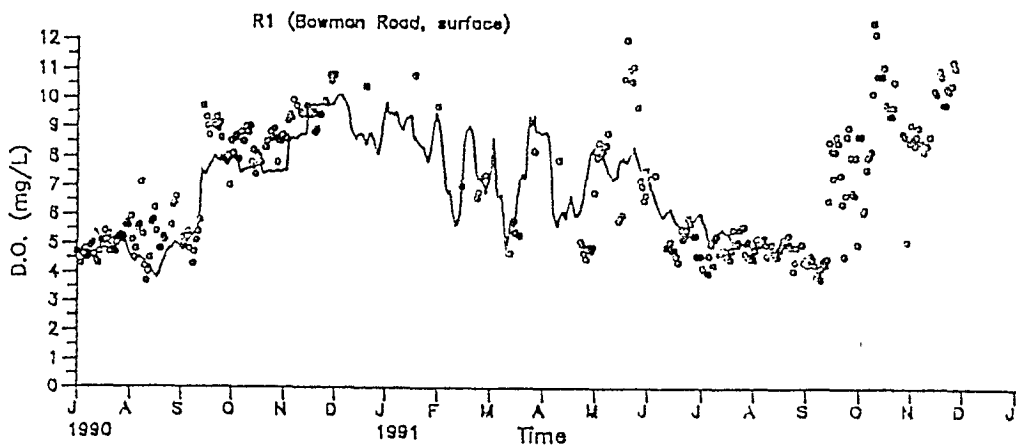
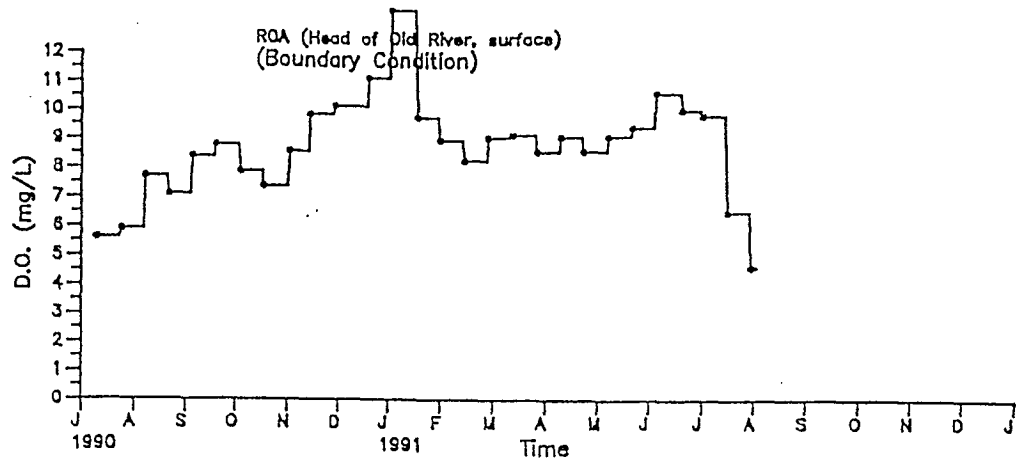
SOURCE: Systech Engineers



Philip Williams & Associates, Ltd.
Consultants in Hydrology

Comparison of Observed and Simulated
Dissolved Oxygen Profiles from 7/90 to 7/91

Figure
VI-12b



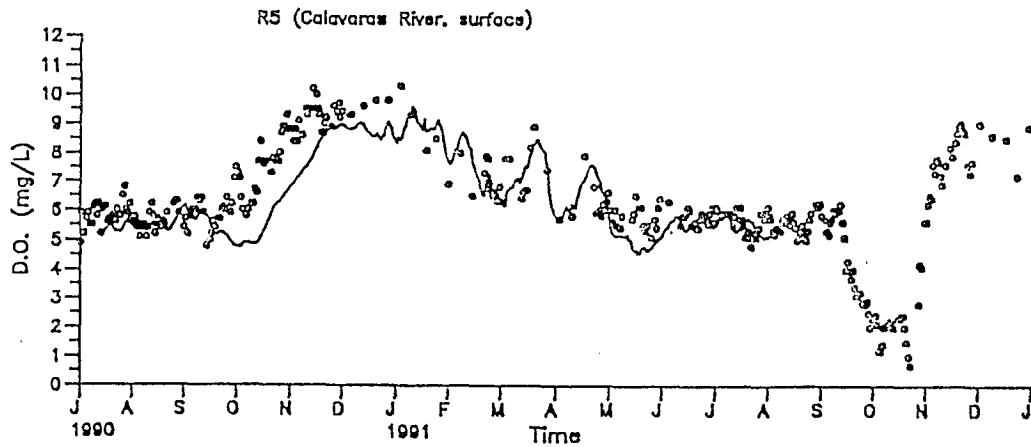
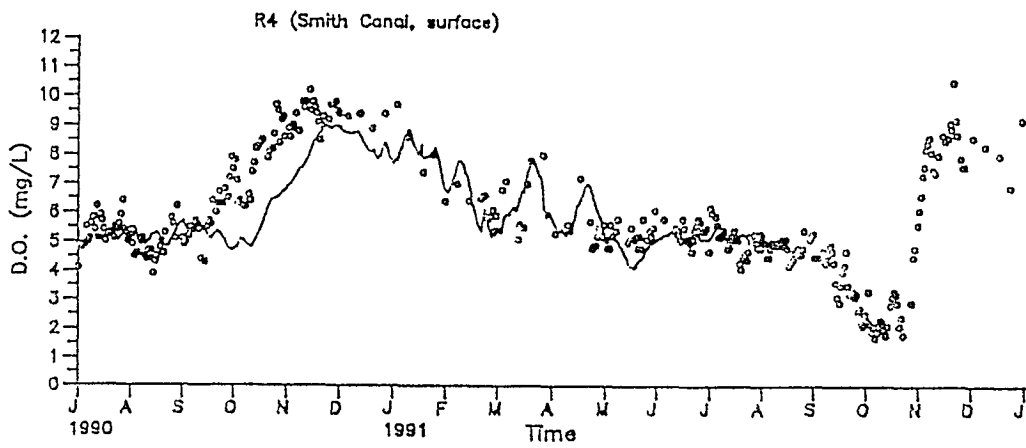
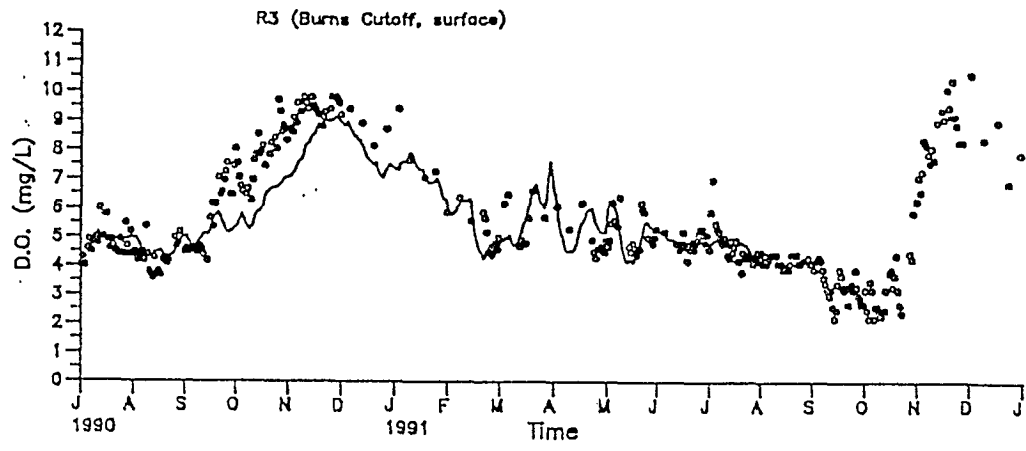
SOURCE: Systech Engineers



Philip Williams & Associates, Ltd.
Consultants in Hydrology

Comparison of Observed and Simulated Dissolved
Oxygen Concentration at Station R0A to R8
From 7/90 to 7/91

Figure
VI-13a



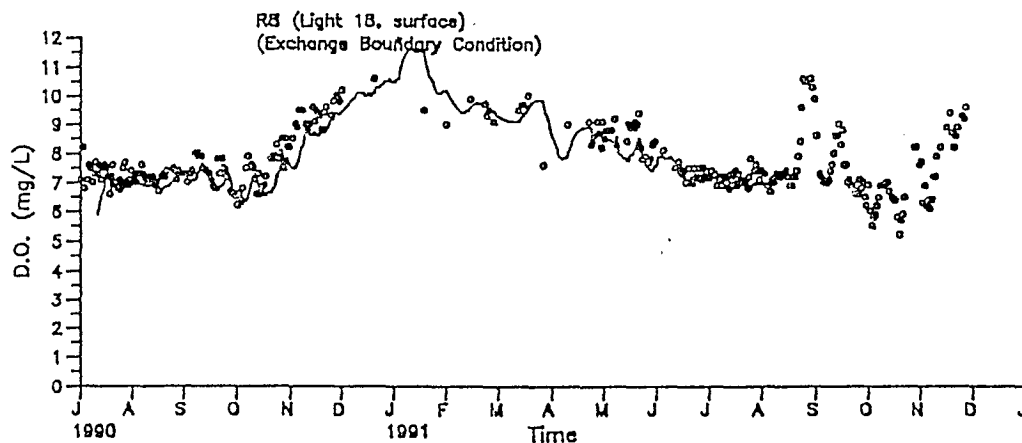
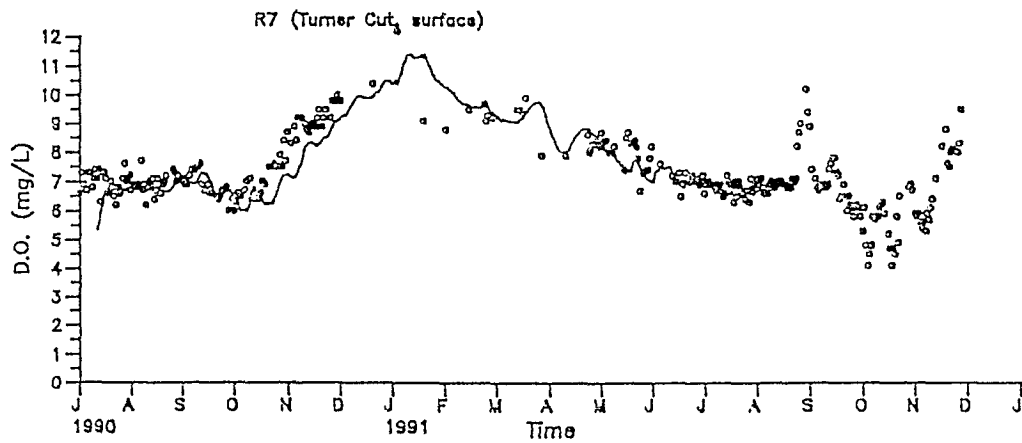
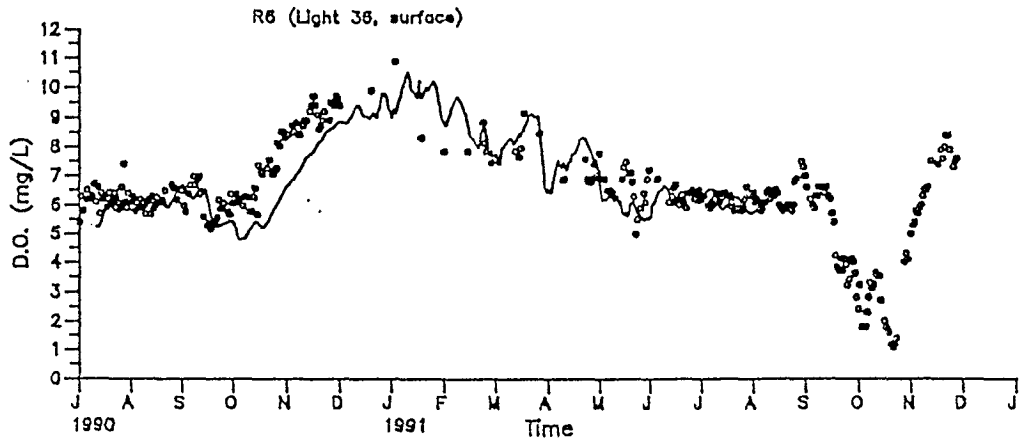
SOURCE: Systech Engineers



Philip Williams & Associates, Ltd.
Consultants in Hydrology

Comparison of Observed and Simulated Dissolved
Oxygen Concentration at Station R0A to R8
From 7/90 to 7/91

Figure
VI-13b



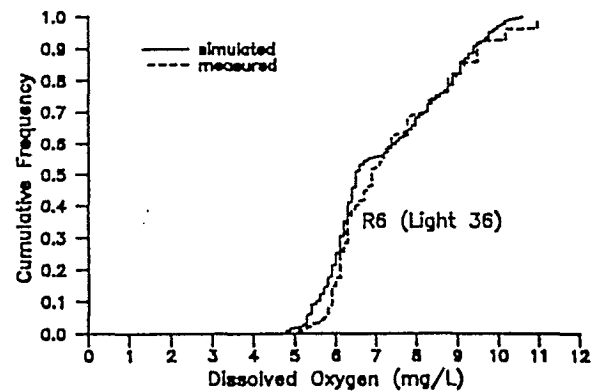
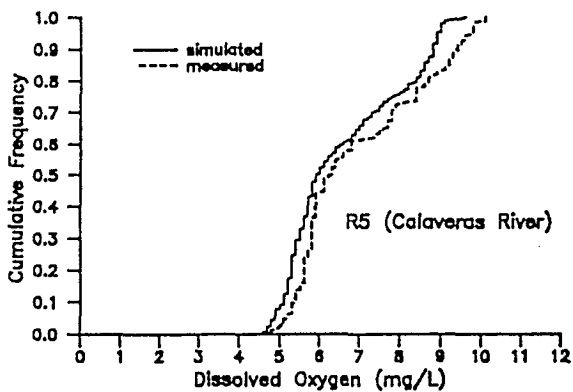
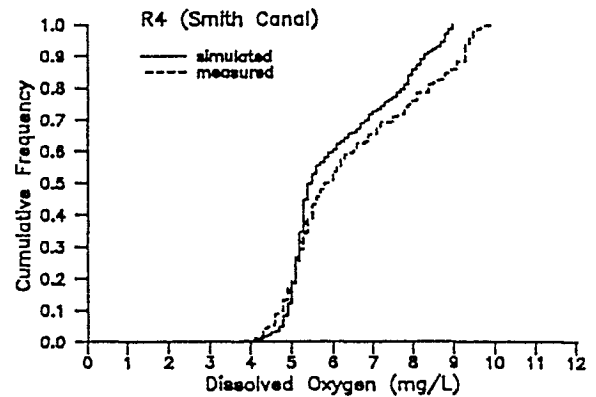
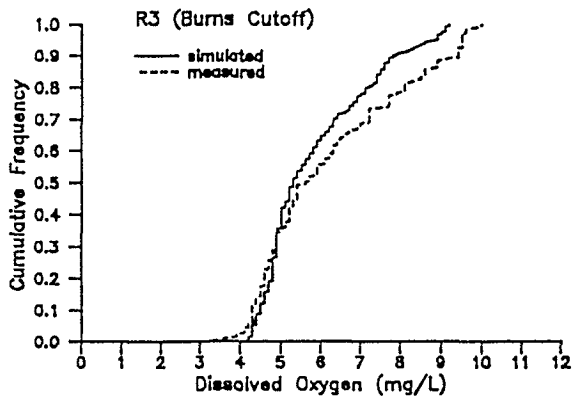
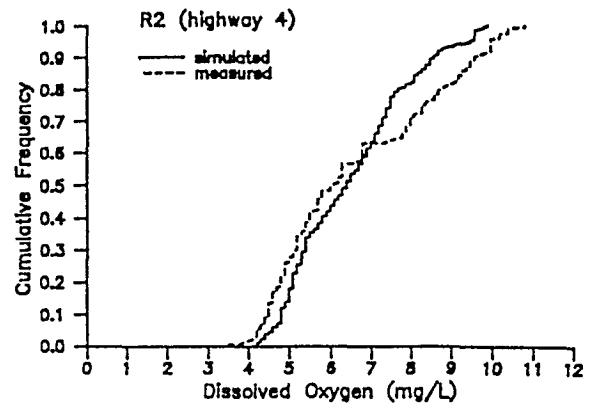
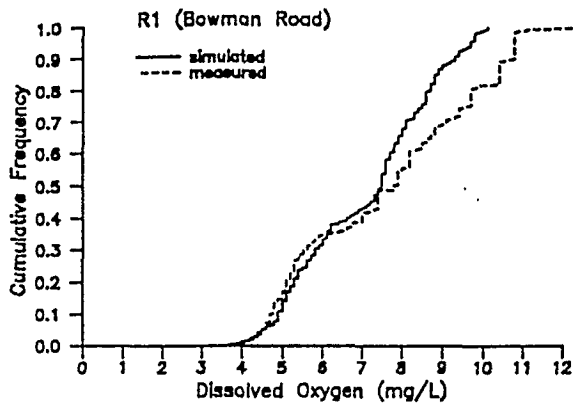
SOURCE: Systech Engineers



Philip Williams & Associates, Ltd.
Consultants in Hydrology

Comparison of Observed and Simulated Dissolved
Oxygen Concentration at Station R0A to R8
From 7/90 to 7/91

Figure
VI-13c



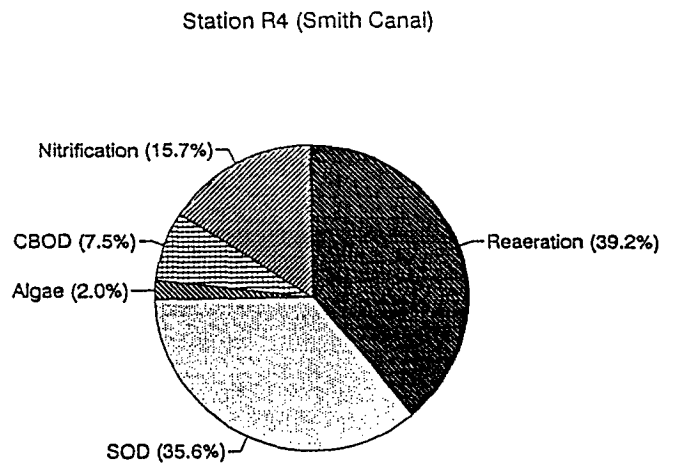
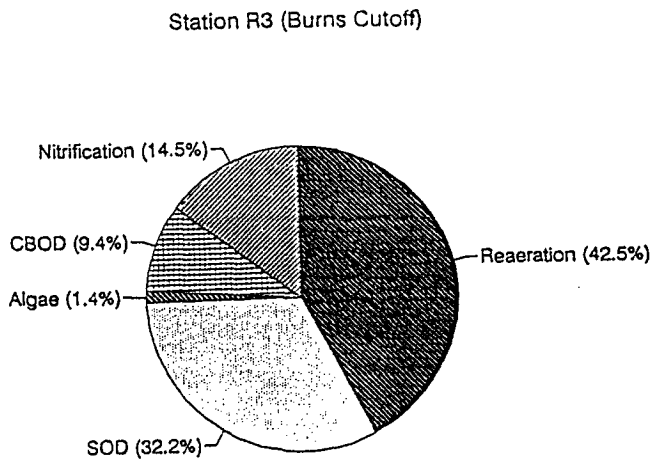
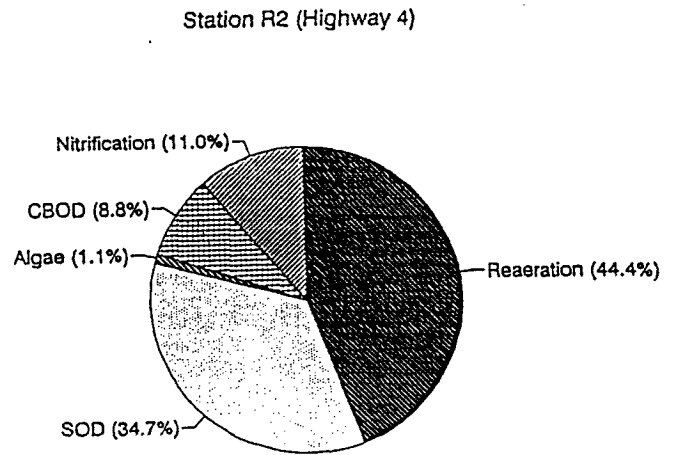
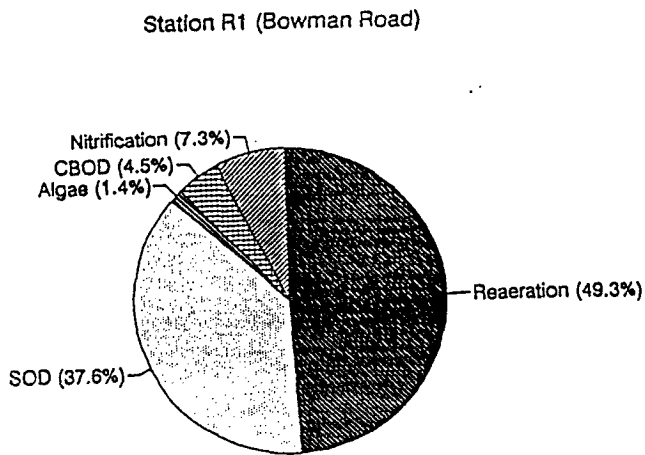
SOURCE: Systech Engineers



Philip Williams & Associates, Ltd.
Consultants in Hydrology

Comparison of Observed and Simulated
Cumulative Frequency of Dissolved Oxygen
for Station R1 to R6 from 7/90 to 7/91

Figure
VI-14



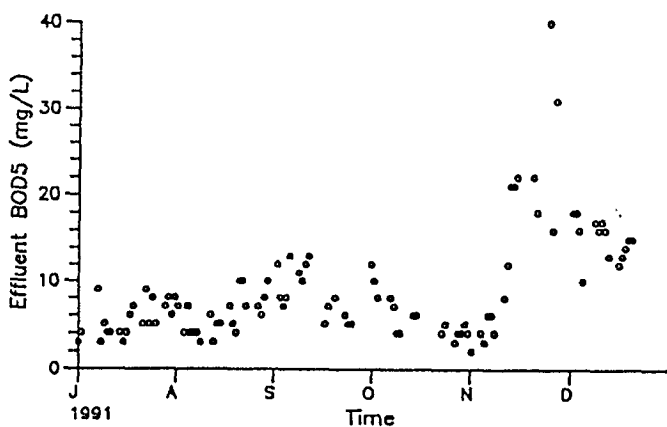
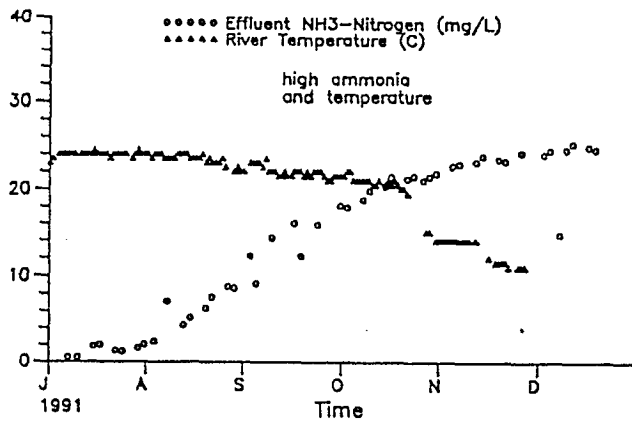
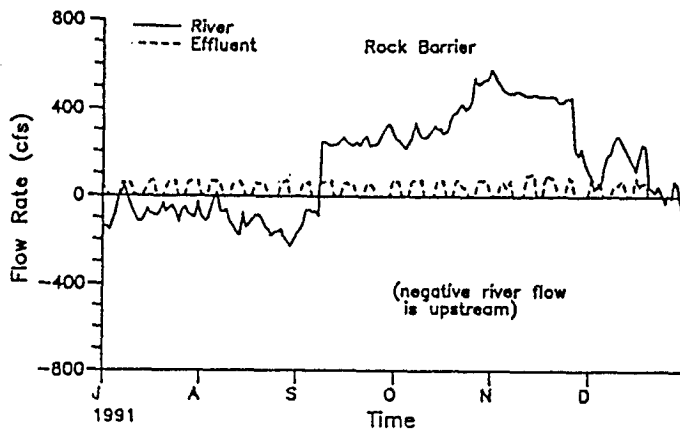
SOURCE: Systech Engineers



Philip Williams & Associates, Ltd.
Consultants in Hydrology

Oxygen Budget at Stations R1 to R4 for
Calibration Period (7/90-7/91)

Figure
VI-15



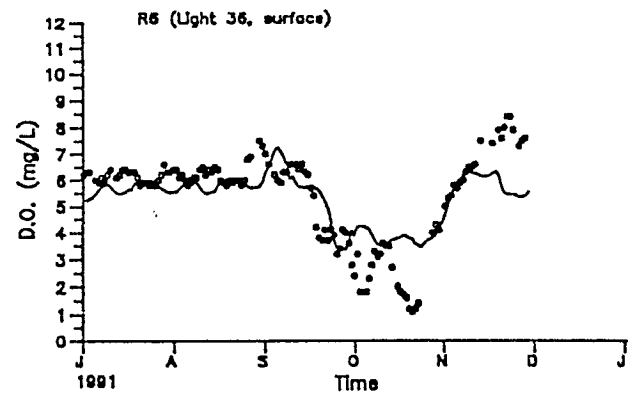
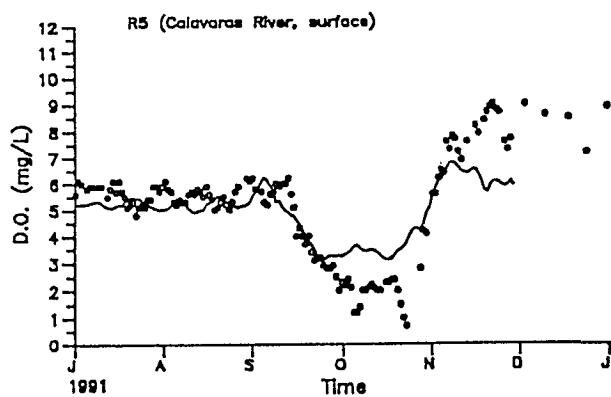
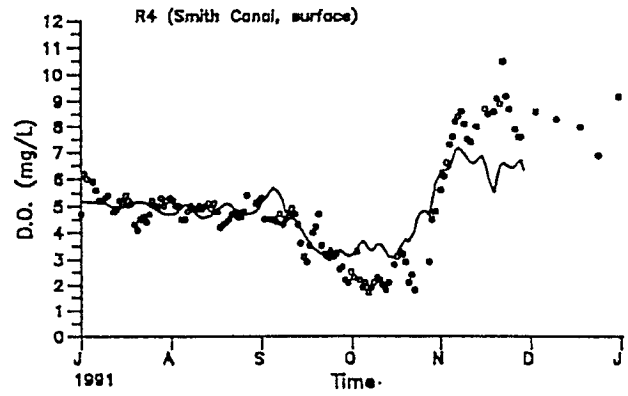
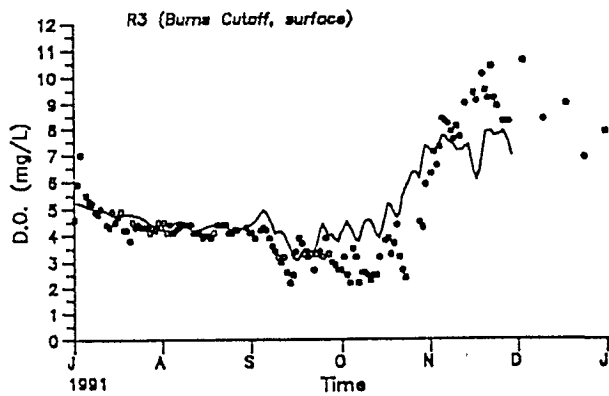
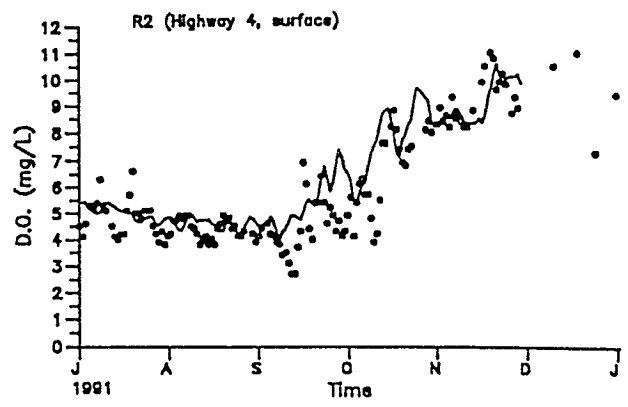
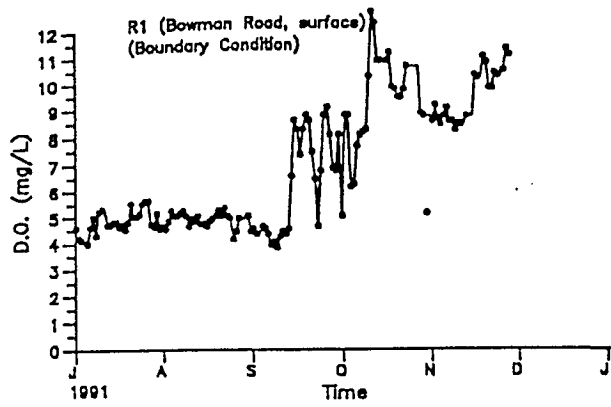
SOURCE: Systech Engineers



Philip Williams & Associates, Ltd.
Consultants in Hydrology

Effluent and River Conditions During
Verification Period (7/91-12/91)

Figure
VI-16



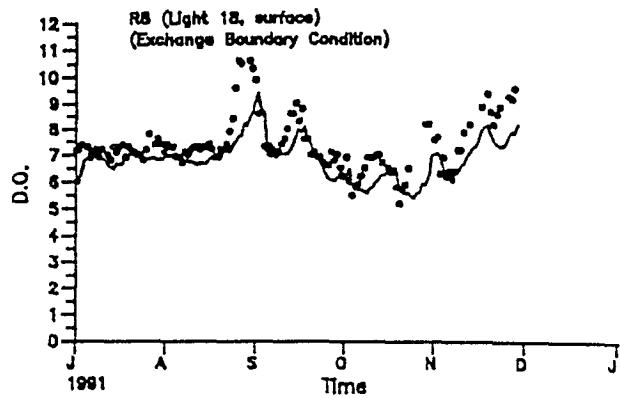
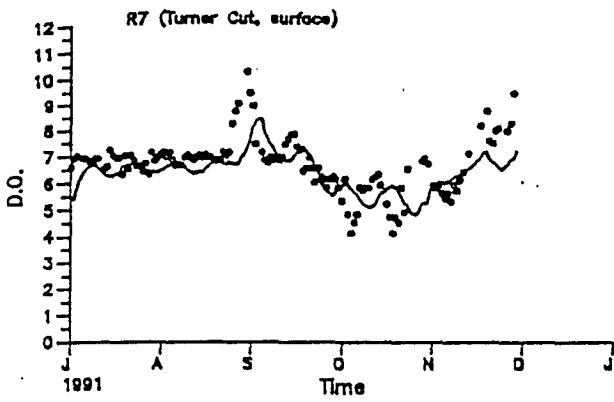
SOURCE: Systech Engineers



Philip Williams & Associates, Ltd.
Consultants in Hydrology

Comparison of Observed and Simulated Dissolved
Oxygen Concentration at Stations R0A to R8
During Verification Period (7/91 to 12/91)

Figure
VI-17a



SOURCE: Systech Engineers



Philip Williams & Associates, Ltd.
Consultants in Hydrology

Comparison of Observed and Simulated Dissolved
Oxygen Concentration at Stations R0A to R8
During Verification Period (7/91 to 12/91)

Figure
VI-17b

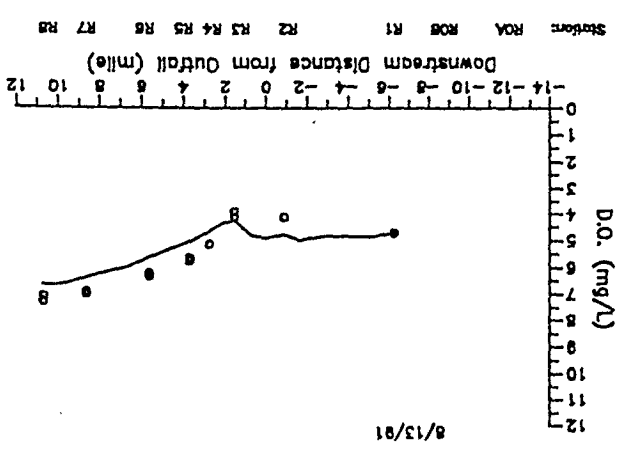
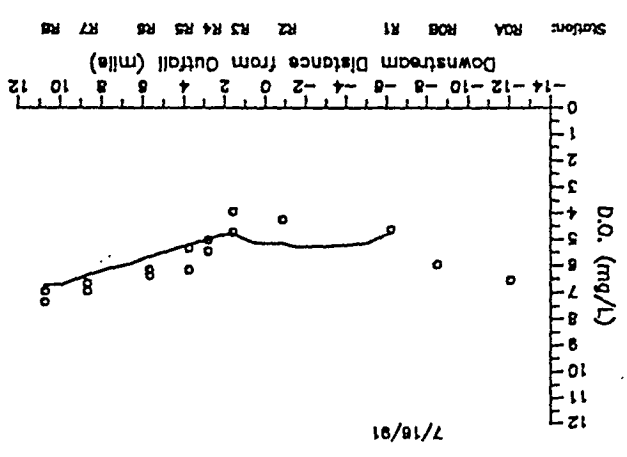
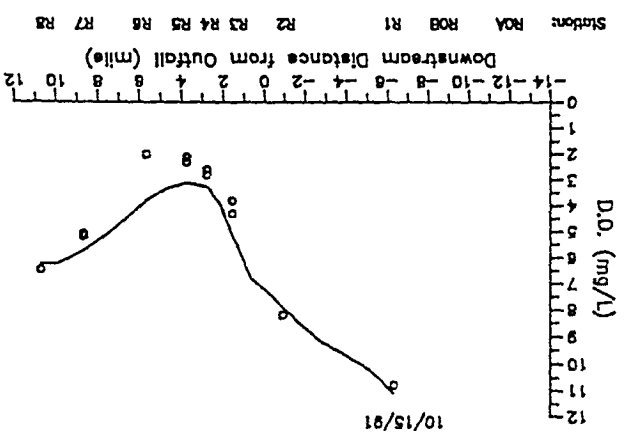
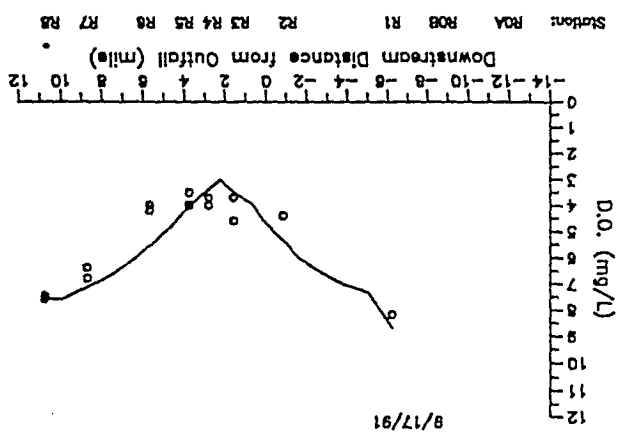
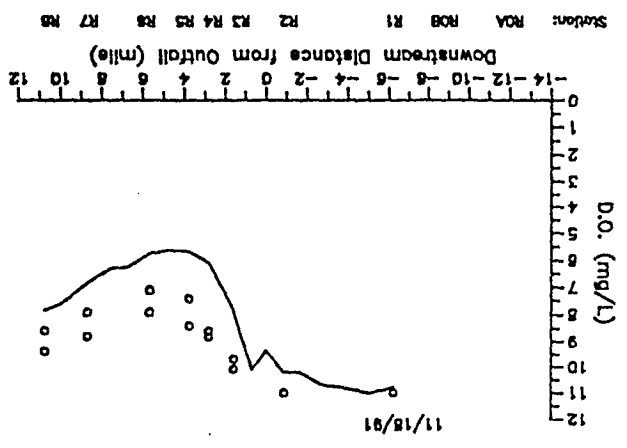


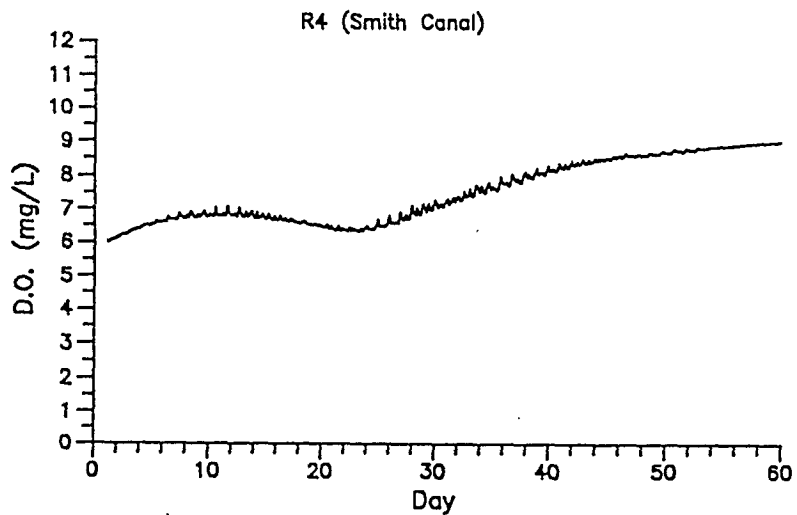
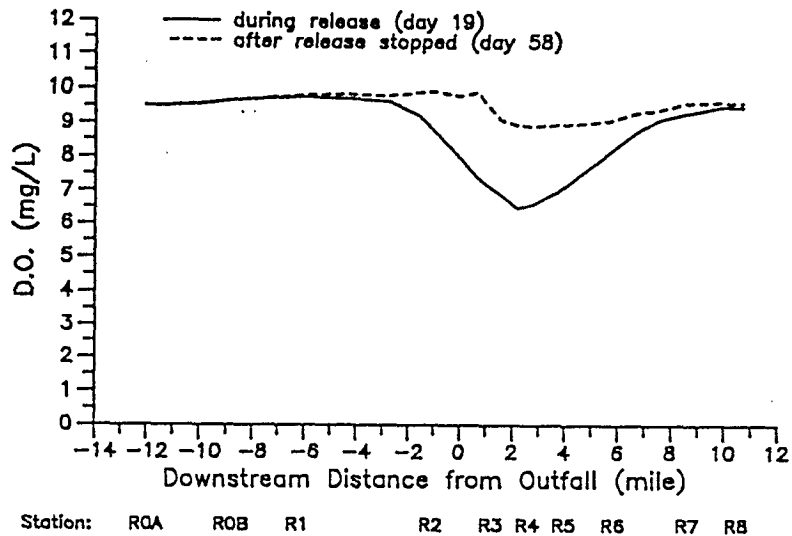
Philip Williams & Associates, Ltd.
Consultants in Hydrology

Comparison of Observed and Simulated Dissolved Oxygen Profiles during Verification Period (7/91-12/91)

Figure VI-18

SOURCE: Systech Engineers





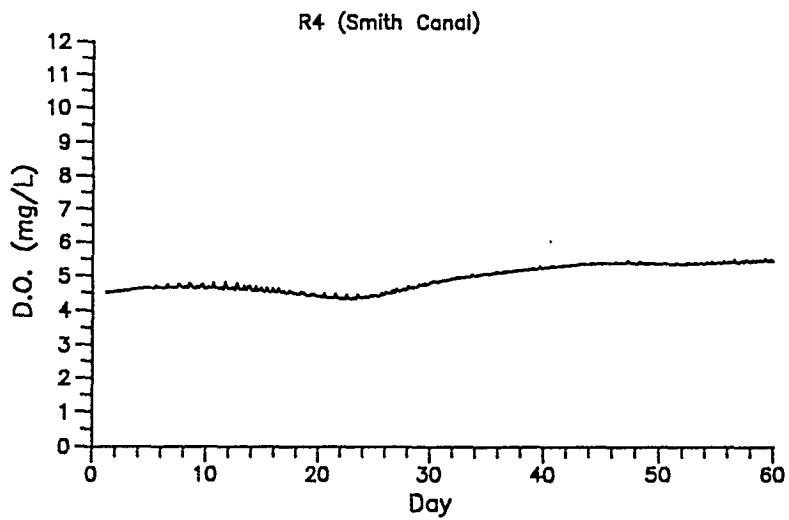
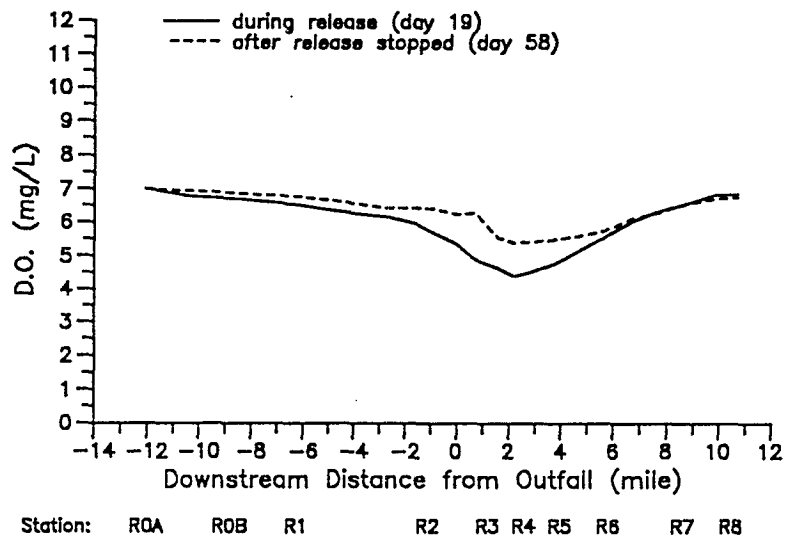
SOURCE: Systech Engineers



Philip Williams & Associates, Ltd.
Consultants in Hydrology

Response of River Dissolved Oxygen to a Plant
Shutdown During Winter Condition with Positive
River Flow

Figure
VI-19



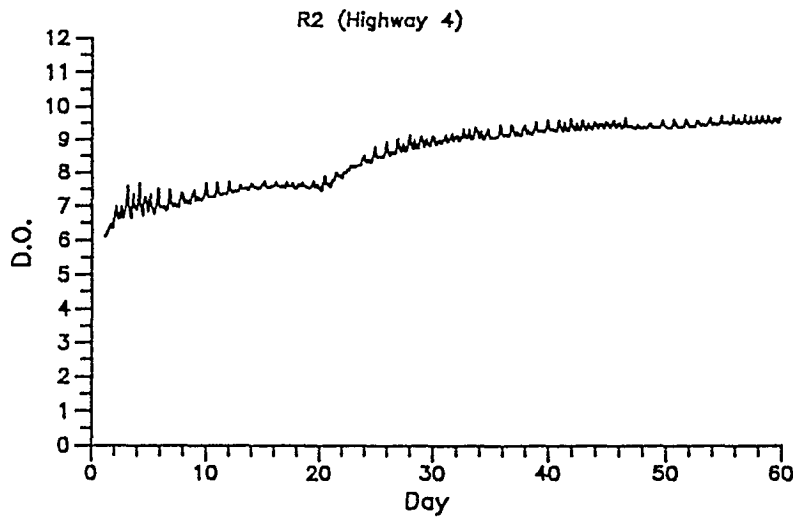
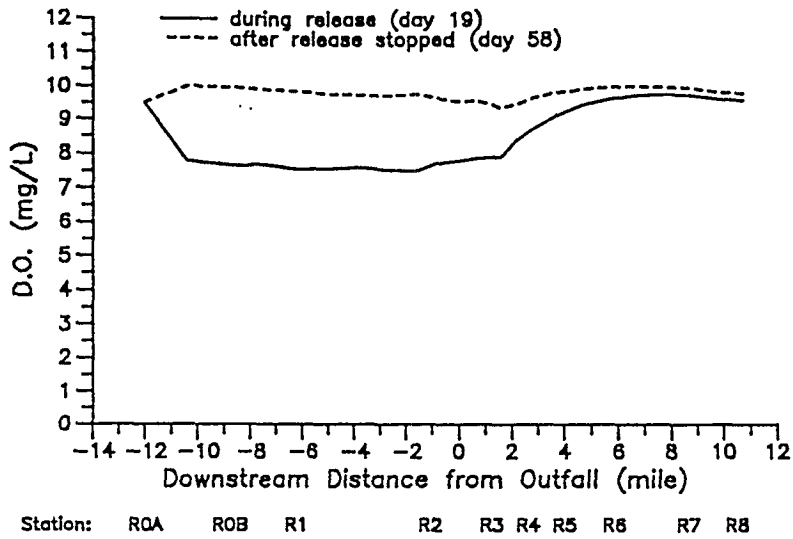
SOURCE: Systech Engineers



Philip Williams & Associates, Ltd.
Consultants in Hydrology

**Response of River Dissolved Oxygen to a
Plant Shutdown during Summer Condition
with Positive River Flow**

Figure
VI-20



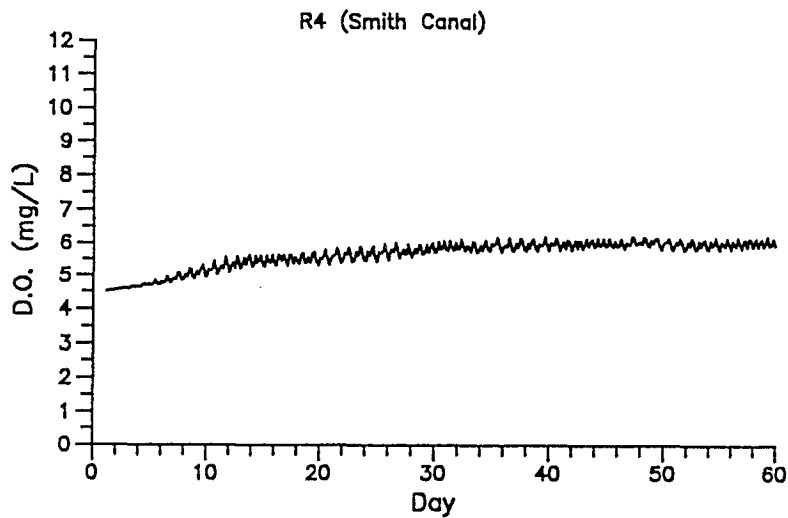
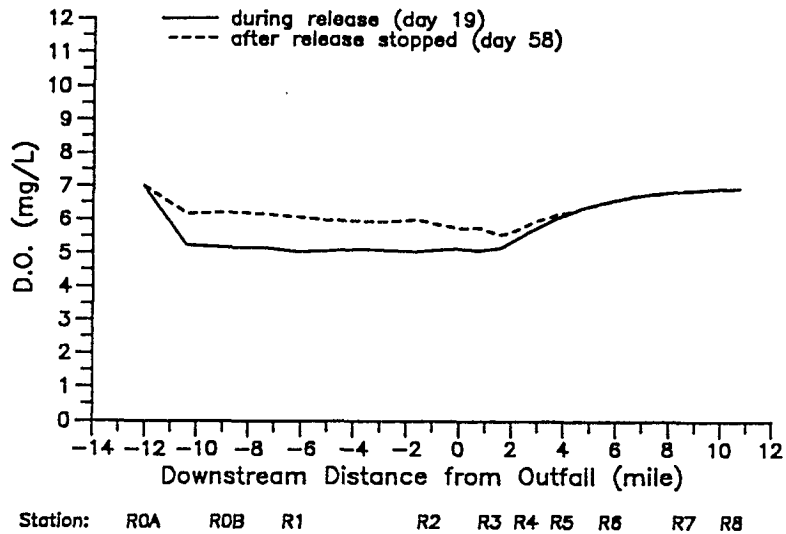
SOURCE: Systech Engineers



Philip Williams & Associates, Ltd.
Consultants in Hydrology

Response of River Dissolved Oxygen to a Plant
Shutdown During Winter Condition with Reverse
River Flow

Figure
VI-21



SOURCE: Systech Engineers



Philip Williams & Associates, Ltd.
Consultants in Hydrology

**Response of River Dissolved Oxygen to a
Plant Shutdown during Summer Conditions
with Reverse River Flow**

**Figure
VI-22**

TABLES

Table II-1. Summary of Corps of Engineers Data on San Joaquin River Tributaries

Location	Period	Minimum Flow (cfs)	Maximum Flow (cfs)	Average Flow (cfs)
Duck Creek near Farmington	1/1/79 - 9/30/91	0.0	243.0	2.0
Mormon Slough at Bellota	1/1/88 - 9/30/91	0.0	8,522.0	460.0
Littlejohn Creek at Farmington	1/1/79 - 12/31/91	0.0	2,452.0	121.0

25\stockton.824\824table\08-06-93

Table II-2. Summary of Peak Flood Discharges in the San Joaquin River at Burns Cutoff

Frequency	Peak Discharge (cfs)
10-Year	11,000
50-Year	17,500
100-Year	21,100
500-Year	41,000

Source: Federal Emergency Management Agency (1989)

Table II-3. Summary of 100-Year Peak Discharges in San Joaquin River Tributaries

Tributary	Drainage Area (square miles)	100-Year Peak Discharge (cfs)
Mormon Slough	533	13,600
Stockton Diverting Canal	533	13,600
Calaveras River	604	14,400
Lower Mosher Slough	13.4	580
Bear Creek	92.3	6,350

Source: Schaaf and Wheeler (1992)

Table II-4. NPDES-Permitted Industrial Discharges in the Stockton Area

Facility	Discharge Point	Maximum Flow Rate	Monitored Constituents
Stockton Cogeneration Company	North Littlejohns Creek	0.66 MGD	COD, Solids, Oil and Grease, Chlorine, Metals, pH, Temperature
Morley Cooling Tower Company	Diverting Canal	0.59 MGD	Chromium, Copper, pH, Arsenic, TDS
Gold Bond Building Products	McDougald Slough	3.5 MGD	COD, Solids, Oil and Grease, Chlorine, pH
McCormick and Baxter Creosoting Co.	Mormon Slough	0.63 MGD	Temperature, pH

Table IV-1. Near Field Study Dosing Conditions, July 20, 1992.

Sampling Time on	Plant Discharge (MGD)	Dose Flow Rate (ml/min)	Dose Conc (g/l)	Effluent Conc (ug/l)
Ebbing 13:00-14:00	33.0	34.1	35.4	13.9
Low Water 16:50-17:46	34.0	35.7	53.1	21.2
Flooding 19:30-20:30	33.5	35.7	70.8	28.7

25\stockton.B24\824table\08-06-93

Table IV-2. Time Lags of Tides at the Downstream Boundaries from the DWR Gage Station at Venice Island.

Location	Time Lag (minutes)	
	Low Tide	High Tide
Paradise Point	19.31	14.75
Light 16	1.43	1.72
Tiki Lagoon	6.30	7.46

25\stockton.824\824table\08-06-93

Table V-1. Survey of Plume Models.

Model	Description	Predictions (initial dilutions)
Fischer (1979)	Analytical solution for a pure jet in a stagnant body of water	May underpredict dilution in near field. Will not account for tidal currents
Wright (1977)	Analytical solution for a pure jet in a cross flow	May overpredict initial dilution.
CORMIX (1992)	Cornell Mixing Zone Expert System for many types of flow cases. Will not handle cross flow situation like the Stockton outfall	Will not run the case. States flow situation too complex. Possible recirculation eddies.
UOUTPLM (1985 EPA Plume Model)	2-D computer model for flowing condition	Overpredicts dilution.
UDKHDEN (1985 EPA Plume Model)	3-D computer model for flowing condition	Slightly overpredicts dilution in near field.

Table V-2. TDS, Temperature, and Density of Effluent and River Water in 1991.

Month	TDS, mg/l		Temp, °C		Density Difference*, kg/m ³
	River	Effluent	River	Effluent	
Jan	618	814	5.6	6.7	-0.18
Feb	635	849	10.7	11.2	-0.19
Mar	495	812	10.7	13.2	-0.90
Apr	418	817	14.7	17.9	+0.05
May	384	809	19.0	17.0	-0.87
Jun	415	921	22.1	23.0	-0.40
Jul	442	882	24.9	25.5	-0.34
Aug	420	942	24.4	24.0	-0.72
Sep	490	1,004	22.8	25.9	+0.16
Oct	660	972	19.6	22.5	+0.26
Nov	545	895	11.6	13.2	-0.23
Dec	488	756	7.1	9.5	-0.16

*density of river water minus the density of effluent

Table V-3. Length Scales During the Tracer Study.

Tidal Condition	Scale Length of Momentum Lm (meters)	Scale Length of Plume Lb (meters)	Ratio Lm/Lb
ebb	6.4	0.12	53
low	11.1	0.63	18
flood	5.6	0.08	70

25\stockton.824\824\table\08-06-93

Table V-4. Modeled Centerline Dilutions from the Stockton Outfall.

Tide	Time, seconds after discharge	Crossflow Distance from West Bank, feet	Downstream Distance From Outfall, feet	Centerline Dilution
Ebb	60	40	52	7.1
Low	60	53	37	7.8
Flood	60	38	56	7.0
Ebb	120	49	96	10
Low	120	64	68	11
Flood	120	46	105	10

25\stockton.824\824table\08-06-93

Table V-5. Measured Centerline Dilutions from the Stockton Outfall.

Tide	Distance Downstream from Outfall, feet	Measured Centerline Dilution
Ebb	60	6
	180	8
	300	10
Low	60	6
	100	9
Flood	60	13
	140	15
	300	19

25\stockton.824\824\table\08-06-93

Table V-6. Initial Dilutions of the Stockton Outfall Under Different Discharge Rates*

Condition	Effluent Discharge (MGD)	Centerline Dilution at 120 seconds
Average	42	12
Low flow	30	10
High flow	54	13
Minimum flow	10	6
Maximum flow	74	15

*Flows based on 1991 data for time of none zero discharges.

Table VI-1. Ammonia Nitrogen at Vernalis.

	Date	Dissolved Ammonia Nitrogen (mg/L)
1990	July 13	0.020
	September 19	0.020
	November 13	<0.100
1991	January 9	0.150
	March 14	0.070
	May 14	0.020
	July 16	0.040

25\stockton.824\824table\08-06-93

Table VI-2. River Flow Rates During Dye Study

Date	River Flow
7/18/92	-27.8
7/19	-26.8
7/20	-14.2
7/21	-24.6
7/22	-31.2
7/23	6.6
7/24	21.7
7/25	16.9
7/26	12.9
7/27	28.9
7/28	2.8
7/29	12.7
7/30	-35.3
7/31	-60.9

25\stockton.824\824\table\08-06-93

Table VI-3. Rate Coefficients.

Coefficients	Typical Range	Calibrated Value at 20°C
CBOD	0.1 to 0.4 per day	0.15 per day
Ammonia decay rate	0.1 to 0.5 per day	0.09 per day
Sediment Oxygen Demand	0.2 to 0.90 g/ft ² /day for municipal sewage sludge aged downstream of outfall	0.12 to 0.29 g/ft ² /day
	0.1 to 0.19 g/ft ² /day for estuarine mud	
	0.02 to 0.09 g/ft ² /day for sandy bottom	
Re-aeration	O'Conner Dobbins Equation and others	O'Conner Dobbins Equation

Note: the literature values were from EPA Rates Manual (1985).

Table VI-4. Temperature Coefficient Used in the Model.

Quality Process	Model Value	Literature Range (EPA Rates Manual 1985)
Nitrification	1.07	1.05 to 1.10
CBOD	1.05	1.02 to 1.15
SOD	1.05	1.02 to 1.09
Re-aeration	1.02	1.022 to 1.024

Table VI-5. Estimated Productivity Rates of Algae in the San Joaquin River Near Stockton.

Date		Productivity (g algae/day/ft ²)
1990	July	0.002
	August	0.002
	September	0.004
	October	0.005
	November	0.006
	December	0.005
	1991	January
February		0.003
March		0.004
April		0.005
May		0.005
June		0.004

Table VI-6. Conditions During Winter and Summer Scenarios.

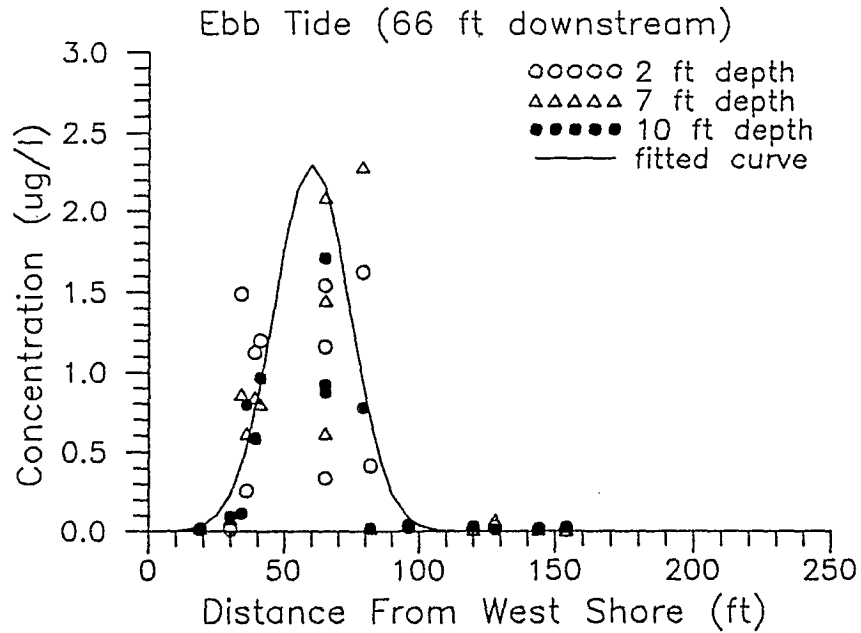
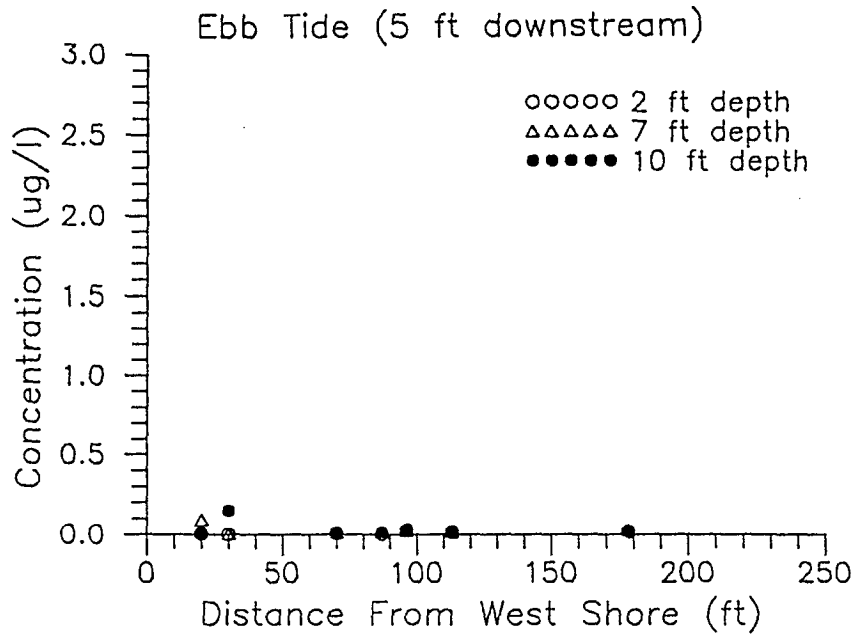
Period	River Temperature °C	DO mg/L	Effluent CBOD mg/L	NH3-N mg/L
Winter	8.0	8.0	14.0	18.0
Summer	22.0	8.0	8.0	4.0

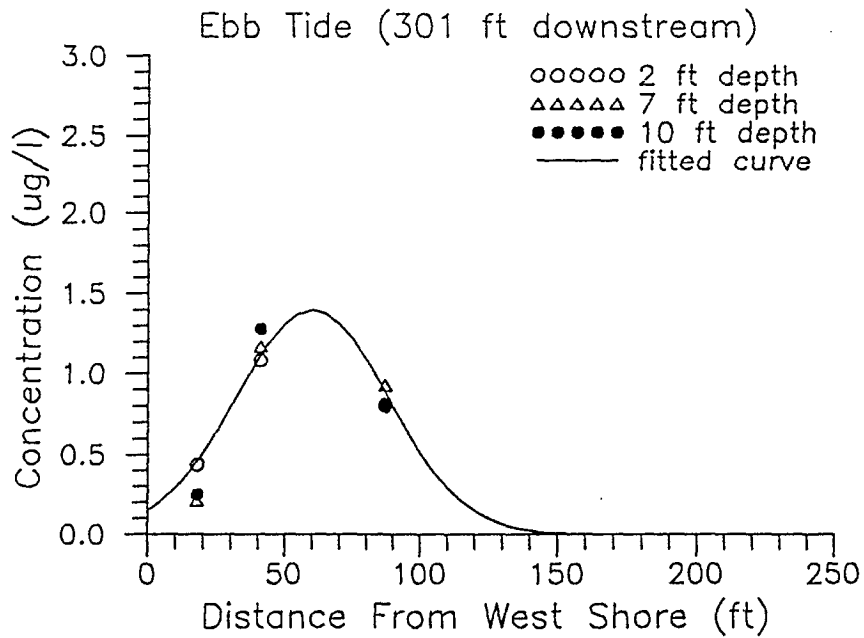
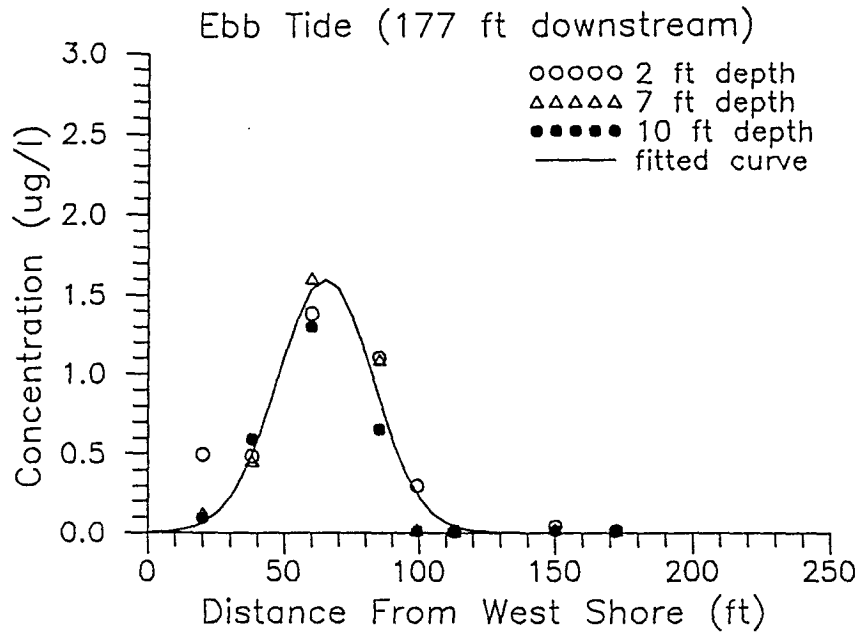
25\stockton.824\824table\08-06-93

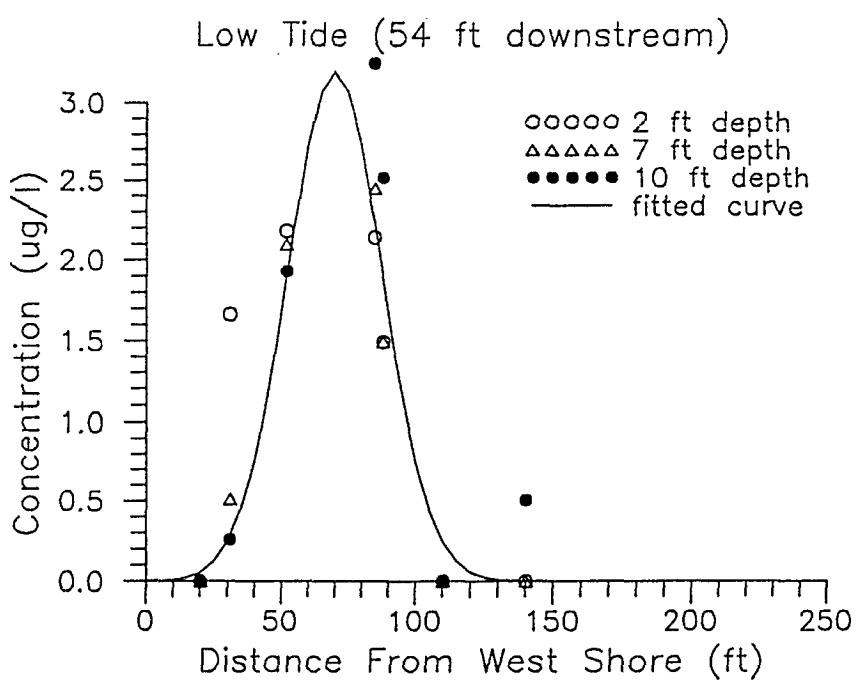
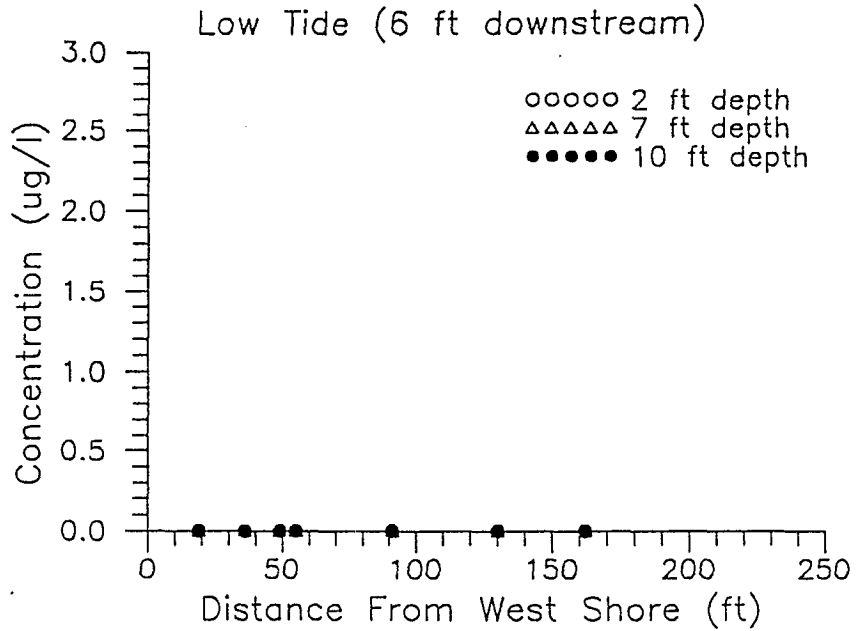
APPENDICES

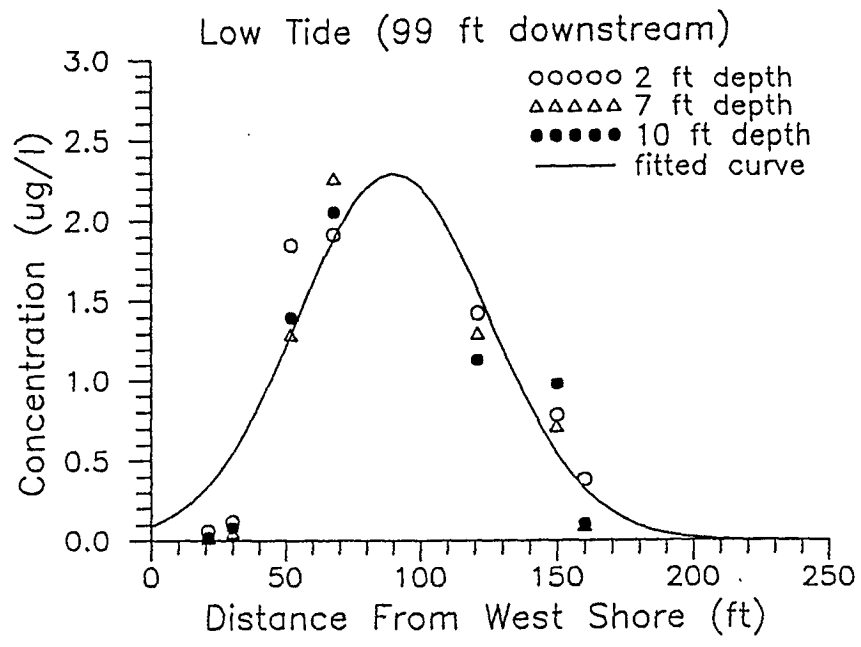
APPENDIX A

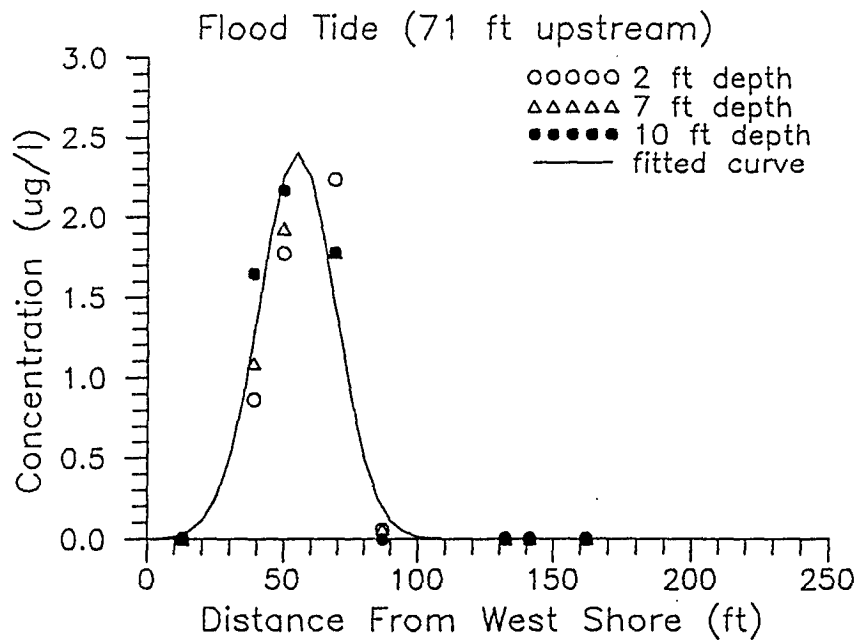
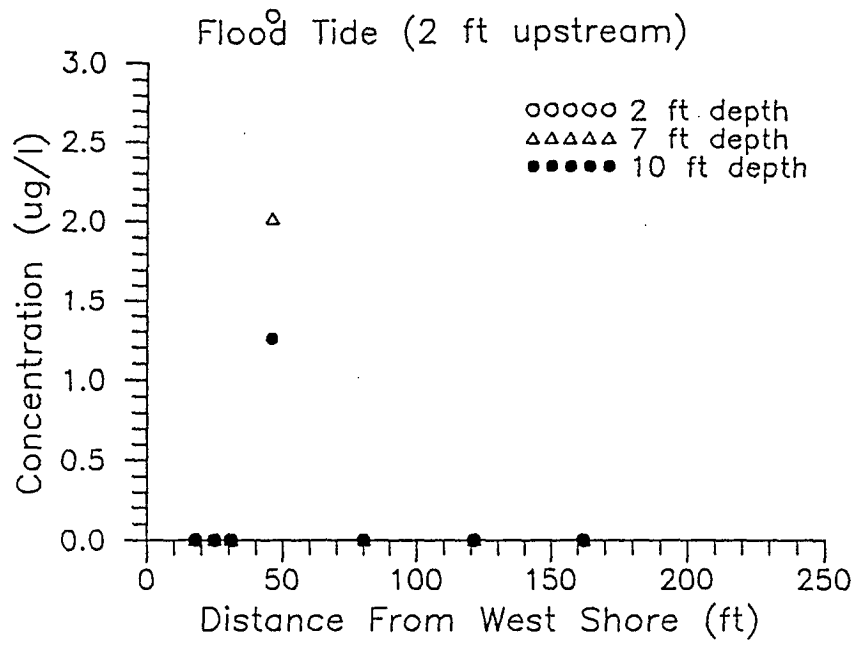
**Dye Concentration Profiles Across
River Transects in the Near Field**

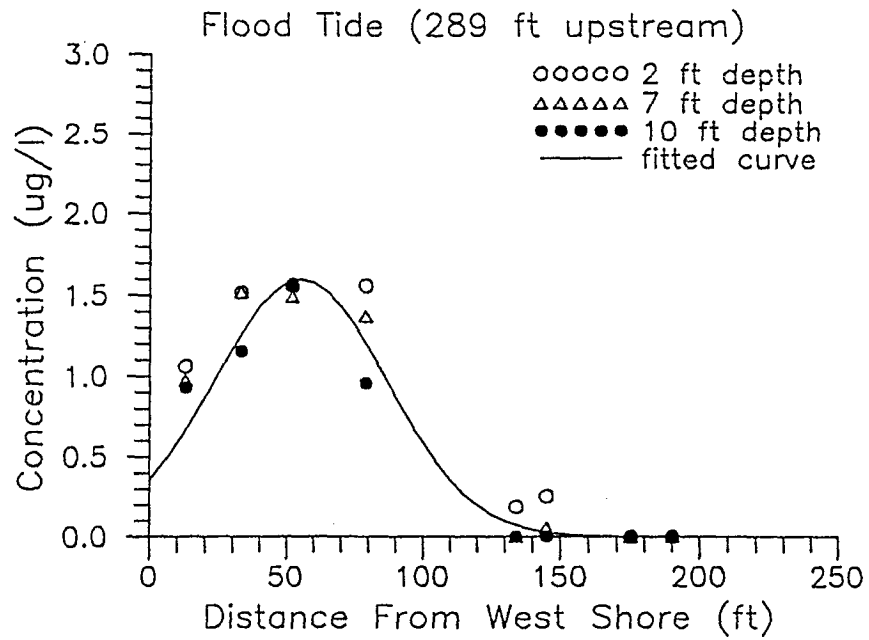
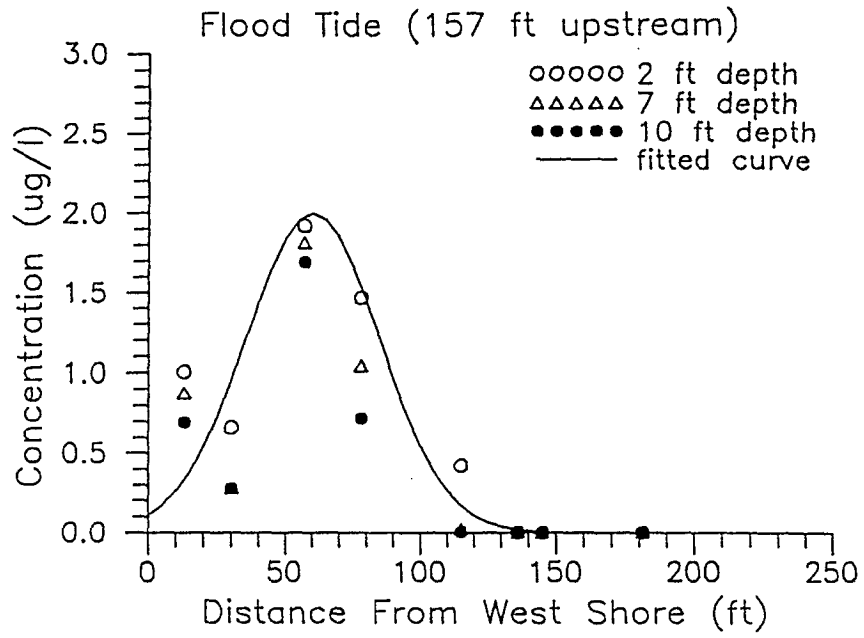






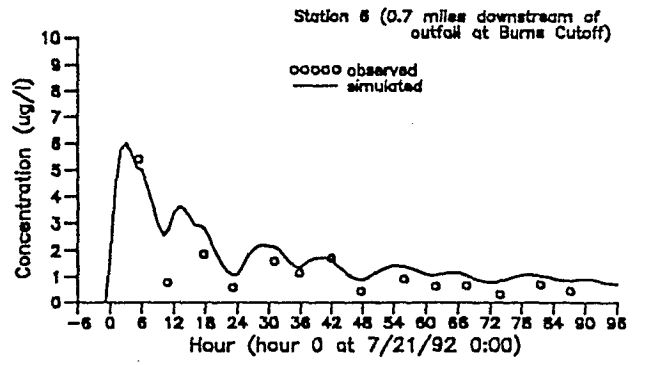
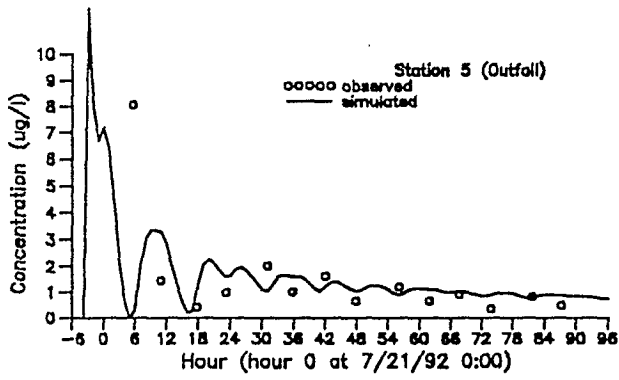
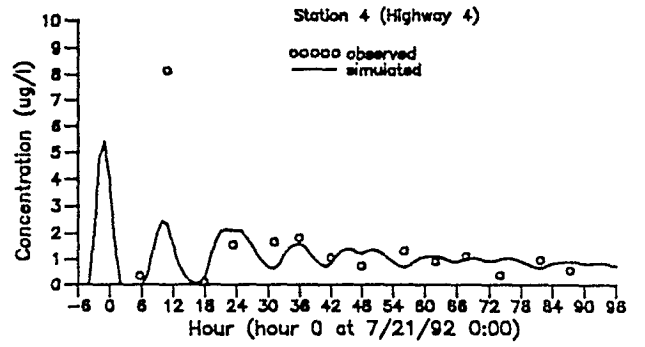
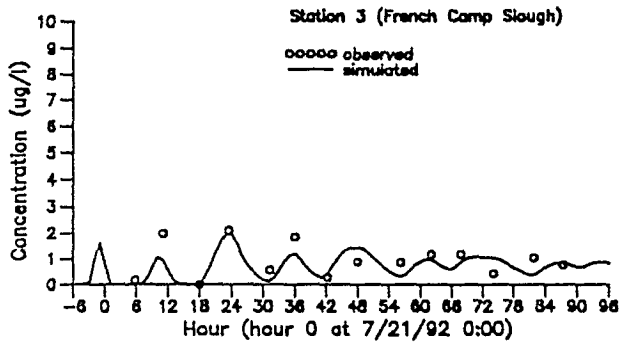
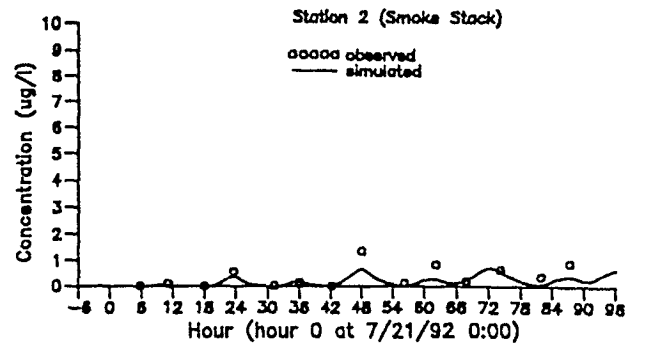
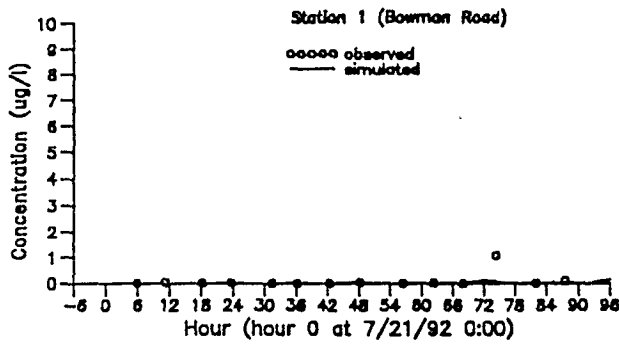


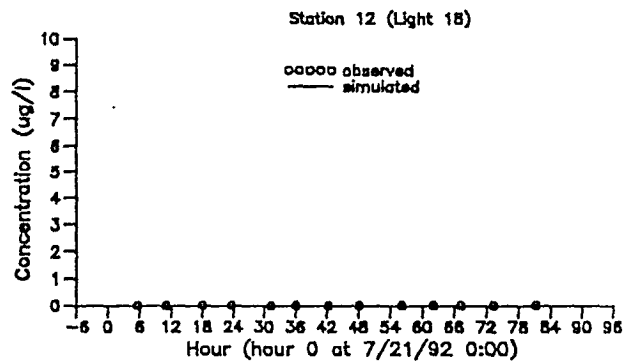
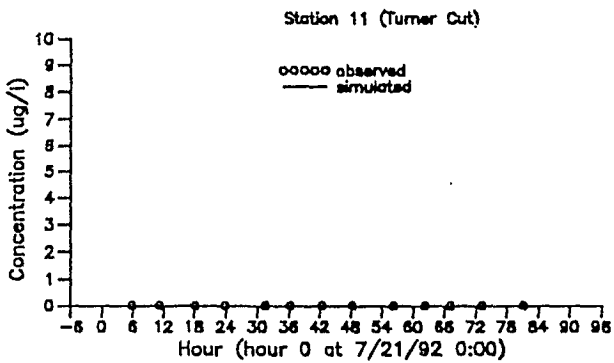
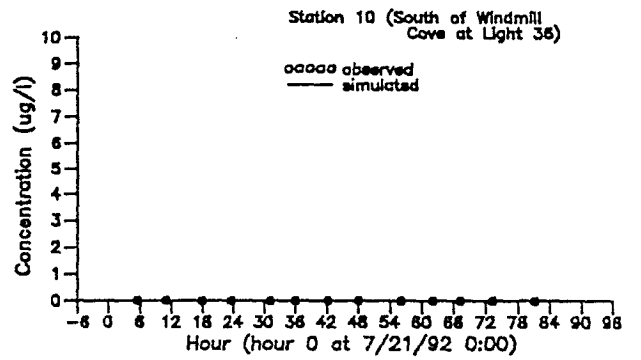
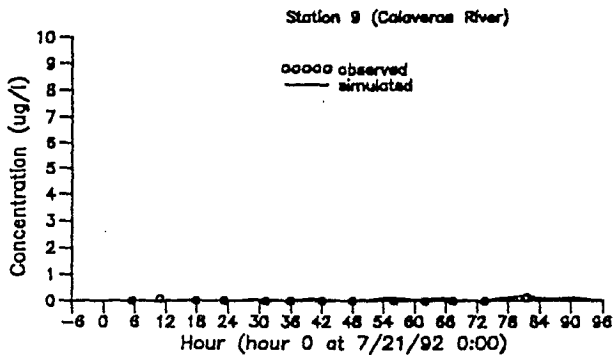
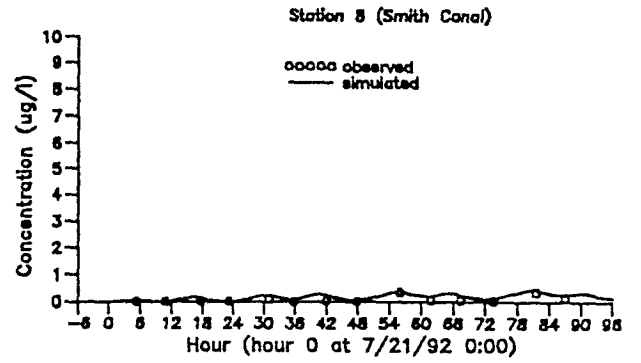
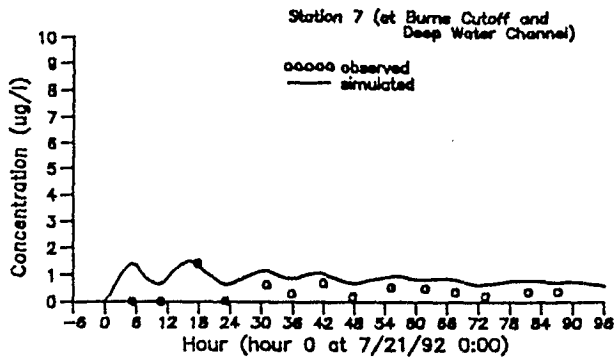




APPENDIX B

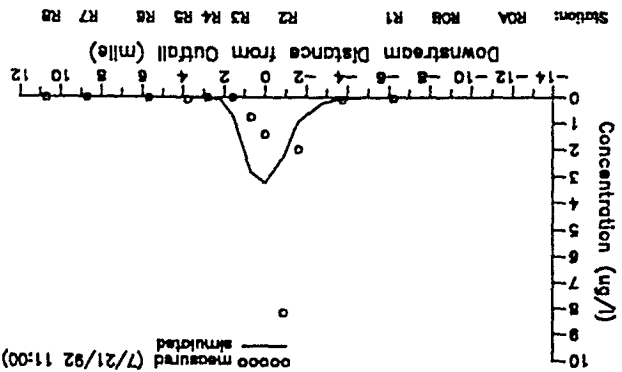
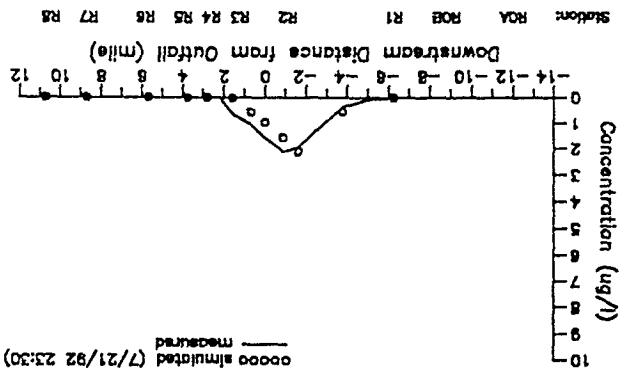
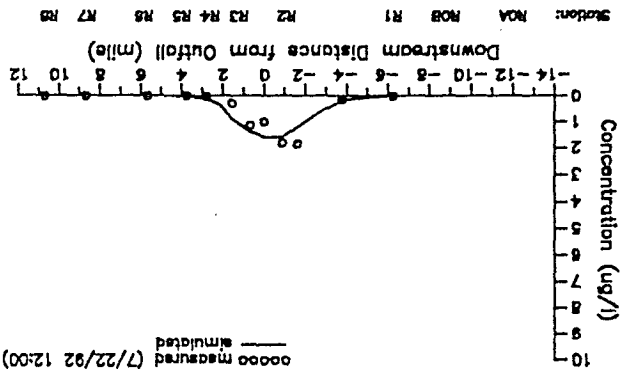
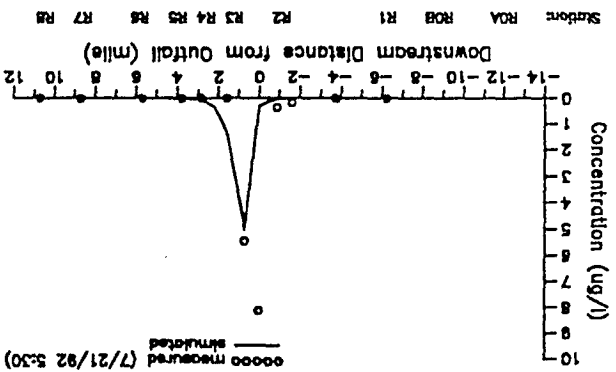
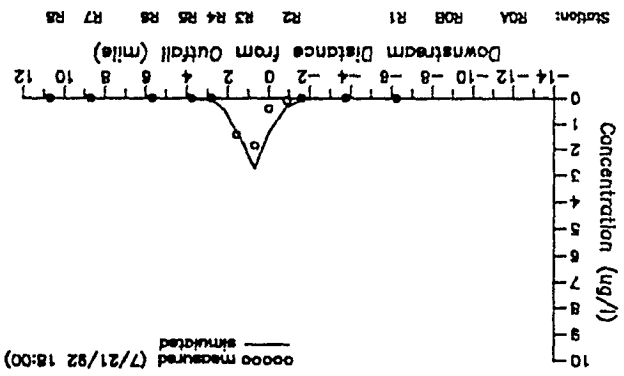
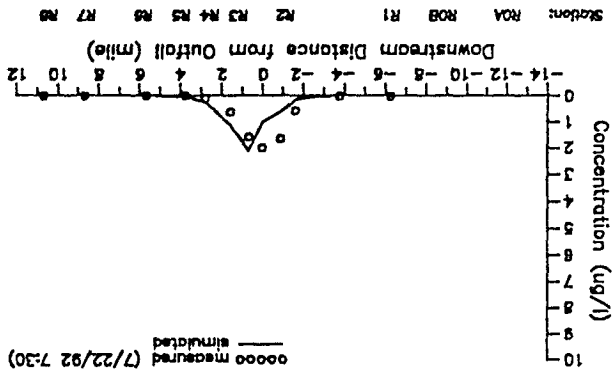
Observed and Simulated Time Concentrations of Dye
at the Far Field Stations

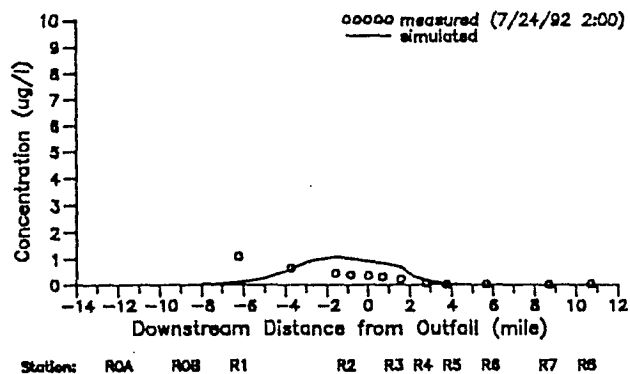
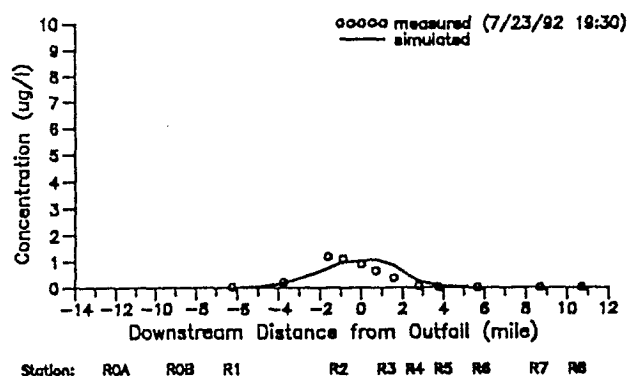
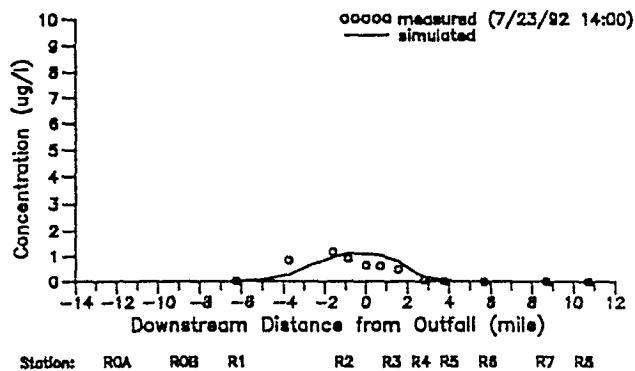
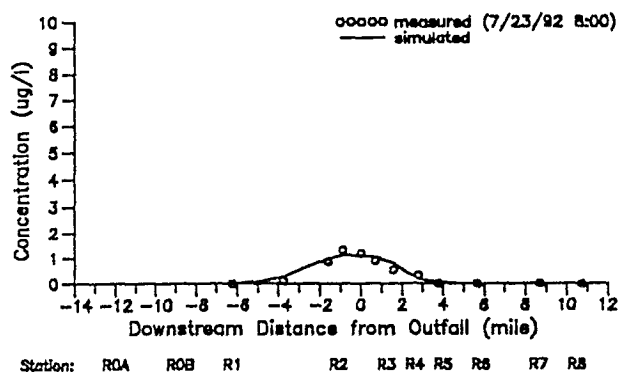
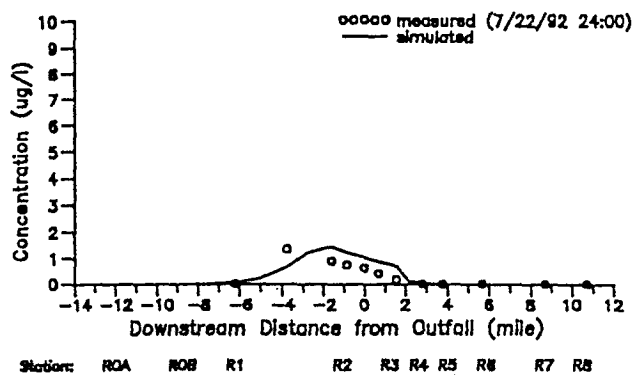
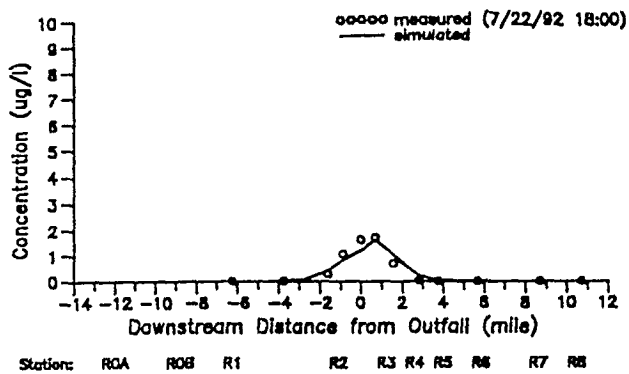


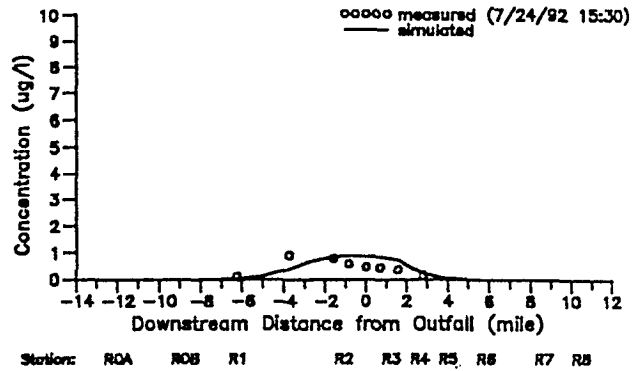
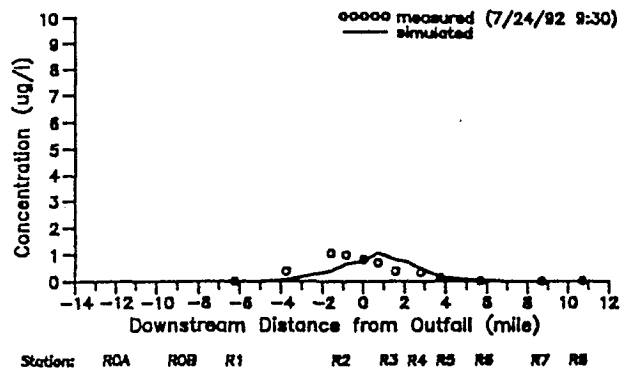


APPENDIX C

Observed and Simulated Dye Concentration
Profiles in the Far Field







APPENDIX D

Method for Estimating San Joaquin River Flows at Stockton
for Times with No Rock Barriers at Old River

METHOD USED FOR ESTIMATION

OF

SAN JOAQUIN RIVER FLOWS AT STOCKTON

Data from the Appendix of DWR Bulliten 76 (April, 1962) is used to estimate the direction and magnitude of the mean (net) daily flow, Q , past Brandt's Bridge [$Q(BB)$] as a function of the San Joaquin River flow at Mossdale and the exports at Tracy/Clifton Court Forebay. The flow past the City of Stockton RWCF Outfall is assumed to be the same as $Q(BB)$. All flows are in cubic feet per second (cfs).

Daily data is available from the U.S. Department of the Interior, Bureau of Reclamation for the San Joaquin River discharge at Vernalis and the exports at Tracy Pump Station and Clifton Court Forebay. San Joaquin River flow at Mossdale is calculated as the discharge at Vernalis, reduced by estimates of diversions (D) for agricultural use (provided by Jerry Cox).

Mean (net) daily flow past outfall = $Q(BB) = Q(\text{Mossdale}) * R_1$

where $R_1 = \frac{Q(BB)}{Q(\text{Mossdale})}$

R_1 is obtained from the reference after calculating R_2 :

$$R_2 = \frac{Q(\text{Export})}{Q(\text{Mossdale})} = \frac{Q(\text{Tracy Pump}) + Q(\text{Clifton Court})}{Q(\text{Vernalis}) - D}$$

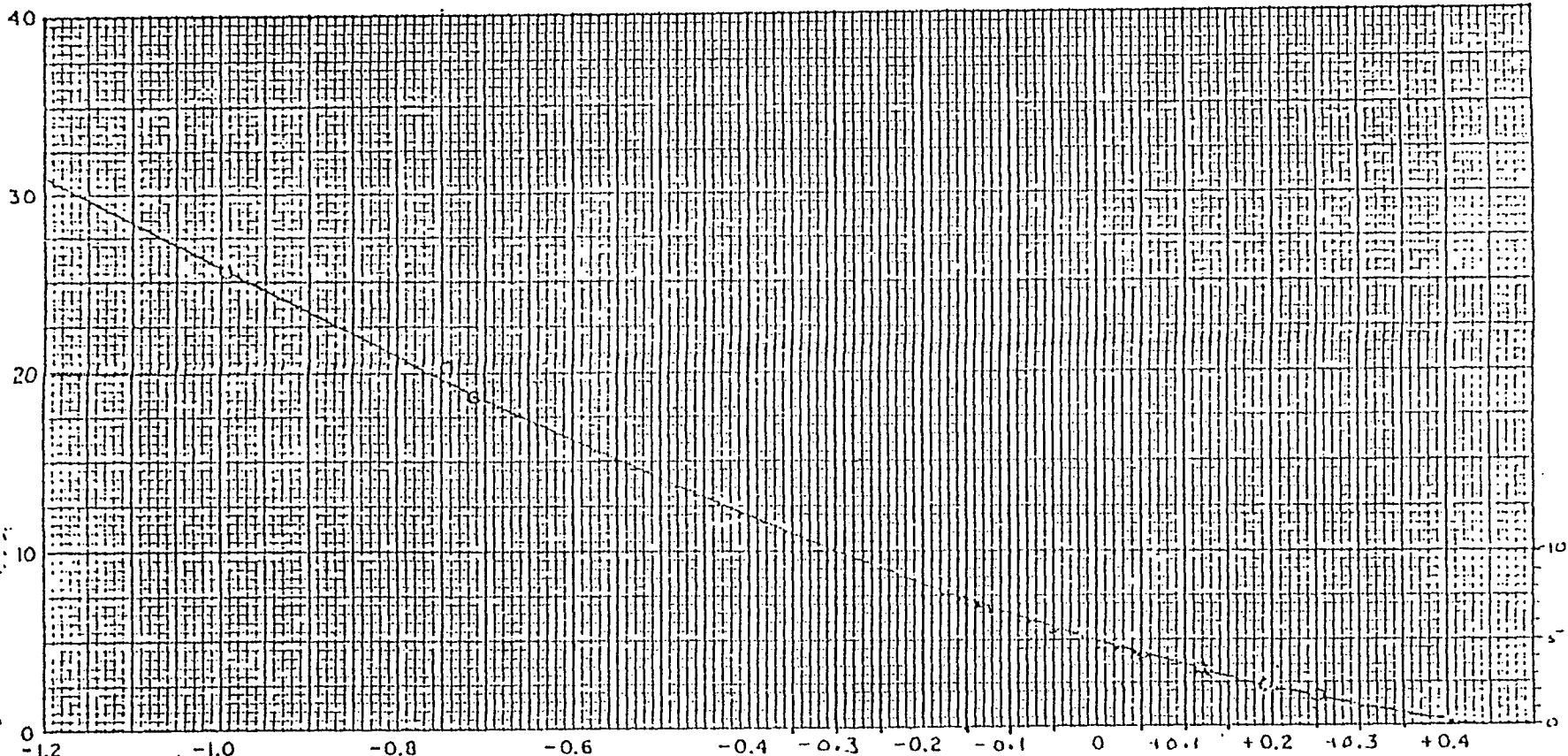
Estimates of Diversion Between
Vernalis and Mossdale

June	-	D	=	191	cfs
July	-	D	=	237	cfs
August	-	D	=	202	cfs
September	-	D	=	122	cfs
October	-	D	=	45	cfs
All other months	-	D	=	0	cfs

Note: The nonlinear referenced graph relating R_1 and R_2 has been reduced to linear segments for use in computer calculation from the raw data.

LEH:lh 5/19/89

RATIO OF DELTA-MENDOTA CANAL PUMPING TO FLOW IN
SAN JOAQUIN RIVER AT MOSSDALE



RATIO OF FLOWS IN SAN JOAQUIN RIVER AT BRANDT BRIDGE TO FLOWS IN
SAN JOAQUIN RIVER AT MOSSDALE

NOTE: Flows in northwesterly direction in San Joaquin River at Brant Bridge positive and in opposite direction negative.

STATE OF CALIFORNIA
THE RESOURCES AGENCY OF CALIFORNIA
DEPARTMENT OF WATER RESOURCES
DELTA BRANCH
DELTA WATER FACILITIES
RATIO OF FLOW AT TWO LOCATIONS
ON SAN JOAQUIN RIVER AS INFLUENCED
BY DELTA-MENDOTA CANAL PUMPING
APRIL 1962

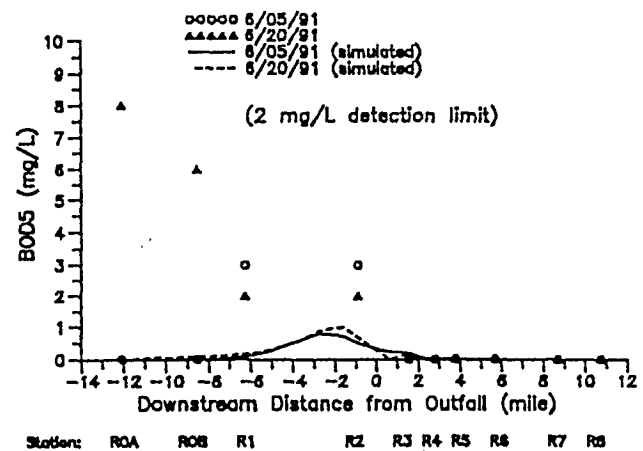
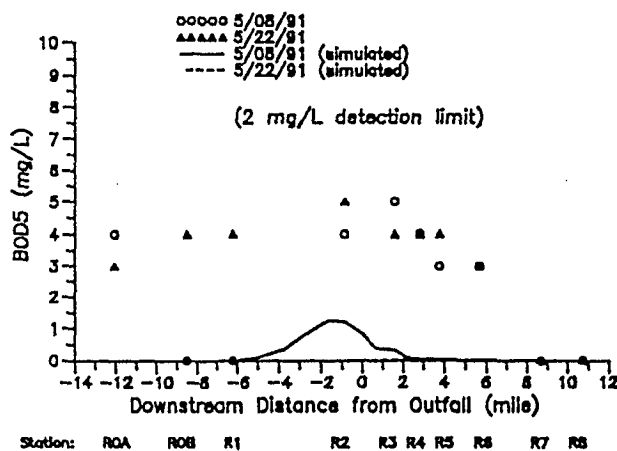
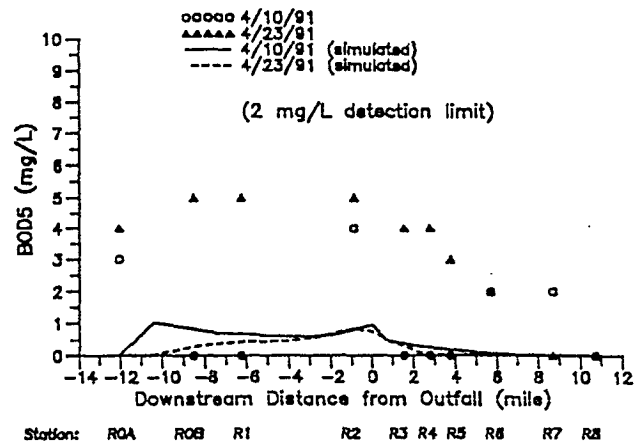
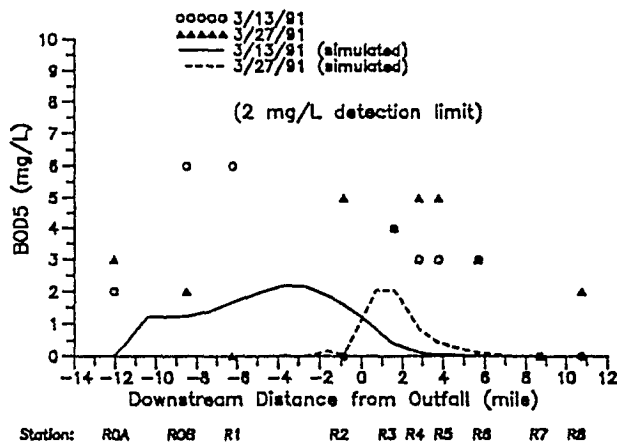
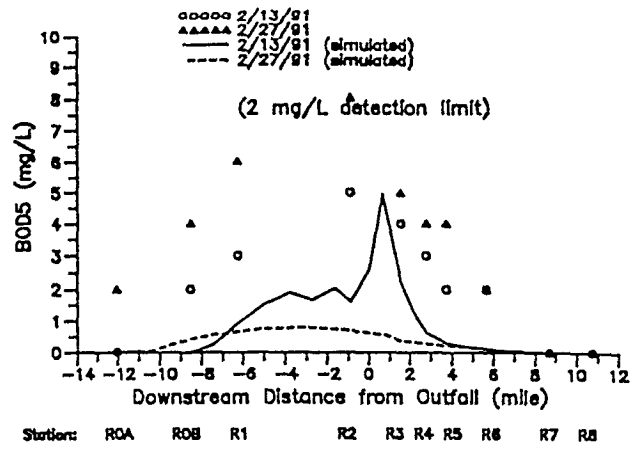
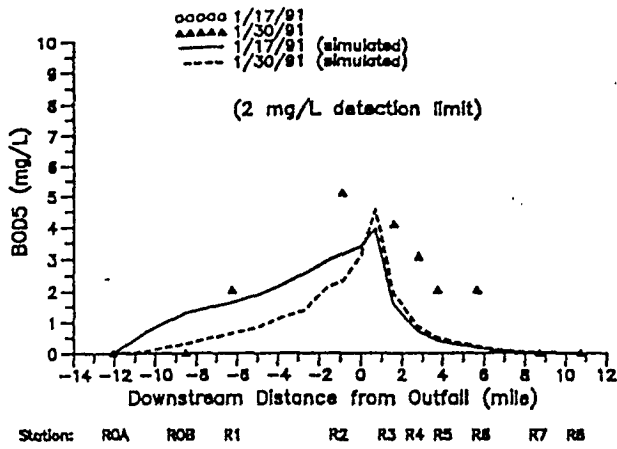
PLATE

D-041387

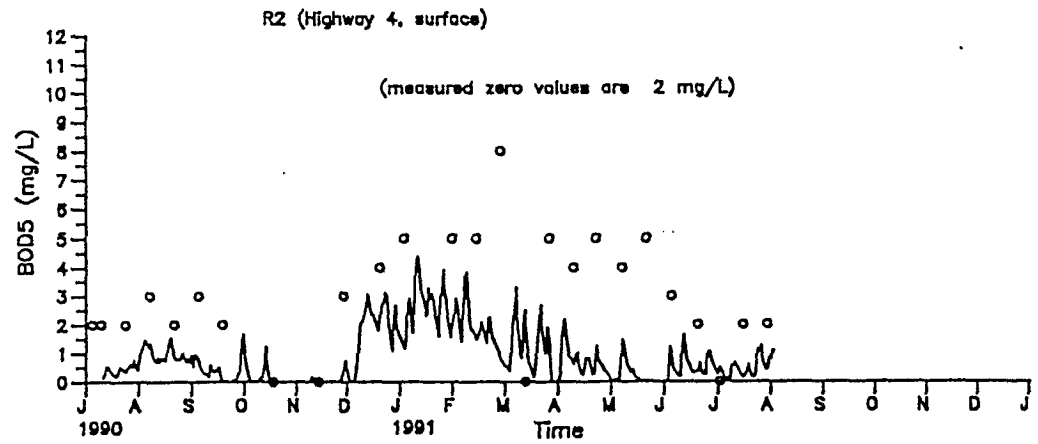
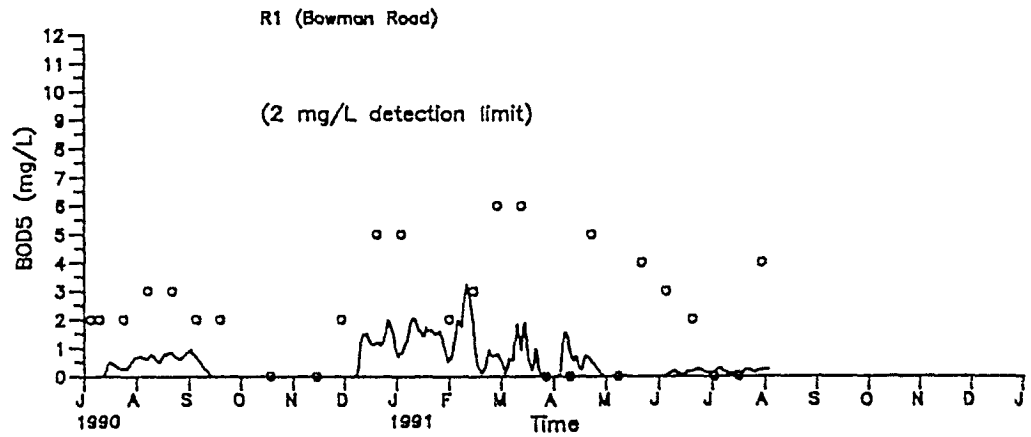
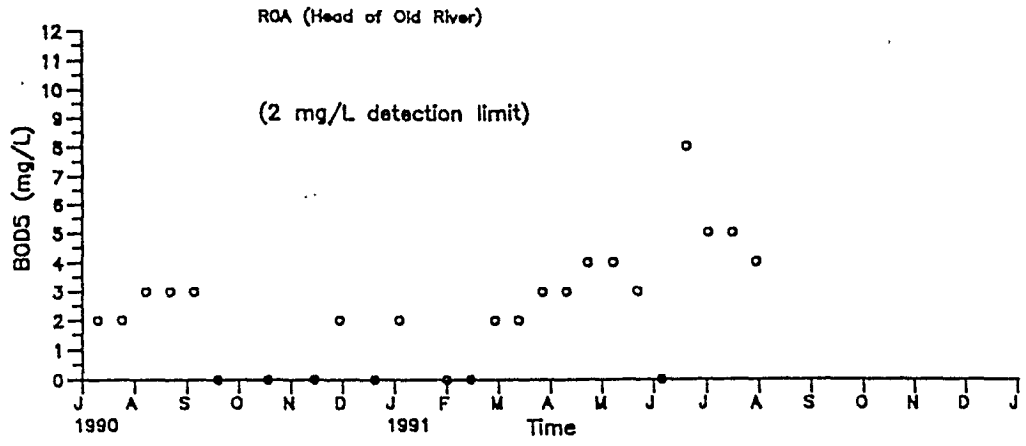
D-041387

APPENDIX E

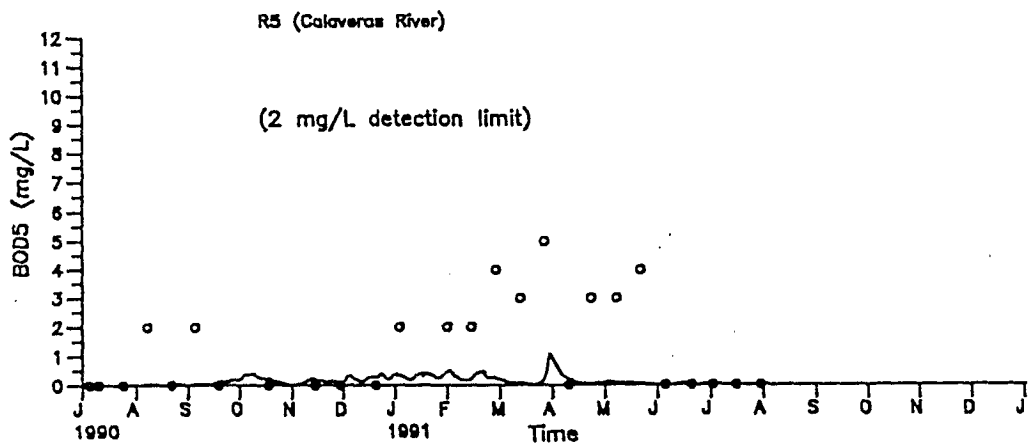
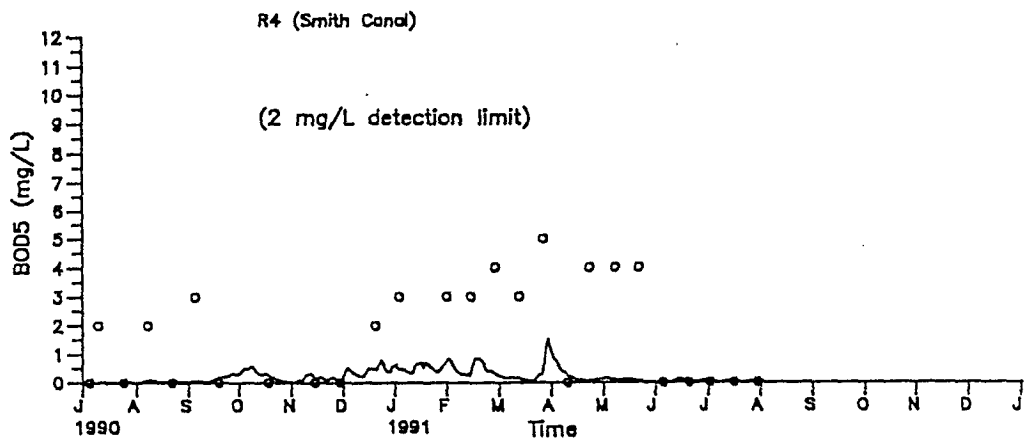
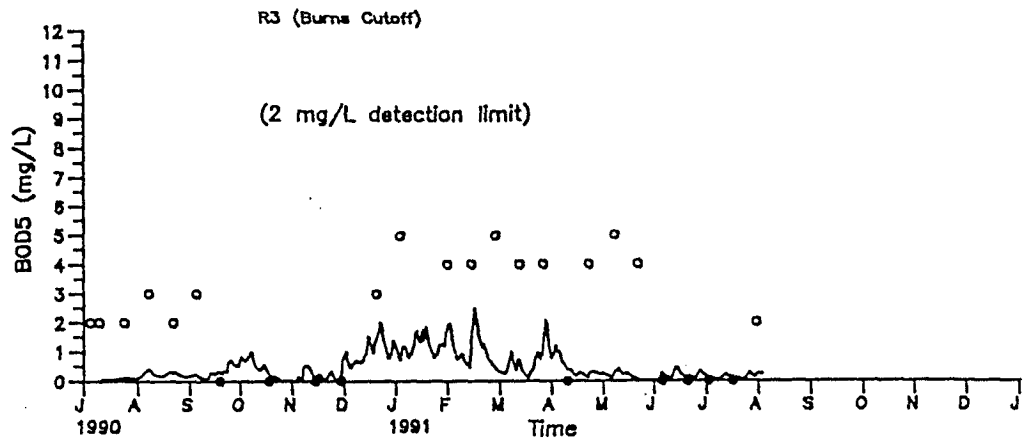
Simulated and Observed Concentration Profiles and
Time Concentrations of Total Dissolved solid From July 1990 to July 1991



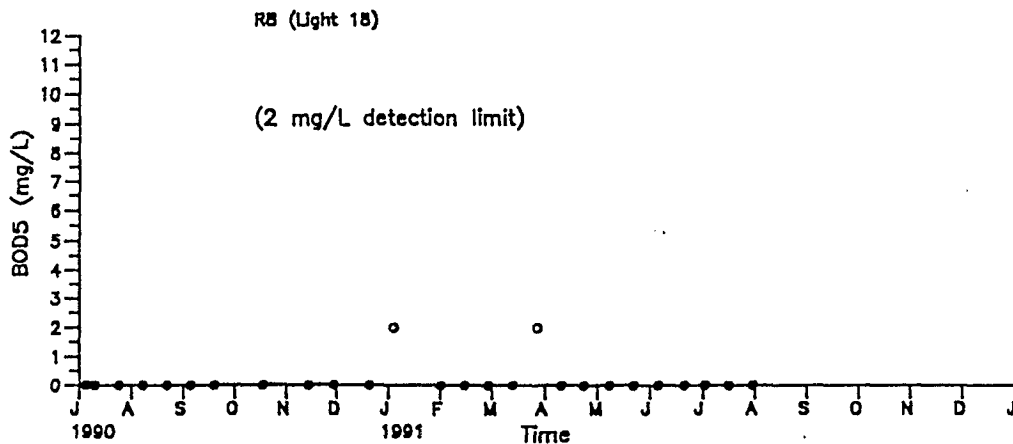
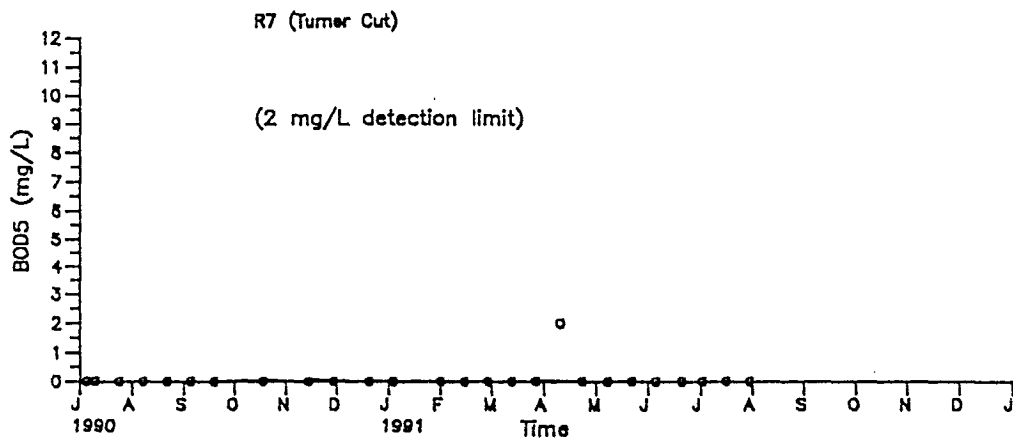
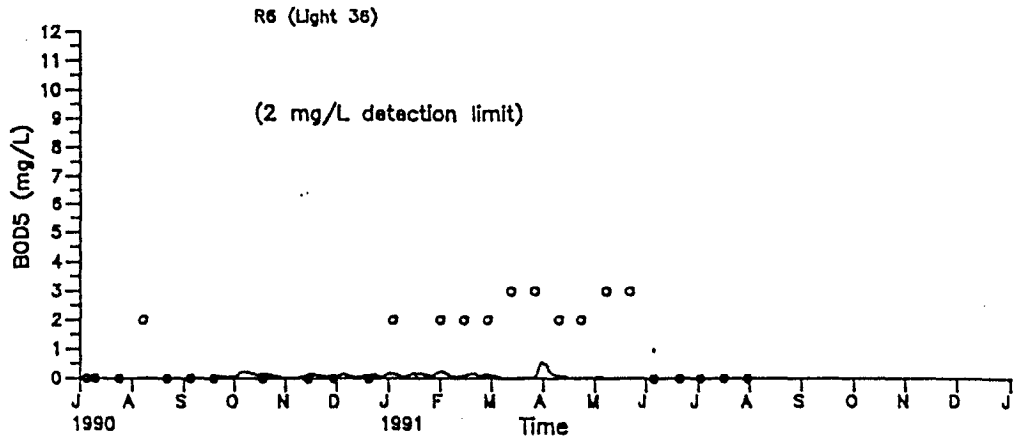
Comparison of Observed and Simulated CBOD Profiles from 7/90 to 7/91 (continued)



Comparison of Observed and Simulated CBOD
Concentration at Stations R0A to R8
From 7/90 to 7/91



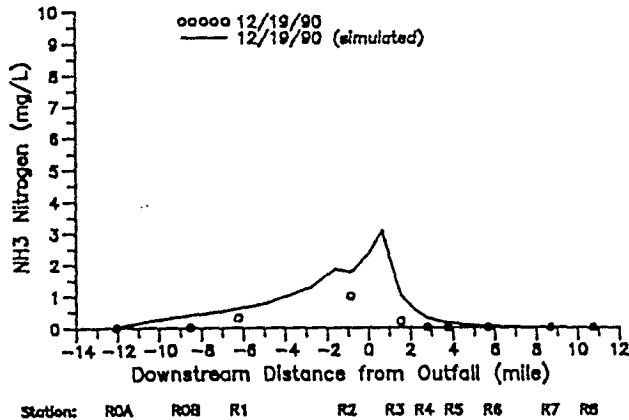
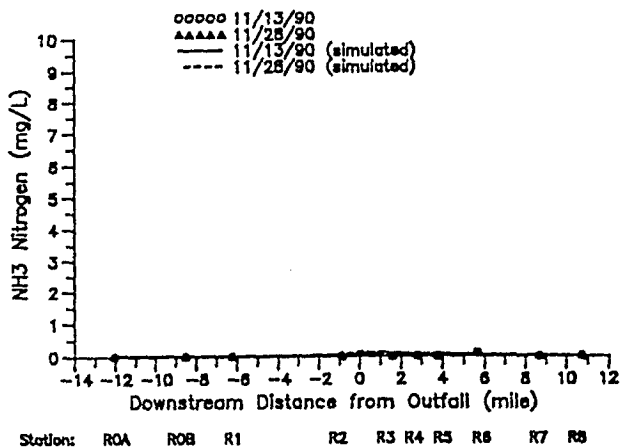
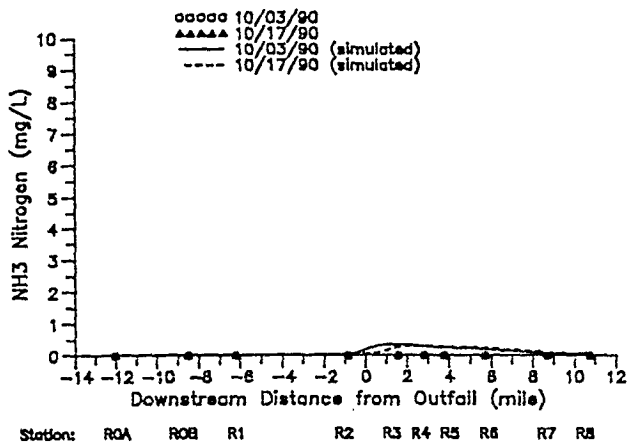
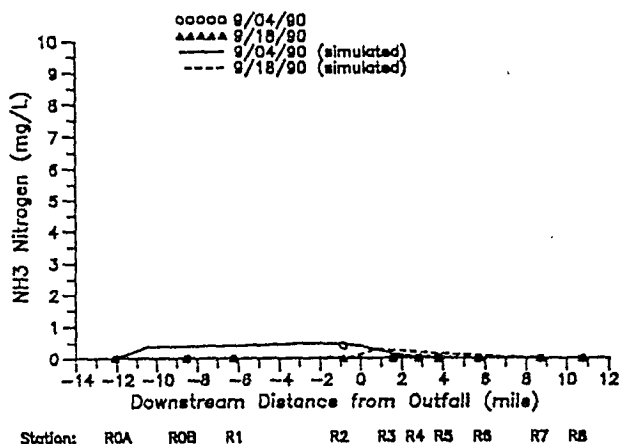
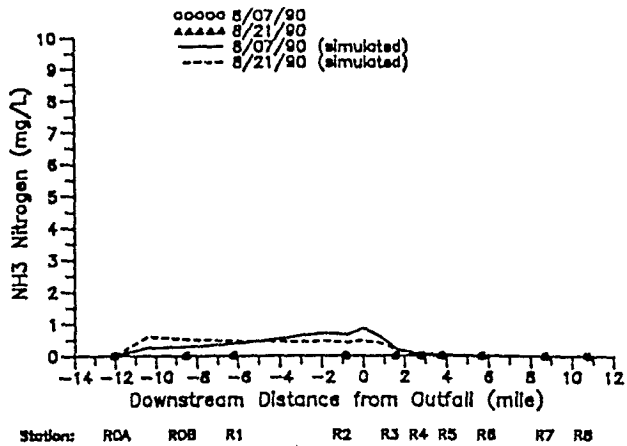
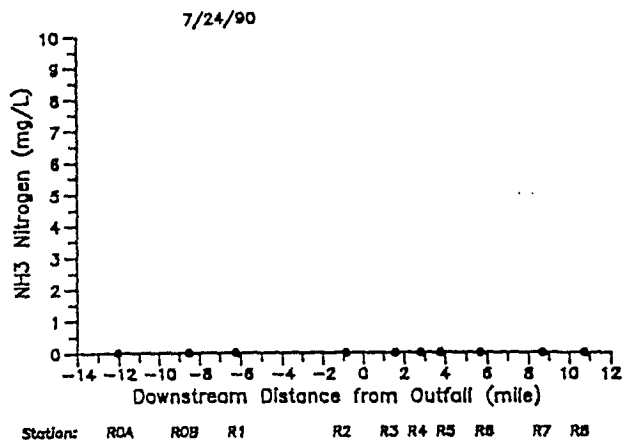
Comparison of Observed and Simulated CBOD
 Concentration at Stations R0A to R8
 From 7/90 to 7/91 (continued)



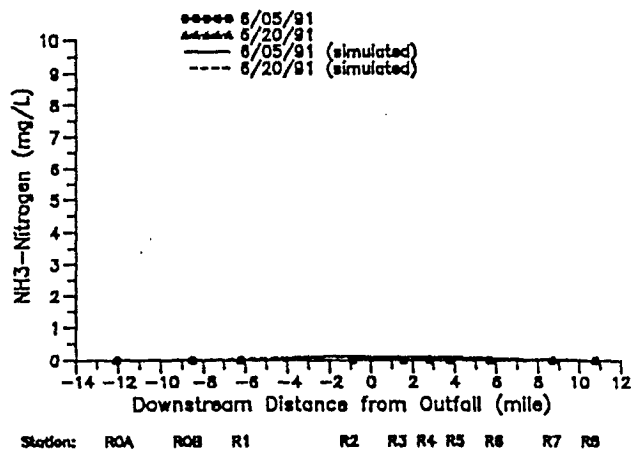
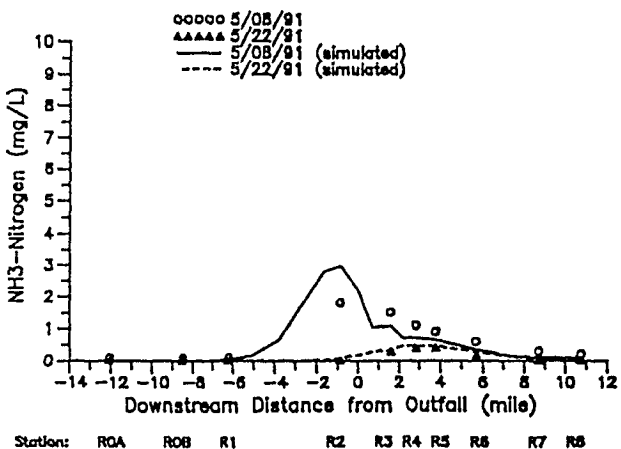
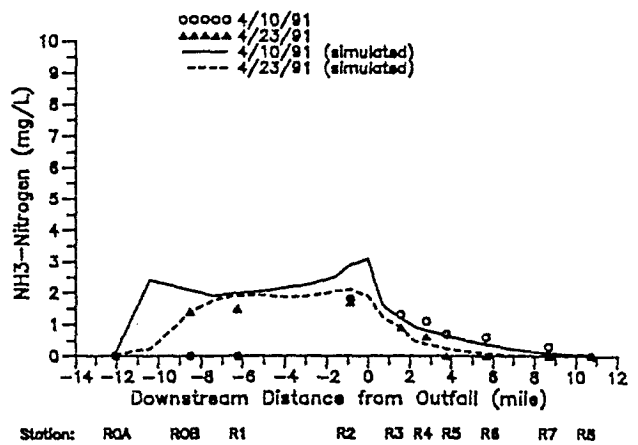
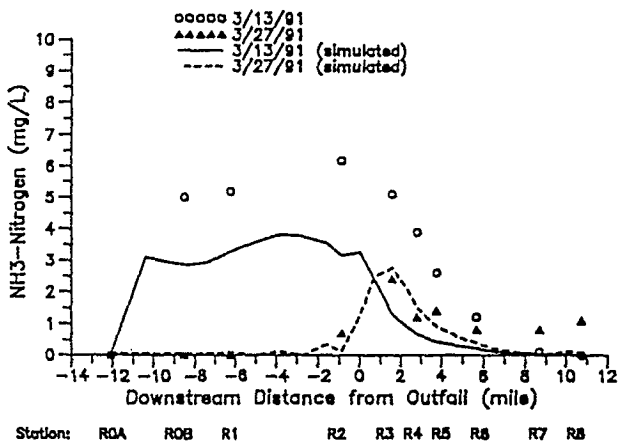
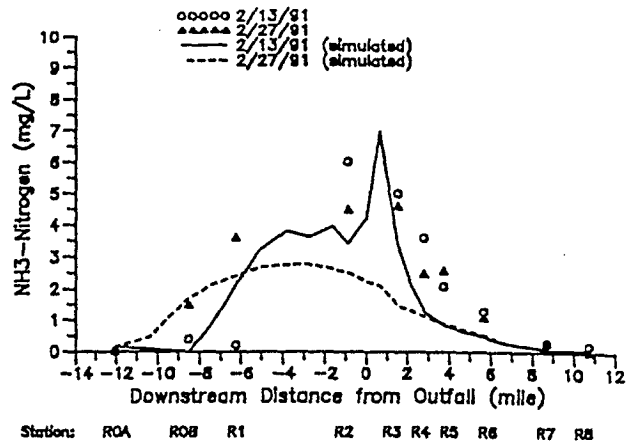
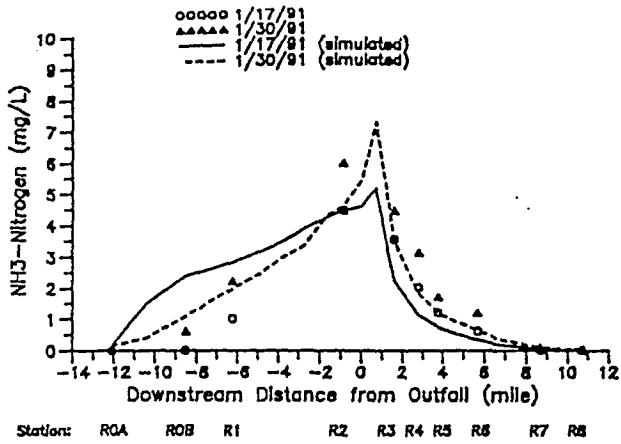
Comparison of Observed and Simulated CBOD
 Concentration at Stations R0A to R8
 From 7/90 to 7/91 (continued)

APPENDIX G

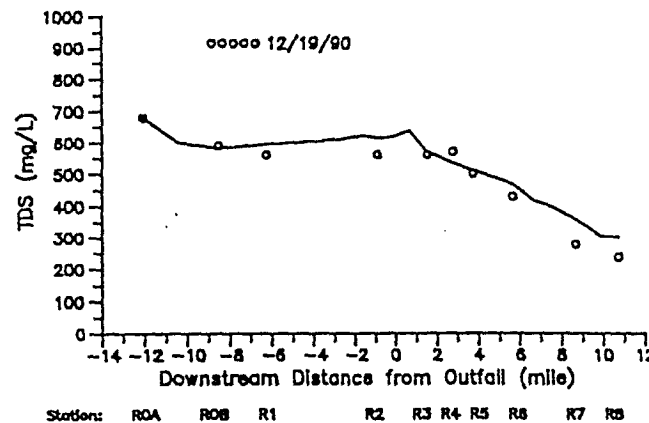
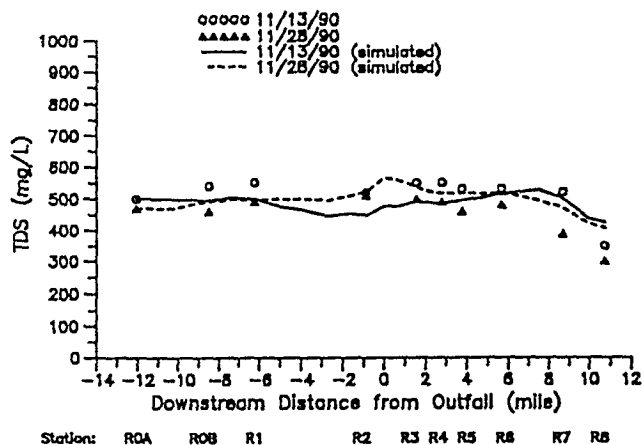
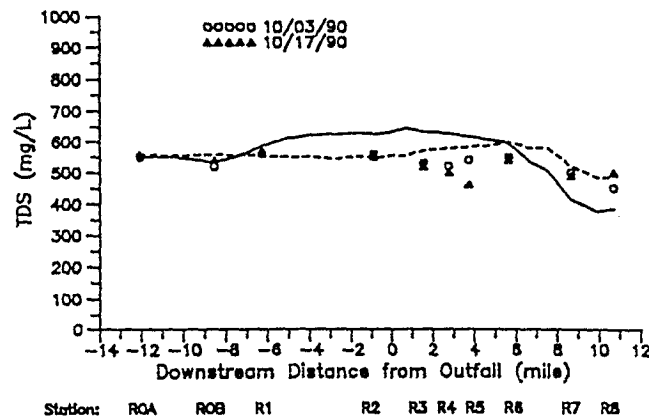
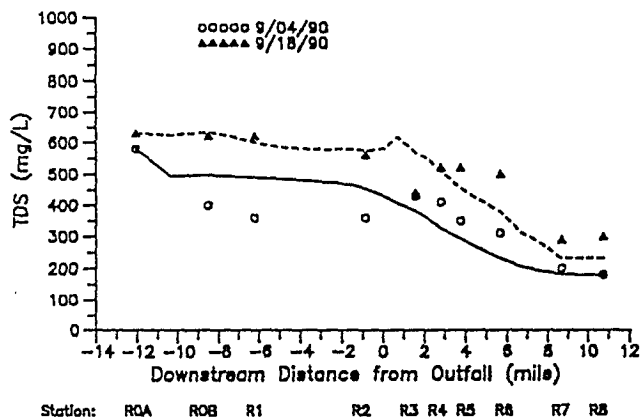
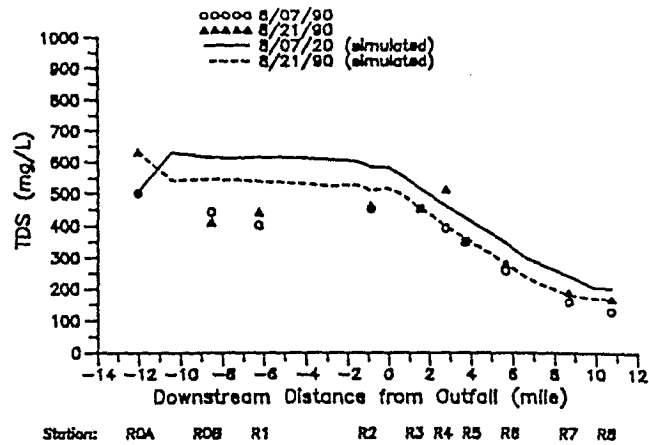
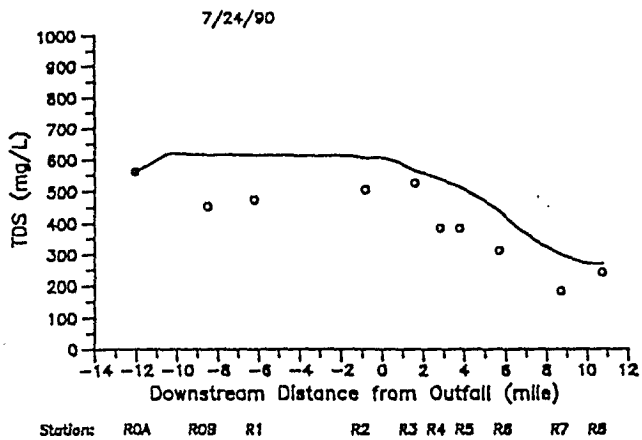
Simulated and Observed Concentration Profiles and
Time Concentrations of Ammonia Nitrogen From July 1990 to July 1991



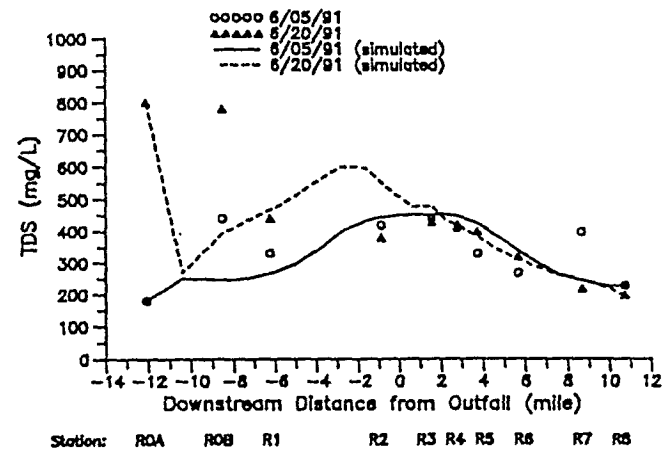
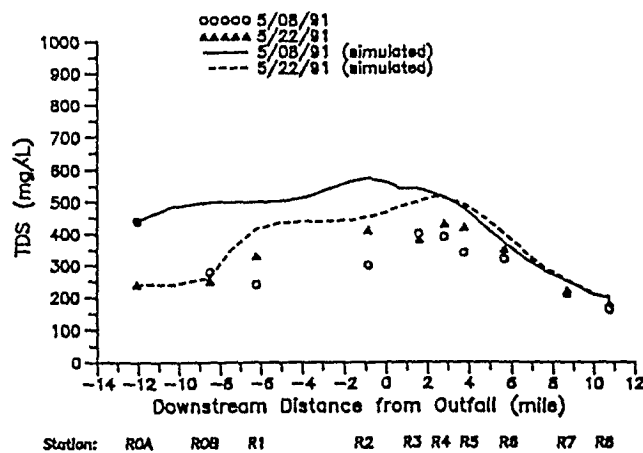
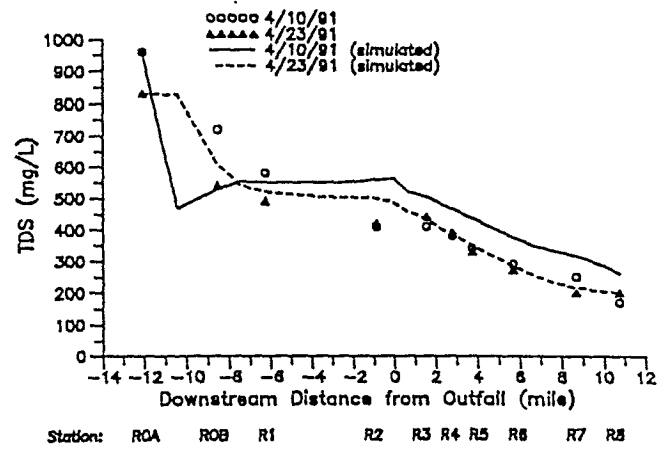
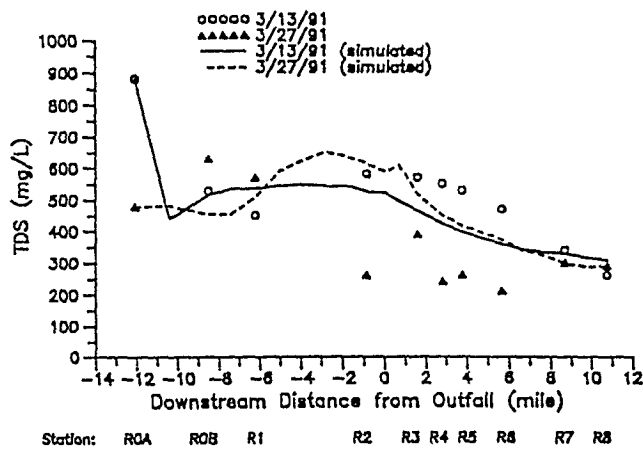
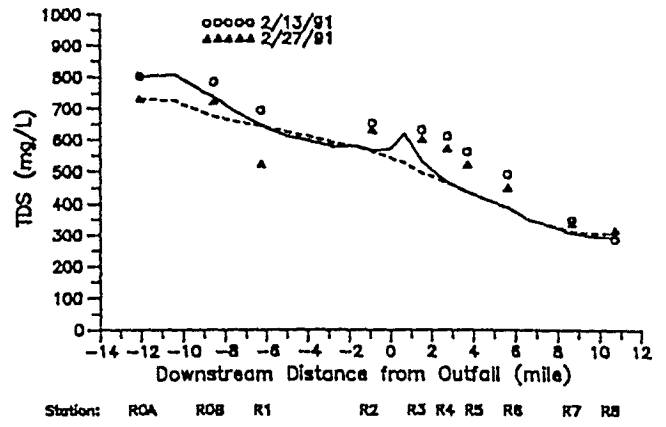
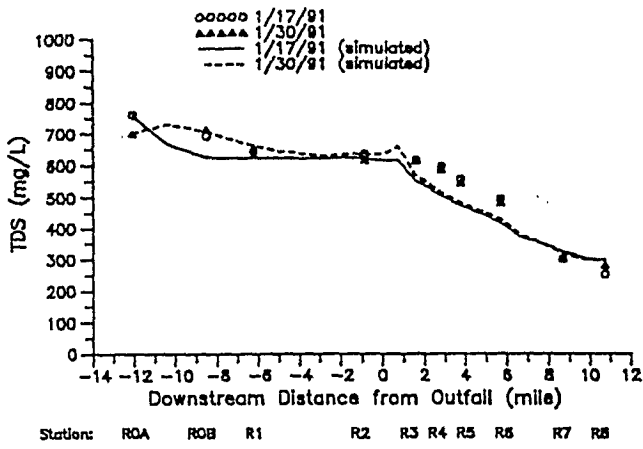
Comparison of Observed and Simulated Ammonia Nitrogen Profiles from 7/90 to 7/91



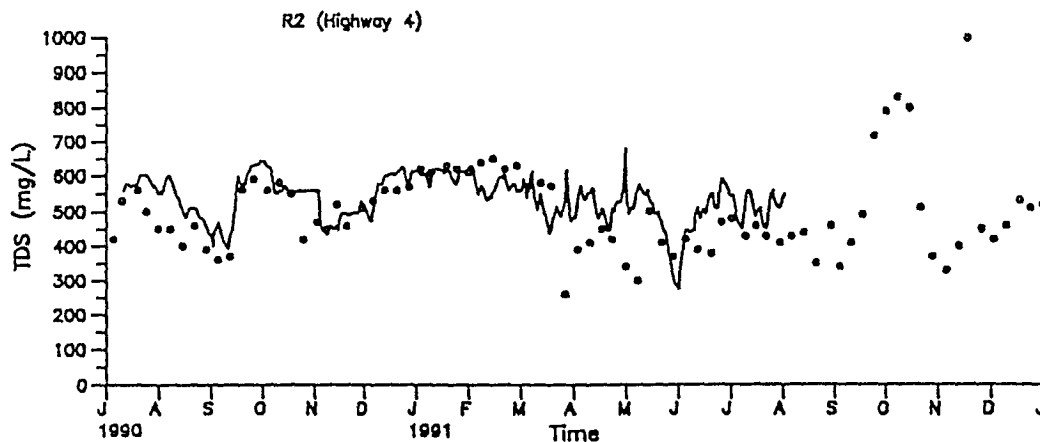
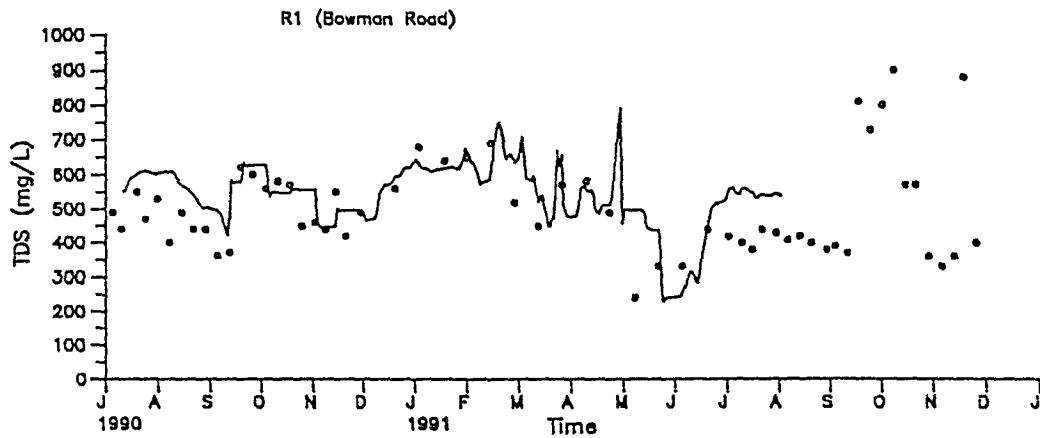
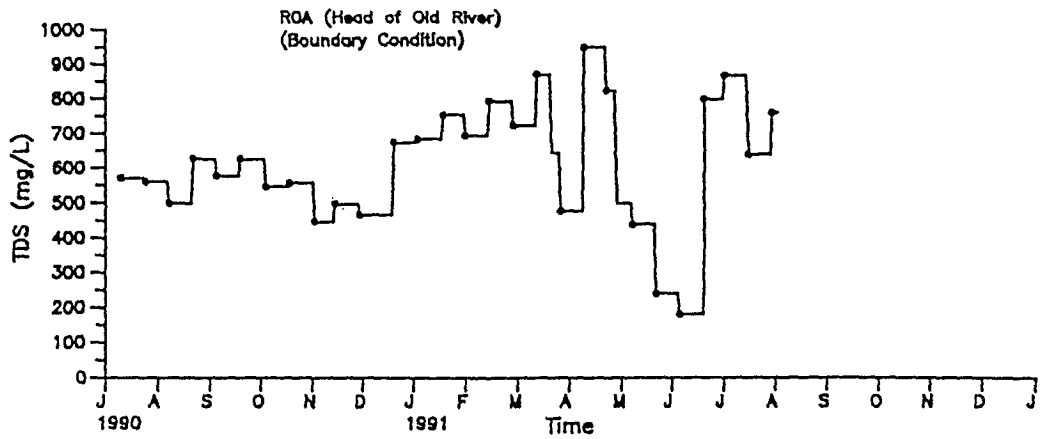
Comparison of Observed and Simulated Ammonia Nitrogen Profiles from 7/90 to 7/91 (continued)



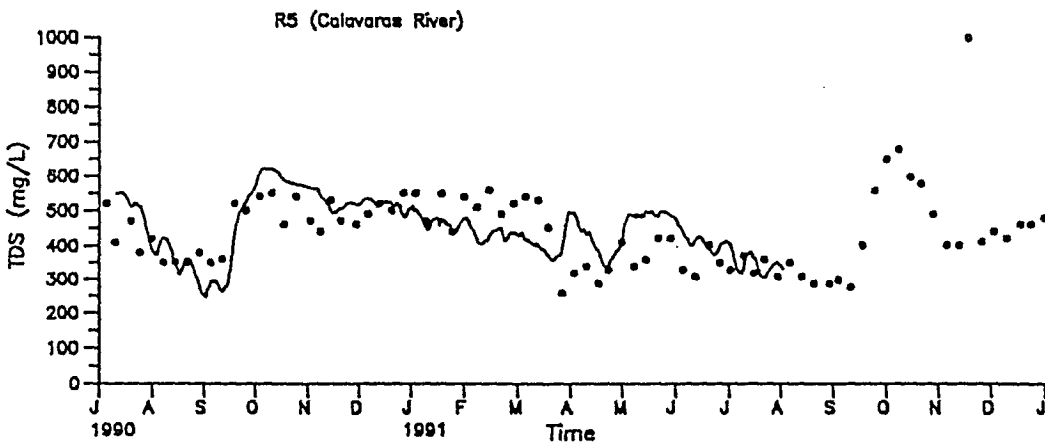
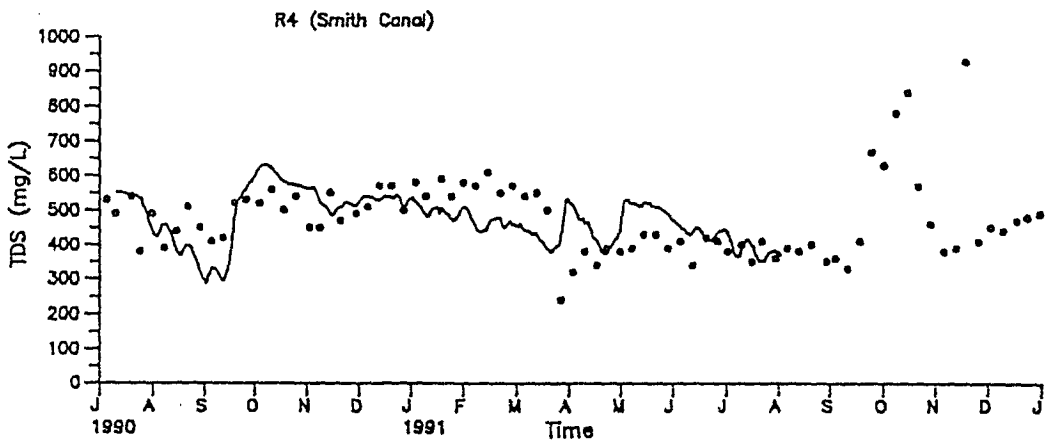
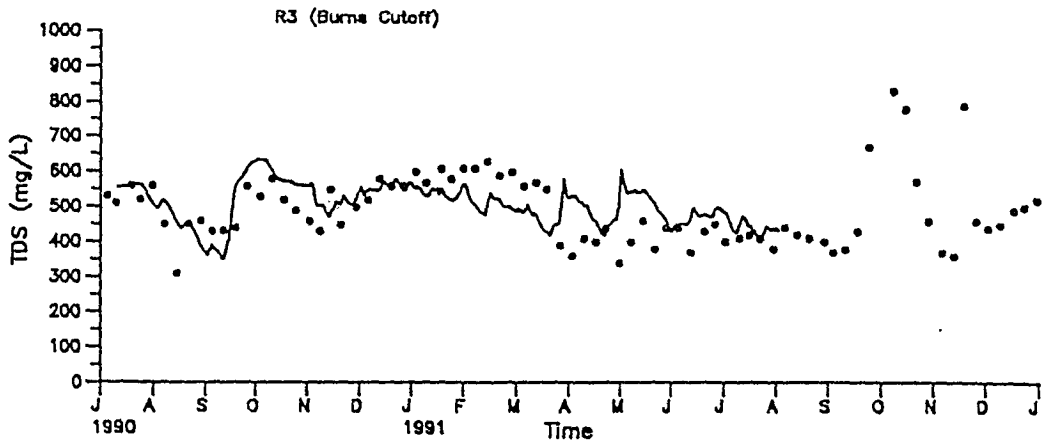
Comparison of Observed and Simulated TDS Profiles from 7/90 to 7/91



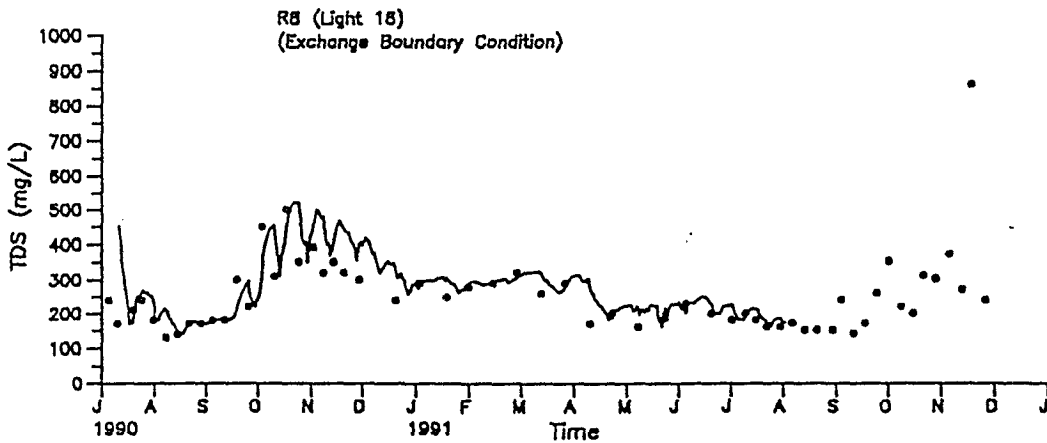
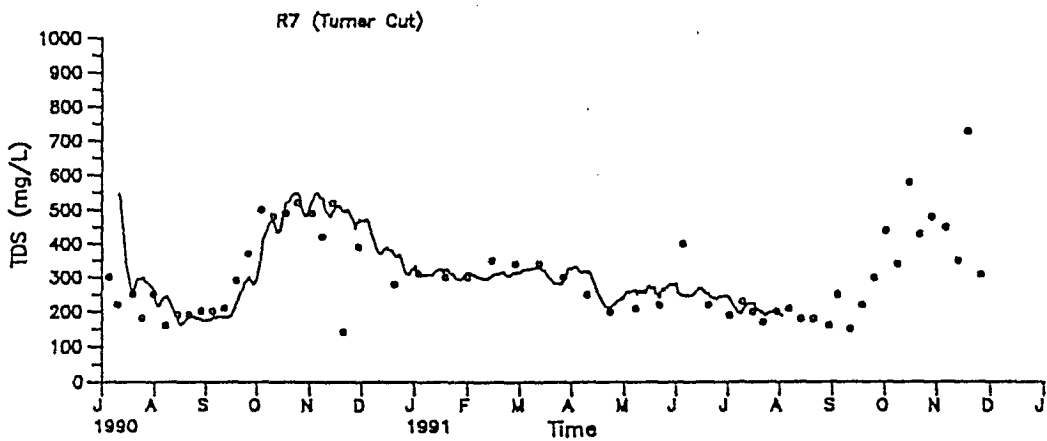
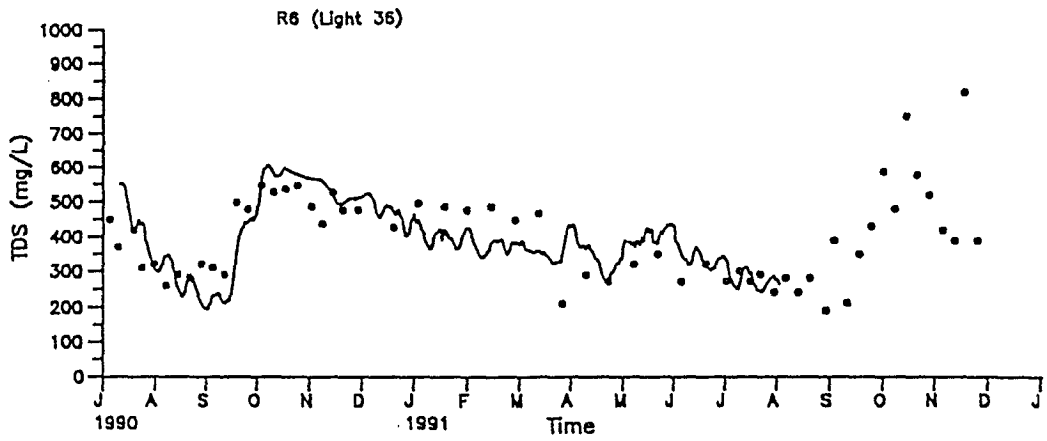
Comparison of Observed and Simulated TDS Profiles from 7/90 to 7/91 (continued)



Comparison of Observed and Simulated TDS
Concentration at Stations ROA to R8
From 7/90 to 7/91



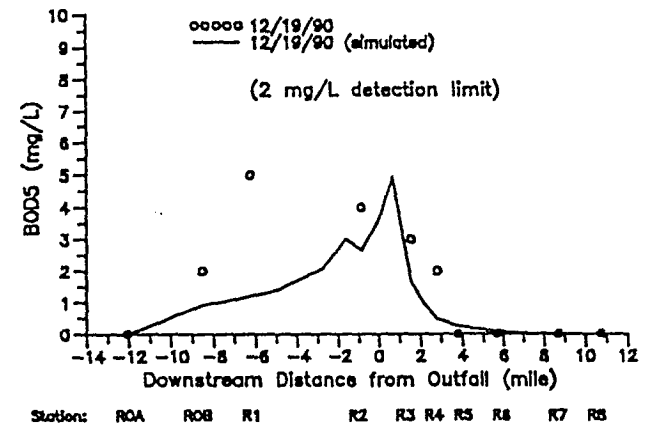
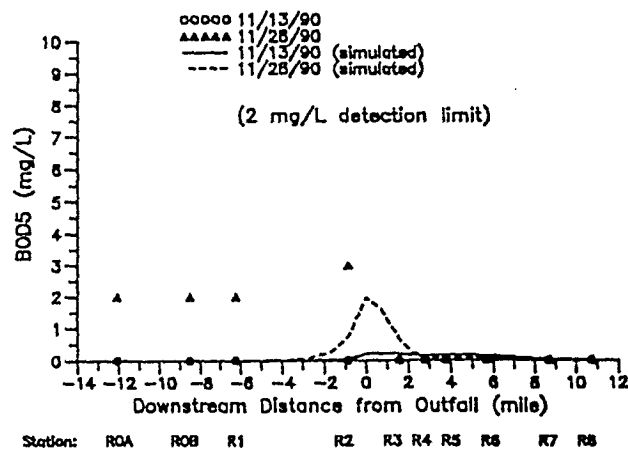
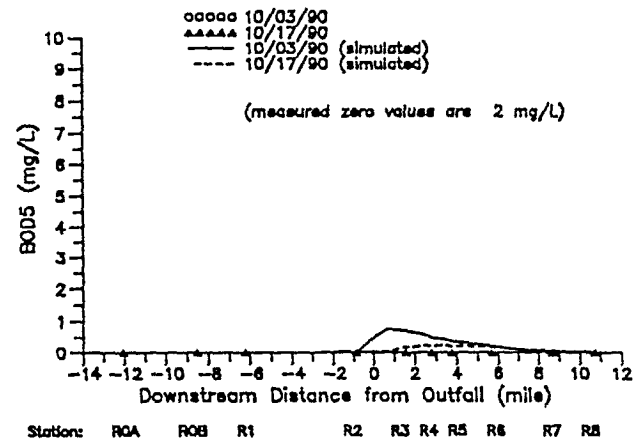
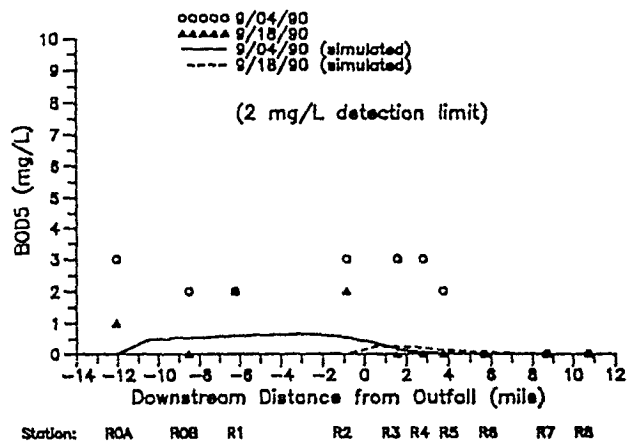
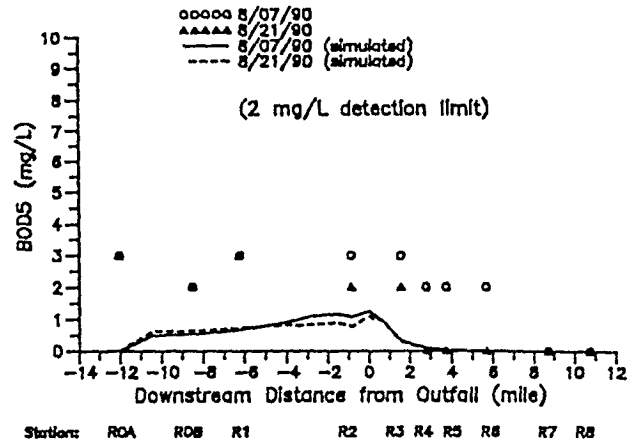
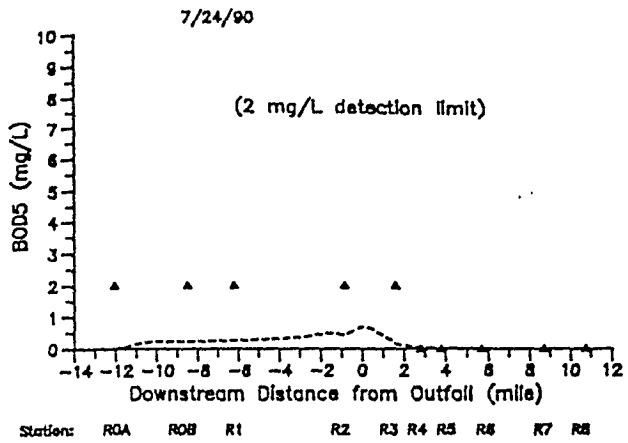
Comparison of Observed and Simulated TDS
 Concentration at Stations R0A to R8
 From 7/90 to 7/91 (continued)



Comparison of Observed and Simulated TDS
Concentration at Stations R0A to R8
From 7/90 to 7/91 (continued)

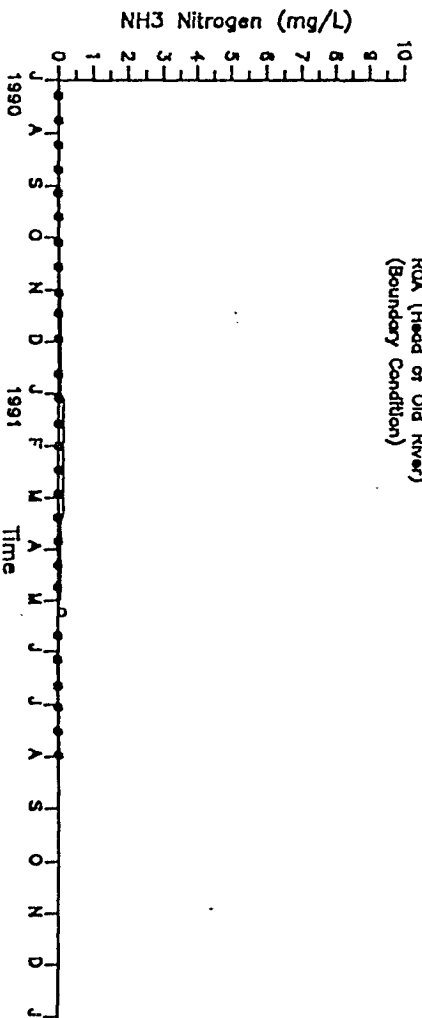
APPENDIX F

Simulated and Observed concentration Profiles and
Time concentrations of Carbonaceous BOD From July 1990 to July 1991

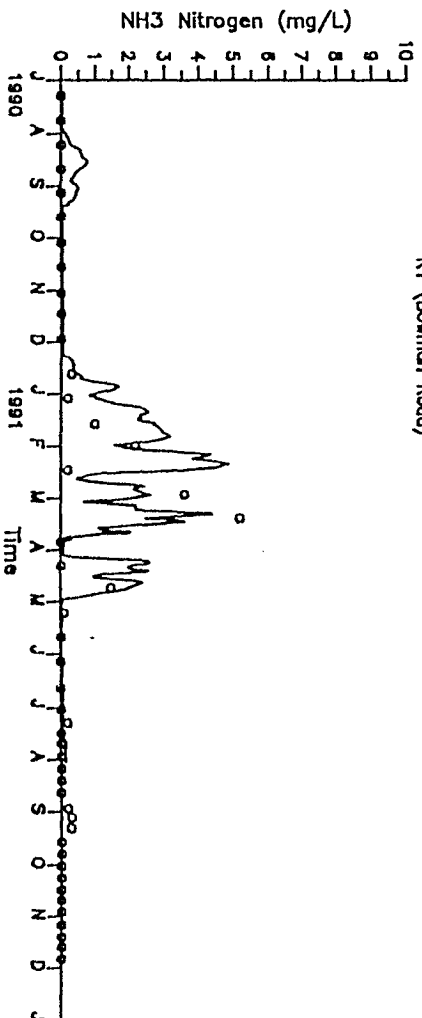


Comparison of Observed and Simulated CBOD Profiles from 7/90 to 7/91

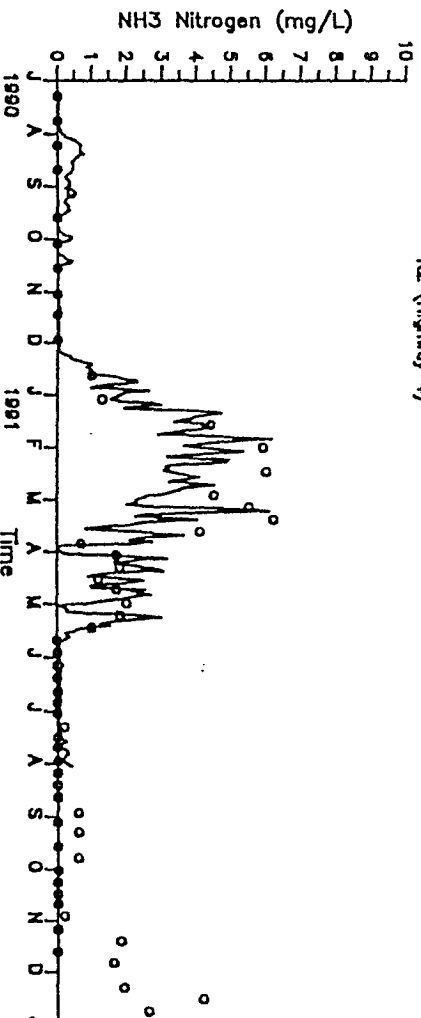
R0A (Head of Old River)
(Boundary Condition)



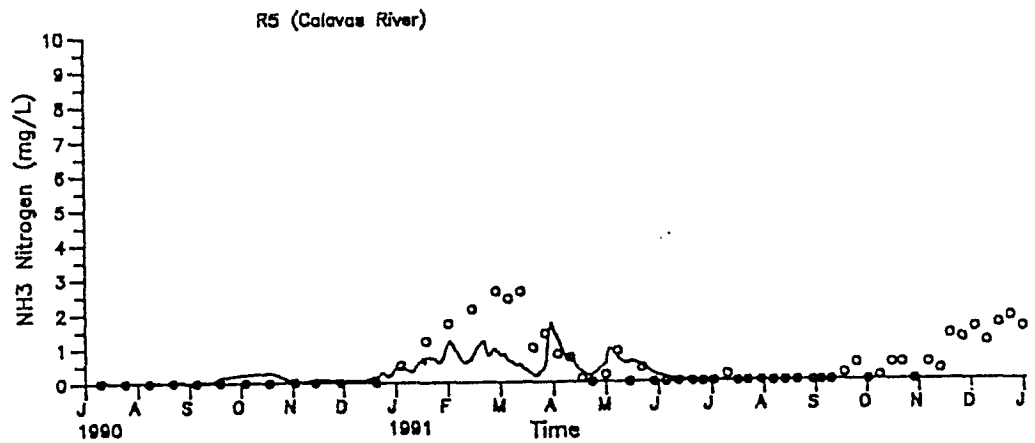
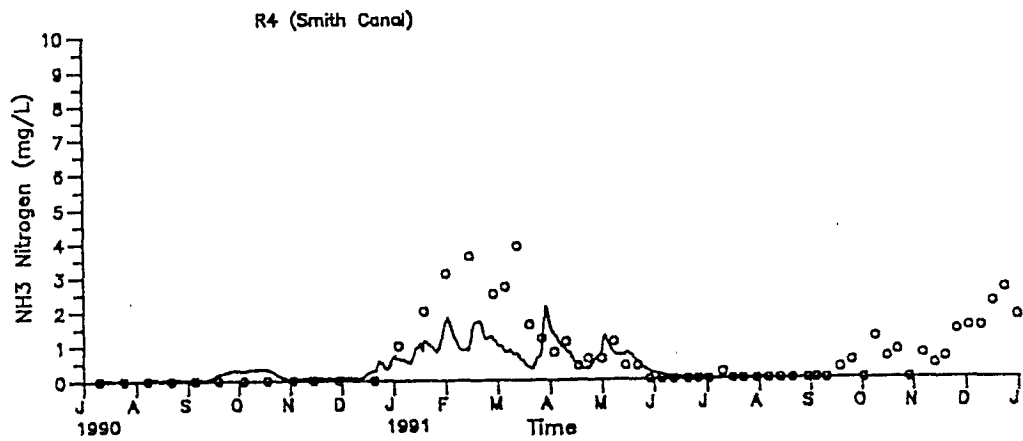
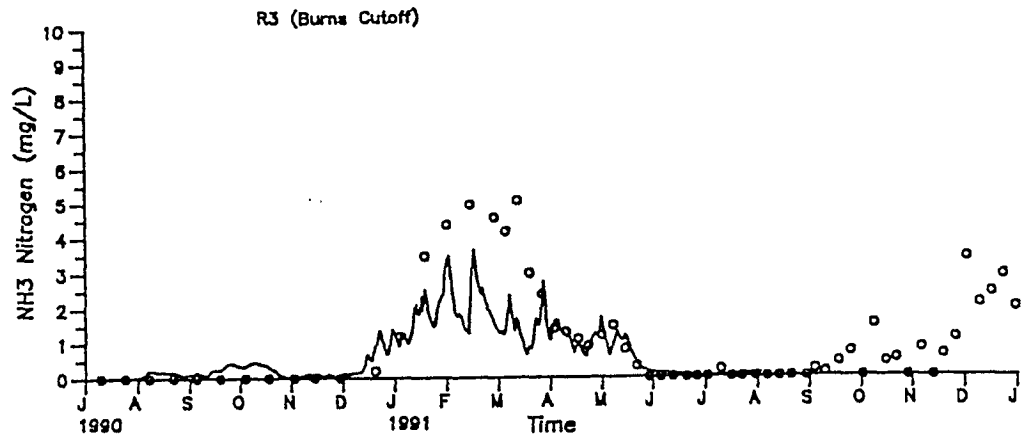
R1 (Bowman Road)



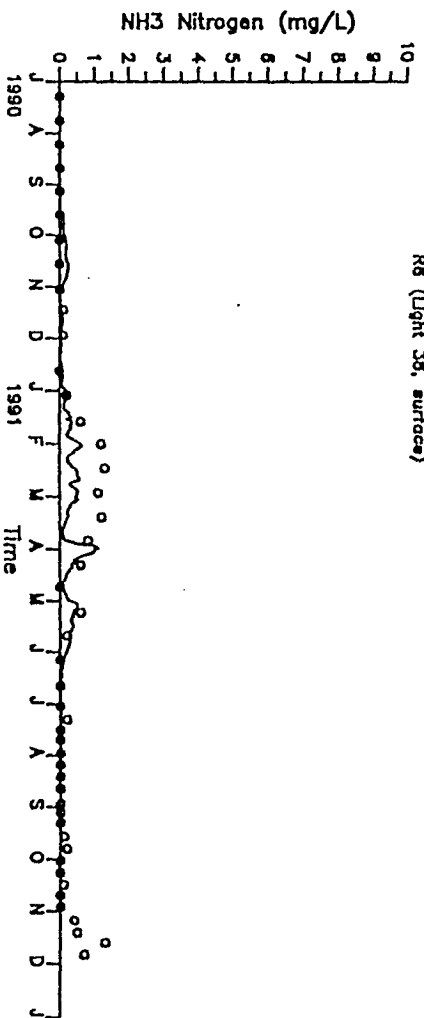
R2 (Highway 4)



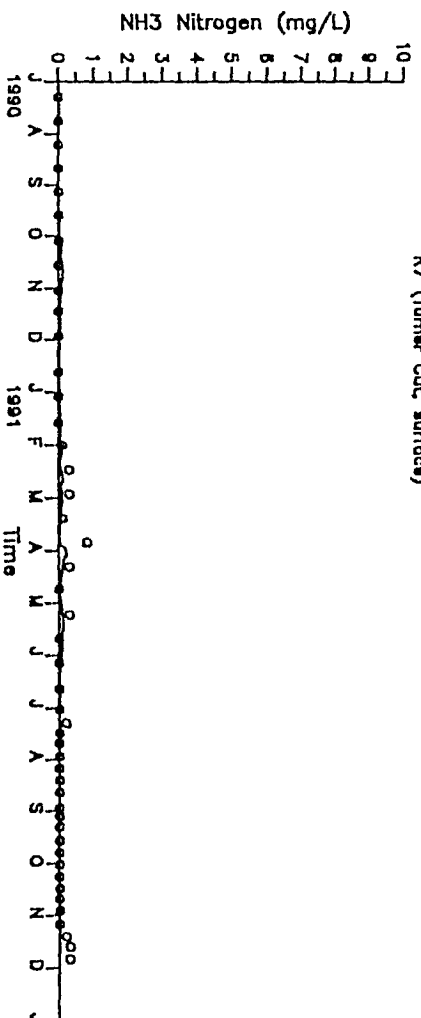
Comparison of Observed and Simulated Ammonia
Nitrogen Concentration at Stations R0A to R8
From 7/90 to 7/91



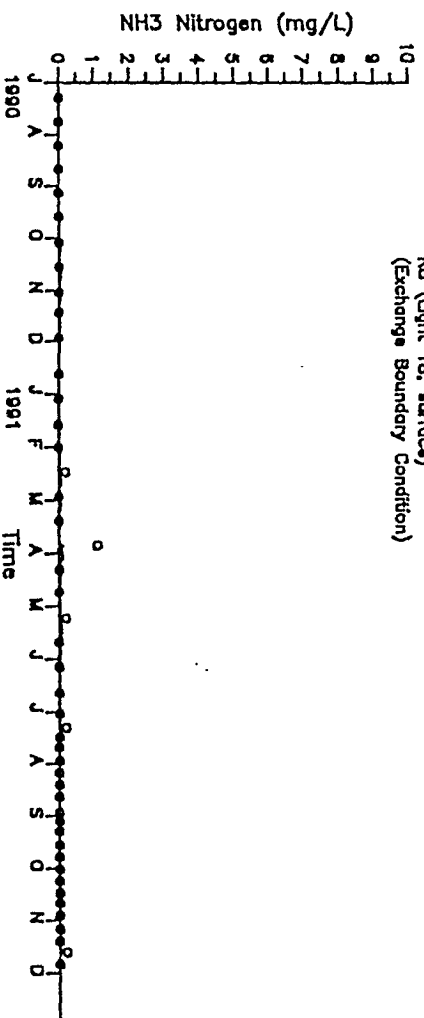
Comparison of Observed and Simulated Ammonia Nitrogen Concentration at Stations R0A to R8 From 7/90 to 7/91 (continued)



R7 (Turner Cut, surface)



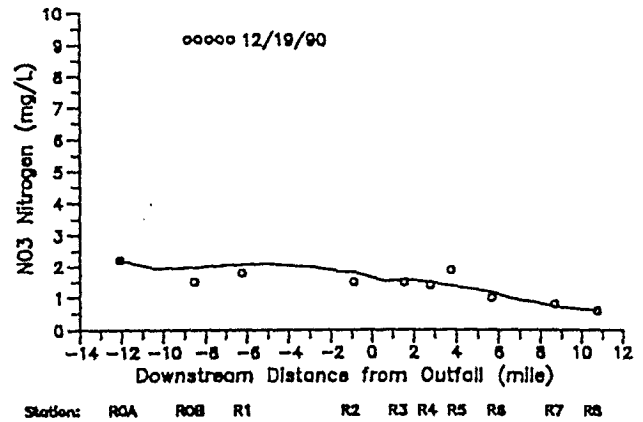
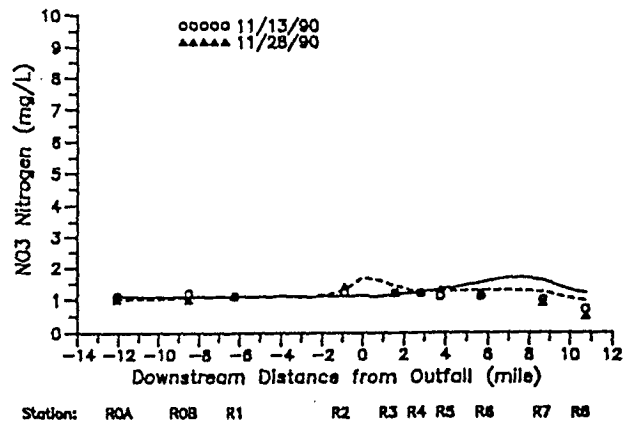
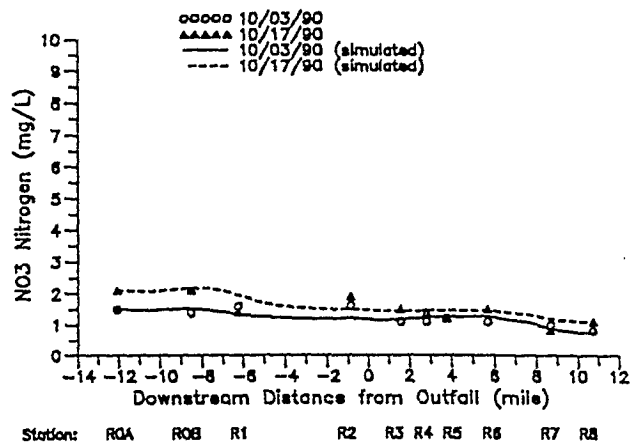
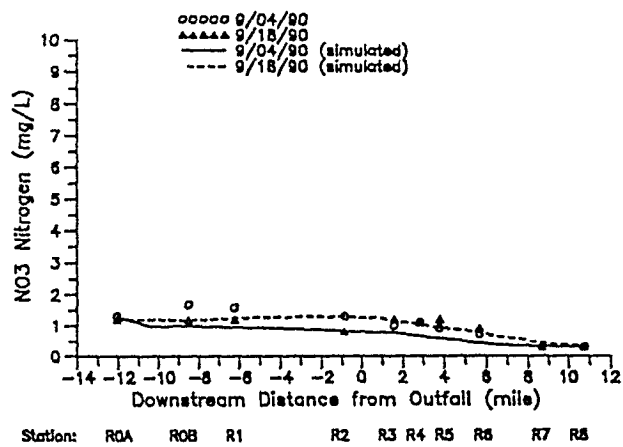
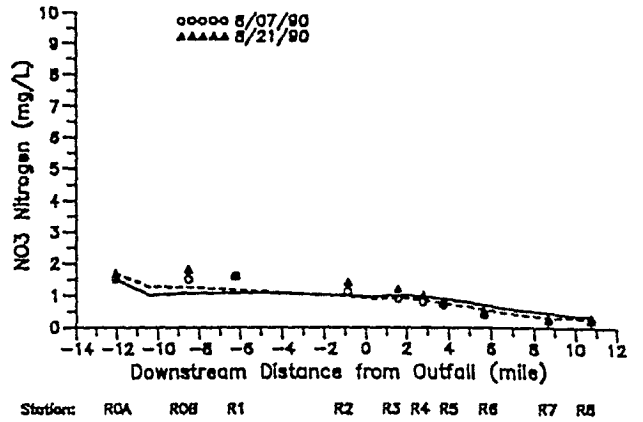
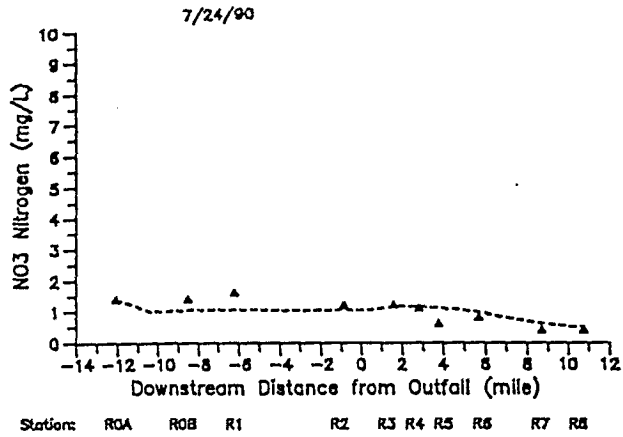
R8 (Light 18, surface)
(Exchange Boundary Condition)



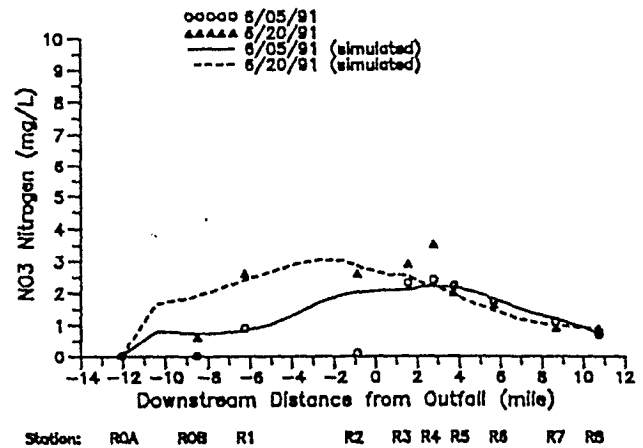
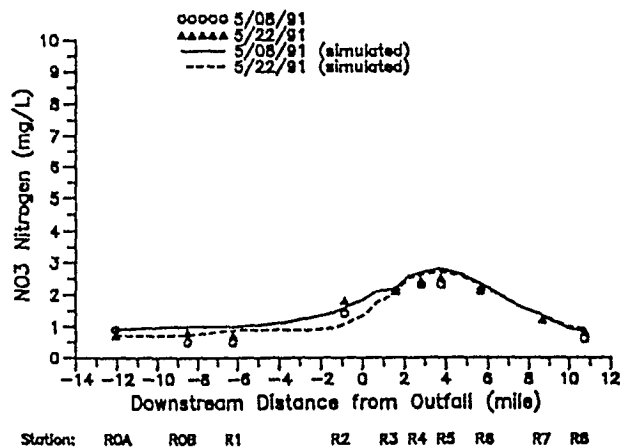
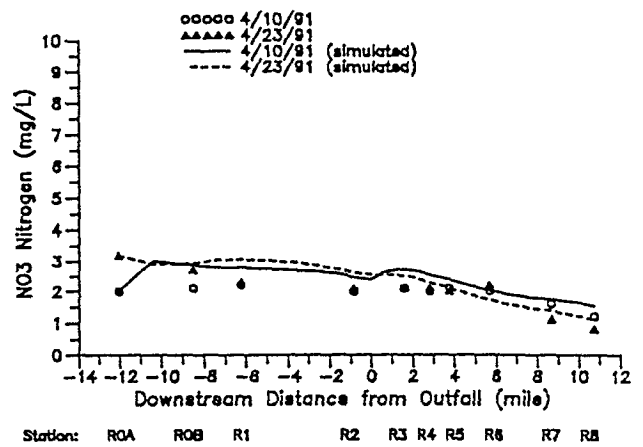
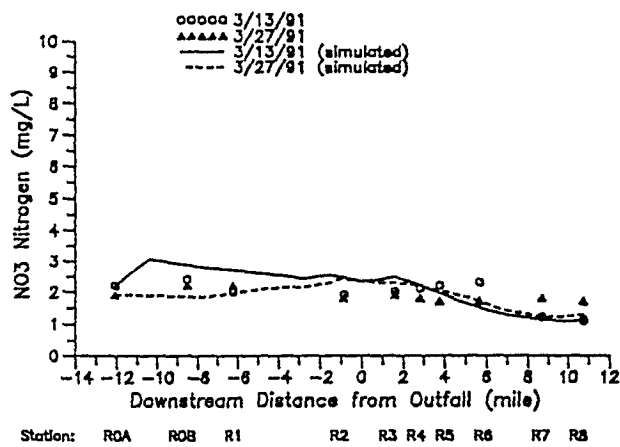
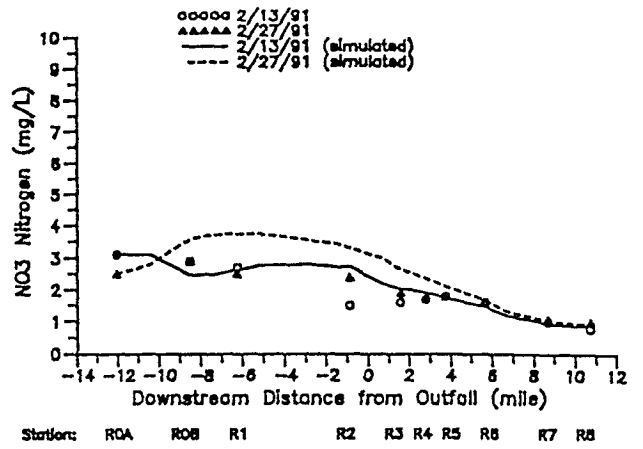
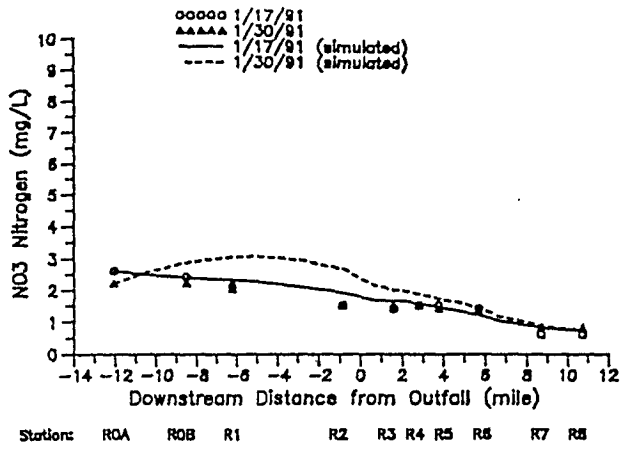
Comparison of Observed and Simulated Ammonia
Nitrogen Concentration at Stations R0A to R8
From 7/90 to 7/91 (continued)

APPENDIX H

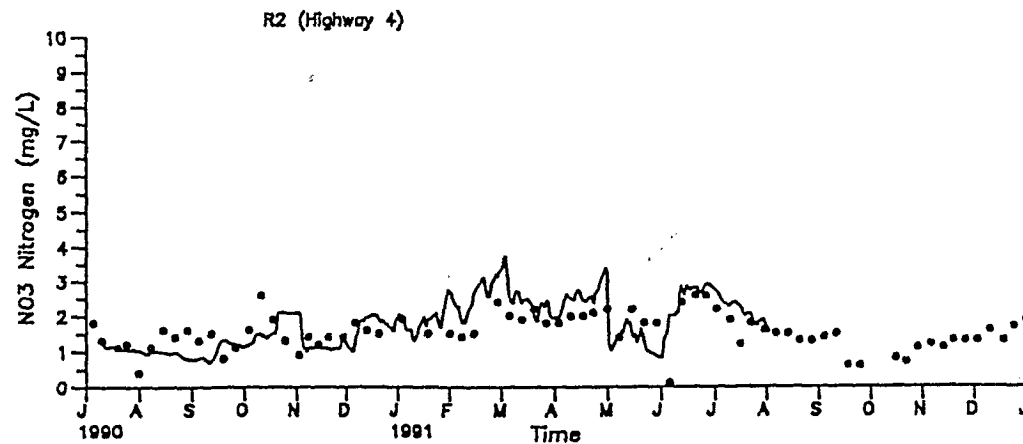
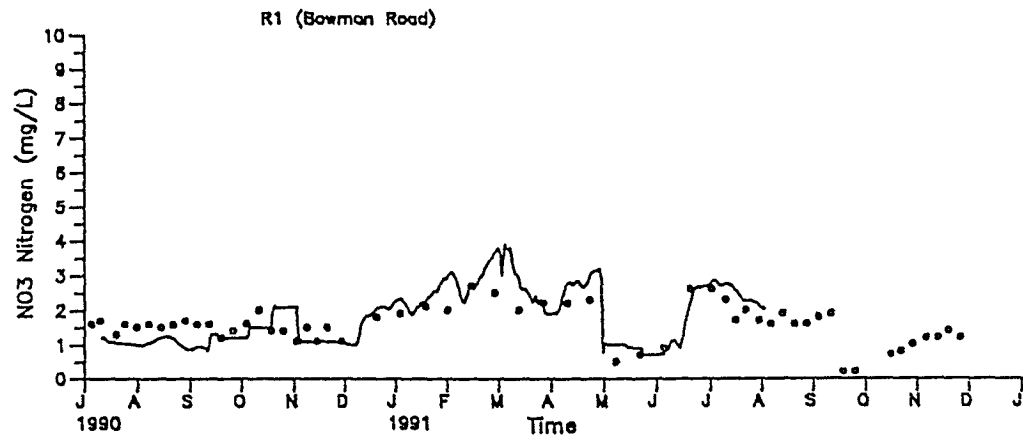
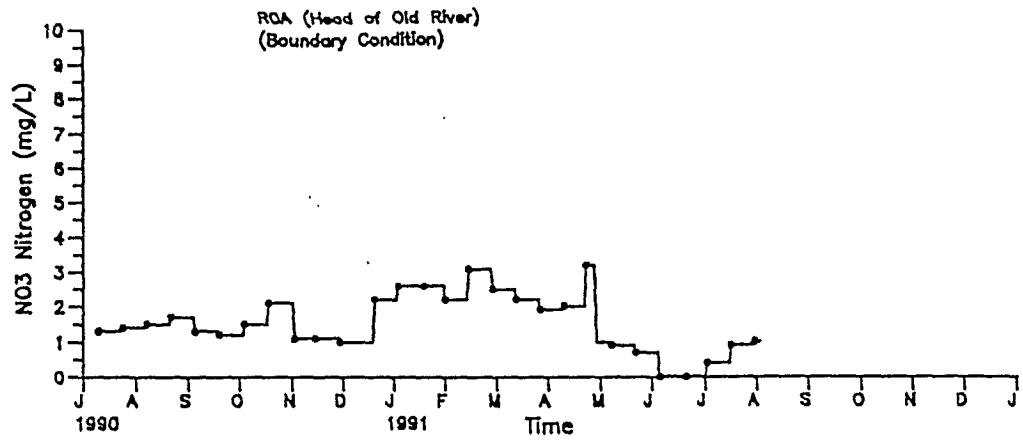
Simulated and Observed concentration Profiles and
Time Concentrations of Nitrate Nitrogen From July 1990 to July 1991



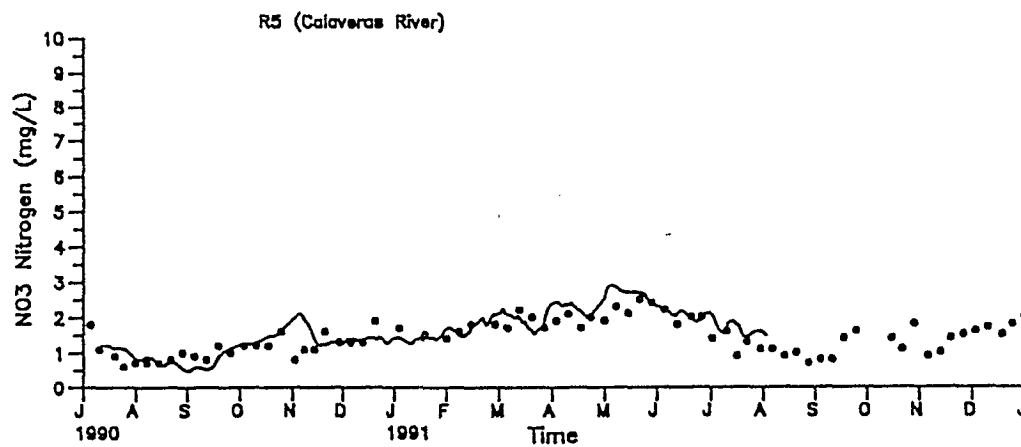
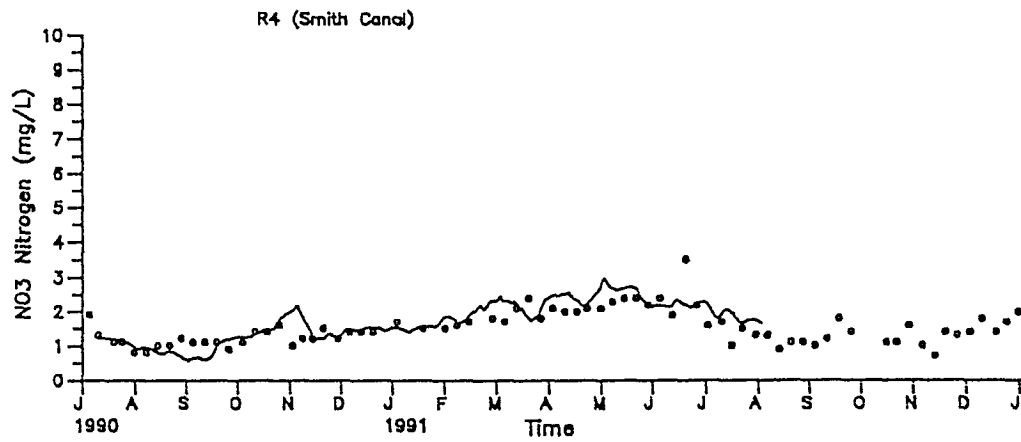
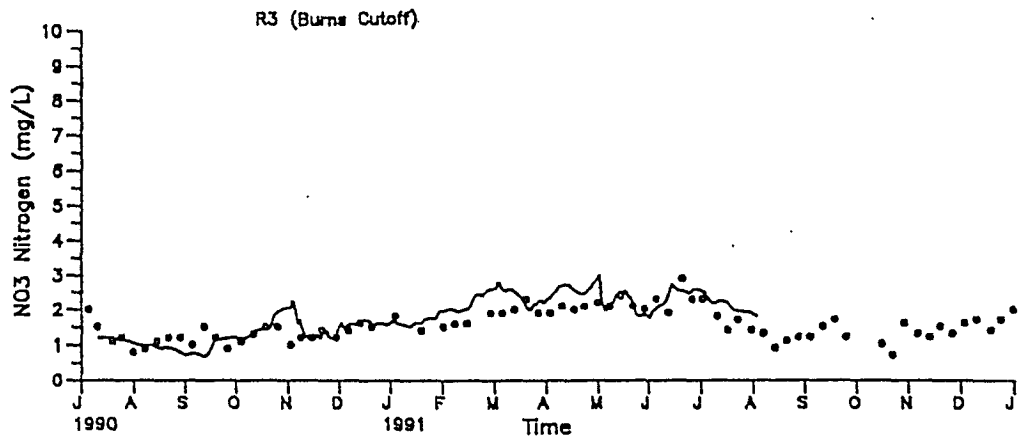
Comparison of Observed and Simulated Nitrate Nitrogen Profiles from 7/90 to 7/91



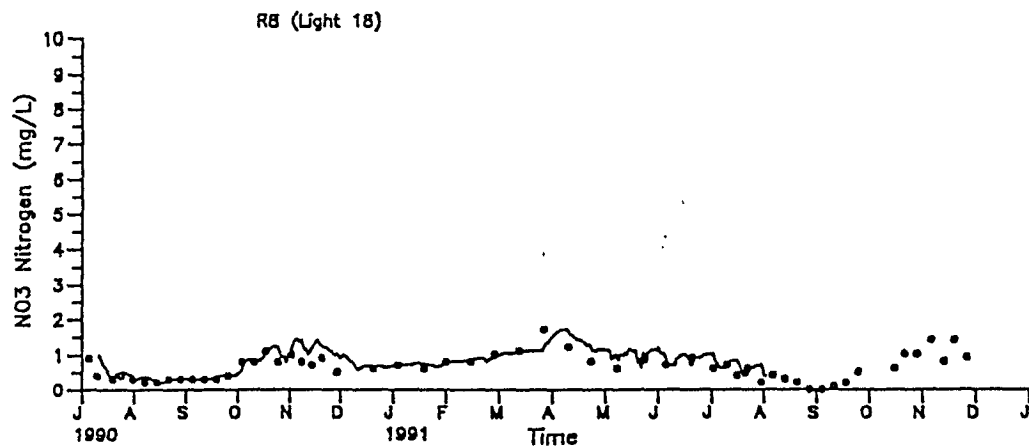
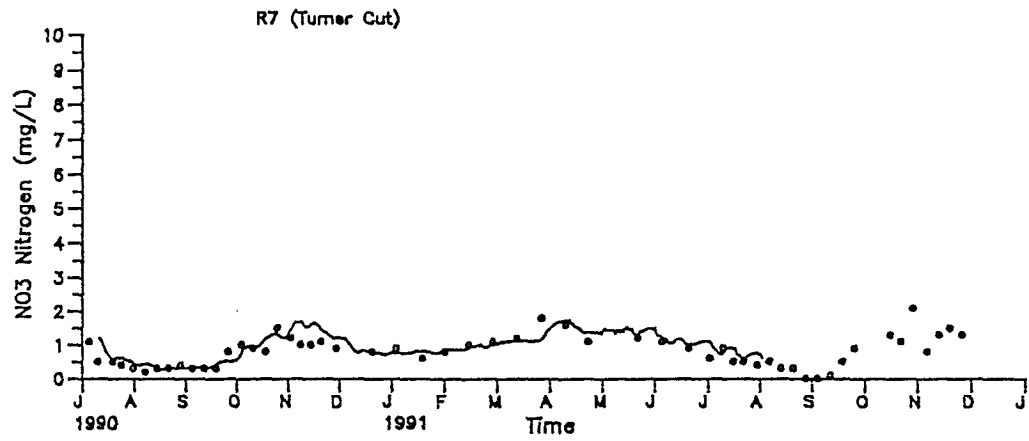
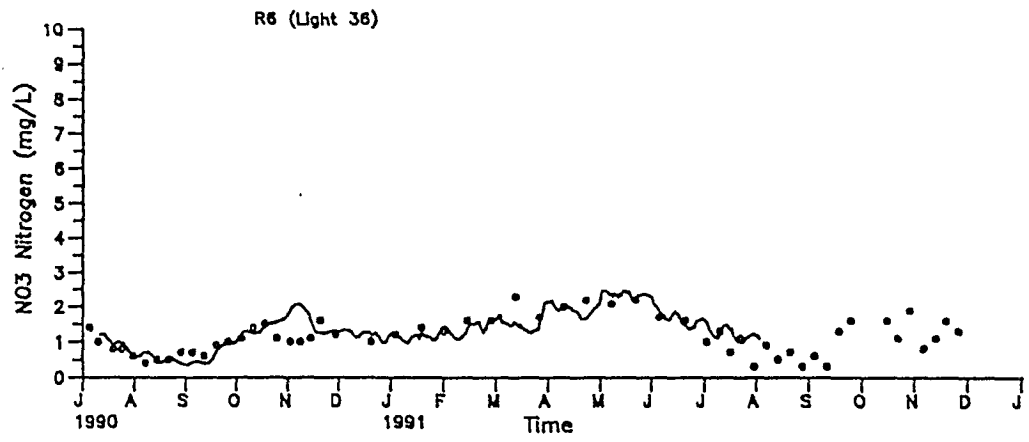
Comparison of Observed and Simulated Nitrate Nitrogen Profiles from 7/90 to 7/91 (continued)



Comparison of Observed and Simulated Nitrate
Nitrogen Concentration at Stations ROA to R8
From 7/90 to 7/91



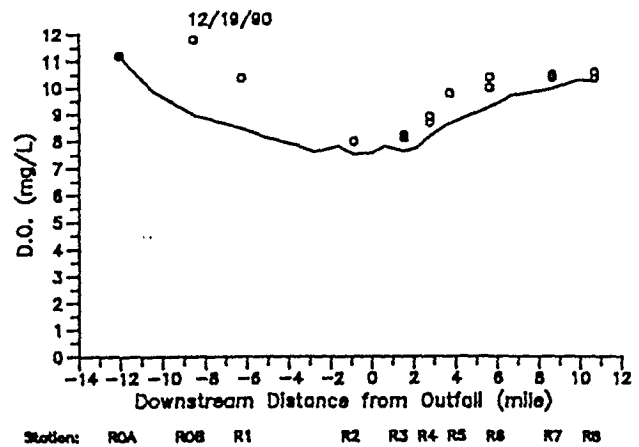
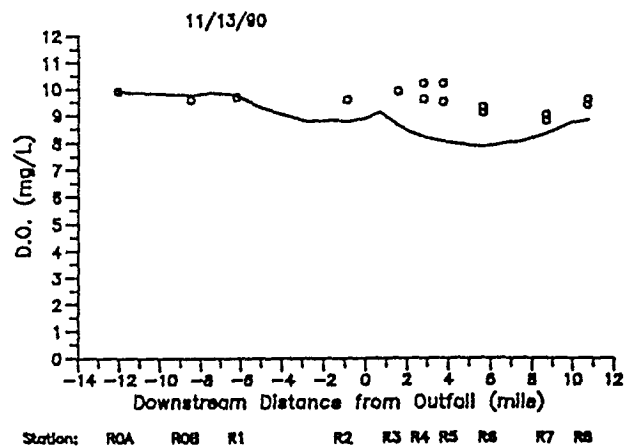
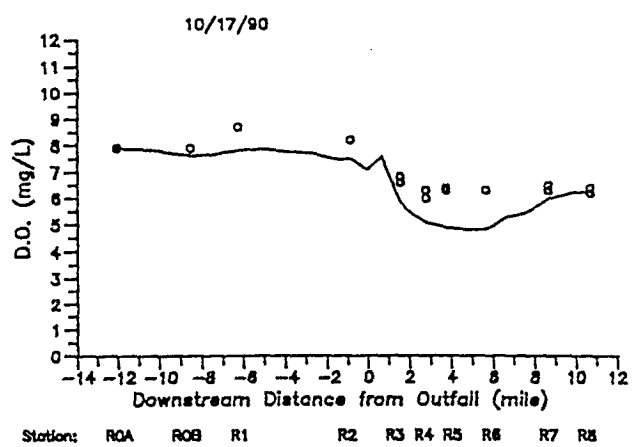
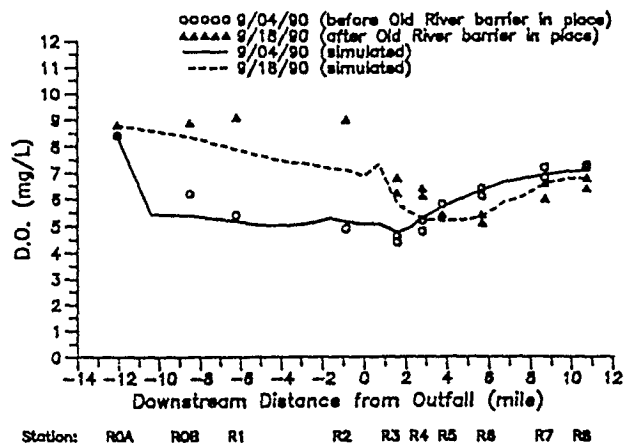
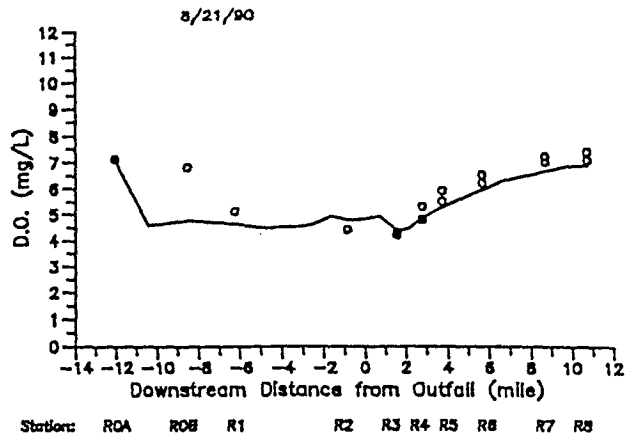
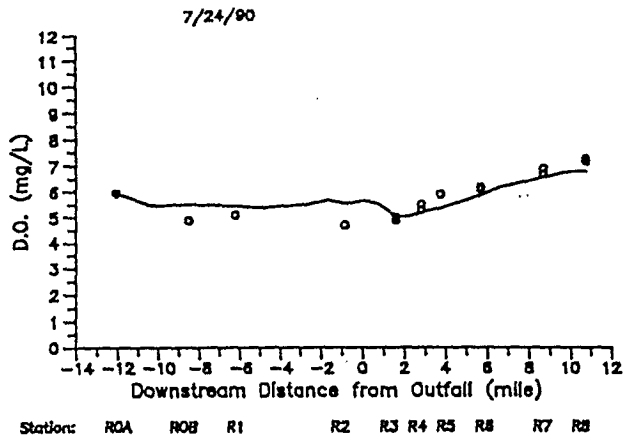
Comparison of Observed and Simulated Nitrate Nitrogen Concentration at Stations R0A to R8 From 7/90 to 7/91 (continued)



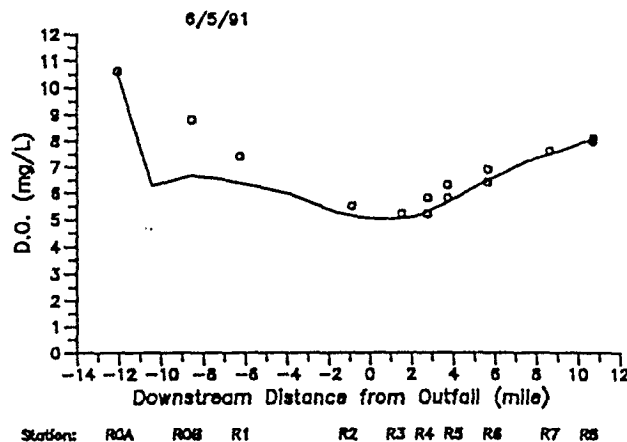
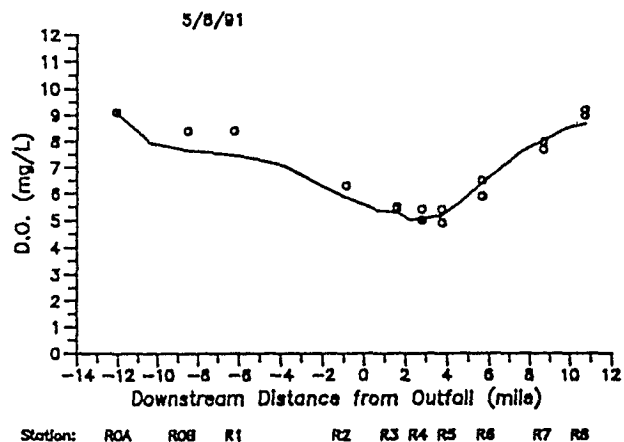
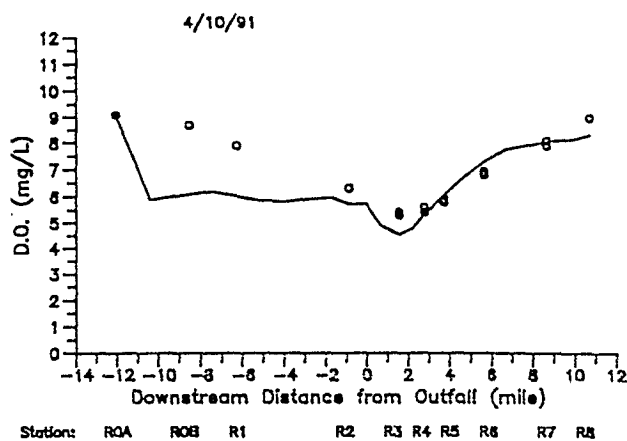
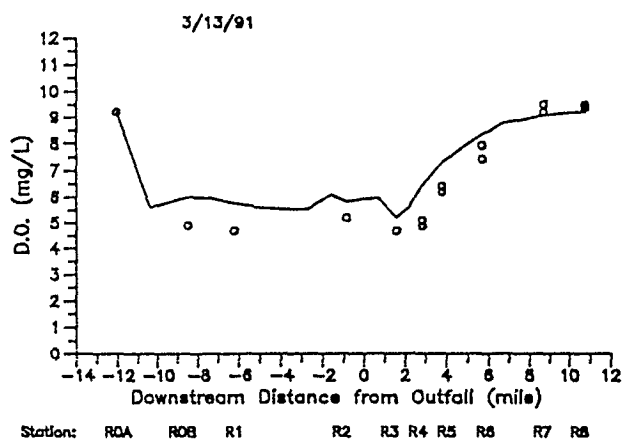
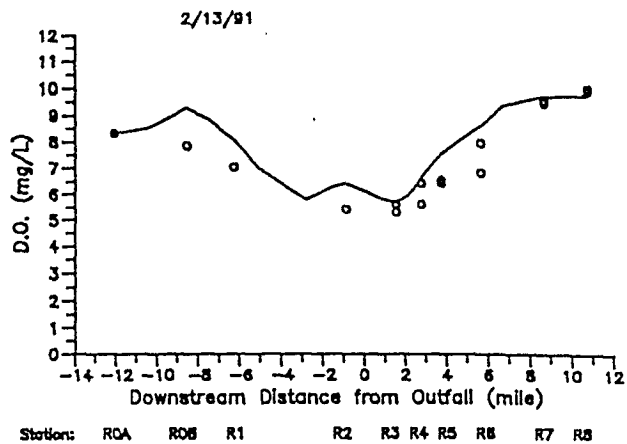
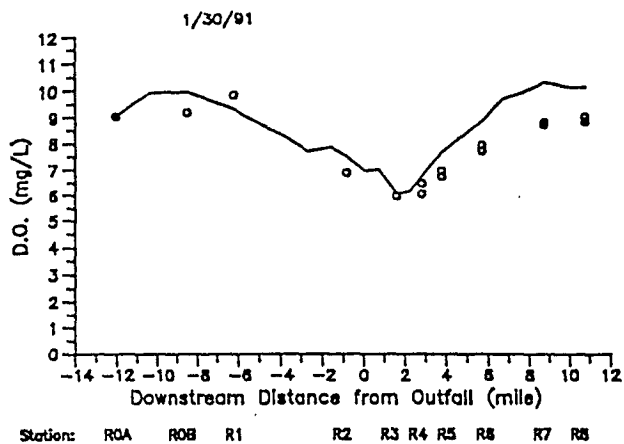
Comparison of Observed and Simulated Nitrate Nitrogen Concentration at Stations R0A to R8 From 7/90 to 7/91 (continued)

APPENDIX I

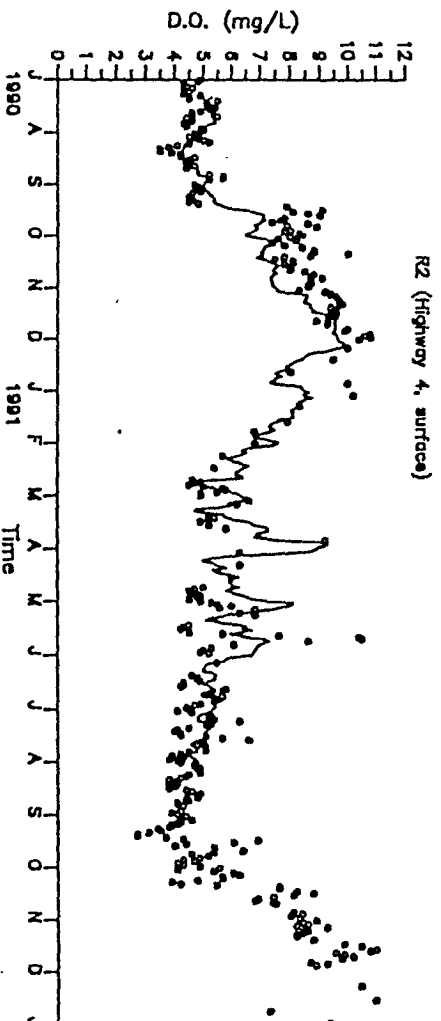
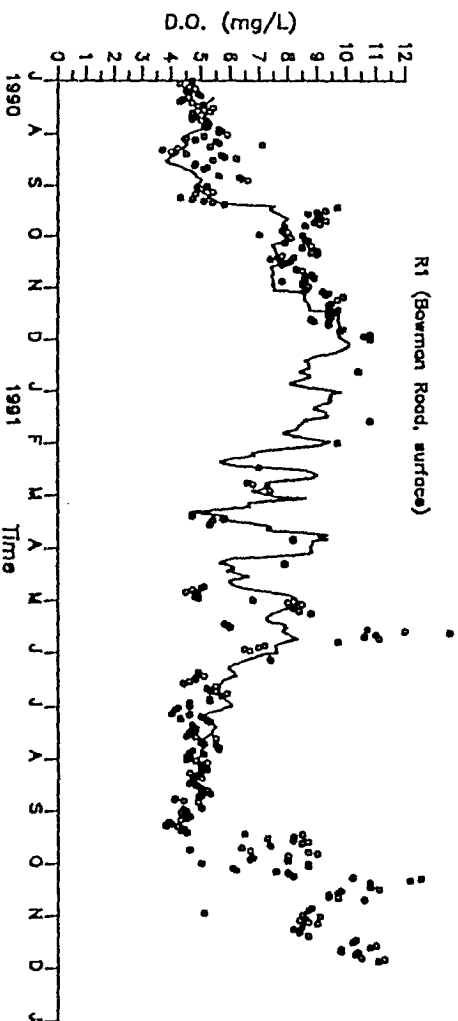
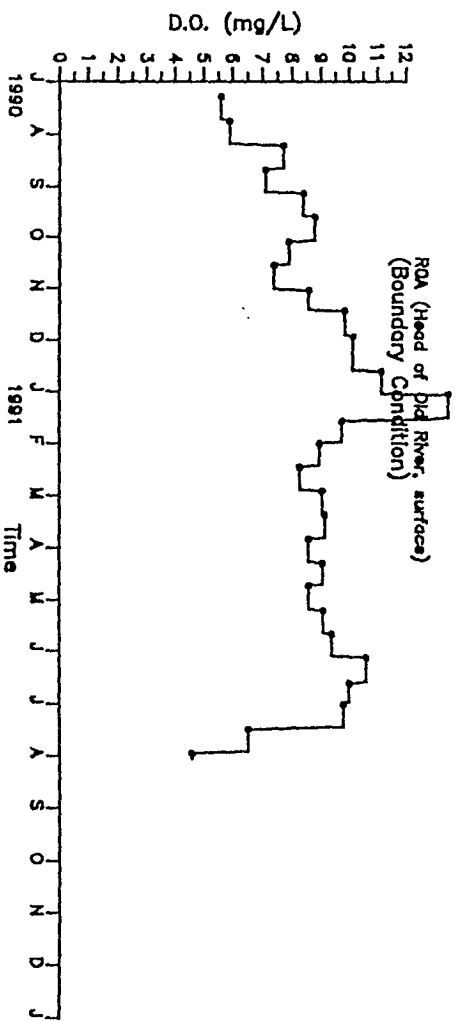
**Simulated and Observed Concentration Profiles and
Time Concentrations of Dissolved Oxygen From July 1990 to July 1991**



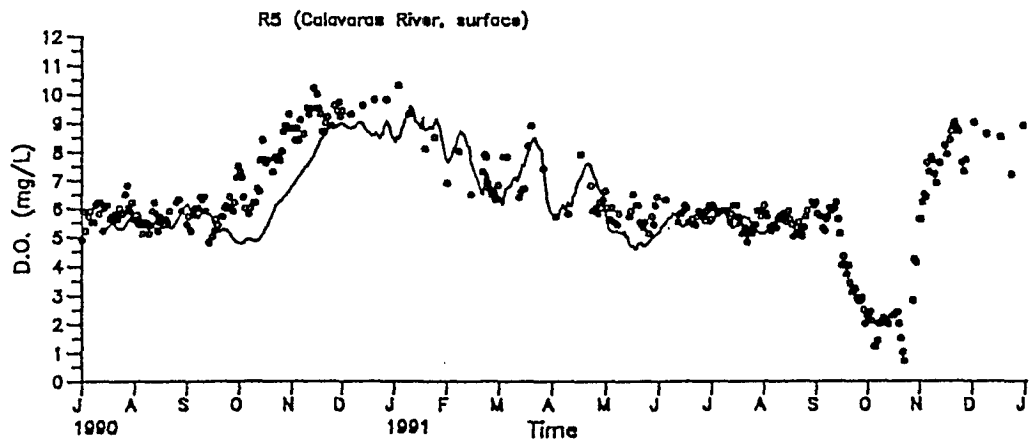
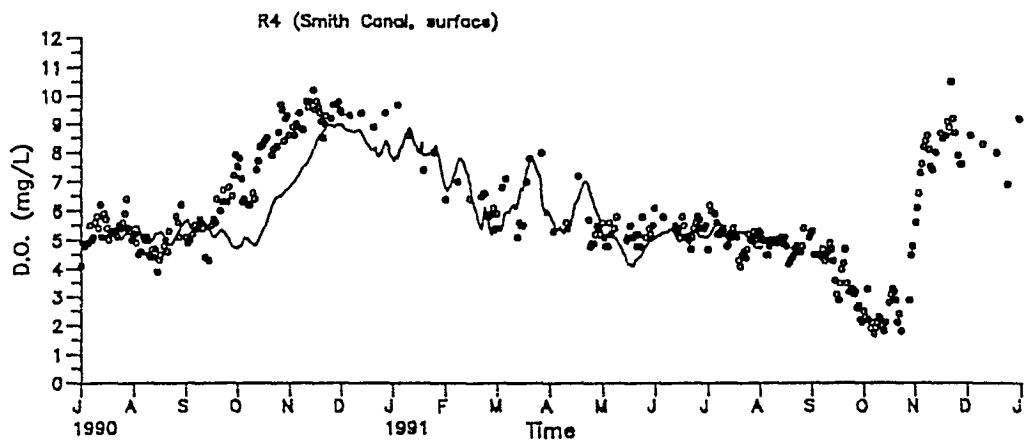
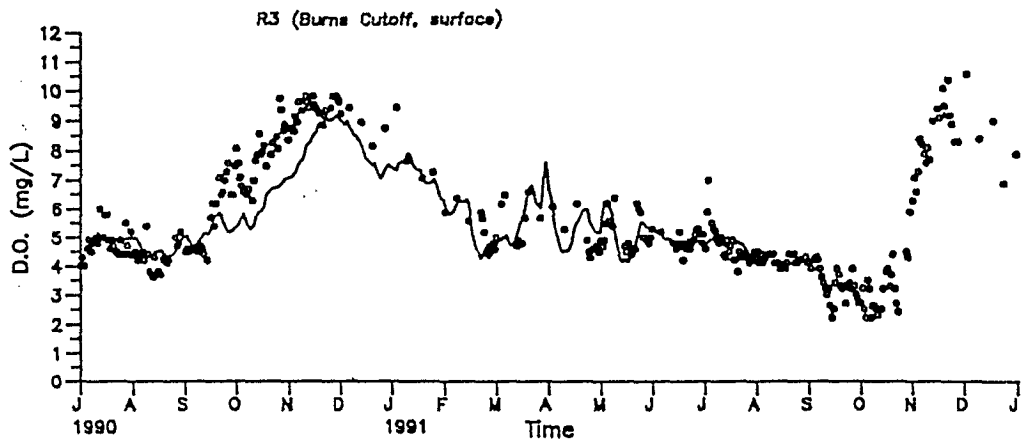
Comparison of Observed and Simulated Dissolved Oxygen Profiles from 7/90 to 7/91



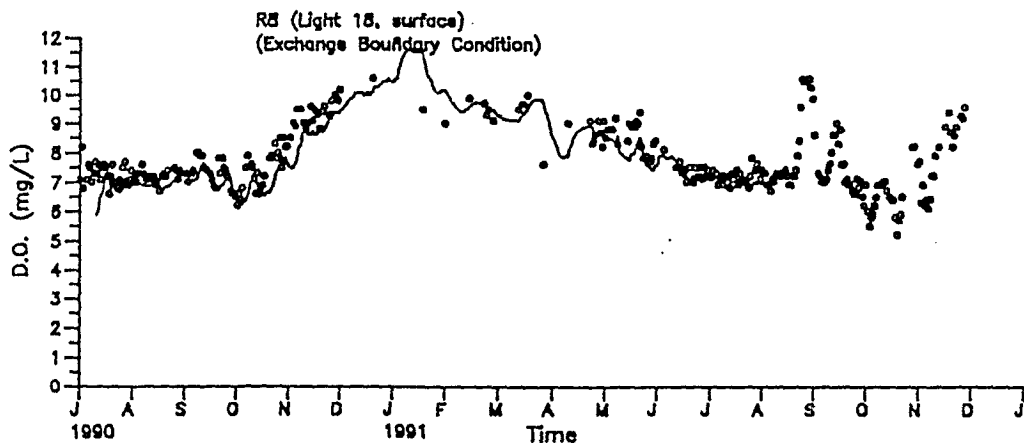
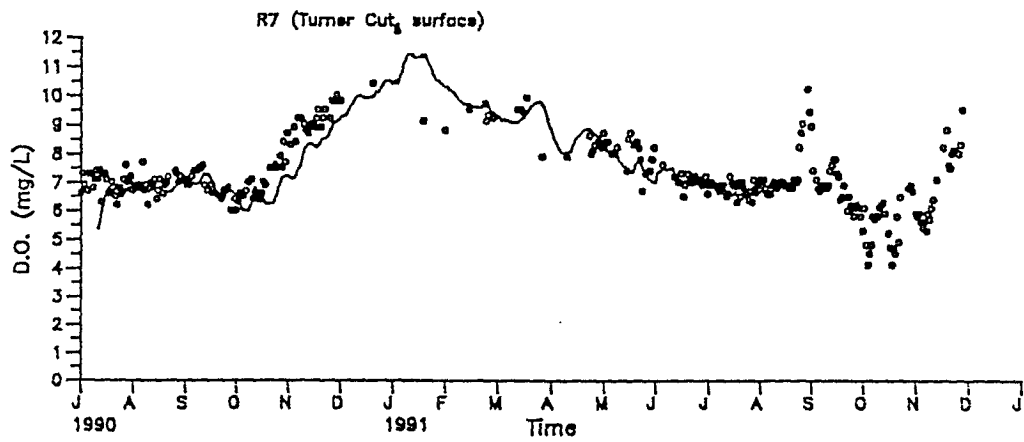
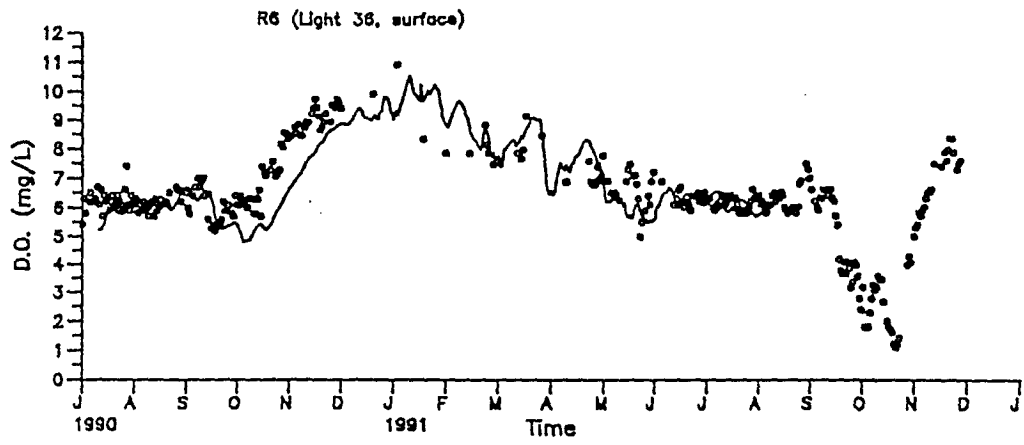
Comparison of Observed and Simulated Dissolved Oxygen Profiles from 7/90 to 7/91 (continued)



Comparison of Observed and Simulated Dissolved
Oxygen Concentration at Station R0A to R8
From 7/90 to 7/91



Comparison of Observed and Simulated Dissolved Oxygen Concentration at Station R0A to R8 From 7/90 to 7/91 (continued)



Comparison of Observed and Simulated Dissolved
Oxygen Concentration at Station R0A to R8
From 7/90 to 7/91 (continued)